Springer Protocols

Janos Minarovits
Hans Helmut Niller *Editors*

Epstein
Barr Virus

Methods and Protocols

Humana Press

Volume 1532
Methods in Molecular Biology

For further volumes: http://www.springer.com/series/7651

Editors

Janos Minarovits and Hans Helmut Niller

Epstein Barr Virus

Methods and Protocols

Editors

Janos Minarovits
University of Szeged, Szeged, Hungary

Hans Helmut Niller
University of Regensburg, Regensburg, Germany

Cover illustration: The picture is derived from the chapter "Functional Analysis of Exosomes Derived from EBV-Infected Cells" of this book, by Gulfaraz Khan and Pretty

S. Philip.

Foreword

The Epstein–Barr virus (EBV) was identified 49 years ago as the causative agent of a long time known disease, infectious mononucleosis (IM, glandular fever). The IM symptoms are not manifested by all individuals at the time of acquisition of the infection. It is highly important that the subclinical primary infection also leads to the virus carrier state for lifetime accompanied by efficient immunity. The "silent" infection is due to a particular strategy of the immune system, based on a finely tuned interaction between T and B lymphocytes. When EBV-carrying B lymphocytes acquire proliferating potential (thus malignant potential) in a well-defined differentiation window in vivo, their multiplication is controlled, and the threat of lymphoma development is eliminated. In vitro experiments show that EBV can induce B cell proliferation directly, without the contribution of additional factors, as demonstrated by the establishment of immortalized lines (LCLs, lymphoblastoid cell lines). It is worth mentioning that LCLs are not only essential tools in basic EBV research, but these lines were indispensable in human genetic studies as well. Using several further strategies EBV contributes to malignant transformation of lymphocytes and also of epithelial and mesenchymal cells. By triggering or perpetuating pathogenic processes, EBV may also play a role in the development of autoimmune syndromes including multiple sclerosis, systemic lupus erythematosus (SLE), and rheumatoid arthritis. The complex and versatile (nonpathogenic and pathogenic) EBV–human interactions are well known. This volume provides a good background for continued studies with details of molecular, immunological, and cell biological methods. Guidelines for the treatment of certain EBV-associated malignancies are also given. "Hot topics" of the field are overviewed in the introductory chapter by the *Editors* , Janos Minarovits (Szeged) and Hans Helmut Niller (Regensburg), followed by the chapters of experts who master the thoroughly described methods. These chapters are highly helpful for both basic and clinical scientists.

Eva Klein
Stockholm, Sweden

Preface

Fifty-two years ago, collaboration between a dedicated surgeon and basic researchers, who applied a combination of as diverse laboratory methods as in vitro cell culture and electron microscopy , paved the way to the discovery of Epstein–Barr virus (EBV), a human herpesvirus (reviewed by Epstein [1]). The detection of herpesvirus particles in Burkitt lymphoma (BL) cells supported the idea—suggested by Denis Burkitt—that an infectious agent may cause BL, a B cell lymphoma highly prevalent among children in Equatorial Africa. Ever since, newer and newer analytic methods were applied to the field of EBV research, shaping our current views as to the natural history of EBV and the pathogenesis of EBV-associated diseases (for a historical perspective, see Ref. [2]). Furthermore, BL was regarded "as a Rosetta stone for understanding the multistep carcinogenesis," i.e., observations such as EBV and *Plasmodium malariae* infection of children with endemic BL and the discovery of *c - myc* translocations in BL cells influenced thinking as to the development of other neoplasms, too [3]. De Thé et al. referred in their paper to a bilingual text, carved in three scripts into a rock stele that was found in the Nile Delta near the town of Rosetta (Rashid); that text—a new research tool, if you wish—was instrumental for the decipherment of Egyptian hieroglyphs by Jean-François Champollion, an achievement that allowed the translation of Ancient Egyptian texts and facilitated the understanding of Egyptian culture and civilization [4]. The data gained by the application of molecular biological methods combined with the applications of up-to-date immunological and cytogenetic methods as well as in vitro and in vivo models of EBV research may offer new solutions to unresolved problems of the EBV field. Some of the hot topics and alternative scenarios as to the viral life cycle, latency, and EBV-associated diseases are overviewed in Chapter 1 of this volume, in the light of the most recent findings, by Janos Minarovits and Hans Helmut Niller. This introductory chapter is followed by typical *Methods* chapters written by experts of the respective areas. Hans Helmut Niller and Georg Bauer give a description of the immunological and molecular methods used in EBV diagnostics (Chapter 2). It is not easy to investigate in vivo EBV infection of B lymphocytes and epithelial cells, the major cell types targeted by EBV. The use of in vitro models facilitates, however, the study of EBV–host cell interactions. Such models include the establishment of "immortalized" lymphoblastoid cell lines by EBV infection of human B lymphocytes, as presented by Noémi Nagy (Chapter 3), and the use of organotypic cultures for the analysis of EBV–epithelial cell interactions, as described thoroughly by Rachel M. Temple, Craig Meyers, and Clare E. Sample (Chapter 4). Identification of the interacting viral and cellular proteins is indispensable for the understanding of interrelationships between EBV and its host cells. In Chapter 5 , Anna A. Georges and Lori Frappier guide us how to use affinity purification- mass

spectroscopy methods for identifying protein–protein interactions in EBV-infected cells. Certain latent EBV proteins influence the nuclear architecture of host cells. Hans Knecht and Sabine May elaborated a spectacular method for the characterization—in three dimensions—of nuclear architecture. They demonstrate how to use 3D Telomere FISH (fluorescent in situ hybridization) to detect nuclear changes, including the alterations of chromosomal ends, induced by LMP1 (latent membrane protein 1, a viral oncoprotein) in Hodgkin lymphoma cells (Chapter 6). Next-generation sequencing methods allow the detailed analysis of transcript structure and abundance in EBV-infected cells. In Chapter 7 , Tina O'Grady, Melody Baddoo, and Erik K. Flemington outline the use of high-throughput RNA sequencing for the analysis of EBV transcription and guide the reader regarding the application of informatics tools for the analysis and visualization of sequence data. Two other approaches, quantitative polymerase chain reaction (qPCR) following conventional RNA isolation and nuclear run-on assay that are suitable for the study of viral promoter activity, are described in Chapter 8 by Kálmán Szenthe and Ferenc Bánáti. In addition to mRNAs, the EBV genome also encodes nontranslated viral microRNAs that modulate the level of both viral and cellular mRNAs and proteins. Furthermore, EBV latency products may alter the level of cellular microRNAs as well. Accordingly, the analysis of viral and cellular microRNAs, the topic of Chapter 9 written by Rebecca L. Skalsky, is of primary importance in the characterization of EBV-infected cells. MicroRNA s and other biomolecules are packaged into exosomes, small lipid vesicles involved in intercellular communication. EBV-infected cells use exosomes for information transfer as well, and the methods for exosome isolation and characterization as well as their functional analysis are detailed in Chapters 10 and 11 by Gulfaraz Khan and Waqar Ahmed, and Gulfaraz Khan and Pretty S. Philip, respectively. Regarding the methods used to study viral DNA, in Chapter 12 Ferenc Bánáti, Anita Koroknai, and Kálmán Szenthe describe how the clonality of a cell population carrying latent EBV episomes can be inferred from the "classical" terminal repeat analysis of the viral genome, whereas Chapter 13 , by Kálmán Szenthe and Ferenc Bánáti, deals with the application of sequencing for the characterization of viral promoters and coding regions. Similarly to cellular promoters, the activity of latent and lytic EBV promoters is also regulated by the binding of viral and cellular regulatory proteins and by epigenetic mechanisms. In Chapter 14 , Anja Godfrey, Sharada Ramasubramanyan, and Alison J. Sinclair demonstrate the use of ChIP-Seq method (chromatin precipitation coupled to DNA sequencing) for the analysis of Zta–DNA interactions. Zta, also called ZEBRA, is an immediate early protein switching on lytic (productive) EBV replication, and there are Zta binding sites both in the viral and in the cellular genome. Host cell phenotype-dependent deposition of epigenetic marks, including DNA methylation and histone modifications, determines the epigenotypes of latent EBV episomes and the activity of the latency promoters. In a detailed protocol, Daniel Salamon describes the use of bisulfite sequencing for the analysis of cytosine

methylation in EBV DNA sequences and lists thoroughly the important steps and caveats of bisulfite modification and PCR amplification (Chapter 15), whereas in Chapter 16 Ferenc Bánáti and Kálmán Szenthe outline how chromatin immunoprecipitation using specific antibodies directed to distinct histone modifications can be applied for the characterization of viral epigenotypes. In vivo experimental models may help to gain insight into important aspects of the EBV life cycle and into the pathogenesis of EBV-associated diseases that are difficult to study in EBV-infected humans . In Chapter 17 , Frank Heuts and Noemi Nagy describe how newborn immunodeficient mice transplanted with human hematopoietic stem cells can be used for the study of immune interactions that occur during EBV infection, whereas in Chapter 18 Ken-Ichi Imadome and Shigeyoshi Fujiwara provide detailed protocols for the preparation and EBV infection of humanized mice and for the monitoring of virological and immunological consequences of the infection. They also describe the development of EBV-associated lymphoproliferative disease in such mice. Finally, Lauren P. McLaughlin, Stephen Gottschalk, Cliona M. Rooney, and Catherine M. Bollard describe, in Chapter 19 , how immunological, virological, tissue culture, and molecular methods can be combined to yield GMP (Good Manufacturing Practice)-compliant EBV-specific T cells for the immunotherapy of EBV-associated post-transplant lymphoproliferative disease (PTLD).

References

1. Epstein A (2015) Why and how Epstein-Barr virus was discovered 50 years ago. Curr Top Microbiol Immunol 390(Pt 1):3–15

2. Klein G (2015) Tumor associations of EBV–Historical Perspectives. Curr Top Microbiol Immunol 390(Pt 1):17–22

3. de Thé G, Gazzolo L, Gessain A (1985) Viruses as risk factors or causes of human leukaemias and lymphomas? Leuk Res. 9(6):691–696

4. Robinson A (2012) Cracking the Egyptian code: the revolutionary life of Jean-François Champollion. Oxford University Press

Janos Minarovits
Hans Helmut Niller
Regensburg, Germany, Budapest, Hungary

Contents

Contributors

Waqar Ahmed
Department of Microbiology and Immunology, College of Medicine and Health Sciences, United Arab Emirates University, Al Ain, United Arab Emirates

Melody Baddoo
Department of Pathology, Tulane University School of Medicine, New Orleans, LA, USA
Tulane Cancer Center, New Orleans, LA, USA

Ferenc Bánáti
RT-Europe Nonprofit Research Ltd., Mosonmagyaróvár, Hungary

Georg Bauer
Institute of Virology, University Medical Centre Freiburg, Freiburg im Breisgau, Germany

Catherine M. Bollard
Center for Cancer and Immunology Research, Children's National Medical Center, Washington, DC, USA
The George Washington University, Washington, DC, USA

Erik K. Flemington
Department of Pathology, Tulane University School of Medicine, New Orleans, LA, USA
Tulane Cancer Center, New Orleans, LA, USA

Lori Frappier
Department of Molecular Genetics, University of Toronto, Toronto, ON, Canada

Shigeyoshi Fujiwara
Department of Allergy and Clinical Immunology, National Research Institute for Child Health and Development, Setagaya-ku, Tokyo, Japan
Division of Hematology and Rheumatology, Department of Medicine, Nihon University School of Medicine, Itabashi-ku, Tokyo, Japan

Anna A. Georges

Department of Molecular Genetics, University of Toronto, Toronto, ON, Canada

Anja Godfrey
School of Life Sciences, University of Sussex, Brighton, UK

Stephen Gottschalk
Texas Children's Cancer Center, Texas Children's Hospital, Baylor College of Medicine, Houston, TX, USA

Frank Heuts
Institute of Immunity and Transplantation, University College London Medical School, London, UK

Ken-Ichi Imadome
Division of Advanced Medicine for Virus Infections, National Research Institute for Child Health and Development, Setagaya-ku, Tokyo, Japan

Gulfaraz Khan
Department of Microbiology and Immunology, College of Medicine and Health Sciences, United Arab Emirates University, Al Ain, United Arab Emirates

Hans Knecht
Division of Hematology, Department of Medicine, Jewish General Hospital, McGill University, Montréal, QC, Canada

Anita Koroknai
Department of Retroviruses, National Center for Epidemiology, Budapest, Hungary

Sabine Mai
Genomic Center for Cancer Research and Diagnosis, Cell Biology, University of Manitoba, CancerCare Manitoba, Winnipeg, MB, Canada

Lauren P. McLaughlin
Department of Hematology/Oncology, Children's National Medical Center, Washington, DC, USA
The George Washington University, Washington, DC, USA

Craig Meyers
Department of Microbiology and Immunology, The Pennsylvania State University College of Medicine, Hershey, PA, USA

The Pennsylvania State Hershey Cancer Institute, Hershey, PA, USA

Janos Minarovits
Department of Oral Biology and Experimental Dental Research, Faculty of Dentistry, University of Szeged, Szeged, Hungary

Noemi Nagy
Department of Microbiology, Tumor and Cell Biology, Karolinska Institutet, Stockholm, Sweden

Hans Helmut Niller
Institute of Medical Microbiology and Hygiene, University of Regensburg, Regensburg, Germany

Tina O'Grady
Department of Pathology, Tulane University School of Medicine, New Orleans, LA, USA

Pretty S. Philip
Department of Microbiology and Immunology, College of Medicine and Health Sciences, United Arab Emirates University, Al Ain, United Arab Emirates

Sharada Ramasubramanyan
V ClinBio Labs Pvt Ltd., Central Research Facility, Sri Ramachandra University, Chennai, India

Cliona M. Rooney
Center for Cell and Gene Therapy, Texas Children's Hospital, Houston Methodist Hospital, Baylor College of Medicine, Houston, TX, USA

Daniel Salamon
Department of Microbiology, Tumor and Cell Biology, Karolinska Institutet, Stockholm, Sweden

Clare E. Sample
Department of Microbiology and Immunology, The Pennsylvania State University College of Medicine, Hershey, PA, USA
The Pennsylvania State Hershey Cancer Institute, Hershey, PA, USA

Alison J. Sinclair

School of Life sciences, University of Sussex, Brighton, UK

Rebecca L. Skalsky
Vaccine and Gene Therapy Institute, Oregon Health and Science University, Beaverton, OR, USA

Kálmán Szenthe
RT-Europe Nonprofit Research Ltd., Mosonmagyaróvár, Hungary

Rachel M. Temple
Department of Microbiology and Immunology, Geisel School of Medicine at Dartmouth, Hanover, NH, USA
Department of Microbiology and Immunology, The Pennsylvania State University College of Medicine, Hershey, PA, USA

1. Current Trends and Alternative Scenarios in EBV Research

Janos Minarovits[1]✉ and Hans Helmut Niller[2]✉

(1) Faculty of Dentistry, Department of Oral Biology and Experimental Dental Research, University of Szeged, Tisza Lajos krt. 64, H-6720 Szeged, Hungary
(2) Institute of Medical Microbiology and Hygiene, University of Regensburg, D-93053 Regensburg, Germany

✉ **Janos Minarovits (Corresponding author)**
Email: minimicrobi@hotmail.com

✉ **Hans Helmut Niller**
Email: Hans-Helmut.Niller@klinik.uni-regensburg.de

Abstract
Epstein-Barr virus (EBV) infection is associated with several distinct hematological and epithelial malignancies, e.g., Burkitt lymphoma, Hodgkin lymphoma, nasopharyngeal carcinoma, gastric carcinoma, and others. The association with several malignant tumors of local and worldwide distribution makes EBV one of the most important tumor viruses. Furthermore, because EBV can cause posttransplant lymphoproliferative disease, transplant medicine has to deal with EBV as a major pathogenic virus second only to cytomegalovirus. In this review, we summarize briefly the natural history of EBV infection and outline some of the recent advances in the pathogenesis of the major EBV-associated neoplasms. We present alternative scenarios and discuss them in the light of most recent experimental data. Emerging research areas including EBV-induced patho-epigenetic alterations in host cells and the putative role of exosome-mediated information transfer in disease development are also within the scope of this review. This book contains an in-depth description of a series of modern methodologies used in EBV research. In this introductory chapter, we thoroughly refer

to the applications of these methods and demonstrate how they contributed to the understanding of EBV-host cell interactions. The data gathered using recent technological advancements in molecular biology and immunology as well as the application of sophisticated in vitro and in vivo experimental models certainly provided deep and novel insights into the pathogenetic mechanisms of EBV infection and EBV-associated tumorigenesis. Furthermore, the development of adoptive T cell immunotherapy has provided a novel approach to the therapy of viral disease in transplant medicine and hematology.

1 Introduction

The virus particles of Epstein-Barr virus (EBV), a human herpesvirus infecting the majority of the population, were discovered by electron microscopy 52 years ago, in the suspension culture of a Burkitt lymphoma-derived cell line [1]. Last year, in connection with the 50th anniversary of the discovery, a series of reviews appeared, dealing with the natural history of EBV, the first human "tumor virus," and the many diseases associated with EBV infection [2, 3]. For this reason, here we wish to give only a brief summary of the basic facts as to the course of EBV infection and its pathologic consequences and focus, in the light of the most recent publications, on some of the emerging new topics and unresolved questions of the field.

2 Epstein-Barr Virus: Basic Facts

Epstein-Barr virus (EBV, also known as human herpesvirus 4) belongs to the *Lymphocryptovirus* genus within the *Gammaherpesvirinae* subfamily of the family *Herpesviridae*. As the name *Lymphocryptovirus* reflects, EBV infects lymphoid cells and "hides," i.e., establishes latency in the B lymphocyte compartment. Latency is a remarkable feature of herpesviruses that are capable to maintain their genomes in host cells for an extended period in the absence of virion production. Similarly to other herpesviruses, the EBV genome packaged into the virion is also a linear double-stranded DNA molecule surrounded by a membrane-coated icosahedral capsid. The prototype B95-8 EBV genome was the first completely sequenced herpesvirus genome [4], and, recently, with the advent of next-generation sequencing, the complete genomes of a series of EBV strains from multiple tumor cell lines, tumor types, and normal infection were determined [5–7] (reviewed by [8]).

EBV is associated with a series of malignant tumors including Burkitt lymphoma (BL), nasopharyngeal carcinoma (NPC) , Hodgkin lymphoma (HL), posttransplant lymphoproliferative disease (PTLD), T/NK cell lymphomas, gastric carcinoma (EBVaGC) , AIDS-associated lymphoma, leiomyosarcoma , and others [9–11]. The expression pattern of viral latent genes in EBV-associated tumor biopsies, in tumor-derived cell lines, and in EBV-infected B cell cultures largely depends on the tumor cell type and on the B cell differentiation status. For a detailed description of the different latent gene expression patterns, we refer to recent reviews [11, 12]. Traditionally, three latency classes I to III and sometimes latency type 0 ("zero") are discerned, accompanied by a few latency types which are situated in between the classical three latency types. In short, latency type 0 in memory B cells is rather restricted to the expression of the EBER RNAs only, possibly accompanied by expression of the BART RNAs or LMP2A in addition, and occasional EBNA1 expression, which is needed for viral genome maintenance when a memory cell is dividing. Latency type I is found in BL cells, with the expression of the EBERs, EBNA1 by transcription from the Q promoter (Qp), and the BART mRNAs and microRNAs . Additional variant expression of latent membrane protein (LMP) 2A is found in EBVaGC. Latency type II, with the additional expression of the LMPs 1 and 2, is found in Hodgkin lymphoma and in nasopharyngeal carcinoma (NPC) with a variable expression of LMP1 . The expression of all viral latent gene products including the BHRF1 microRNAs is found in EBV-transformed lymphoblastoid cell lines (LCL), in most early-onset PTLD cases and also in leiomyosarcomas of immune-suppressed patients. In this case, all EBNA proteins are expressed by transcription from the C promoter . This gene expression pattern has been termed "latency type III" or "Cp-on latency." This condition is also referred to as "the growth program" [13].

Besides the classical latent gene products, there are also specific gene products normally attributed to the lytic viral replication cycle which are regularly expressed in tumor tissue. For example, in NPC and EBVaGC , expression of the BARF1 protein is regularly found [14–16] (reviewed by [17]). However, there is more to be found among lytic genes which are regularly expressed in tumor tissue. Whole genome analysis of RNA-seq data has the power to uncover previously overlooked or hidden gene expression patterns, novel genes, and splice junctions, but also the contamination of cell lines [18–24]. A recent analysis of RNA-seq data of a series of EBVaGC revealed the expression of the BNLF2A reading frame in nearly half of all EBVaGC [25, 26]. BNLF2A codes for an inhibitor of MHC class I-TAP-mediated antigenic peptide transport and thereby provides immune evasion properties to latently infected tumor cells [27]. Furthermore, an RNA-seq analysis of NPC tissue and the NPC cell line C666.1 showed diverse latency gene expression patterns besides latency type II and a considerable amount of lytic regulatory gene expression [28].

Besides its classical role as a viral transcription and replication factor binding to

oriP, latent protein EBNA1 is also expressed in the lytic viral infection mode and has manifold cellular impact. Affinity purification coupled with mass spectrometry (AP-MS) and tandem affinity purification (TAP-tagging) approaches have successfully been used to uncover the interaction of viral proteins with its cellular binding partners [29]. Through its direct interaction with the ubiquitin-specific protease (USP) 7 (also termed HAUSP), EBNA1 interferes with p53 and Mdm2 binding to the same binding pocket on USP7 in vitro [30, 31]. Thus, EBNA1 may contribute antiapoptotic functions to tumorigenesis in NPC or EBVaGC by lowering p53 levels in response to DNA damage [32, 33]. By disrupting PML nuclear bodies, similar to other herpesviruses, EBNA1 may contribute to the reactivation of the lytic viral replication cycle [34]. The situation is complex, however, because in epithelial cell lines EBNA1 upregulated a set of cellular microRNAs , including let-7a that represses EBV reactivation [35].

PML disruption through EBNA1 is mediated by the cellular kinase CK2 [30, 36]. Because the loss of PML proteins or nuclear bodies also impairs apoptosis [37], it is interesting that latent EBNA1 has been found to induce the loss of PML proteins in NPC and EBVaGC cells. Thereby, EBNA1 may contribute additional antiapoptotic functions to the establishment of EBV-associated malignancies [32, 33]. A further interaction partner of EBNA1 which is relevant to antiapoptosis and EBV-associated tumorigenesis is the proapoptotic tumor suppressor protein Nm23-H1, a suppressor of metastasis whose functions are suppressed by EBNA1 [38]. By binding and activating the promoter of the gene for apoptosis inhibitor survivin, EBNA1 contributes a further mechanism to antiapoptosis [39].

3 Establishment of EBV Latency in Memory B Cells: Alternative Scenarios

It has been well documented that latent EBV genomes reside mainly in isotype-switched memory B cells in the peripheral blood (reviewed by [40]). There are, however, several possibilities for the virus to reach the memory B cell compartment. The traditional view, supported by several lines of evidence, suggests that the virus infects and activates naïve tonsillar B cells which traverse the germinal center (GC) , where they proliferate, undergo immunoglobulin gene rearrangements, accumulate mutations, and change their gene expression program and phenotype several times, in parallel with successive alterations in the activity of the EBV latency promoters. At the end of the differentiation process, the memory B cells would contain almost silent EBV episomes [13]. How the activity of the latent viral promoters is regulated in parallel with the modulation of the B cell phenotype in the GC remains to be established. In a recent study, Heuts et al. used EBV-infected humanized mice to analyze the activity of the major latent EBV promoters in B cells after primary infection. They observed that in

addition to the activity of the C promoter (Cp), where the primary transcripts for six Epstein-Barr virus nuclear antigens (EBNAs) are initiated, in activated, proliferating B cells the activity of an alternative promoter (Q promoter, Qp) could also be detected. Only transcripts coding for a single nuclear antigen, EBNA1 , are initiated at Qp that is typically used in lymphoma and carcinoma cells (BL, HL, NPC) and B cells with a non-activated phenotype. Qp usage could not be detected, however, in CD4$^+$ T cell-depleted mice. These data suggested that interaction of helper T cells with EBV-infected B cells may induce a switch in EBV promoter usage in vivo, which may contribute to a reprogramming of viral gene expression during primary infection [41].

Another scenario is also based on the in vitro-infection of naïve B lymphocytes, but claims that polyclonally activated B cells may accumulate Ig gene mutations and acquire Ig memory genotypes via a GC -independent pathway [42]. An analysis using microdissection of lymphoid tissue obtained from patients undergoing infectious mononucleosis showed that the virus is actually able to infect memory B cells directly [43, 44]. In a humanized mouse model of Rag2$^{-/-}$ γc$^{-/-}$ mice, i.e., *Rag2/Il2rg* compound mutant animals exhibiting T cell, B cell, and NK cell immunodeficiencies, Cocco et al. studied EBV infection of the lymphoid organs that developed following transplantation of human CD34+ cord blood cells. They observed that EBV-infected cells expressing distinct combinations of viral latency products—as assessed by in situ hybridization and immunochemistry—were scattered both in GCs and in areas with no GC structure [45]. Others found evidence for EBV infection of extrafollicular B cells in tonsils of infectious mononucleosis patients undergoing primary infection [46], and a recent study on memory B cell reconstitution following allogeneic hematopoietic stem cell transplantation also points to the possibility of extrafollicular EBV infection, i.e., the infection of mature donor B cells that were either transferred in the stem cell graft or differentiated from donor stem cells in the host organism [47]. Thus, in infectious mononucleosis, memory B cells are directly infected by EBV. However, under experimental conditions, in animal models, and under certain clinical conditions, there might be more than one route for EBV to access the memory B cell compartment.

4 The EBV Lytic Replication Cycle: New Insights

Latent EBV infection is characterized by a restricted, host cell phenotype-dependent expression of the viral genes. The latent RNAs and proteins encoded by the EBV genome modulate the epigenotype, gene expression pattern , and phenotype of the host cells (reviewed by [48]). In contrast, all of the viral genes are transcribed during lytic or productive EBV replication, due to the successive activation of immediate early, early, and late EBV promoters. In parallel, expression of BGLF5 , a protein encoded by one of the lytic cycle genes, results in a dramatic decrease, i.e., shutoff, in host protein synthesis [49]. In spite of this observation, a recent transcriptome analysis revealed that

expression of the immediate early protein Zta (ZEBRA, BZLF1) , a major transactivator of a subset of EBV genes, had, unexpectedly, a significant effect on the cellular transcriptome: it upregulated the transcription of 1679 cellular genes and reduced the expression of 584. Among the upregulated genes were 190 genes involved in cell morphogenesis, suggesting that they may contribute to the assembly and egress of the virions. Thus, EBV may reprogram the cellular genome to utilize cellular mechanisms during productive replication. Analysis of cellular Zta binding sites revealed that they are located distal to the regulated promoters, implicating that they may act by reorganizing the 3D structure of the cellular genome [50].

Although the association of EBV with neoplasms of epithelial origin such as NPC and EBVaGC is well documented, the lack of a suitable in vitro experimental model hindered, for a long time, the analysis of the viral life cycle in the epithelial cell compartment. Recently, Temple et al. established organotypic raft cultures of primary human keratinocytes derived from either gingiva or tonsil tissue and observed productive, lytic EBV replication in the suprabasal layers of the stratified epithelium infected by the virus in vitro. However, latently infected cells could not be observed, and EBV did not induce epithelial cell proliferation in the raft cultures. These data suggested that oral mucosal epithelial cells may contribute significantly to the production of EBV in high levels and play an important role in the spread of the virus, via saliva, in the host population [51].

5 Endemic Burkitt Lymphoma and Sporadic Burkitt Lymphoma: Alternative Pathogenic Pathways

Although deregulated expression of *C-MYC(MYC)* appears to be indispensable in the molecular pathogenesis of Burkitt lymphoma (BL), the strong association of latent EBV genomes with endemic BL cases (eBL) suggested that the virus is an important factor in the generation of eBL, and direct transformation by EBV was implicated in the pathogenesis of other lymphomas as well [52, 53]. However, chronic infection by various microbial species may also affect lymphomagenesis indirectly, by continuous antigen stimulation resulting in clonal B cell expansion [52]. A recent next-generation sequencing (NGS) study revealed that the mutation pattern of cellular genes and the somatic hypermutation status of the immunoglobulin genes in eBL differ from the patterns observed in sporadic Burkitt lymphoma (sBL) [54]. Only a fraction of sBL cases is associated with EBV, and it was demonstrated earlier that mutations of the *TCF3* and *ID3* genes may activate, in an intrinsic way, the B cell receptor (BCR) pathway in sBL cells [55–57]. *TCF3* codes for a transcription factor activating a pro-survival pathway, whereas *ID3* encodes a negative regulator of TCF3. This antigen-independent, "tonic" form of BCR activation may facilitate sBL development. In

contrast, by sequencing of immunoglobulin heavy chain variable region genes (*IGHV* genes), Amato et al. found molecular signatures reflecting an active somatic hypermutation process in eBL, but much less in sBL [54]. Thus, extrinsic antigenic signaling may play a role in the pathogenesis of eBL, an idea supported by the observed intraclonal diversity of eBL and the detection of replacement mutations that probably remodeled the structure of immunoglobulins [54]. Amato et al. argued that extrinsic stimulation by antigens of *Plasmodium falciparum* malaria in BL-endemic areas may facilitate clonal outgrowth of memory B cells expressing distinct immunoglobulin receptors . They also speculated—based on the frequent use of the autoreactive antibody-encoding VH4-34 gene by BL cells—that in addition to *Plasmodium falciparum* antigens, autoreactive antigens may also play a role in the pathogenesis of BL [54]. Sequencing of PCR amplified *IGHV* genes in an earlier study also revealed higher mutation rates in eBL versus sBL or EBV-positive BL versus EBV-negative BL samples [58]. Based on their findings, Bellan et al. speculated that EBV-negative BLs may originate from early centroblasts, whereas EBV-positive BLs may originate either from late germinal center B cells on the pathway of differentiation to memory B cells or from memory B cells [58]. This is in accordance with earlier models for the pathogenesis of endemic BL, where the strong antigenic drive provided by malaria or alternatively also by other parasites or viral infections has already been pointed out to be a crucial condition [59–64].

6 Endemic Burkitt Lymphoma: Pathogenesis via Multiple Interacting Risk Factors?

Based on its geographical association with malaria and the presence of EBV genomes in virtually 100 % of tumors, endemic Burkitt lymphoma was traditionally depicted as a consequence of sustained B cell proliferation elicited by these pathogens [53, 65, 66]. Both *Plasmodium falciparum* and EBV are capable to interact with memory B cells, and both pathogens may induce the enzymatic machinery involved in class switch recombination and somatic hypermutation of B cells [67–74]. Occasional off target action of activation-induced cytidine deaminase (AID) as well as RAG1 and RAG2, the products of recombination activating genes 1 and 2, may result in DNA breakage, genetic instability, and chromosomal translocations leading to deregulated expression of *MYC*, a gene coding for a nuclear protein that drives the proliferation of BL cells, the putative descendants of centroblasts located to the dark zone of the germinal center [74–77]. Although *MYC* is not expressed in the bulk of germinal center cells, its expression is required for the cyclic reentry of B cells from the light zone into the dark zone of the germinal center where B cells undergo the selection process adapting their immunoglobulin genes through somatic hypermutation . Inhibition of *MYC* expression

led to a collapse of germinal centers. Thus, the cyclically regulated expression of *MYC* is of utmost importance for a physiological germinal center reaction [78]. A recent epidemiologic study performed using blood samples collected in western Kenya indicated that *Plasmodium falciparum* and EBV may act in concert to upregulate AID expression in peripheral blood mononuclear cells of children living in malaria holoendemic areas [79]. In addition to AID, RAG1, and RAG2, EBV also induces DNA polymerase η, an error-prone enzyme involved in short-patch DNA synthesis that may play a role in the generation of oncogene mutations in B cells [69, 80]. Interestingly, the EBV early lytic cycle protein BALF2 and its homolugue, the herpes simplex virus protein ICP8 are members of the family of DDE/RNAse H-like fold recombinases which also include RAG1 [81].

Although there is a single example, based on histological examination, for the occurrence of a Burkitt-like lymphoma in a mouse immunized with *Plasmodium yoelii* [82] that could be attributed to the persistent immune stimulation by the malaria parasite per se, eBL is usually regarded as a disease of polymicrobial etiology [66, 70, 83]. In addition to the synergistic action of Epstein-Barr virus and *Plasmodium falciparum* malaria, infection with arboviruses, including the potentially oncogenic chikungunya virus , may also play a role in the genesis of eBL, especially in situations when unexpected shifts were observed in space-time case clusters of the disease [84–86]. Furthermore, it was also suggested that tumor promoters and immunomodulators present in the extracts of *Euphorbia tirucalli* could induce *MYC* translocation , productive EBV replication, and may facilitate B cell transformation (reviewed by [86, 87]). There is an overlap regarding the geographic distribution of *E. tirucalli* and the "lymphoma belt," i.e., the areas where BL is endemic in Africa. *E. tirucalli* extracts are used as traditional herbal remedy, and the phorbol esters produced by the plant are also secreted into the soil [88]. Using FISH, Mannucci et al. observed chromosome 8 polysomy in 17 % of cells of an EBV-immortalized LCL and a freshly established cord blood-derived EBV-positive cell line treated with *E. tirucalli* plant extracts. *MYC* is located to chromosome 8, and treatment with the plant extract upregulated the expression of *MYC* as well as that of *BCL2* , although there were no chromosome abnormalities affecting chromosome 18 carrying the latter gene that encodes an antiapoptotic protein. In parallel, upregulation of certain EBV lytic cycle proteins (BZLF1; early antigen, EA) and latency proteins (LMP1 , EBNA1 , EBNA2) was detected as well. All of these changes may contribute to the pathogenesis of eBL [89].

In addition to environmental factors, genetic predisposition may also influence the susceptibility of children to eBL. Sequence polymorphisms of cytokine genes may affect the levels of cytokines affecting tumor growth. In pediatric BL patients from Southeast Brazil, distinct genotypes at position-1082 of the *IL10* gene, coding for a regulatory cytokine, were more frequent, compared to healthy individuals from the same geographic region; carriers of genotypes associated with higher IL-10 production had a

worse event-free survival [90]. In contrast, the same IL-10 promoter haplotypes or an IL-6 promoter polymorphism were not associated with an elevated risk of eBL in a study in western Kenya [91].

Heterozygotes carrying a single copy of the mutant hemoglobin β gene called the sickle cell gene usually do not have symptoms of sickle cell disease and are protected against malaria . Because *Plasmodium falciparum* infection is an important risk factor of eBL, it was suggested that heterozygosity (HbAS, sickle cell trait) may also protect against the development of eBL [92]. Mulama et al. observed, however, that there was no significant difference in HbAS frequency between children with eBL and the corresponding controls, indicating that protection against clinical malaria or high-density parasitemia may not curb lymphomagenesis [93]. Further studies may reveal the potential influence of additional genetic traits on the pathogenesis of eBL.

7 EBNA2 -Driven LCL-Like Cells Are Dispensable for the Genesis of Endemic Burkitt Lymphoma (eBL): The Alternative Model

"Classical" scenarios proposed for the pathogenesis of eBL, a lymphoma that is 100 % EBV positive, argued that either an EBV-immortalized, LCL-like B cell undergoes *myc* translocation or an overstimulated B cell with a translocated *myc* gene is infected by EBV [59, 94]. These pathogenic pathways rely either on severe T cell suppression to accommodate the latency type III lymphoblasts or on a latency promoter switch (from Cp to Qp) to downregulate the expression of immunogenic latency proteins. Substantial reorganization of the cellular chromatin may also be a precondition for the accompanying phenotypic switch of the cell. We elaborated an alternative molecular model which avoids these difficulties [63, 64]. We proposed that the precursor of the eBL cell is an EBV-infected, antigen-stimulated memory B cell, participating in the germinal center reaction. We argued that the binding of MYC, a nuclear matrix - attachment factor present in increased amounts in the latency type I B cell after the *Ig-MYC* translocation, may help to maintain the latent viral genomes in the cell by binding to the EBV episomes and anchoring them to the nuclear matrix. In parallel, the type I EBV latency products expressed may counteract the strong proapoptotic effect of *myc*. As a matter of fact, both EBNA1 and the non-translated viral RNAs, including the EBERs and certain EBV-encoded microRNAs that are expressed in type I EBV latency, have antiapoptotic functions (reviewed by [95]). BL might develop as a result of the clonal proliferation of the surviving cell carrying a *myc* translocation and—based on terminal repeat analysis—monoclonal EBV genomes [62–64, 96].

We think that—according to Sir Karl Popper's criteria—our molecular model for the pathogenesis of endemic BL, proposed more than a decade ago [62–64, 96], has not

been falsified. Actually, as far as we know, it has been preferentially supported by the experimental data which have been created since then. Figure 1 shows the essential features of our eBL model, i.e., the rescue of an apoptosis- bound B cell which has undergone a *MYC*-translocation in a germinal center reaction through antiapoptotic functions provided by a latent EBV genome.
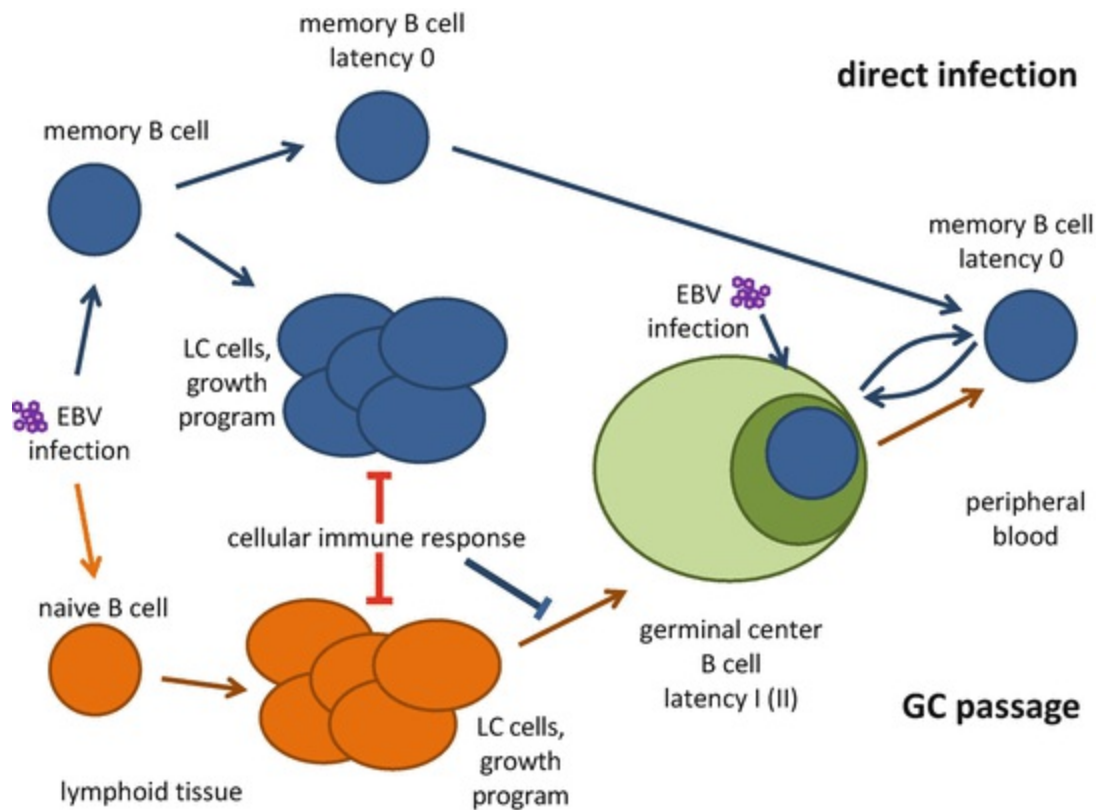
Fig. 1 Pathogenesis of endemic Burkitt lymphoma. Germinal center passage model (*below*, *brown arrows*; [13]): upon EBV infection of naïve B cells in the tonsils, they become growth-transformed cells exhibiting a viral latency type III gene expression pattern (growth program). Some cells which are not extinguished by the cellular immune response undergo a germinal center passage, where they switch from the growth program to latency types I or II, mediated either by a promoter switch from Cp to Qp or by deletion of the EBNA2 reading frame [103], upon which they end up as memory B cells [13]. Direct GC infection model (*above*, *blue arrows*; [44, 62]): upon EBV infection of memory or germinal center B cells in the tonsils, the incoming viral genomes are circularized and enter latency types 0, I, or II. All naïve or memory B cells which upon infection enter the EBV growth program are extinguished by the cellular immune response. B cells having deleted the EBNA2-reading frame from their viral genomes may enter latency again and thereby survive the immune response. EBV-infected cells exhibiting latency type III generally avoid GC reactions

It was observed that the presence of EBER -positive cells in a germinal center reaction is a rare event [9, 60, 61, 97]. Furthermore, the viral latency type III program has not been found to be compatible with a regular germinal center reaction [61, 97–102]. In malaria patients, however, the probability of a latently EBV-infected blood B cell, light zone B cell, or memory B cell which express latency types I or II to enter or reenter a GC reaction is increased. By binding to its recognition site within the locus control region of the latent EBV genome, the *myc* oncoprotein increases the probability

of viral antiapoptotic functions, or viral factors that induce cellular antiapoptotic functions, to be expressed. Thus, latency class 0 or I EBV infection of a B cell which undergoes a *MYC*-translocation in a GC reaction increases the probability of a "crashed" B cell to survive both the strong proapoptotic security measures within the germinal center and the strong proapoptotic drive of the translocated *myc* gene [62–64]. The lymphoblastoid transformation of B cells expressing the EBV growth program is expendable for the pathogenesis of endemic BL [103], but not debarred from it, because it increases the overall viral load. In principle, even the antiapoptotic role which EBV plays for the pathogenesis of endemic BL is expendable: it may be replaced by additional mutations in EBV-negative sporadic BLs , such as *TCF3* and *ID3* mutations [55–57]. Because oncogene translocations occur in physiological germinal center reactions as molecular accidents with low frequency [104–106], stochastic rules permit that even the exaggerated antigenic stimulus for B cells is expendable in sporadic cases. The complementary contributions of malaria and EBV are therefore just increasing, however considerably, the probability of a *myc*-translocation to happen and the probability of a crashed B cell to survive and become the founder cell of a Burkitt lymphoma, respectively.

When our antiapoptosis model for the pathogenesis of eBL has first been established [62–64, 96], a blind eye was turned to it by some proponents of the transformation model [107], and only part of it [108] has been highlighted in a one-sided debate [109]. It has taken some time to have "the alternative pathogenetic pathways" concept [63] discussed on a level playing field, with the focus shifted from transformation to antiapoptosis, regrettably, however, mostly without giving reference, e.g., [9, 110–114]. Although the role of EBV in the origin of eBL has been repetitively claimed over the years to be unclear [107, 115], our eBL model has stood the test of time (for greater detail on the establishment of viral latency, see [11, 116]). Due to its predictive power and plausibility, it has not come as a surprise that a slow adaptation to our eBL model took place [113], and more recently it has just been taken for granted that the role of EBV is mainly to provide antiapoptotic functions to a *myc*-translocated B cell to survive the GC reaction, with transformation or the growth program not being mentioned at all anymore [117].

We think that our alternative molecular model is compatible with a role for multiple risk factors in the pathogenesis of eBL. We propose that during primary EBV infection in BL-endemic areas, memory B cells or outgoing germinal center B cells are directly infected by EBV, as observed in certain infectious mononucleosis patients [43, 44]. We speculate that disruption of the normal architecture of the lymphoid organs by malaria infection [118] may facilitate direct EBV infection of memory B cells or GC B cells as well as EBV infection of extrafollicular B cells. It may facilitate the reentry of EBV-infected B cells into germinal centers, too. The antigenic stimulus provided for B cells by *Plasmodium falciparum*, parasites other than plasmodium [60, 61, 74], viruses like

HIV in the early phase of infection [59, 119], arboviruses [84–86], or EBV increases the frequency of germinal center reactions and thereby the probability of molecular accidents, i.e., the translocation of *MYC* and other oncogenes.

During the development of eBL, in parallel with the B cell antigenic drive, the cellular immune response is compromised by plasmodium or HIV infection; as a consequence, there is an increase in the number of latently EBV-infected memory cells [74, 120]. In vivo experimental models revealed that plasmodium infection may suppress the maturation and modulate the function of dendritic cells, causing immune hyporesponsiveness [121]. In addition, PfMIF (*P. falciparum* MIF), an ortholog of human MIF (macrophage migration inhibitory factor), could be detected in sera of malaria patients, and the corresponding recombinant *P. berghei* MIF (PbMIF) modulated inflammatory cytokine production and decreased CD4+ T cell recall responses in experimental animals [122]. Furthermore, White et al. observed that *Plasmodium yoelii* coinfection of mice reduced the CD8+ T cell response to heterologous *Listeria monocytogenes* infection [123]. Thus, plasmodium infection may interfere at several points with the adaptive immune response.

The various combinations of B cell antigenic drive and immune suppression may result in the development of EBV-positive lymphomas with distinct cellular phenotypes and viral gene expression patterns. Whereas eBL, corresponding to EBV latency type I, is the predominant lymphoma type in malaria endemic areas, proliferation of EBV-transformed latency class III B cells forms the basis of most cases of early-onset posttransplant lymphoproliferative disease (PTLD) developing in transplant patients undergoing iatrogenic immune suppression (reviewed by [124, 125]). In the latter patients, an increase in the number of EBV-infected memory B cells may precede the outgrowth of lymphoma cells [126]. PTLDs may be first polymorphic, then monomorphic, if immune suppression is continuing [127]. If immune control is restored in time, through the reduction of immunosuppressive treatment for transplant patients, polymorphic B cells expressing the growth program are extinguished, as long as they have not undergone further mutations which turn them into malignant clones [128].

In patients with acquired immunodeficiency syndrome (AIDS), HIV- associated cytopathic effects result in the destruction of CD4+ memory T cells, and regenerative processes only partially compensate for the loss (reviewed by [129]). The decline in CD4+ T cell number and the dysregulation of the immune response open the way for opportunistic infections and facilitate the development of opportunistic, virus-associated neoplasms, including EBV-positive lymphomas. In contrast to endemic BLs, PTLDs arising in transplant patients and EBV-positive AIDS-associated B cell lymphomas represent a diverse group of tumors which represent the three major EBV latency types [124, 130, 131]. EBV latency type I was observed in AIDS-associated BL and centroblastic DLBCL (diffuse large B cell lymphoma). EBV frequently coinfects primary effusion lymphomas (PELs) caused by Kaposi's sarcoma-associated

herpesvirus (KSHV); these tumors also belong to EBV latency type I. Type II latency is represented by Hodgkin lymphomas (HLs), and it is remarkable that 100 % of HLs occurring in AIDS patients are EBV positive. Finally, latency type III is characteristic for primary CNS lymphomas developing in the brain, an immuno-privileged site. The immunoblastic type of DLBCL also belongs to type III latency among the EBV-positive, AIDS-associated lymphomas [130, 131]. Thus, immunodeficient states caused by HIV may facilitate the development of a series of EBV-associated B cell lymphoma types, most of which maintain a characteristic pattern of latent EBV gene expression . It is remarkable that the incidence of EBV-positive PTLD is low in early HIV infection, in spite of the fact that both *P. falciparum* and HIV suppress CD4+ T cell recall responses [122, 129].

The composite pattern of the antigenic stimulus for B cells and the suppression of T cell function in the abovementioned clinical conditions, acting either simultaneously or at different times and degrees, certainly influenced the ideas regarding the pathogenesis of eBL [63]. In addition, lytic induction of the EBV replication cycle, e.g., mediated by *Euphorbia tirucalli* or by *P. falciparum* infection, increases the viral load and may affect the number of EBV-positive B cells that are the potential precursors of eBL cells [89, 132].

8 Molecular Pathogenesis of Hodgkin Lymphoma: A Role for LMP1- Induced Genomic Instability

Latent membrane protein 1 (LMP1) is an EBV-encoded oncoprotein capable to cause tumorigenic transformation of rodent cells [133]. LMP1, a pleiotropic regulator activating multiple cellular pathways, is expressed in LCLs immortalized by EBV in vitro and in PTLDs with type III latency phenotype; it can also be detected in the majority of NPCs and in EBV-positive Hodgkin lymphomas (HDs) (reviewed by [134, 135]). Although most studies focused on the signaling activities of LMP1 and their contribution to B cell immortalization, lymphomagenesis, and carcinogenesis, LMP1 may play an important role in the reorganization of the nuclear architecture as well. Lajoie et al. observed that expression of LMP1 from a plasmid construct in the EBV-negative BL line BJAB downregulated the levels of shelterin proteins that protect telomeres from DNA repair mechanisms in mammalian cells and also downregulated the transcription of several genes encoding members of the shelterin protein complex; in parallel, LMP1 expression increased the number of multinucleated cells [136, 137]. The decreased levels of telomere repeat factors (TRF) 1 and 2 and protection of telomere (POT) 1 proteins may result in genomic instability due to an altered 3D nuclear organization of telomeres, formation of telomere aggregates, generation of unprotected short telomeres, and formation of end-to-end telomere fusions of chromosomes

(reviewed by [138]). LMP1 may contribute to the pathogenesis of HL by facilitating the transition from mononuclear Hodgkin cells to multinuclear Reed-Sternberg cells [138, 139]. In addition, as also supported by recent superresolution microscopy analysis, there are distinct changes in the nuclear architecture in therapy refractory versus relapsing HL [138, 140, 141].

9 Patho-epigenetics of EBV-Associated Disease

Recent technical advances have made it possible to sequence, with nucleotide resolution, the entire cellular epigenomes. Thus, complete bisulfite sequence maps of a couple of LCLs [142], one eBL cell line Daudi [143], and a series of eBL tumor tissues [144] have been generated. Furthermore, a whole genome epigenomic analysis of B cells on their way through maturation and differentiation showed that, compared to naïve B cells, a significant loss of methylation takes place in GC B cells and even more in memory B cells. Compared to their normal counterparts, B cell lymphomas frequently acquire methylation changes in genomic regions already undergoing methylation changes during normal B cell differentiation [145].

Compared to normal B cell epigenomes, EBV-transformed LCLs exhibit a massive hypomethylation comprising approximately two thirds of their genome. Contrary, the eBL cell line Daudi showed a 69 % methylation of all genomic CpG dinucleotides with a majority of methylation islands at polycomb repressive complex (PRC) 2 target genes, reflecting an earlier epigenetic analysis of mature aggressive B cell lymphomas [143, 146, 147]. However, cell lines do not necessarily reflect tumor tissue. Thus, the epigenomic analysis of native GC B cells versus follicular lymphoma (FL) and BL tissue is most interesting. Overall, the degree of CpG methylation was significantly lower in FL and BL than in GC B cells, despite the GC origin of both lymphoma types. However, considerable gains in methylation were observed in BL and FL especially at CpGs carrying a low-level methylation in GC B cells [144].

For NPC and EBVaGC, complete epigenomes have not yet been established. However, a methylated DNA immune precipitation (MeDIP) analysis has been conducted for NPC [148] and methylation array-based analyses for EBVaGC, in addition to a great number of prior candidate gene studies. Both NPC and EBVaGC belong to the group of CpG island methylator phenotype (CIMP) cancers (reviewed by [11, 149–151]). Actually, EBVaGC is among the highest methylated of all cancers studied so far [26]. For tumor virology in general and the EBV field, it would be interesting to have a pairwise direct comparison of the complete cellular epigenomes of BL and LCL cell lines and of the NPC, EBVaGC, eBL , sBL , HL, and early-onset PTLD tumor tissues. Especially the pairs EBVaGC-NPC, eBL-sBL, eBL-LCL, LCL-DLBCL (early-onset PTLD), and HL-DLBCL (late-onset PTLD) would be most interesting to study.

10 EBV-Associated Diseases: A Role for Exosome-Mediated Information Transfer?

Exosomes are nano-sized, endosome-derived membrane vesicles released by a series of different mammalian cell types into the extracellular space [152, 153]. They carry protein, RNA, DNA, and lipid molecules and may play a role in intercellular communication between neighboring cells as well as in long-distance information transfer via the body fluids they enter [152, 154, 155]. It was proposed that such nano-vesicles are especially suitable for the transfer of small regulatory RNA molecules (microRNAs) [156]. Exosomes are internalized by their target cells as single vesicles at the base of filopodia [157]. Interestingly, exosomes somewhat resemble the "gemmules" which Charles Darwin first postulated in his Pangenesis theory, published in his book of 1868 *The Variation of Animals and Plants under Domestication* [158].

Nanbo et al. observed that exosomes released from EBV-infected clones of the BL line Mutu as well as exosomes derived from an EBV-negative Mutu subclone were internalized via caveola-dependent endocytosis by the recipient EBV-negative epithelial cells [159]. Depending on the source of the exosomes, the outcome of exosome-recipient cell interaction varied: exosomes produced by latency type III Mutu cells increased a significantly higher expression of ICAM-1 (intracellular adhesion molecule 1) in the EBV-negative nasopharyngeal carcinoma cell line CNE1 than the exosomes derived from EBV-negative or latency type I Mutu cells. This difference in phenotypic modulation of CNE1 cells was attributed to the exosomal transfer of LMP1 (latent membrane protein 1) from the latency type III Mutu cells expressing LMP1. Nanbo et al. speculated that exosomes may also play a role in the transfer of EBV from infected B lymphocytes to epithelial cells by stabilizing the contacts between the interacting cells [159].

The first hint for the association of the EBV oncoprotein LMP1 with exosomes came from the work of Dukers et al., who detected LMP1 in pellets obtained by differential centrifugation from supernatants of EBV-positive lymphoblastoid cells [160]. They also pinpointed, based on homology search, two sequences in the first transmembrane domain of LMP1 that may mediate the in vitro immunosuppressive effects of LMP1. These data and further experiments suggested that LMP1-positive exosomes secreted by EBV-positive, LMP1-expressing tumor cells may block antitumor immune responses mediated by tumor-infiltrating T cells and NK cells in vivo [160, 161].

LMP1 may also affect intercellular communication indirectly, by enhancing the expression or exosomal packaging of distinct cellular proteins into exosomes. Ceccarelli et al. observed that LMP1 expression in a human nasopharyngeal carcinoma cell line facilitated the release of exosomes containing fibroblast growth factor 2 (FGF-2), a potent inducer of angiogenesis. They suggested that LMP1/FGF-2 double-positive

exosomes may promote neoangiogenesis and tumor progression [162]. A recent study demonstrated that LMP1 may also increase the exosomal level of hypoxia-inducible factor 1-alpha (HIF1α), a component of the HIF1 transcription factor [163]. HIF1 is a master regulator coordinating cellular responses to hypoxia, and HIF1 overexpression may play a role in tumor angiogenesis and tumor progression [164, 165]. Aga et al. found that LMP1-carrying exosomes increased the migration and invasiveness of human immortalized nasopharyngeal epithelial cells; in parallel, the cellular phenotype changed as well, and there was a decrease in E-cadherin and an increase in N-cadherin expression, a change possibly supported by exosomal HIF1α. These data suggested that exosomes produced by LMP1-positive nasopharyngeal carcinoma cells may facilitate epithelial-mesenchymal transition (EMT) and metastasis formation [163].

In nasopharyngeal carcinoma cells, expression of LMP1 was associated with an increased level of epithelial growth factor receptor (EGFR) in exosomes. Internalization of such exosomes by human umbilical vein endothelial cells (HUVECs) resulted in the activation of signaling pathways involved in the regulation of cell growth and the activation of VEGF (vascular endothelial growth factor) expression [166]. Similarly to LMP1, another EBV-encoded latent membrane protein, LMP2A , was also found to be secreted via exosomes into the culture media of lymphoid cell lines [167].

Ariza et al. observed that BLLF3 , a deoxyuridine triphosphate nucleotidohydrolase (dUTPase) encoded by a lytic cycle gene of EBV, was secreted in exosomes from chemically induced Raji cells [168]. Ariza et al. speculated that BLLF3—when expressed in vivo under certain EBV-associated pathological conditions including NPC , NK/T cell lymphoma , infectious mononucleosis , and oral hairy leukoplakia —may induce, unrelated to its enzymatic activity, an inflammatory reaction by interacting with TLR2, a toll-like receptor [168].

A proteomic study revealed that in lymphoid cells infected by either EBV or KSHV (Kaposi's sarcoma-associated herpesvirus, another human gammaherpesvirus), the protein components of the exosomes changed, compared to the exosomes of BJAB, an uninfected B cell line: there were 93 proteins unique to exosomes from EBV-infected cells and 22 proteins specific for exosomes derived from KSHV-infected cells. LMP1 expression had a significant impact on the exosome-associated proteome: there were 60 proteins present in LMP1-positive exosomes that were not detected in their LMP1-negative counterparts [169].

EBV infection of human B cells in vitro resulted in the release of exosomes that harbor LMP1, and LMP1-containing exosomes released from an EBV-negative, LMP1-transfected BL line were internalized by human B cells. The internalized LMP1-containing exosomes modulated the phenotype and altered the genotype of the recipient cells: they induced cell proliferation and upregulated AID (activation-induced cytidine deaminase), a key enzyme in class switch recombination. Accordingly, hallmarks of class switch recombination, i.e., the production of circle and germline transcripts for

IgG1, were observed in B cells exposed to the LMP1-harboring exosomes. In parallel, differentiation toward a plasmablast-like phenotype was also recorded. These data suggested that exosomes released from EBV-infected lymphoid cells may alter the fate of noninfected B cells [170].

As outlined above, the uptake of exosomes released from EBV-positive cells may affect the phenotype of recipient cells via the cellular and viral proteins transmitted. Another possibility for phenotypic modulation of target cells by EBV-infected lymphoblastoid cells is based on the exosomal transfer of viral mRNAs encoding the latent EBV proteins LMP1, LMP2 , EBNA1, and EBNA2 [171].

The non-translated, highly abundant EBV-encoded RNAs, EBER1 , and EBER2 were also detected in exosomal fractions purified from cell culture supernatants of EBV-positive lymphoid cell lines. The very same exosomes also contained the cellular La protein, suggesting EBER-La complexes may be co-packaged into exosomes. La was present, however, in exosomes derived from EBV-negative cells as well [172]. The putative role of EBER1 and EBER2 in the pathogenesis of EBV-associated neoplasms was reviewed recently [173–175]. We would like to emphasize, however, that EBER-La complexes released from EBV-positive cells either in exosomes or via active secretion of La may activate Toll-like receptor 3 (TLR3) recognizing double-stranded RNAs [176]. The resulting immune activation could possibly initiate the development or facilitate the progression of EBV-associated autoimmune diseases [177]. The use of novel experimental models, such as EBV-infected new-generation humanized mice , may clarify the role of EBERs in the pathogenesis of certain autoimmune diseases, including EBV-associated hemophagocytic lymphohistiocytosis and rheumatoid arthritis (reviewed by [178]). Internalization of EBER1-loaded exosomes by human plasmacytoid dendritic cells (pDCs) and the infiltration of skin lesions of systemic lupus erythematosus (SLE) patients by pDCs support the idea that EBER1, detected in high levels in such lesions, may play a role in the pathogenesis of SLE as well [179].

In addition to the EBERs, exosomes released by EBV-infected cells contain other non-translated viral and cellular RNA molecules, including microRNAs (miRNAs) as well. Similarly to their cellular counterparts, EBV-encoded microRNAs are also transcribed and processed in the nucleus and transported to the cytoplasm, where they are further processed, and finally interact with their cellular and viral mRNA targets as single-stranded miRNAs. Such interactions, usually at the 3′-untranslated region of mRNAs, result in the destabilization of the target mRNAs and suppress their translation. Pegtel et al. observed that EBV-encoded miRNAs accumulated in exosomes of EBV-infected B cells, and were transmitted, during in vitro cocultivation, into monocyte-derived dendritic cells [180]. Based on their observation and on the role of miRNAs in immune regulation (reviewed by [181]), Pegtel et al. suggested that exosome-transmitted miRNAs may act like paracrine factors, reaching a relatively high level in lymph nodes or in the microenvironment of malignant tumors [180]. Others observed the

uptake of EBV-miRNAs, carried by exosomes released from an EBV-positive NPC cell line, by endothelial cells [166]. In addition, EBV-miRNAs, generated before splicing of the BamHI A rightward transcripts (BARTs) , were detected in secreted exosomes in plasma samples of nude mice carrying NPC xenografts. They were also present in plasma samples of NPC patients [182].

How miRNAs and other RNA molecules are loaded into exosomes remains to be elucidated. Janas et al. proposed recently that affinity to the raft-like regions in the outer layer of the multivesicular body membrane plays an important role in this process [183]. The presence of EBV may affect the selection of cellular RNAs loaded into exosomes because co-culture of EBV-positive Raji BL cells , but not that of the EBV-negative Ramos BL cells increased the level of the cellular miR-155 in recipient retinal pigment epithelial cells [184]. An increased miR-155 level may elicit pro-angiogenic changes in the exosome-recipient cells.

EBV latency products may affect the level of cellular miRNAs by upregulating their expression. One may speculate that cellular miRNA levels may influence the abundance of distinct, exosome-packaged miRNAs. Similarly to other RNA transcripts, the transcription of primary miRNAs is also regulated by epigenetic mechanisms that are subjected to modulation by latent EBV proteins [185, 186].

Transfer of cellular miRNAs from oral epithelial cells to B cells carrying latent EBV genomes may result in the induction of productive virus replication. Lin et al. observed that members of the epithelium-specific cellular miR-200 microRNA family are present in high levels both in oral and tonsillar epithelia and saliva. Transfer of exosomes loaded with the members of the miR-200 family reactivated and induced lytic replication of latent EBV genomes in B cells cultivated in vitro, suggesting that exosomes may facilitate the exchange of EBV between the B cell compartment and the epithelial cell compartment [187].

11 Adoptive T Cell Immunotherapy

Besides CMV primary infection and reactivation, EBV-associated posttransplant lymphoproliferative disease (PTLD) , both of the early- and late-onset type, is a major cause of mortality in recipients of solid organs or allogeneic stem cells. When reduction of immune suppression and treatment with B cell depleting anti-CD20 monoclonal antibodies fail to alleviate the disease, classical chemotherapy is frequently the last resort, with rather poor success rates. Especially for latency type III expressing early-onset PTLD, adoptive T cell therapy has had great success with very little side effects. However, unfortunately, this therapy is not yet available even in major university clinics on a regular basis, due to the high demand for skill and infrastructure and due to technical challenges, in spite of the great progress made over the last two decades in developing such therapies and making them amenable for routine application (reviewed

by [188]). Antigen-specific T cell therapy has also been used for virus-associated cancer or lymphoma in immune competent patients [189–193] (reviewed by [194]). Engineered EBV-specific T cells carrying genetic modifications making them resistant against the immune-suppressive local tumor environment are under development [195–198]. Latency III, especially through peptides derived from the EBNA3 proteins, offers a better working surface for cellular immune attack than latency I or II. Therefore, malignancies expressing the full complement of latency III gene products, e.g., early-onset PTLD, are better suited for treatment with EBV-specific T cells than those expressing latency types I or II, e.g., most late-onset PTLD, BL, EBVaGC, HL, or NPC . The activation and expansion of T cells specifically directed against LMP1 and LMP2A may be a promising solution. Beyond viruses, gene-modified T cells have also shown promising results in the treatment of common malignancies [199–201].

There are differences between the PTLD tumors of solid organ transplant (SOT) and hematopoietic stem cell transplant (HSCT) patients. In HSCT patients PTLD mostly originate from donor lymphocytes. Thus, donor lymphocyte infusion is effective for PTLD, but is significantly prone to graft versus host disease (GVHD) . To avoid GVHD, EBV-specific T cells were activated and expanded. For this purpose, donor LCL had to be established as antigen presenting cells in each individual case. Regarding clinical outcome and cost, this treatment compared favorably with other treatment modalities for PTLD [202]. In SOT patients, PTLDs originate mostly from recipient lymphocytes. This gives the advantage of timely establishment of LCLs, but has to deal with iatrogenic immune suppression which usually cannot be reduced in order to prevent graft rejection. Therefore, the development of genetically modified specific T cells which are resistant to immunosuppressive treatment is a promising option [203–206].

Since time is the most limiting factor in aggressive PTLD, and the generation of new individually tailored EBV-specific T cells takes around 12 weeks, it is almost impossible to obtain such T cells in time to be of clinical relevance. Therefore, the rapid isolation of pre-existing EBV-specific T cells has been tried with success [207, 208]. Furthermore, to overcome the problem of limited numbers of specific donor T cells, the rapid in vitro stimulation and expansion of functioning multi-virus-specific T cells from donor blood was achieved within less than 1 month [209]. However, the very rapid progression of PTLD may not even leave 1 week's time for the patient. Therefore, banks containing off-the-shelf third-party T cells, with a best-possible HLA match, were established and successfully tried by several transplant centers [210–212].

12 Concluding Remarks

We have briefly outlined some exciting trends in EBV research and the interconnected clinical issues. Research developments during recent years were facilitated through the generation of novel methods, novel high throughput techniques, and through significant

technological progress of already existing methods. One of the aims of the new volume "Epstein-Barr virus—Methods and Protocols" is to contribute to the advancement of EBV research through the transfer of avant-garde techniques into daily laboratory routine and the transfer of new knowledge into clinical work. Thus, it remains to be hoped that the new book will find many interested readers and users.

References

1. Epstein MA, Achong BG, Barr YM (1964) Virus particles in cultured lymphoblasts from Burkitt's lymphoma. Lancet 1:702–703
[PubMed]

2. Munz C (Ed) (2015) Epstein Barr virus volume 1: one herpes virus: many diseases. In: Current Topics in Microbiology and Immunology, vol 390. Springer International Publishing, New York. doi:10.1007/978-3-319-22822-8

3. Munz C (Ed) (2015) Epstein Barr virus volume 2: one herpes virus: many diseases. In: Current topics in microbiology and immunology, vol 391. Springer International Publishing, New York. doi:10.1007/978-3-319-22834-1

4. Baer R, Bankier AT, Biggin MD, Deininger PL, Farrell PJ, Gibson TJ, Hatfull G, Hudson GS, Satchwell SC, Seguin C (1984) DNA sequence and expression of the B95-8 Epstein-Barr virus genome. Nature 310(5974):207–211
[PubMed]

5. Lin Z, Wang X, Strong MJ, Concha M, Baddoo M, Xu G, Baribault C, Fewell C, Hulme W, Hedges D, Taylor CM, Flemington EK (2013) Whole-genome sequencing of the Akata and Mutu Epstein-Barr virus strains. J Virol 87(2):1172–1182. doi:10.1128/JVI.02517-12
[PubMed][PubMedCentral]

6. Kwok H, Wu CW, Palser AL, Kellam P, Sham PC, Kwong DL, Chiang AK (2014) Genomic diversity of Epstein-Barr virus genomes isolated from primary nasopharyngeal carcinoma biopsy samples. J Virol 88(18):10662–10672. doi:10.1128/JVI.01665-14
[PubMed][PubMedCentral]

7. Palser AL, Grayson NE, White RE, Corton C, Correia S, Ba Abdullah MM, Watson SJ, Cotten M, Arrand JR, Murray PG, Allday MJ, Rickinson AB, Young LS, Farrell PJ, Kellam P (2015) Genome diversity of Epstein-Barr virus from multiple tumor types and normal infection. J Virol 89(10):5222–5237. doi:10.1128/JVI.03614-14
[PubMed][PubMedCentral]

8. Farrell PJ (2015) Epstein-Barr virus strain variation. Curr Top Microbiol Immunol 390(Pt 1):45–69. doi:10.1007/978-3-319-22822-8_4
[PubMed]

9. Vockerodt M, Yap LF, Shannon-Lowe C, Curley H, Wei W, Vrzalikova K, Murray PG (2015) The Epstein-Barr virus and the pathogenesis of lymphoma. J Pathol 235(2):312–322. doi:10.1002/path.4459
[PubMed]

10. Tsao SW, Tsang CM, To KF, Lo KW (2015) The role of Epstein-Barr virus in epithelial malignancies. J Pathol

235(2):323–333. doi:10.1002/path.4448

[PubMed]

11. Niller HH, Banati F, Salamon D, Minarovits J (2016) Epigenetic alterations in Epstein-Barr virus-associated diseases. Adv Exp Med Biol 879:39–69. doi:10.1007/978-3-319-24738-0_3

[PubMed]

12. Longnecker R, Kieff E, Cohen JI (2013) Epstein Barr virus. In: Knipe DM, Howley PM (eds) Fields virology, 6th edn. Lippincott Williams & Wilkins, Philadelphia, pp 1898–1959

13. Thorley-Lawson DA (2001) Epstein-Barr virus: exploiting the immune system. Nat Rev Immunol 1(1):75–82. doi:10.1038/35095584

[PubMed]

14. Decaussin G, Sbih-Lammali F, de Turenne-Tessier M, Bouguermouh A, Ooka T (2000) Expression of BARF1 gene encoded by Epstein-Barr virus in nasopharyngeal carcinoma biopsies. Cancer Res 60(19):5584–5588

[PubMed]

15. zur Hausen A, Brink AA, Craanen ME, Middeldorp JM, Meijer CJ, van den Brule AJ (2000) Unique transcription pattern of Epstein-Barr virus (EBV) in EBV-carrying gastric adenocarcinomas: expression of the transforming BARF1 gene. Cancer Res 60(10):2745–2748

[PubMed]

16. Seto E, Yang L, Middeldorp J, Sheen TS, Chen JY, Fukayama M, Eizuru Y, Ooka T, Takada K (2005) Epstein-Barr virus (EBV)-encoded BARF1 gene is expressed in nasopharyngeal carcinoma and EBV-associated gastric carcinoma tissues in the absence of lytic gene expression. J Med Virol 76(1):82–88. doi:10.1002/jmv.20327

[PubMed]

17. Takada K (2012) Role of EBER and BARF1 in nasopharyngeal carcinoma (NPC) tumorigenesis. Semin Cancer Biol 22(2):162–165. doi:10.1016/j.semcancer.2011.12.007

[PubMed]

18. Lin Z, Xu G, Deng N, Taylor C, Zhu D, Flemington EK (2010) Quantitative and qualitative RNA-Seq-based evaluation of Epstein-Barr virus transcription in type I latency Burkitt's lymphoma cells. J Virol 84(24):13053–13058. doi:10.1128/JVI.01521-10

[PubMed][PubMedCentral]

19. Concha M, Wang X, Cao S, Baddoo M, Fewell C, Lin Z, Hulme W, Hedges D, McBride J, Flemington EK (2012) Identification of new viral genes and transcript isoforms during Epstein-Barr virus reactivation using RNA-Seq. J Virol 86(3):1458–1467. doi:10.1128/JVI.06537-11

[PubMed][PubMedCentral]

20. Dobin A, Davis CA, Schlesinger F, Drenkow J, Zaleski C, Jha S, Batut P, Chaisson M, Gingeras TR (2013) STAR: ultrafast universal RNA-seq aligner. Bioinformatics 29(1):15–21. doi:10.1093/bioinformatics/bts635

[PubMed]

21. O'Grady T, Cao S, Strong MJ, Concha M, Wang X, Splinter Bondurant S, Adams M, Baddoo M, Srivastav SK, Lin Z, Fewell C, Yin Q, Flemington EK (2014) Global bidirectional transcription of the Epstein-Barr virus genome during reactivation. J Virol 88(3):1604–1616. doi:10.1128/JVI.02989-13

[PubMed][PubMedCentral]

22. Strong MJ, Baddoo M, Nanbo A, Xu M, Puetter A, Lin Z (2014) Comprehensive high-throughput RNA sequencing analysis reveals contamination of multiple nasopharyngeal carcinoma cell lines with HeLa cell

genomes. J Virol 88(18):10696–10704. doi:10.1128/JVI.01457-14
[PubMed][PubMedCentral]

23. Cao S, Strong MJ, Wang X, Moss WN, Concha M, Lin Z, O'Grady T, Baddoo M, Fewell C, Renne R, Flemington EK (2015) High-throughput RNA sequencing-based virome analysis of 50 lymphoma cell lines from the Cancer Cell Line Encyclopedia project. J Virol 89(1):713–729. doi:10.1128/JVI.02570-14
[PubMed]

24. Cao S, Moss W, O'Grady T, Concha M, Strong MJ, Wang X, Yu Y, Baddoo M, Zhang K, Fewell C, Lin Z, Dong Y, Flemington EK (2015) New noncoding lytic transcripts derived from the Epstein-Barr virus latency origin of replication, oriP, are hyperedited, bind the paraspeckle protein, NONO/p54nrb, and support viral lytic transcription. J Virol 89(14):7120–7132. doi:10.1128/JVI.00608-15
[PubMed][PubMedCentral]

25. Barretina J, Caponigro G, Stransky N, Venkatesan K, Margolin AA, Kim S, Wilson CJ, Lehar J, Kryukov GV, Sonkin D, Reddy A, Liu M, Murray L, Berger MF, Monahan JE, Morais P, Meltzer J, Korejwa A, Jane-Valbuena J, Mapa FA, Thibault J, Bric-Furlong E, Raman P, Shipway A, Engels IH, Cheng J, Yu GK, Yu J, Aspesi P Jr, de Silva M, Jagtap K, Jones MD, Wang L, Hatton C, Palescandolo E, Gupta S, Mahan S, Sougnez C, Onofrio RC, Liefeld T, MacConaill L, Winckler W, Reich M, Li N, Mesirov JP, Gabriel SB, Getz G, Ardlie K, Chan V, Myer VE, Weber BL, Porter J, Warmuth M, Finan P, Harris JL, Meyerson M, Golub TR, Morrissey MP, Sellers WR, Schlegel R, Garraway LA (2012) The Cancer Cell Line Encyclopedia enables predictive modelling of anticancer drug sensitivity. Nature 483(7391):603–607. doi:10.1038/nature11003
[PubMed][PubMedCentral]

26. Cancer Genome Atlas Research Network (2014) Comprehensive molecular characterization of gastric adenocarcinoma. Nature 513(7517):202–209. doi:10.1038/nature13480

27. Strong MJ, Laskow T, Nakhoul H, Blanchard E, Liu Y, Wang X, Baddoo M, Lin Z, Yin Q, Flemington EK (2015) Latent expression of the Epstein-Barr virus (EBV)-encoded major histocompatibility complex class I TAP inhibitor, BNLF2a, in EBV-positive gastric carcinomas. J Virol 89(19):10110–10114. doi:10.1128/JVI.01110-15
[PubMed][PubMedCentral]

28. Hu L, Lin Z, Wu Y, Dong J, Zhao B, Cheng Y, Huang P, Xu L, Xia T, Xiong D, Wang H, Li M, Guo L, Kieff E, Zeng Y, Zhong Q, Zeng M (2016) Comprehensive profiling of EBV gene expression in nasopharyngeal carcinoma through paired-end transcriptome sequencing. Front Med 10(1):61–75. doi:10.1007/s11684-016-0436-0
[PubMed]

29. Georges AA, Frappier L (2015) Proteomics methods for discovering viral-host interactions. Methods 90:21–27. doi:10.1016/j.ymeth.2015.05.001
[PubMed]

30. Holowaty MN, Zeghouf M, Wu H, Tellam J, Athanasopoulos V, Greenblatt J, Frappier L (2003) Protein profiling with Epstein-Barr nuclear antigen-1 reveals an interaction with the herpesvirus-associated ubiquitin-specific protease HAUSP/USP7. J Biol Chem 278(32):29987–29994. doi:10.1074/jbc.M303977200
[PubMed]

31. Saridakis V, Sheng Y, Sarkari F, Holowaty MN, Shire K, Nguyen T, Zhang RG, Liao J, Lee W, Edwards AM, Arrowsmith CH, Frappier L (2005) Structure of the p53 binding domain of HAUSP/USP7 bound to Epstein-Barr nuclear antigen 1 implications for EBV-mediated immortalization. Mol Cell 18(1):25–36. doi:10.1016/j.molcel.2005.02.029
[PubMed]

32. Sivachandran N, Sarkari F, Frappier L (2008) Epstein-Barr nuclear antigen 1 contributes to nasopharyngeal

carcinoma through disruption of PML nuclear bodies. PLoS Pathog 4(10):e1000170. doi:10.1371/journal.ppat.1000170
[PubMed][PubMedCentral]

33. Sivachandran N, Dawson CW, Young LS, Liu FF, Middeldorp J, Frappier L (2012) Contributions of the Epstein-Barr virus EBNA1 protein to gastric carcinoma. J Virol 86(1):60–68. doi:10.1128/JVI.05623-11
[PubMed][PubMedCentral]

34. Sivachandran N, Wang X, Frappier L (2012) Functions of the Epstein-Barr virus EBNA1 protein in viral reactivation and lytic infection. J Virol 86(11):6146–6158. doi:10.1128/JVI.00013-12
[PubMed][PubMedCentral]

35. Mansouri S, Pan Q, Blencowe BJ, Claycomb JM, Frappier L (2014) Epstein-Barr virus EBNA1 protein regulates viral latency through effects on let-7 microRNA and dicer. J Virol 88(19):11166–11177. doi:10.1128/JVI.01785-14
[PubMed][PubMedCentral]

36. Sivachandran N, Cao JY, Frappier L (2010) Epstein-Barr virus nuclear antigen 1 Hijacks the host kinase CK2 to disrupt PML nuclear bodies. J Virol 84(21):11113–11123. doi:10.1128/JVI.01183-10
[PubMed][PubMedCentral]

37. Wang ZG, Ruggero D, Ronchetti S, Zhong S, Gaboli M, Rivi R, Pandolfi PP (1998) PML is essential for multiple apoptotic pathways. Nat Genet 20(3):266–272. doi:10.1038/3073
[PubMed]

38. Murakami M, Lan K, Subramanian C, Robertson ES (2005) Epstein-Barr virus nuclear antigen 1 interacts with Nm23-H1 in lymphoblastoid cell lines and inhibits its ability to suppress cell migration. J Virol 79(3):1559–1568. doi:10.1128/JVI.79.3.1559-1568.2005
[PubMed][PubMedCentral]

39. Lu J, Murakami M, Verma SC, Cai Q, Haldar S, Kaul R, Wasik MA, Middeldorp J, Robertson ES (2011) Epstein-Barr virus nuclear antigen 1 (EBNA1) confers resistance to apoptosis in EBV-positive B-lymphoma cells through up-regulation of survivin. Virology 410(1):64–75. doi:10.1016/j.virol.2010.10.029
[PubMed]

40. Thorley-Lawson DA (2015) EBV persistence—introducing the virus. Curr Top Microbiol Immunol 390(Pt 1):151–209. doi:10.1007/978-3-319-22822-8_8
[PubMed]

41. Heuts F, Rottenberg ME, Salamon D, Rasul E, Adori M, Klein G, Klein E, Nagy N (2014) T cells modulate Epstein-Barr virus latency phenotypes during infection of humanized mice. J Virol 88(6):3235–3245. doi:10.1128/JVI.02885-13
[PubMed][PubMedCentral]

42. Heath E, Begue-Pastor N, Chaganti S, Croom-Carter D, Shannon-Lowe C, Kube D, Feederle R, Delecluse HJ, Rickinson AB, Bell AI (2012) Epstein-Barr virus infection of naive B cells in vitro frequently selects clones with mutated immunoglobulin genotypes: implications for virus biology. PLoS Pathog 8(5):e1002697. doi:10.1371/journal.ppat.1002697
[PubMed][PubMedCentral]

43. Kurth J, Hansmann ML, Rajewsky K, Kuppers R (2003) Epstein-Barr virus-infected B cells expanding in germinal centers of infectious mononucleosis patients do not participate in the germinal center reaction. Proc Natl Acad Sci U S A 100(8):4730–4735
[PubMed][PubMedCentral]

44. Kurth J, Spieker T, Wustrow J, Strickler GJ, Hansmann LM, Rajewsky K, Kuppers R (2000) EBV-infected B cells in infectious mononucleosis: viral strategies for spreading in the B cell compartment and establishing latency. Immunity 13(4):485–495
[PubMed]

45. Cocco M, Bellan C, Tussiwand R, Corti D, Traggiai E, Lazzi S, Mannucci S, Bronz L, Palummo N, Ginanneschi C, Tosi P, Lanzavecchia A, Manz MG, Leoncini L (2008) CD34+ cord blood cell-transplanted Rag2–/–gamma(c)–/– mice as a model for Epstein-Barr virus infection. Am J Pathol 173(5):1369–1378. doi:10.2353/ajpath.2008.071186
[PubMed][PubMedCentral]

46. Chaganti S, Heath EM, Bergler W, Kuo M, Buettner M, Niedobitek G, Rickinson AB, Bell AI (2009) Epstein-Barr virus colonization of tonsillar and peripheral blood B-cell subsets in primary infection and persistence. Blood 113(25):6372–6381. doi:10.1182/blood-2008-08-175828
[PubMed]

47. Burns DM, Tierney R, Shannon-Lowe C, Croudace J, Inman C, Abbotts B, Nagra S, Fox CP, Chaganti S, Craddock CF, Moss P, Rickinson AB, Rowe M, Bell AI (2015) Memory B-cell reconstitution following allogeneic hematopoietic stem cell transplantation is an EBV-associated transformation event. Blood 126(25):2665–2675. doi:10.1182/blood-2015-08-665000
[PubMed][PubMedCentral]

48. Niller HH, Szenthe K, Minarovits J (2014) Epstein-Barr virus-host cell interactions: an epigenetic dialog? Front Genet 5:367. doi:10.3389/fgene.2014.00367
[PubMed][PubMedCentral]

49. Rowe M, Glaunsinger B, van Leeuwen D, Zuo J, Sweetman D, Ganem D, Middeldorp J, Wiertz EJ, Ressing ME (2007) Host shutoff during productive Epstein-Barr virus infection is mediated by BGLF5 and may contribute to immune evasion. Proc Natl Acad Sci U S A 104(9):3366–3371. doi:10.1073/pnas.0611128104
[PubMed][PubMedCentral]

50. Ramasubramanyan S, Osborn K, Al-Mohammad R, Naranjo Perez-Fernandez IB, Zuo J, Balan N, Godfrey A, Patel H, Peters G, Rowe M, Jenner RG, Sinclair AJ (2015) Epstein-Barr virus transcription factor Zta acts through distal regulatory elements to directly control cellular gene expression. Nucleic Acids Res 43(7):3563–3577. doi:10.1093/nar/gkv212
[PubMed][PubMedCentral]

51. Temple RM, Zhu J, Budgeon L, Christensen ND, Meyers C, Sample CE (2014) Efficient replication of Epstein-Barr virus in stratified epithelium in vitro. Proc Natl Acad Sci U S A 111(46):16544–16549. doi:10.1073/pnas.1400818111
[PubMed][PubMedCentral]

52. Suarez F, Lortholary O, Hermine O, Lecuit M (2006) Infection-associated lymphomas derived from marginal zone B cells: a model of antigen-driven lymphoproliferation. Blood 107(8):3034–3044. doi:10.1182/blood-2005-09-3679
[PubMed]

53. Magrath I (2012) Epidemiology: clues to the pathogenesis of Burkitt lymphoma. Br J Haematol 156(6):744–756. doi:10.1111/j.1365-2141.2011.09013.x
[PubMed]

54. Amato T, Abate F, Piccaluga P, Iacono M, Fallerini C, Renieri A, De Falco G, Ambrosio MR, Mourmouras V, Ogwang M, Calbi V, Rabadan R, Hummel M, Pileri S, Leoncini L, Bellan C (2016) Clonality analysis of

immunoglobulin gene rearrangement by next-generation sequencing in endemic Burkitt lymphoma suggests antigen drive activation of BCR as opposed to sporadic Burkitt lymphoma. Am J Clin Pathol 145(1):116–127. doi:10.1093/ajcp/aqv011
[PubMed]

55. Richter J, Schlesner M, Hoffmann S, Kreuz M, Leich E, Burkhardt B, Rosolowski M, Ammerpohl O, Wagener R, Bernhart SH, Lenze D, Szczepanowski M, Paulsen M, Lipinski S, Russell RB, Adam-Klages S, Apic G, Claviez A, Hasenclever D, Hovestadt V, Hornig N, Korbel JO, Kube D, Langenberger D, Lawerenz C, Lisfeld J, Meyer K, Picelli S, Pischimarov J, Radlwimmer B, Rausch T, Rohde M, Schilhabel M, Scholtysik R, Spang R, Trautmann H, Zenz T, Borkhardt A, Drexler HG, Moller P, MacLeod RA, Pott C, Schreiber S, Trumper L, Loeffler M, Stadler PF, Lichter P, Eils R, Kuppers R, Hummel M, Klapper W, Rosenstiel P, Rosenwald A, Brors B, Siebert R, Project IM-S (2012) Recurrent mutation of the ID3 gene in Burkitt lymphoma identified by integrated genome, exome and transcriptome sequencing. Nat Genet 44(12):1316–1320. doi:10.1038/ng.2469
[PubMed]

56. Schmitz R, Young RM, Ceribelli M, Jhavar S, Xiao W, Zhang M, Wright G, Shaffer AL, Hodson DJ, Buras E, Liu X, Powell J, Yang Y, Xu W, Zhao H, Kohlhammer H, Rosenwald A, Kluin P, Muller-Hermelink HK, Ott G, Gascoyne RD, Connors JM, Rimsza LM, Campo E, Jaffe ES, Delabie J, Smeland EB, Ogwang MD, Reynolds SJ, Fisher RI, Braziel RM, Tubbs RR, Cook JR, Weisenburger DD, Chan WC, Pittaluga S, Wilson W, Waldmann TA, Rowe M, Mbulaiteye SM, Rickinson AB, Staudt LM (2012) Burkitt lymphoma pathogenesis and therapeutic targets from structural and functional genomics. Nature 490(7418):116–120. doi:10.1038/nature11378
[PubMed][PubMedCentral]

57. Love C, Sun Z, Jima D, Li G, Zhang J, Miles R, Richards KL, Dunphy CH, Choi WW, Srivastava G, Lugar PL, Rizzieri DA, Lagoo AS, Bernal-Mizrachi L, Mann KP, Flowers CR, Naresh KN, Evens AM, Chadburn A, Gordon LI, Czader MB, Gill JI, Hsi ED, Greenough A, Moffitt AB, McKinney M, Banerjee A, Grubor V, Levy S, Dunson DB, Dave SS (2012) The genetic landscape of mutations in Burkitt lymphoma. Nat Genet 44(12):1321–1325. doi:10.1038/ng.2468
[PubMed][PubMedCentral]

58. Bellan C, Lazzi S, Hummel M, Palummo N, de Santi M, Amato T, Nyagol J, Sabattini E, Lazure T, Pileri SA, Raphael M, Stein H, Tosi P, Leoncini L (2005) Immunoglobulin gene analysis reveals 2 distinct cells of origin for EBV-positive and EBV-negative Burkitt lymphomas. Blood 106(3):1031–1036. doi:10.1182/blood-2005-01-0168
[PubMed]

59. Lenoir GM, Bornkamm G (1987) Burkitt's lymphoma, a human cancer model for the study of the multistep development of cancer: proposal for a new scenario. In: Klein G (ed) Advances in viral oncology, vol 7. Raven, New York, pp 173–206

60. Araujo I, Foss HD, Bittencourt A, Hummel M, Demel G, Mendonca N, Herbst H, Stein H (1996) Expression of Epstein-Barr virus-gene products in Burkitt's lymphoma in northeast Brazil. Blood 87(12):5279–5286
[PubMed]

61. Araujo I, Foss HD, Hummel M, Anagnostopoulos I, Barbosa HS, Bittencourt A, Stein H (1999) Frequent expansion of Epstein-Barr virus (EBV) infected cells in germinal centres of tonsils from an area with a high incidence of EBV-associated lymphoma. J Pathol 187(3):326–330. doi:10.1002/(SICI)1096-9896(199902)187:3<326::AID-PATH242>3.0.CO;2-N
[PubMed]

62. Niller HH, Salamon D, Ilg K, Koroknai A, Banati F, Bauml G, Rucker O, Schwarzmann F, Wolf H, Minarovits J (2003) The in vivo binding site for oncoprotein c-Myc in the promoter for Epstein-Barr virus (EBV) encoding RNA (EBER) 1 suggests a specific role for EBV in lymphomagenesis. Med Sci Monit 9(1):HY1–HY9

[PubMed]

63. Niller HH, Salamon D, Ilg K, Koroknai A, Banati F, Schwarzmann F, Wolf H, Minarovits J (2004) EBV-associated neoplasms: alternative pathogenetic pathways. Med Hypotheses 62(3):387–391. doi:10.1016/j.mehy.2003.11.001
[PubMed]

64. Niller HH, Salamon D, Banati F, Schwarzmann F, Wolf H, Minarovits J (2004) The LCR of EBV makes Burkitt's lymphoma endemic. Trends Microbiol 12(11):495–499
[PubMed]

65. Orem J, Mbidde EK, Lambert B, de Sanjose S, Weiderpass E (2007) Burkitt's lymphoma in Africa, a review of the epidemiology and etiology. Afr Health Sci 7(3):166–175. doi:10.5555/afhs.2007.7.3.166
[PubMed][PubMedCentral]

66. Moormann AM, Snider CJ, Chelimo K (2011) The company malaria keeps: how co-infection with Epstein-Barr virus leads to endemic Burkitt lymphoma. Curr Opin Infect Dis 24(5):435–441. doi:10.1097/QCO.0b013e328349ac4f
[PubMed][PubMedCentral]

67. Kuhn-Hallek I, Sage DR, Stein L, Groelle H, Fingeroth JD (1995) Expression of recombination activating genes (RAG-1 and RAG-2) in Epstein-Barr virus-bearing B cells. Blood 85(5):1289–1299
[PubMed]

68. He B, Raab-Traub N, Casali P, Cerutti A (2003) EBV-encoded latent membrane protein 1 cooperates with BAFF/BLyS and APRIL to induce T cell-independent Ig heavy chain class switching. J Immunol 171(10):5215–5224
[PubMed][PubMedCentral]

69. Epeldegui M, Hung YP, McQuay A, Ambinder RF, Martinez-Maza O (2007) Infection of human B cells with Epstein-Barr virus results in the expression of somatic hypermutation-inducing molecules and in the accrual of oncogene mutations. Mol Immunol 44(5):934–942. doi:10.1016/j.molimm.2006.03.018
[PubMed]

70. Chene A, Donati D, Orem J, Mbidde ER, Kironde F, Wahlgren M, Bejarano MT (2009) Endemic Burkitt's lymphoma as a polymicrobial disease: new insights on the interaction between Plasmodium falciparum and Epstein-Barr virus. Semin Cancer Biol 19(6):411–420. doi:10.1016/j.semcancer.2009.10.002
[PubMed]

71. Iskra S, Kalla M, Delecluse HJ, Hammerschmidt W, Moosmann A (2010) Toll-like receptor agonists synergistically increase proliferation and activation of B cells by Epstein-Barr virus. J Virol 84(7):3612–3623. doi:10.1128/JVI.01400-09
[PubMed][PubMedCentral]

72. Simone O, Bejarano MT, Pierce SK, Antonaci S, Wahlgren M, Troye-Blomberg M, Donati D (2011) TLRs innate immunereceptors and Plasmodium falciparum erythrocyte membrane protein 1 (PfEMP1) CIDR1alpha-driven human polyclonal B-cell activation. Acta Trop 119(2–3):144–150. doi:10.1016/j.actatropica.2011.05.005
[PubMed][PubMedCentral]

73. Shannon-Lowe C, Rowe M (2011) Epstein-Barr virus infection of polarized epithelial cells via the basolateral surface by memory B cell-mediated transfer infection. PLoS Pathog 7(5):e1001338. doi:10.1371/journal.ppat.1001338
[PubMed][PubMedCentral]

74. Torgbor C, Awuah P, Deitsch K, Kalantari P, Duca KA, Thorley-Lawson DA (2014) A multifactorial role for P. falciparum malaria in endemic Burkitt's lymphoma pathogenesis. PLoS Pathog 10(5):e1004170. doi:10.1371/journal.ppat.1004170
[PubMed][PubMedCentral]

75. Victora GD, Dominguez-Sola D, Holmes AB, Deroubaix S, Dalla-Favera R, Nussenzweig MC (2012) Identification of human germinal center light and dark zone cells and their relationship to human B-cell lymphomas. Blood 120(11):2240–2248. doi:10.1182/blood-2012-03-415380
[PubMed][PubMedCentral]

76. Schmitz R, Ceribelli M, Pittaluga S, Wright G, Staudt LM (2014) Oncogenic mechanisms in Burkitt lymphoma. Cold Spring Harb Perspect Med 4(2):a014282. doi:10.1101/cshperspect.a014282
[PubMed][PubMedCentral]

77. Robbiani DF, Deroubaix S, Feldhahn N, Oliveira TY, Callen E, Wang Q, Jankovic M, Silva IT, Rommel PC, Bosque D, Eisenreich T, Nussenzweig A, Nussenzweig MC (2015) Plasmodium infection promotes genomic instability and AID-dependent B cell lymphoma. Cell 162(4):727–737. doi:10.1016/j.cell.2015.07.019
[PubMed][PubMedCentral]

78. Dominguez-Sola D, Victora GD, Ying CY, Phan RT, Saito M, Nussenzweig MC, Dalla-Favera R (2012) The proto-oncogene MYC is required for selection in the germinal center and cyclic reentry. Nat Immunol 13(11):1083–1091. doi:10.1038/ni.2428
[PubMed][PubMedCentral]

79. Wilmore JR, Asito AS, Wei C, Piriou E, Sumba PO, Sanz I, Rochford R (2015) AID expression in peripheral blood of children living in a malaria holoendemic region is associated with changes in B cell subsets and Epstein-Barr virus. Int J Cancer 136(6):1371–1380. doi:10.1002/ijc.29127
[PubMed]

80. Faili A, Aoufouchi S, Weller S, Vuillier F, Stary A, Sarasin A, Reynaud CA, Weill JC (2004) DNA polymerase eta is involved in hypermutation occurring during immunoglobulin class switch recombination. J Exp Med 199(2):265–270. doi:10.1084/jem.20031831
[PubMed][PubMedCentral]

81. Bryant KF, Yan Z, Dreyfus DH, Knipe DM (2012) Identification of a divalent metal cation binding site in herpes simplex virus 1 (HSV-1) ICP8 required for HSV replication. J Virol 86(12):6825–6834. doi:10.1128/JVI.00374-12
[PubMed][PubMedCentral]

82. Malagon F, Gonzalez-Angulo J, Carrasco E, Robert L (2011) Etiopathogenesis of Burkitt's lymphoma: a lesson from a BL-like in CD1 mouse immune to Plasmodium yoelii yoelii. Infect Agent Cancer 6(1):10. doi:10.1186/1750-9378-6-10
[PubMed][PubMedCentral]

83. Rochford R, Cannon MJ, Moormann AM (2005) Endemic Burkitt's lymphoma: a polymicrobial disease? Nat Rev Microbiol 3(2):182–187. doi:10.1038/nrmicro1089
[PubMed]

84. van den Bosch C, Lloyd G (2000) Chikungunya fever as a risk factor for endemic Burkitt's lymphoma in Malawi. Trans R Soc Trop Med Hyg 94(6):704–705
[PubMed]

85. van den Bosch C (2012) A role for RNA viruses in the pathogenesis of Burkitt's lymphoma: the need for reappraisal. Adv Hematol 2012:494758. doi:10.1155/2012/494758

[PubMed]

86. van den Bosch CA (2004) Is endemic Burkitt's lymphoma an alliance between three infections and a tumour promoter? Lancet Oncol 5(12):738–746
[PubMed]

87. Aya T, Kinoshita T, Imai S, Koizumi S, Mizuno F, Osato T, Satoh C, Oikawa T, Kuzumaki N, Ohigashi H et al (1991) Chromosome translocation and c-MYC activation by Epstein-Barr virus and Euphorbia tirucalli in B lymphocytes. Lancet 337(8751):1190
[PubMed]

88. Mizuno F, Koizumi S, Osato T, Kokwaro JO, Ito Y (1983) Chinese and african euphorbiaceae plant extracts: markedly enhancing effect on Epstein-Barr virus-induced transformation. Cancer Lett 19(2):199–205
[PubMed]

89. Mannucci S, Luzzi A, Carugi A, Gozzetti A, Lazzi S, Malagnino V, Simmonds M, Cusi MG, Leoncini L, van den Bosch CA, De Falco G (2012) EBV reactivation and chromosomal polysomies: Euphorbia tirucalli as a possible cofactor in endemic burkitt lymphoma. Adv Hematol 2012:149780. doi:10.1155/2012/149780
[PubMed][PubMedCentral]

90. Minnicelli C, Barros MH, Klumb CE, Romano SO, Zalcberg IR, Hassan R (2012) Relationship of Epstein-Barr virus and interleukin 10 promoter polymorphisms with the risk and clinical outcome of childhood Burkitt lymphoma. PLoS One 7(9):e46005. doi:10.1371/journal.pone.0046005
[PubMed][PubMedCentral]

91. Oduor CI, Chelimo K, Ouma C, Mulama DH, Foley J, Vulule J, Bailey JA, Moormann AM (2014) Interleukin-6 and interleukin-10 gene promoter polymorphisms and risk of endemic Burkitt lymphoma. Am J Trop Med Hyg 91(3):649–654. doi:10.4269/ajtmh.13-0616
[PubMed][PubMedCentral]

92. Pike MC, Morrow RH, Kisuule A, Mafigiri J (1970) Burkitt's lymphoma and sickle cell trait. Br J Prev Soc Med 24(1):39–41
[PubMed][PubMedCentral]

93. Mulama DH, Bailey JA, Foley J, Chelimo K, Ouma C, Jura WG, Otieno J, Vulule J, Moormann AM (2014) Sickle cell trait is not associated with endemic Burkitt lymphoma: an ethnicity and malaria endemicity-matched case–control study suggests factors controlling EBV may serve as a predictive biomarker for this pediatric cancer. Int J Cancer 134(3):645–653. doi:10.1002/ijc.28378
[PubMed]

94. Klein G (1987) In defense of the "old" Burkitt lymphoma scenario. In: Klein G (ed) Advances in viral oncology, vol 7. Raven, New York, pp 207–211

95. Allday MJ (2009) How does Epstein-Barr virus (EBV) complement the activation of Myc in the pathogenesis of Burkitt's lymphoma? Semin Cancer Biol 19(6):366–376. doi:10.1016/j.semcancer.2009.07.007
[PubMed][PubMedCentral]

96. Niller HH, Salamon D, Rahmann S, Ilg K, Koroknai A, Banati F, Schwarzmann F, Wolf H, Minarovits J (2004) A 30 kb region of the Epstein-Barr virus genome is colinear with the rearranged human immunoglobulin gene loci: implications for a "ping-pong evolution" model for persisting viruses and their hosts. A review. Acta Microbiol Immunol Hung 51(4):469–484. doi:10.1556/AMicr.51.2004.4.7
[PubMed]

97.

Khan G (2006) Epstein-Barr virus and the germinal center B cells. Exp Hematol 34(6):695–696. doi:10.1016/j.exphem.2006.02.021
[PubMed]

98. Panagopoulos D, Victoratos P, Alexiou M, Kollias G, Mosialos G (2004) Comparative analysis of signal transduction by CD40 and the Epstein-Barr virus oncoprotein LMP1 in vivo. J Virol 78(23):13253–13261. doi:10.1128/JVI.78.23.13253-13261.2004
[PubMed][PubMedCentral]

99. Tobollik S, Meyer L, Buettner M, Klemmer S, Kempkes B, Kremmer E, Niedobitek G, Jungnickel B (2006) Epstein-Barr virus nuclear antigen 2 inhibits AID expression during EBV-driven B-cell growth. Blood 108(12):3859–3864. doi:10.1182/blood-2006-05-021303
[PubMed]

100. Boccellato F, Anastasiadou E, Rosato P, Kempkes B, Frati L, Faggioni A, Trivedi P (2007) EBNA2 interferes with the germinal center phenotype by downregulating BCL6 and TCL1 in non-Hodgkin's lymphoma cells. J Virol 81(5):2274–2282. doi:10.1128/JVI.01822-06
[PubMed]

101. Roughan JE, Thorley-Lawson DA (2009) The intersection of Epstein-Barr virus with the germinal center. J Virol 83(8):3968–3976. doi:10.1128/JVI.02609-08
[PubMed][PubMedCentral]

102. Roughan JE, Torgbor C, Thorley-Lawson DA (2010) Germinal center B cells latently infected with Epstein-Barr virus proliferate extensively but do not increase in number. J Virol 84(2):1158–1168. doi:10.1128/JVI.01780-09
[PubMed]

103. Kelly G, Bell A, Rickinson A (2002) Epstein-Barr virus-associated Burkitt lymphomagenesis selects for downregulation of the nuclear antigen EBNA2. Nat Med 8(10):1098–1104. doi:10.1038/nm758
[PubMed]

104. Limpens J, Stad R, Vos C, de Vlaam C, de Jong D, van Ommen GJ, Schuuring E, Kluin PM (1995) Lymphoma-associated translocation t(14;18) in blood B cells of normal individuals. Blood 85(9):2528–2536
[PubMed]

105. Muller JR, Janz S, Goedert JJ, Potter M, Rabkin CS (1995) Persistence of immunoglobulin heavy chain/c-myc recombination-positive lymphocyte clones in the blood of human immunodeficiency virus-infected homosexual men. Proc Natl Acad Sci U S A 92(14):6577–6581
[PubMed][PubMedCentral]

106. Klein G (2000) Dysregulation of lymphocyte proliferation by chromosomal translocations and sequential genetic changes. Bioessays 22(5):414–422. doi:10.1002/(SICI)1521-1878(200005)22:5<414::AID-BIES3>3.0.CO;2-5
[PubMed]

107. Thorley-Lawson DA, Gross A (2004) Persistence of the Epstein-Barr virus and the origins of associated lymphomas. N Engl J Med 350(13):1328–1337. doi:10.1056/NEJMra032015
[PubMed]

108. Rossi G, Bonetti F (2004) EBV and Burkitt's lymphoma. N Engl J Med 350(25):2621
[PubMed]

109. Thorley-Lawson DA (2004) EBV and Burkitt's lymphoma. N Engl J Med 350(25):2621

110. Kelly GL, Milner AE, Baldwin GS, Bell AI, Rickinson AB (2006) Three restricted forms of Epstein-Barr virus latency counteracting apoptosis in c-myc-expressing Burkitt lymphoma cells. Proc Natl Acad Sci U S A 103(40):14935–14940. doi:10.1073/pnas.0509988103
[PubMed][PubMedCentral]

111. Rowe M, Kelly GL, Bell AI, Rickinson AB (2009) Burkitt's lymphoma: the Rosetta Stone deciphering Epstein-Barr virus biology. Semin Cancer Biol 19(6):377–388. doi:10.1016/j.semcancer.2009.07.004
[PubMed][PubMedCentral]

112. Schulz TF, Cordes S (2009) Is the Epstein-Barr virus EBNA-1 protein an oncogen? Proc Natl Acad Sci U S A 106(7):2091–2092. doi:10.1073/pnas.0812575106
[PubMed][PubMedCentral]

113. Gromminger S, Mautner J, Bornkamm GW (2012) Burkitt lymphoma: the role of Epstein-Barr virus revisited. Br J Haematol 156(6):719–729
[PubMed]

114. Rickinson AB (2014) Co-infections, inflammation and oncogenesis: future directions for EBV research. Semin Cancer Biol 26:99–115. doi:10.1016/j.semcancer.2014.04.004
[PubMed]

115. Bornkamm GW (2009) Epstein-Barr virus and its role in the pathogenesis of Burkitt's lymphoma: an unresolved issue. Semin Cancer Biol 19(6):351–365. doi:10.1016/j.semcancer.2009.07.002
[PubMed]

116. Niller HH, Banati F, Ay E, Minarovits J (2012) Epigenetic changes in virus-associated neoplasms. In: Minarovits J, Niller HH (eds) Patho-epigenetics of disease. Springer, New York, pp 179–225

117. Nunes-Alves C (2014) Parasite biology: Piecing it together. Nat Rev Microbiol 12(7):462–463

118. Piguet PF, Da Laperrousaz C, Vesin C, Donati Y (2001) Incidence of apoptosis in the lymphoid organs of normal or malaria infected mice is decreased in CD18 and urokinase-receptor (UPAR, CD87) deficient mice. Dev Immunol 8(3–4):183–191
[PubMed][PubMedCentral]

119. Kalter SP, Riggs SA, Cabanillas F, Butler JJ, Hagemeister FB, Mansell PW, Newell GR, Velasquez WS, Salvador P, Barlogie B et al (1985) Aggressive non-Hodgkin's lymphomas in immunocompromised homosexual males. Blood 66(3):655–659
[PubMed]

120. Richard Y, Amiel C, Jeantils V, Mestivier D, Portier A, Dhello G, Feuillard J, Creidy R, Nicolas JC, Raphael M (2010) Changes in blood B cell phenotypes and Epstein-Barr virus load in chronically human immunodeficiency virus-infected patients before and after antiretroviral therapy. J Infect Dis 202(9):1424–1434. doi:10.1086/656479
[PubMed]

121. Millington OR, Di Lorenzo C, Phillips RS, Garside P, Brewer JM (2006) Suppression of adaptive immunity to heterologous antigens during Plasmodium infection through hemozoin-induced failure of dendritic cell function. J Biol 5(2):5. doi:10.1186/jbiol34
[PubMed][PubMedCentral]

122. Sun T, Holowka T, Song Y, Zierow S, Leng L, Chen Y, Xiong H, Griffith J, Nouraie M, Thuma PE, Lolis E, Janse CJ, Gordeuk VR, Augustijn K, Bucala R (2012) A plasmodium-encoded cytokine suppresses T-cell immunity during malaria. Proc Natl Acad Sci U S A 109(31):E2117–E2126. doi:10.1073/pnas.1206573109

[PubMed][PubMedCentral]

123. White CE, Villarino NF, Sloan SS, Ganusov VV, Schmidt NW (2015) Plasmodium suppresses expansion of T cell responses to heterologous infections. J Immunol 194(2):697–708. doi:10.4049/jimmunol.1401745
[PubMed]

124. Schober T, Framke T, Kreipe H, Schulz TF, Grosshennig A, Hussein K, Baumann U, Pape L, Schubert S, Wingen AM, Jack T, Koch A, Klein C, Maecker-Kolhoff B (2013) Characteristics of early and late PTLD development in pediatric solid organ transplant recipients. Transplantation 95(1):240–246. doi:10.1097/TP.0b013e318277e344
[PubMed]

125. Tse E, Kwong YL (2015) Epstein Barr virus-associated lymphoproliferative diseases: the virus as a therapeutic target. Exp Mol Med 47:e136. doi:10.1038/emm.2014.102
[PubMed][PubMedCentral]

126. Babcock GJ, Decker LL, Freeman RB, Thorley-Lawson DA (1999) Epstein-Barr virus-infected resting memory B cells, not proliferating lymphoblasts, accumulate in the peripheral blood of immunosuppressed patients. J Exp Med 190(4):567–576
[PubMed][PubMedCentral]

127. Morscio J, Dierickx D, Tousseyn T (2013) Molecular pathogenesis of B-cell posttransplant lymphoproliferative disorder: what do we know so far? Clin Dev Immunol 2013:150835. doi:10.1155/2013/150835
[PubMed][PubMedCentral]

128. Petrara MR, Giunco S, Serraino D, Dolcetti R, De Rossi A (2015) Post-transplant lymphoproliferative disorders: from epidemiology to pathogenesis-driven treatment. Cancer Lett 369(1):37–44. doi:10.1016/j.canlet.2015.08.007
[PubMed]

129. Okoye AA, Picker LJ (2013) CD4(+) T-cell depletion in HIV infection: mechanisms of immunological failure. Immunol Rev 254(1):54–64. doi:10.1111/imr.12066
[PubMed][PubMedCentral]

130. Bibas M, Antinori A (2009) EBV and HIV-related lymphoma. Mediterr J Hematol Infect Dis 1(2):e2009032. doi:10.4084/MJHID.2009.032
[PubMed][PubMedCentral]

131. Carbone A, Cesarman E, Spina M, Gloghini A, Schulz TF (2009) HIV-associated lymphomas and gamma-herpesviruses. Blood 113(6):1213–1224. doi:10.1182/blood-2008-09-180315
[PubMed]

132. Chene A, Donati D, Guerreiro-Cacais AO, Levitsky V, Chen Q, Falk KI, Orem J, Kironde F, Wahlgren M, Bejarano MT (2007) A molecular link between malaria and Epstein-Barr virus reactivation. PLoS Pathog 3(6):e80. doi:10.1371/journal.ppat.0030080
[PubMed][PubMedCentral]

133. Wang D, Liebowitz D, Kieff E (1985) An EBV membrane protein expressed in immortalized lymphocytes transforms established rodent cells. Cell 43(3 Pt 2):831–840
[PubMed]

134. Kieser A, Sterz KR (2015) The latent membrane protein 1 (LMP1). Curr Top Microbiol Immunol 391:119–149. doi:10.1007/978-3-319-22834-1_4
[PubMed]

135.

Kempkes B, Robertson ES (2015) Epstein-Barr virus latency: current and future perspectives. Curr Opin Virol 14:138–144. doi:10.1016/j.coviro.2015.09.007
[PubMed]

136. Lajoie V, Lemieux B, Sawan B, Lichtensztejn D, Lichtensztejn Z, Wellinger R, Mai S, Knecht H (2015) LMP1 mediates multinuclearity through downregulation of shelterin proteins and formation of telomeric aggregates. Blood 125(13):2101–2110. doi:10.1182/blood-2014-08-594176
[PubMed][PubMedCentral]

137. de Lange T (2005) Shelterin: the protein complex that shapes and safeguards human telomeres. Genes Dev 19(18):2100–2110. doi:10.1101/gad.1346005
[PubMed]

138. Knecht H, Righolt C, Mai S (2013) Genomic instability: the driving force behind refractory/relapsing Hodgkin's lymphoma. Cancers (Basel) 5(2):714–725. doi:10.3390/cancers5020714

139. Knecht H, Bruderlein S, Wegener S, Lichtensztejn D, Lichtensztejn Z, Lemieux B, Moller P, Mai S (2010) 3D nuclear organization of telomeres in the Hodgkin cell lines U-HO1 and U-HO1-PTPN1: PTPN1 expression prevents the formation of very short telomeres including "t-stumps". BMC Cell Biol 11:99. doi:10.1186/1471-2121-11-99
[PubMed][PubMedCentral]

140. Righolt CH, Guffei A, Knecht H, Young IT, Stallinga S, van Vliet LJ, Mai S (2014) Differences in nuclear DNA organization between lymphocytes, Hodgkin and Reed-Sternberg cells revealed by structured illumination microscopy. J Cell Biochem 115(8):1441–1448. doi:10.1002/jcb.24800
[PubMed][PubMedCentral]

141. Righolt CH, Knecht H, Mai S (2016) DNA superresolution structure of Reed-Sternberg cells differs between long-lasting remission versus relapsing Hodgkin's lymphoma patients. J Cell Biochem 117(7):1633–1637. doi:10.1002/jcb.25456
[PubMed]

142. Hansen KD, Sabunciyan S, Langmead B, Nagy N, Curley R, Klein G, Klein E, Salamon D, Feinberg AP (2014) Large-scale hypomethylated blocks associated with Epstein-Barr virus-induced B-cell immortalization. Genome Res 24(2):177–184. doi:10.1101/gr.157743.113
[PubMed][PubMedCentral]

143. Kreck B, Richter J, Ammerpohl O, Barann M, Esser D, Petersen BS, Vater I, Murga Penas EM, Bormann Chung CA, Seisenberger S, Lee Boyd V, Smallwood S, Drexler HG, Macleod RA, Hummel M, Krueger F, Hasler R, Schreiber S, Rosenstiel P, Franke A, Siebert R (2013) Base-pair resolution DNA methylome of the EBV-positive Endemic Burkitt lymphoma cell line DAUDI determined by SOLiD bisulfite-sequencing. Leukemia 27(8):1751–1753. doi:10.1038/leu.2013.4
[PubMed][PubMedCentral]

144. Kretzmer H, Bernhart SH, Wang W, Haake A, Weniger MA, Bergmann AK, Betts MJ, Carrillo-de-Santa-Pau E, Doose G, Gutwein J, Richter J, Hovestadt V, Huang B, Rico D, Juhling F, Kolarova J, Lu Q, Otto C, Wagener R, Arnolds J, Burkhardt B, Claviez A, Drexler HG, Eberth S, Eils R, Flicek P, Haas S, Hummel M, Karsch D, Kerstens HH, Klapper W, Kreuz M, Lawerenz C, Lenze D, Loeffler M, Lopez C, MacLeod RA, Martens JH, Kulis M, Martin-Subero JI, Moller P, Nagel I, Picelli S, Vater I, Rohde M, Rosenstiel P, Rosolowski M, Russell RB, Schilhabel M, Schlesner M, Stadler PF, Szczepanowski M, Trumper L, Stunnenberg HG, ICGC MMML-Seq Project, BLUEPRINT Project, Kuppers R, Ammerpohl O, Lichter P, Siebert R, Hoffmann S, Radlwimmer B (2015) DNA methylome analysis in Burkitt and follicular lymphomas identifies differentially methylated regions

linked to somatic mutation and transcriptional control. Nat Genet 47(11):1316–1325. doi:10.1038/ng.3413
[PubMed]

145. Kulis M, Merkel A, Heath S, Queiros AC, Schuyler RP, Castellano G, Beekman R, Raineri E, Esteve A, Clot G, Verdaguer-Dot N, Duran-Ferrer M, Russinol N, Vilarrasa-Blasi R, Ecker S, Pancaldi V, Rico D, Agueda L, Blanc J, Richardson D, Clarke L, Datta A, Pascual M, Agirre X, Prosper F, Alignani D, Paiva B, Caron G, Fest T, Muench MO, Fomin ME, Lee ST, Wiemels JL, Valencia A, Gut M, Flicek P, Stunnenberg HG, Siebert R, Kuppers R, Gut IG, Campo E, Martin-Subero JI (2015) Whole-genome fingerprint of the DNA methylome during human B cell differentiation. Nat Genet 47(7):746–756. doi:10.1038/ng.3291
[PubMed]

146. Martin-Subero JI, Ammerpohl O, Bibikova M, Wickham-Garcia E, Agirre X, Alvarez S, Bruggemann M, Bug S, Calasanz MJ, Deckert M, Dreyling M, Du MQ, Durig J, Dyer MJ, Fan JB, Gesk S, Hansmann ML, Harder L, Hartmann S, Klapper W, Kuppers R, Montesinos-Rongen M, Nagel I, Pott C, Richter J, Roman-Gomez J, Seifert M, Stein H, Suela J, Trumper L, Vater I, Prosper F, Haferlach C, Cruz Cigudosa J, Siebert R (2009) A comprehensive microarray-based DNA methylation study of 367 hematological neoplasms. PLoS One 4(9), e6986. doi:10.1371/journal.pone.0006986
[PubMed][PubMedCentral]

147. Martin-Subero JI, Kreuz M, Bibikova M, Bentink S, Ammerpohl O, Wickham-Garcia E, Rosolowski M, Richter J, Lopez-Serra L, Ballestar E, Berger H, Agirre X, Bernd HW, Calvanese V, Cogliatti SB, Drexler HG, Fan JB, Fraga MF, Hansmann ML, Hummel M, Klapper W, Korn B, Kuppers R, Macleod RA, Moller P, Ott G, Pott C, Prosper F, Rosenwald A, Schwaenen C, Schubeler D, Seifert M, Sturzenhofecker B, Weber M, Wessendorf S, Loeffler M, Trumper L, Stein H, Spang R, Esteller M, Barker D, Hasenclever D, Siebert R, Molecular Mechanisms in Malignant Lymphomas Network Project of the Deutsche Krebshilfe (2009) New insights into the biology and origin of mature aggressive B-cell lymphomas by combined epigenomic, genomic, and transcriptional profiling. Blood 113(11):2488–2497. doi:10.1182/blood-2008-04-152900
[PubMed]

148. Li L, Zhang Y, Fan Y, Sun K, Su X, Du Z, Tsao SW, Loh TK, Sun H, Chan AT, Zeng YX, Chan WY, Chan FK, Tao Q (2015) Characterization of the nasopharyngeal carcinoma methylome identifies aberrant disruption of key signaling pathways and methylated tumor suppressor genes. Epigenomics 7(2):155–173. doi:10.2217/epi.14.79
[PubMed]

149. Kaneda A, Matsusaka K, Aburatani H, Fukayama M (2012) Epstein-Barr virus infection as an epigenetic driver of tumorigenesis. Cancer Res 72(14):3445–3450. doi:10.1158/0008-5472.CAN-11-3919
[PubMed]

150. Lo KW, Chung GT, To KF (2012) Deciphering the molecular genetic basis of NPC through molecular, cytogenetic, and epigenetic approaches. Semin Cancer Biol 22(2):79–86. doi:10.1016/j.semcancer.2011.12.011
[PubMed]

151. Niller HH, Banati F, Minarovits J (2014) Epigenetic alterations in nasopharyngeal carcinoma and Epstein-Barr virus (EBV) associated gastric carcinoma: a lesson in contrasts. J Nasopharyng Carcinoma 1:e9. doi:10.15383/jnpc.9

152. Yoon YJ, Kim OY, Gho YS (2014) Extracellular vesicles as emerging intercellular communicasomes. BMB Rep 47(10):531–539
[PubMed][PubMedCentral]

153. Meckes DG Jr (2015) Exosomal communication goes viral. J Virol 89(10):5200–5203. doi:10.1128/JVI.02470-14
[PubMed][PubMedCentral]

154. Record M, Carayon K, Poirot M, Silvente-Poirot S (2014) Exosomes as new vesicular lipid transporters involved in cell-cell communication and various pathophysiologies. Biochim Biophys Acta 1841(1):108–120. doi:10.1016/j.bbalip.2013.10.004
[PubMed]

155. San Lucas FA, Allenson K, Bernard V, Castillo J, Kim DU, Ellis K, Ehli EA, Davies GE, Petersen JL, Li D, Wolff R, Katz M, Varadhachary G, Wistuba I, Maitra A, Alvarez H (2016) Minimally invasive genomic and transcriptomic profiling of visceral cancers by next-generation sequencing of circulating exosomes. Ann Oncol 27(4):635–641. doi:10.1093/annonc/mdv604
[PubMed]

156. Zomer A, Vendrig T, Hopmans ES, van Eijndhoven M, Middeldorp JM, Pegtel DM (2010) Exosomes: fit to deliver small RNA. Commun Integr Biol 3(5):447–450. doi:10.4161/cib.3.5.12339
[PubMed][PubMedCentral]

157. Heusermann W, Hean J, Trojer D, Steib E, von Bueren S, Graff-Meyer A, Genoud C, Martin K, Pizzato N, Voshol J, Morrissey DV, Andaloussi SE, Wood MJ, Meisner-Kober NC (2016) Exosomes surf on filopodia to enter cells at endocytic hot spots, traffic within endosomes, and are targeted to the ER. J Cell Biol 213(2):173–184. doi:10.1083/jcb.201506084
[PubMed][PubMedCentral]

158. Liu Y, Li X (2012) Darwin's pangenesis and molecular medicine. Trends Mol Med 18(9):506–508. doi:10.1016/j.molmed.2012.07.002
[PubMed]

159. Nanbo A, Kawanishi E, Yoshida R, Yoshiyama H (2013) Exosomes derived from Epstein-Barr virus-infected cells are internalized via caveola-dependent endocytosis and promote phenotypic modulation in target cells. J Virol 87(18):10334–10347. doi:10.1128/JVI.01310-13
[PubMed][PubMedCentral]

160. Dukers DF, Meij P, Vervoort MB, Vos W, Scheper RJ, Meijer CJ, Bloemena E, Middeldorp JM (2000) Direct immunosuppressive effects of EBV-encoded latent membrane protein 1. J Immunol 165(2):663–670
[PubMed]

161. Flanagan J, Middeldorp J, Sculley T (2003) Localization of the Epstein-Barr virus protein LMP 1 to exosomes. J Gen Virol 84(Pt 7):1871–1879. doi:10.1099/vir.0.18944-0
[PubMed]

162. Ceccarelli S, Visco V, Raffa S, Wakisaka N, Pagano JS, Torrisi MR (2007) Epstein-Barr virus latent membrane protein 1 promotes concentration in multivesicular bodies of fibroblast growth factor 2 and its release through exosomes. Int J Cancer 121(7):1494–1506. doi:10.1002/ijc.22844
[PubMed]

163. Aga M, Bentz GL, Raffa S, Torrisi MR, Kondo S, Wakisaka N, Yoshizaki T, Pagano JS, Shackelford J (2014) Exosomal HIF1alpha supports invasive potential of nasopharyngeal carcinoma-associated LMP1-positive exosomes. Oncogene 33(37):4613–4622. doi:10.1038/onc.2014.66
[PubMed][PubMedCentral]

164. Mujcic H, Hill RP, Koritzinsky M, Wouters BG (2014) Hypoxia signaling and the metastatic phenotype. Curr Mol Med 14(5):565–579
[PubMed]

165. Zwaans BM, Lombard DB (2014) Interplay between sirtuins, MYC and hypoxia-inducible factor in cancer-

associated metabolic reprogramming. Dis Model Mech 7(9):1023–1032. doi:10.1242/dmm.016287
[PubMed][PubMedCentral]

166. Meckes DG Jr, Shair KH, Marquitz AR, Kung CP, Edwards RH, Raab-Traub N (2010) Human tumor virus utilizes exosomes for intercellular communication. Proc Natl Acad Sci U S A 107(47):20370–20375. doi:10.1073/pnas.1014194107
[PubMed][PubMedCentral]

167. Ikeda M, Longnecker R (2007) Cholesterol is critical for Epstein-Barr virus latent membrane protein 2A trafficking and protein stability. Virology 360(2):461–468. doi:10.1016/j.virol.2006.10.046
[PubMed]

168. Ariza ME, Rivailler P, Glaser R, Chen M, Williams MV (2013) Epstein-Barr virus encoded dUTPase containing exosomes modulate innate and adaptive immune responses in human dendritic cells and peripheral blood mononuclear cells. PLoS One 8(7), e69827. doi:10.1371/journal.pone.0069827
[PubMed][PubMedCentral]

169. Meckes DG Jr, Gunawardena HP, Dekroon RM, Heaton PR, Edwards RH, Ozgur S, Griffith JD, Damania B, Raab-Traub N (2013) Modulation of B-cell exosome proteins by gamma herpesvirus infection. Proc Natl Acad Sci U S A 110(31):E2925–E2933. doi:10.1073/pnas.1303906110
[PubMed][PubMedCentral]

170. Gutzeit C, Nagy N, Gentile M, Lyberg K, Gumz J, Vallhov H, Puga I, Klein E, Gabrielsson S, Cerutti A, Scheynius A (2014) Exosomes derived from Burkitt's lymphoma cell lines induce proliferation, differentiation, and class-switch recombination in B cells. J Immunol 192(12):5852–5862. doi:10.4049/jimmunol.1302068
[PubMed][PubMedCentral]

171. Canitano A, Venturi G, Borghi M, Ammendolia MG, Fais S (2013) Exosomes released in vitro from Epstein-Barr virus (EBV)-infected cells contain EBV-encoded latent phase mRNAs. Cancer Lett 337(2):193–199. doi:10.1016/j.canlet.2013.05.012
[PubMed]

172. Ahmed W, Philip PS, Tariq S, Khan G (2014) Epstein-Barr virus-encoded small RNAs (EBERs) are present in fractions related to exosomes released by EBV-transformed cells. PLoS One 9(6):e99163. doi:10.1371/journal.pone.0099163
[PubMed][PubMedCentral]

173. Ahmed W, Khan G (2014) The labyrinth of interactions of Epstein-Barr virus-encoded small RNAs. Rev Med Virol 24(1):3–14. doi:10.1002/rmv.1763
[PubMed]

174. Skalsky RL, Cullen BR (2015) EBV noncoding RNAs. Curr Top Microbiol Immunol 391:181–217. doi:10.1007/978-3-319-22834-1_6
[PubMed]

175. Iwakiri D (2016) Multifunctional non-coding Epstein-Barr virus encoded RNAs (EBERs) contribute to viral pathogenesis. Virus Res 212:30–38. doi:10.1016/j.virusres.2015.08.007
[PubMed]

176. Iwakiri D, Zhou L, Samanta M, Matsumoto M, Ebihara T, Seya T, Imai S, Fujieda M, Kawa K, Takada K (2009) Epstein-Barr virus (EBV)-encoded small RNA is released from EBV-infected cells and activates signaling from Toll-like receptor 3. J Exp Med 206(10):2091–2099. doi:10.1084/jem.20081761

[PubMed][PubMedCentral]

177. Niller HH, Wolf H, Minarovits J (2008) Regulation and dysregulation of Epstein-Barr virus latency: implications for the development of autoimmune diseases. Autoimmunity 41(4):298–328. doi:10.1080/08916930802024772 [PubMed]

178. Fujiwara S, Imadome K, Takei M (2015) Modeling EBV infection and pathogenesis in new-generation humanized mice. Exp Mol Med 47:e135. doi:10.1038/emm.2014.88 [PubMed][PubMedCentral]

179. Baglio SR, van Eijndhoven MA, Koppers-Lalic D, Berenguer J, Lougheed SM, Gibbs S, Leveille N, Rinkel RN, Hopmans ES, Swaminathan S, Verkuijlen SA, Scheffer GL, van Kuppeveld FJ, de Gruijl TD, Bultink IE, Jordanova ES, Hackenberg M, Piersma SR, Knol JC, Voskuyl AE, Wurdinger T, Jimenez CR, Middeldorp JM, Pegtel DM (2016) Sensing of latent EBV infection through exosomal transfer of 5′pppRNA. Proc Natl Acad Sci U S A 113(5):E587–E596. doi:10.1073/pnas.1518130113 [PubMed][PubMedCentral]

180. Pegtel DM, Cosmopoulos K, Thorley-Lawson DA, van Eijndhoven MA, Hopmans ES, Lindenberg JL, de Gruijl TD, Wurdinger T, Middeldorp JM (2010) Functional delivery of viral miRNAs via exosomes. Proc Natl Acad Sci U S A 107(14):6328–6333. doi:10.1073/pnas.0914843107 [PubMed][PubMedCentral]

181. Lodish HF, Zhou B, Liu G, Chen CZ (2008) Micromanagement of the immune system by microRNAs. Nat Rev Immunol 8(2):120–130. doi:10.1038/nri2252 [PubMed]

182. Gourzones C, Gelin A, Bombik I, Klibi J, Verillaud B, Guigay J, Lang P, Temam S, Schneider V, Amiel C, Baconnais S, Jimenez AS, Busson P (2010) Extra-cellular release and blood diffusion of BART viral micro-RNAs produced by EBV-infected nasopharyngeal carcinoma cells. Virol J 7:271. doi:10.1186/1743-422X-7-271 [PubMed][PubMedCentral]

183. Janas T, Janas MM, Sapon K, Janas T (2015) Mechanisms of RNA loading into exosomes. FEBS Lett 589(13):1391–1398. doi:10.1016/j.febslet.2015.04.036 [PubMed]

184. Yoon C, Kim J, Park G, Kim S, Kim D, Hur DY, Kim B, Kim YS (2016) Delivery of miR-155 to retinal pigment epithelial cells mediated by Burkitt's lymphoma exosomes. Tumour Biol 37(1):313–321. doi:10.1007/s13277-015-3769-4 [PubMed]

185. Szenthe K, Koroknai A, Banati F, Bathori Z, Lozsa R, Burgyan J, Wolf H, Salamon D, Nagy K, Niller HH, Minarovits J (2013) The 5′ regulatory sequences of active miR-146a promoters are hypomethylated and associated with euchromatic histone modification marks in B lymphoid cells. Biochem Biophys Res Commun 433(4):489–495. doi:10.1016/j.bbrc.2013.03.022 [PubMed]

186. Yin Q, Wang X, Roberts C, Flemington EK, Lasky JA (2016) Methylation status and AP1 elements are involved in EBV-mediated miR-155 expression in EBV positive lymphoma cells. Virology 494:158–167. doi:10.1016/j.virol.2016.04.005 [PubMed]

187. Lin Z, Swan K, Zhang X, Cao S, Brett Z, Drury S, Strong MJ, Fewell C, Puetter A, Wang X, Ferris M, Sullivan DE, Li L, Flemington EK (2016) Secreted oral epithelial cell membrane vesicles induce Epstein-Barr virus

reactivation in latently infected B cells. J Virol 90(7):3469–3479. doi:10.1128/JVI.02830-15
[PubMed][PubMedCentral]

188. Gottschalk S, Rooney CM (2015) Adoptive T-cell immunotherapy. Curr Top Microbiol Immunol 391:427–454. doi:10.1007/978-3-319-22834-1_15
[PubMed][PubMedCentral]

189. Bollard CM, Aguilar L, Straathof KC, Gahn B, Huls MH, Rousseau A, Sixbey J, Gresik MV, Carrum G, Hudson M, Dilloo D, Gee A, Brenner MK, Rooney CM, Heslop HE (2004) Cytotoxic T lymphocyte therapy for Epstein-Barr virus + Hodgkin's disease. J Exp Med 200(12):1623–1633. doi:10.1084/jem.20040890
[PubMed][PubMedCentral]

190. Bollard CM, Gottschalk S, Leen AM, Weiss H, Straathof KC, Carrum G, Khalil M, Wu MF, Huls MH, Chang CC, Gresik MV, Gee AP, Brenner MK, Rooney CM, Heslop HE (2007) Complete responses of relapsed lymphoma following genetic modification of tumor-antigen presenting cells and T-lymphocyte transfer. Blood 110(8):2838–2845. doi:10.1182/blood-2007-05-091280
[PubMed][PubMedCentral]

191. Louis CU, Straathof K, Bollard CM, Ennamuri S, Gerken C, Lopez TT, Huls MH, Sheehan A, Wu MF, Liu H, Gee A, Brenner MK, Rooney CM, Heslop HE, Gottschalk S (2010) Adoptive transfer of EBV-specific T cells results in sustained clinical responses in patients with locoregional nasopharyngeal carcinoma. J Immunother 33(9):983–990. doi:10.1097/CJI.0b013e3181f3cbf4
[PubMed][PubMedCentral]

192. Chia WK, Teo M, Wang WW, Lee B, Ang SF, Tai WM, Chee CL, Ng J, Kan R, Lim WT, Tan SH, Ong WS, Cheung YB, Tan EH, Connolly JE, Gottschalk S, Toh HC (2014) Adoptive T-cell transfer and chemotherapy in the first-line treatment of metastatic and/or locally recurrent nasopharyngeal carcinoma. Mol Ther 22(1):132–139. doi:10.1038/mt.2013.242
[PubMed]

193. Bollard CM, Gottschalk S, Torrano V, Diouf O, Ku S, Hazrat Y, Carrum G, Ramos C, Fayad L, Shpall EJ, Pro B, Liu H, Wu MF, Lee D, Sheehan AM, Zu Y, Gee AP, Brenner MK, Heslop HE, Rooney CM (2014) Sustained complete responses in patients with lymphoma receiving autologous cytotoxic T lymphocytes targeting Epstein-Barr virus latent membrane proteins. J Clin Oncol 32(8):798–808. doi:10.1200/JCO.2013.51.5304
[PubMed]

194. Manzo T, Heslop HE, Rooney CM (2015) Antigen-specific T cell therapies for cancer. Hum Mol Genet 24(R1):R67–R73. doi:10.1093/hmg/ddv270
[PubMed][PubMedCentral]

195. Dotti G, Savoldo B, Pule M, Straathof KC, Biagi E, Yvon E, Vigouroux S, Brenner MK, Rooney CM (2005) Human cytotoxic T lymphocytes with reduced sensitivity to Fas-induced apoptosis. Blood 105(12):4677–4684. doi:10.1182/blood-2004-08-3337
[PubMed][PubMedCentral]

196. Foster AE, Dotti G, Lu A, Khalil M, Brenner MK, Heslop HE, Rooney CM, Bollard CM (2008) Antitumor activity of EBV-specific T lymphocytes transduced with a dominant negative TGF-beta receptor. J Immunother 31(5):500–505. doi:10.1097/CJI.0b013e318177092b
[PubMed][PubMedCentral]

197. Perna SK, De Angelis B, Pagliara D, Hasan ST, Zhang L, Mahendravada A, Heslop HE, Brenner MK, Rooney CM, Dotti G, Savoldo B (2013) Interleukin 15 provides relief to CTLs from regulatory T cell-mediated inhibition:

implications for adoptive T cell-based therapies for lymphoma. Clin Cancer Res 19(1):106–117. doi:10.1158/1078-0432.CCR-12-2143
[PubMed]

198. Leen AM, Sukumaran S, Watanabe N, Mohammed S, Keirnan J, Yanagisawa R, Anurathapan U, Rendon D, Heslop HE, Rooney CM, Brenner MK, Vera JF (2014) Reversal of tumor immune inhibition using a chimeric cytokine receptor. Mol Ther 22(6):1211–1220. doi:10.1038/mt.2014.47
[PubMed][PubMedCentral]

199. Rosenberg SA, Dudley ME (2009) Adoptive cell therapy for the treatment of patients with metastatic melanoma. Curr Opin Immunol 21(2):233–240. doi:10.1016/j.coi.2009.03.002
[PubMed][PubMedCentral]

200. Brentjens RJ, Davila ML, Riviere I, Park J, Wang X, Cowell LG, Bartido S, Stefanski J, Taylor C, Olszewska M, Borquez-Ojeda O, Qu J, Wasielewska T, He Q, Bernal Y, Rijo IV, Hedvat C, Kobos R, Curran K, Steinherz P, Jurcic J, Rosenblat T, Maslak P, Frattini M, Sadelain M (2013) CD19-targeted T cells rapidly induce molecular remissions in adults with chemotherapy-refractory acute lymphoblastic leukemia. Sci Transl Med 5(177):177ra138. doi:10.1126/scitranslmed.3005930

201. Grupp SA, Kalos M, Barrett D, Aplenc R, Porter DL, Rheingold SR, Teachey DT, Chew A, Hauck B, Wright JF, Milone MC, Levine BL, June CH (2013) Chimeric antigen receptor-modified T cells for acute lymphoid leukemia. N Engl J Med 368(16):1509–1518. doi:10.1056/NEJMoa1215134
[PubMed][PubMedCentral]

202. Heslop HE, Slobod KS, Pule MA, Hale GA, Rousseau A, Smith CA, Bollard CM, Liu H, Wu MF, Rochester RJ, Amrolia PJ, Hurwitz JL, Brenner MK, Rooney CM (2010) Long-term outcome of EBV-specific T-cell infusions to prevent or treat EBV-related lymphoproliferative disease in transplant recipients. Blood 115(5):925–935. doi:10.1182/blood-2009-08-239186
[PubMed][PubMedCentral]

203. De Angelis B, Dotti G, Quintarelli C, Huye LE, Zhang L, Zhang M, Pane F, Heslop HE, Brenner MK, Rooney CM, Savoldo B (2009) Generation of Epstein-Barr virus-specific cytotoxic T lymphocytes resistant to the immunosuppressive drug tacrolimus (FK506). Blood 114(23):4784–4791. doi:10.1182/blood-2009-07-230482
[PubMed][PubMedCentral]

204. Brewin J, Mancao C, Straathof K, Karlsson H, Samarasinghe S, Amrolia PJ, Pule M (2009) Generation of EBV-specific cytotoxic T cells that are resistant to calcineurin inhibitors for the treatment of posttransplantation lymphoproliferative disease. Blood 114(23):4792–4803. doi:10.1182/blood-2009-07-228387
[PubMed]

205. Huye LE, Nakazawa Y, Patel MP, Yvon E, Sun J, Savoldo B, Wilson MH, Dotti G, Rooney CM (2011) Combining mTor inhibitors with rapamycin-resistant T cells: a two-pronged approach to tumor elimination. Mol Ther 19(12):2239–2248. doi:10.1038/mt.2011.179
[PubMed][PubMedCentral]

206. Ricciardelli I, Blundell MP, Brewin J, Thrasher A, Pule M, Amrolia PJ (2014) Towards gene therapy for EBV-associated posttransplant lymphoma with genetically modified EBV-specific cytotoxic T cells. Blood 124(16):2514–2522. doi:10.1182/blood-2014-01-553362
[PubMed][PubMedCentral]

207. Moosmann A, Bigalke I, Tischer J, Schirrmann L, Kasten J, Tippmer S, Leeping M, Prevalsek D, Jaeger G, Ledderose G, Mautner J, Hammerschmidt W, Schendel DJ, Kolb HJ (2010) Effective and long-term control of

EBV PTLD after transfer of peptide-selected T cells. Blood 115(14):2960–2970. doi:10.1182/blood-2009-08-236356
[PubMed]

208. Icheva V, Kayser S, Wolff D, Tuve S, Kyzirakos C, Bethge W, Greil J, Albert MH, Schwinger W, Nathrath M, Schumm M, Stevanovic S, Handgretinger R, Lang P, Feuchtinger T (2013) Adoptive transfer of Epstein-Barr virus (EBV) nuclear antigen 1-specific t cells as treatment for EBV reactivation and lymphoproliferative disorders after allogeneic stem-cell transplantation. J Clin Oncol 31(1):39–48. doi:10.1200/JCO.2011.39.8495
[PubMed]

209. Gerdemann U, Katari UL, Papadopoulou A, Keirnan JM, Craddock JA, Liu H, Martinez CA, Kennedy-Nasser A, Leung KS, Gottschalk SM, Krance RA, Brenner MK, Rooney CM, Heslop HE, Leen AM (2013) Safety and clinical efficacy of rapidly-generated trivirus-directed T cells as treatment for adenovirus, EBV, and CMV infections after allogeneic hematopoietic stem cell transplant. Mol Ther 21(11):2113–2121. doi:10.1038/mt.2013.151
[PubMed][PubMedCentral]

210. Haque T, Wilkie GM, Jones MM, Higgins CD, Urquhart G, Wingate P, Burns D, McAulay K, Turner M, Bellamy C, Amlot PL, Kelly D, MacGilchrist A, Gandhi MK, Swerdlow AJ, Crawford DH (2007) Allogeneic cytotoxic T-cell therapy for EBV-positive posttransplantation lymphoproliferative disease: results of a phase 2 multicenter clinical trial. Blood 110(4):1123–1131. doi:10.1182/blood-2006-12-063008
[PubMed]

211. Doubrovina E, Oflaz-Sozmen B, Prockop SE, Kernan NA, Abramson S, Teruya-Feldstein J, Hedvat C, Chou JF, Heller G, Barker JN, Boulad F, Castro-Malaspina H, George D, Jakubowski A, Koehne G, Papadopoulos EB, Scaradavou A, Small TN, Khalaf R, Young JW, O'Reilly RJ (2012) Adoptive immunotherapy with unselected or EBV-specific T cells for biopsy-proven EBV+ lymphomas after allogeneic hematopoietic cell transplantation. Blood 119(11):2644–2656. doi:10.1182/blood-2011-08-371971
[PubMed][PubMedCentral]

212. Leen AM, Bollard CM, Mendizabal AM, Shpall EJ, Szabolcs P, Antin JH, Kapoor N, Pai SY, Rowley SD, Kebriaei P, Dey BR, Grilley BJ, Gee AP, Brenner MK, Rooney CM, Heslop HE (2013) Multicenter study of banked third-party virus-specific T cells to treat severe viral infections after hematopoietic stem cell transplantation. Blood 121(26):5113–5123. doi:10.1182/blood-2013-02-486324
[PubMed][PubMedCentral]

2. Epstein-Barr Virus: Clinical Diagnostics

Hans-Helmut Niller[1] ✉ and Georg Bauer[2]

(1)   Institute of Medical Microbiology and Hygiene, University of Regensburg, Franz-Josef-Strauß-Allee 11, D-93053 Regensburg, Germany
(2)   Institute of Virology, University Medical Centre Freiburg, Hermann-Herder-Straße 11, Freiburg im Breisgau, D-79106, Germany

✉ **Hans-Helmut Niller**
    Email: hans-helmut.niller@klinik.uni-regensburg.de

Abstract
The vast majority of the human adult population is infected with Epstein-Barr virus (EBV), and the majority of the EBV-infected individuals tolerates the infection well, without any further symptoms after primary infection. In cases of individuals which undergo primary infection in the form of an infectious mononucleosis, or which have undergone primary infection in their past, it is sometimes important to appraise symptomatic disease or differentiate infectious mononucleosis from other conditions. In these cases, serological methods, i.e., immunofluorescence, ELISA, or Western blot, are the methods of choice to come to an unequivocal diagnostic conclusion, while the detection and quantification of viral DNA through PCR plays a minor role.

On the other hand, in a minority of the human population, EBV infection is associated or causally linked with autoimmune or malignant disease. Especially in the bone marrow or solid organ transplanted, or in otherwise severely immune-suppressed patients, prolonged EBV primary infection or EBV reactivation from latency may be a serious and life-threatening complication which needs to be diagnosed the faster the better, in order to take therapeutic steps in time. Determining the serostatus correctly is also important in these cases. However, the direct and quantitative detection of viral DNA are of importance for the diagnosis of serious EBV disease and its monitoring.

In the following, we give an overview of diagnostic methods to accurately determine EBV serostatus and viral load. We evaluate the advantages and disadvantages

of each method and report on the diagnostic significance of each and how to resolve diagnostic problems in case of uncertainties. For practical procedures, we refer to the detailed instruction manuals of the respective test kit manufacturers which have to be closely followed for reliable results.

---

1 Epstein-Barr Virus

Epstein-Barr virus was discovered by electron microscopy in cells from biopsies of Burkitt lymphomas more than 50 years ago [1]. Since then, the research on this multifaceted virus has tremendously stimulated tumor biology, tumor immunology, molecular virology, clinical virology, and virus diagnostics.

Initially, due to the history of its discovery, the focus was especially on the tumor biological aspects of EBV. The detection of the EBV genome in Burkitt lymphomas was a milestone for human tumor virology. Thereby, EBV became the first established human tumor virus, and the discovery of EBV in nasopharyngeal carcinoma (NPC) biopsies [2], and specifically in the epithelial tumor cells of NPC [3], prepared for the discovery of further human tumor viruses in epithelial cancers from a conceptual perspective. The role of the virus in tumor development in humans was later expanded as a result of the detection of EBV genomes in gastric carcinomas, certain forms of classical Hodgkin's lymphoma, rare T-cell lymphomas, and parotid tumors. The PTLD (posttransplant lymphoproliferative disease)-related lymphomas, lymphomas in patients with Purtilo syndrome, and AIDS-related lymphomas are mechanistically related, but different in their pathogenetic details [4, 5]. This group of lymphomas directly highlights the importance of an intact immune system to control EBV-infected cells and points to the role of viral latency and to the impact of EBV-driven proliferation and antiapoptotic effects. The effects of EBV on transformation and cell proliferation, however, certainly do not represent all of the aspects which are important for the participation of EBV in tumor development [6]. With respect to the distinct viral functions involved in tumorigenesis in each case, the molecular pathogenesis of diverse EBV-associated tumors must not be lumped together [7]. Based on the discovery of a binding site for *c*-Myc in the central locus control region of the EBV genome [8], a clear distinction between transformative and antiapoptotic functions for the molecular pathogenesis of PTLD -like tumors and Burkitt tumors, respectively, has been made [9]. Because recent history-centered reviews [10, 11] keep ignoring the central viral myc-binding site [8] and the interconnected concept of alternative pathogenetic pathways [9], they have to engage in low-key work-arounds and, thus, to approach the obvious solution to the

Burkitt problem, at a slower pace. Possibly, more recent data [12–14], strongly supportive of the alternative BL model [7, 15], may finally deflate the older transformation -based Burkitt lymphoma models.

The in vivo binding site for the oncoprotein *c*-Myc in the locus control region of the EBV genome suggested a specific, antiapoptotic role for EBV in Burkitt lymphomagenesis and for the first time provided a direct link between oncogene function and the viral genome in a vulnerable phase of the germinal center precursor cell for a Burkitt lymphoma [8]. This was supplemented by the understanding of the role of epigenetic control [16] and the complex effects of reactive oxygen species (ROS) [17–19], the production of which is initiated by the latency protein EBNA-1.

Primarily, the interest in the tumor biological aspects of EBV and the availability of new methods in cell biology and molecular biology enhanced the characterization of latency-related proteins of EBV such as EBNA-1, EBNA-2, EBNA-3A, EBNA-3B, EBNA-3C, LMP-1, and LMP-2, immediate early antigens (IEA), and early antigens (EA) that control the coordinated synthesis of the structural proteins VCA (viral capsid antigen) and MA (membrane antigen) and of the viral DNA in the replicative phase of the virus. This comprehensive pioneering work was of great advantage when the view on EBV was widened with respect to its importance in clinical virology.

Rather unexpected for a tumor virus, it was found that EBV infects the majority of the human population and that a distinct percentage of infected people develops mononucleosis for which EBV was proven to be the causative agent. Thereby the age at infection seemed to influence the probability of development of clinical symptoms. EBV-dependent mononucleosis was soon recognized as a clinical entity with a nonuniform appearance. Classical symptoms include large lymph nodes, pharyngitis, headache, fever, hepatosplenomegaly, hepatitis, mononuclear cells in the blood, and neurological symptoms. Due to the variability of the combination of symptoms, EBV-associated mononucleosis needs to be differentiated from primary infection with CMV , HHV-6 , HIV , rubella virus, mumps virus, and classical hepatitis viruses HAV, HBV, HCV, and HEV. There is symptomatic overlap with toxoplasmosis, brucellosis, leptospirosis, and diphtheria. Clinically overt EBV infection can be misinterpreted as leukemia and lymphoma, and the neurological symptoms require distinction from a wide variety of neurotropic infections. It is less known that acute EBV infection may become overt just as a severe infection of the respiratory tract, especially in younger children (an age group, where clinical symptoms after primary infection with EBV are usually less expected).

The potential of EBV to drive the proliferation of lymphocytes has a strong side effect on the serological diagnosis of other infections that may lead to false interpretations. EBV infection can cause polyclonal stimulation of IgG -producing memory cells, but can also trigger the proliferation of IgM -producing cells without the need of presence of the respective specific antigen. This may lead to an increase in IgG

titers directed against a random antigen and to detectable IgM responses without underlying specific interaction of the immune system with the respective agent. This situation may be especially problematic in cases where the symptoms of an EBV infection are misunderstood as being indicative of rubella infection. In this case, appearance of rubella-specific IgM due to polyclonal stimulation by EBV may be misinterpreted as indication for rubella infection. Therefore, in many cases (and all cases during pregnancy), the determination of the significance of IgM responses needs to be assured by parallel testing of serological EBV markers. If these exclude acute EBV infection, EBV-driven polyclonal stimulation is not likely. If, however, a primary EBV infection is diagnosed, further diagnostic measures need to differentiate between polyclonal stimulation due to EBV without infection with rubella virus and the less frequent, but occurring situation of double infection with both viruses. In the case of HHV-6, where IgG levels often drop below detectability a few years after primary infection, EBV infection later in live through polyclonal stimulation may cause a rise in IgG levels that even impress an experienced performer of viral diagnosis as seroconversion that seems to prove primary infection with HHV-6 [20]. In addition to the phenomenon of polyclonal stimulation, the transient immunosuppressive effect of EBV infection can lead to reactivation of other latent herpes viruses such as HHV-6, CMV , or VZV . This may lead to a strong increase in the level of VZV-IgA that is usually regarded as being indicative for primary infection with VZV or zoster [21].

Likewise, controlled latency of EBV can be influenced by iatrogenic immunosuppression or immunosuppression induced by infectious agents. As a consequence, the pool of cells that are latently infected with EBV may increase. This enhances the chance of induction of viral replication and increase the concentration of viral antigens, which in turn provokes an immunological response that may be misunderstood as indication of EBV being the cause of the clinical situation, while EBV is the target in this case. As massive immunosuppression may lead to the loss of anti-EBNA-1, an EBV-specific marker that is indicative of past infection, serological analysis may become rather ambiguous and require a broader approach for resolution.

2 EBV Serology Using Immunofluorescence

Classical EBV serology was based on the detection of VCA-IgM , VCA-IgG , and anti-EBNA-IgG, supplemented by the determination of anti-EA-IgG, using immunofluorescence techniques [22, 23]. If performed by experienced investigators, using excellent equipment and taking care of standardization, these methods were nicely reproducible and allowed quantitative measurements based on titration. VCA-IgG and VCA-IgM determinations were performed using indirect immunofluorescence with Burkitt lymphoma cell lines like P3HR-1 that were characterized by a small percentage of virus-producing cells surrounded by a surplus of latently infected, nonproductive

cells that served as internal negative control. Due to the localization and relatively high local concentration of VCA in the nucleus, anti-VCA-IgG or anti-VCA-IgM was prominent as a bright stain of VCA-positive nuclei, surrounded by the surplus of negative nuclei (Fig. 1). EA-IgG determinations were performed by indirect immunofluorescence as well, using cell lines like Raji that showed no virus replication, but allowed induction of early antigen expression in a distinct percentage of cells. As early antigens are regulatory proteins, their concentration is much lower than that of structural proteins like VCA. Therefore, classical EA-IgG tests in contrast to VCA-IgG and VCA-IgM represented test systems with a suboptimal concentration of antigen and therefore only gave a positive response when very high concentrations of anti-EA antibodies were present. Therefore, using indirect immunofluorescence, EA-IgG was usually found positive in exceptional cases and was regarded as a marker for virus reactivation, often in connection with clinically problematic cases. Measurement of EA-IgG in healthy people with past EBV infection was rare. As EBNA proteins are found in extremely low concentrations in EBV-positive cells, detection of antibodies directed against EBNA was not possible when the indirect immunofluorescence technique was used. First of all, this is a good message, because otherwise VCA-antibody determination would not have been possible due to overlap with anti-EBNA reactivity. For the detection of anti-EBNA, an additional amplificatory step was required. This step took advantage from the intriguing finding that antibodies against EBNA always seem to be complement-binding antibodies, even years after primary infection, although complement-binding antibodies are usually shorter-lived. After binding of anti-EBNA to its target protein, the assays were washed, and the antibody complexed to EBNA was confronted with human complement that bound to the complex and built a platform for subsequent binding of many anticomplement IgGs labeled with the fluorescence label (Fig. 2).
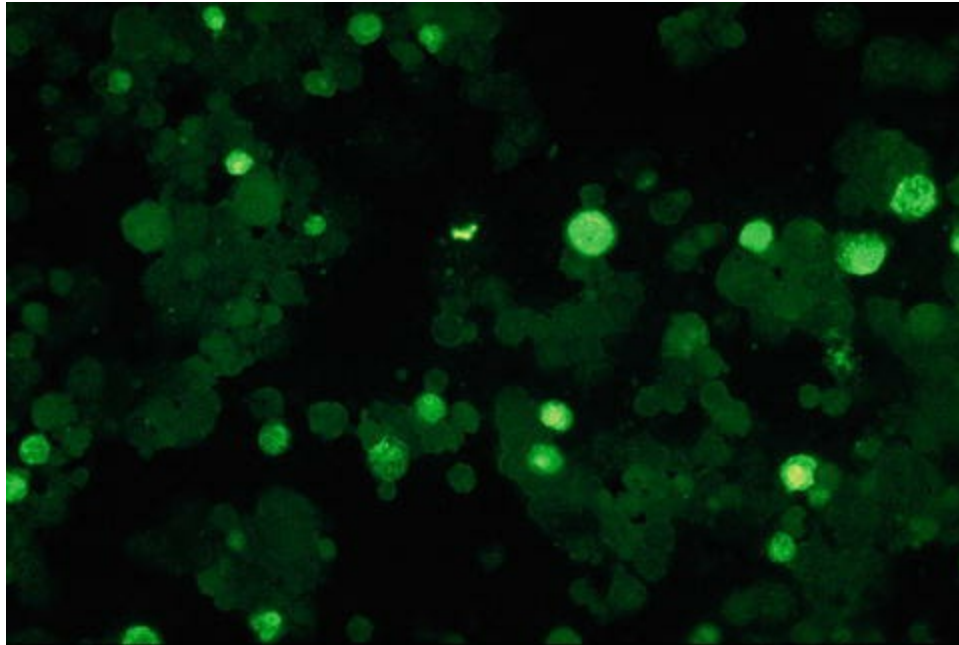
Fig. 1 Determination of VCA-IgG using indirect immunofluorescence
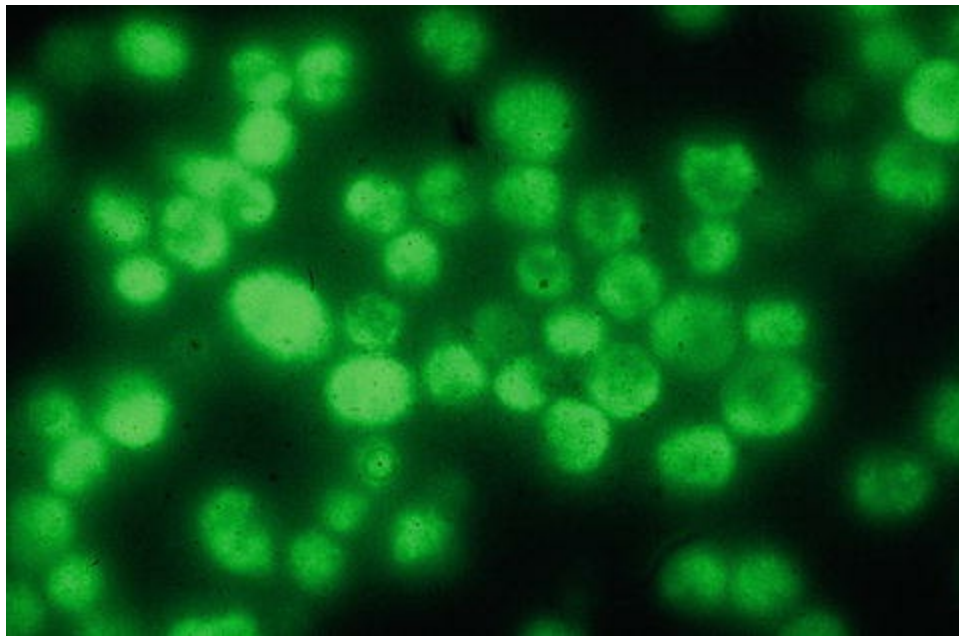
Fig. 2 Anti-EBNA-1 test using anticomplementary immunofluorescence

A positive VCA-IgG and VCA-IgM finding was considered as evidence for an acute EBV infection. Negative VCA-IgM in case of positive VCA-IgG was considered as past infection. Retrospective analysis showed that this approach did not lead to correct conclusions in all cases and therefore had a high degree of insecurity when an individual case had to be diagnosed. The major problem was associated with IgM tests. Competition between IgG and IgM caused suppression of IgM detection, and therefore the determination of the true IgM status would have required the removal of IgG in all

serum samples before the IgM test. But even then, a significant percentage of sera from patients with secured primary EBV infection did not show positive IgM responses. In the study by Schillinger et al. (1993), nearly 20 % of sera from acute infections were IgM negative. Several reasons sum up to this problematic number: (1) the IgM response is below the detection level; (2) the IgM response would have been detectable only for an extremely short period, and the first serum was taken too late; (3) the IgM test was not sufficiently sensitive; and (4) the competing IgG was not sufficiently removed. On the other side, VCA-IgM responses persisted for up to a year and more after acute infection, causing misinterpretation if only the late sera were tested [23, 24]. It was therefore neither possible to derive a reliable indication for an acute EBV infection from a positive VCA-IgM finding nor could an acute infection be ruled out with absolute certainty on the basis of the absence of an IgM response. Therefore, many laboratories used anti-EBNA testing as regular supplementary method, as anti-EBNA was regarded as a late marker. Therefore, its positivity was taken as clear exclusion of acute EBV infection. However, it was soon realized by many investigators that nonselective anti-EBNA testing by anticomplementary immunofluorescence was not as specific as initially anticipated. The reason for this is due to anti-EBNA-2 positivity in about 30 % of acute infections at the onset of clinical symptoms [24]. The problem was solved through the use of Burkitt lymphoma cells with deleted EBNA-2 gene that allowed to focus on anti-EBNA-1 responses specifically. A positive anti-EBNA-1 response therefore was indicative of secured past infection with EBV, provided parallel testing with an EBV-negative Burkitt lymphoma cell line produced evidence for the absence of anticellular reactivities that mimicked anti-EBNA-1 responses in some cases. The problem of anticellular reactivity was especially overt for anti-EBNA testing, as all cells contain EBNA, and therefore the test in its classical version has no internal negative antigen control. As anti-EBNA-1 is detectable at the earliest 4 weeks after the onset of the disease after acute EBV infection, it was possible to rule out with certainty an acute EBV infection in the case of positive anti-EBNA-1. Whereas a specifically positive anti-EBNA-1 response (especially in combination with a positive VCA-IgG) clearly excluded an acute EBV infection, negative anti-EBNA-1 in combination with VCA-IgG did not allow a conclusive interpretation, though this constellation was regularly found in acute infections. The reason for this failure is the fact that about 6 % of healthy persons with past EBV infection never develop a detectable anti-EBNA-1 response and that previously anti-EBNA-positive people may lose anti-EBNA-1 selectively during massive immunosuppression due to iatrogenic intervention or immunosuppression based on infections, immune disorders, or tumors.

Therefore, even optimally performed and controlled EBV serology using immunofluorescence tests found its limitation by (1) about 5 % of unresolvable cases due to anticellular reactivities and (2) insecure differentiation between negative anti-EBNA-1 due to primary infection from negative anti-EBNA-1 due the failure to develop

this marker or due to secondary loss of this marker. Therefore, a high degree of uncertainty with respect to the unequivocal diagnosis of acute EBV infections was not resolvable, whereas past EBV infections were diagnosed with high confidentiality. Though these cases represent the majority in routine diagnosis, the situation as a total was not bearable and required further steps for improvements. The use of avidity determination as an additional diagnostic tool in combination with immunofluorescence techniques will be discussed in a later section. The following sections discuss the use of recombinant viral proteins for further improvement of EBV serology.

The majority of diagnostic labs is not using the anti-EBV indirect immunofluorescence assay anymore. Among those labs, only a very small minority of experts are preparing their glass slides which carry infected cells expressing EBV antigens by themselves. Therefore, here we do not provide a step-by-step protocol for preparing glass slides and performing the indirect anti-EBV immunofluorescence assay. For those who choose to use it routinely, there are several manufacturers who sell ready-to-use assay IFT kits with detailed instruction manuals included.

3 The Use of Recombinant EBV Proteins in Western Blots and Line Assays

The development of immunoblots (Western blots) with recombinant antigens represents an important milestone in the improvement of EBV diagnostics [25]. In particular, p72 (EBNA-1, viral gene BKRF1, i.e., BamHI restriction fragment K, rightward frame 1), p23 (BLRF2, a component of VCA), and the early proteins p54 (BMRF1) and p138 (BALF2) were used in the first generation of commercially available Western blots [26]. Later, p18 (BFRF3) , another component of VCA, was added in various assays. It is important to note that the antibody response to unprocessed p18 is similar to that directed against p23, i.e., it is a marker that is detected relatively early in infection and that defines specific seropositivity. In contrast, Mikrogen patented a processed p18 that provided only epitopes that are recognized late in infection, and thus this marker is useful as a late marker, in analogy to p72. Sera from patients with acute EBV infection are regularly negative for p18(mod)-IgG during the first 3 weeks after onset of disease.

Compared to assays based on immunofluorescence, the blot had several advantages. (1) Because recombinant, highly purified antigens were used, the problem of anticellular reactivity (a problem in 5 % cases tested by immunofluorescence) was no longer an issue. (2) Due to the use of recombinant antigens, the test system now contained sufficiently high concentrations of antigens. Thus, the test result was solely dependent on the concentration of antibody and therefore their precise quantitation was relatively easy.

Whereas the patterns of antibodies directed at VCA and EBNA-1 were rather

congruent, independently of whether they were detected by immunofluorescence or immunoblots, the determination of anti-EA-IgG showed major differences and was the cause of frequent misinterpretation. Due to the low concentration of EA proteins in immunofluorescence, only sera with very high titers gave a significant response with this method. Frequently, these were cases with acute infections or reactivations after immunosuppression. EA-IgG (detected by immunofluorescence) was therefore regarded as a marker indicative for recent active interaction between the immune system and EBV. In contrast, the high concentration of recombinant EA in immunoblots allowed to determine the true serostatus with respect to anti-EA. Depending on the EA markers used, at least 20 % of healthy people with past EBV infection were positive [27, 28]. Also, unexpectedly and in contrast to the experience obtained before with immunofluorescence, EA-IgG detectable by immunoblot very frequently stayed positive over very long periods. In addition, the kinetics of appearance of EA-IgG during acute EBV infection showed a major difference, depending on the method used. Whereas EA-IgG determined by immunofluorescence usually became detectable after VCA-IgG, EA-IgG detected by sufficiently high concentrations of recombinant EA usually was the first positive marker in acute EBV infection analyzed by immunoblot.

Whereas the molecular weight of viral proteins determined their position on the immunoblot (Western blot) stripes, the line assay, in which recombinant antigens were transferred onto nitrocellulose after extensive purification, allowed to group the antigens according to early and late antibody response with respect to the onset of disease. A high degree of purification of proteins was necessary to ensure that the degree of specificity of responses determined by the line assay was the same as determined by immunoblot [29]. It has to be pointed out that not the blotting procedure itself determines the specificity reached by either method, but the degree of purity of the applied proteins.

The distribution of a specific protein within a band on immunoblots is characterized as Gaussian distribution, due to the movement of the proteins during electrophoresis. In contrast, purified proteins applied to the line assay show an equal concentration over the area of a distinct band. This difference has a major impact on the antigen/antibody reaction and its quantification. Antibodies interacting with a protein band on immunoblots face the highest antigen concentration in the middle of the band, with decreasing concentrations to both sides. Therefore, the reaction kinetics with a given antibody concentration is the highest in the middle and decreases within the band. This complex reaction is the basis for the finding that testing of serum dilutions in an immunoblot does not only lead to a decrease in staining but is paralleled by a change in the broadness of the band (Fig. 3). In contrast, testing dilutions of sera on line assays results in a decrease of the intensity, but not in the size or shape of the bands (Fig. 4). This is due to the equal distribution of antigen within the band leading to homogenous reaction kinetics at all sites of the band. Therefore, tests that require rather precise

measurements, like avidity determination, are preferably established by line assays.
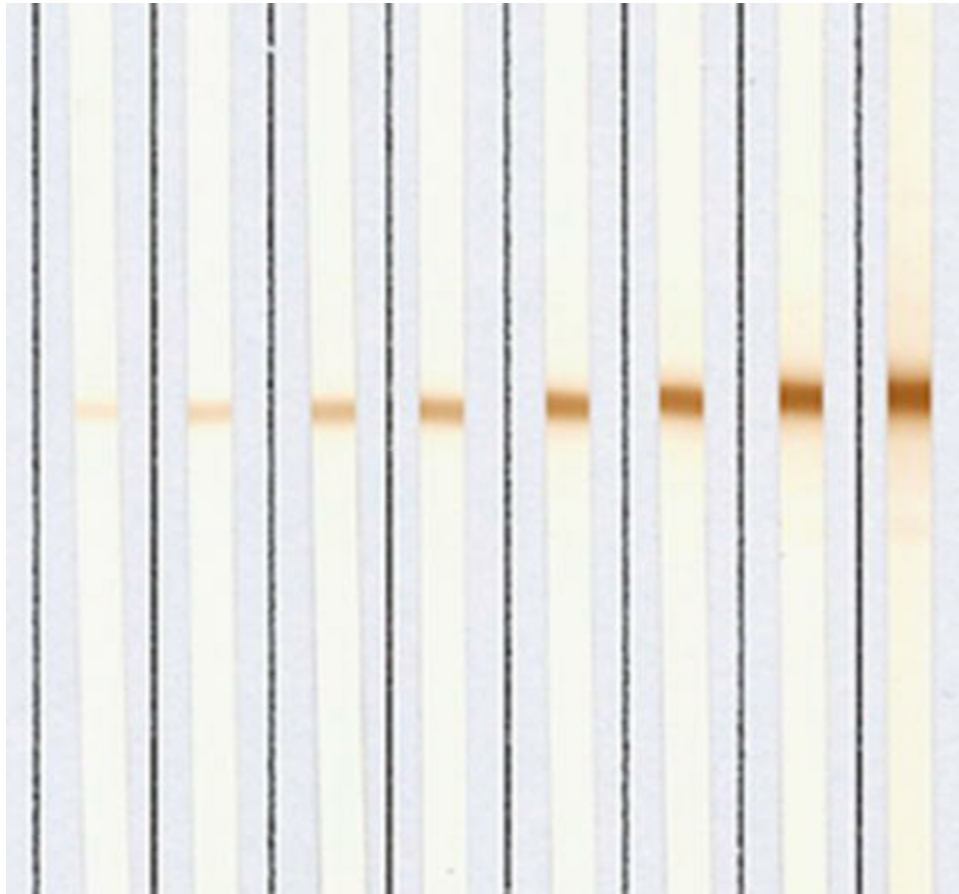
Fig. 3 Titration of a positive serum using immunoblot stripes. Dilution of the serum (from *right* to *left*) causes a decrease in intensity as well as a change in the size of the band
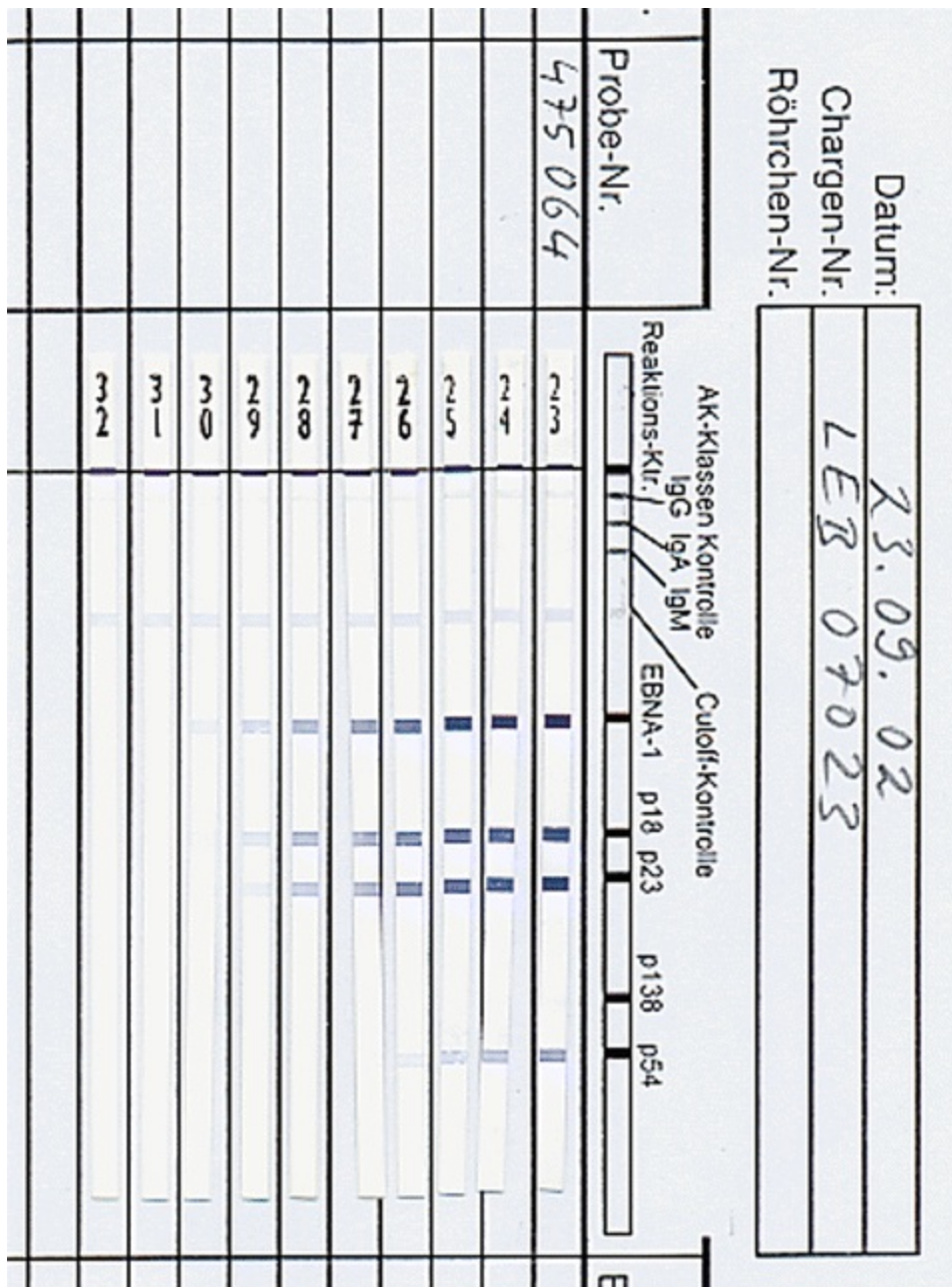
Fig. 4 Titration of a positive serum using a line assay. Dilution of the serum (from *right* to *left*) causes a decrease in intensity without a change in the size of the band

For the practical blot procedure, we refer to the test manuals which are always included in the assay kits of the respective supplier and have to be followed in detail. Test strips, dilution and washing buffers, and conjugate and substrate solutions are always included in assay kits. In the following, we give an exemplary short description for a blotting procedure:

1. Pipet 2 mL of dilution or wash buffer into each well on an incubation tray. Wash buffer is a phosphate-buffered salt solution containing skim milk powder to block

nonspecific binding of serum antibodies to the test strips.

2. Using a plastic forceps, place a nitrocellulose test strip into the wells without skin contact and without damaging the strip.

3. Submerge the strip through gentle shaking.

4. Add 20 μL of the serum to be analyzed.

5. Cover the tray with a plastic lid and shake gently for 1 h on a horizontal shaker at room temperature.

6. After 1 h of serum incubation, pipet off the liquid, using a fresh pipet tip for each well or an aspirating device.

7. Wash off serum traces by three cycles of adding 2 mL of washing buffer, shaking 5 min, and pipetting off the washing buffer, always taking care to avoid cross contamination with serum antibodies between the wells.

8. Add 2 mL of freshly prepared conjugate solution and shake for 45 min at room temperature, while the tray is covered with a plastic lid. Conjugate contains an antihuman rabbit antibody labeled with horseradish peroxidase (HRP). Conjugates are specific for human IgG , IgM , or IgA . Thus, take care to choose the appropriate conjugate for the type of strip (IgG, IgA, or IgM) to be analyzed.

9. Pipet off the conjugate solution, using a fresh pipet for each well or aspirating device.

10. Wash off conjugate traces three times as above.

11. Add 1.5 mL of substrate solution and incubate for 5–10 min, by shaking gently at room temperature. Substrate solution contains the chromogenic substrate tetramethylbenzidine which is oxidized by the HRP that is conjugated to the secondary rabbit antibodies.

12. Pipet off the substrate solution or use an aspirating device.

13. Wash three times with deionized water as above.

14. Dry test strips for 2 h between two layers of absorbent paper.

15. Read out results according to the respective manufacturer's instruction manual.

16. Store the strips dry and protected from exposure to light.

---

4 Avidity Determination as an Additional Diagnostic Tool

Affinity maturation of the IgG response is known as a unidirectional and regularly occurring process during the establishment of an immune response [30]. The biological basis for this process is determined (1) by the need of IgG-expressing B-cell clones to receive the specific antigen as stimulus for survival and proliferation and (2) by constant mutagenesis in the Fab structure. A few cell clones thus may eventually present IgG that binds the antigen with higher affinity. These clones are positively selected, whereas proliferation and survival of the parental clones is impaired. Stepwise cycles of mutagenesis and selection finally lead to clones that generate IgG with high affinity for the specific epitope structure. Plasma cells derived from these clones will be the source of high-affinity IgG. Affinity represents a complex biophysical principle that is not trivial to measure. For routine diagnosis, therefore, the determination is restricted to the strength of the binding between antigen and antibody. This measurement has been termed avidity determination and is representative for overall affinity. Please note that formerly the term avidity was also used to describe the complexity of antibody populations, e.g., against flagella of bacteria. The historic term has a different biological background and is not suitable in the context of avidity as defined above. Avidity determination has been applied to EBV serology and has been found to resolve certain problematic diagnostic cases [31, 32]. These initial studies used quantitative immunofluorescence and 6 M urea for the disaggregation of antibody/antigen complexes. Test slides were incubated with serum dilutions, and parallel slides were either treated with secondary fluorescent antibodies as usual or were treated with 6 M urea for 3 min, washed, and then processed like the control. The comparison between the titers was used to determine the avidity index. This procedure required a high standardization of quantitation of immunofluorescence titers. The maturation kinetics of VCA-IgG avidity was very fast. Only during the first 10 days after the onset of disease all sera from acute EBV infections showed low avidity. Thus, the application was more or less restricted to sera that were taken immediately after the onset of disease (a rare situation in present health management). Avidity determination was established for

immunoblots and line assays in a patented application form. This approach has the advantage that the avidity of antibodies directed against several distinct antigens can be determined in one test. The major advantage was, however, that due to the larger concentration of recombinant antigen in the test system, the measured kinetics of avidity determination was much slower and with a later onset than the determination by immunofluorescence . This seemingly paradoxical finding is explained by less competition between antibodies with high, intermediate, and low affinity in the immunoblot and line assay. In the immunofluorescence test with its lower concentration of antigen, high-affinity antibodies will compete out antibodies with intermediate or low affinity and thus overestimate high affinity. When this competition is lowered through supply with higher concentrations of antigen (immunoblot and line assay), sera containing a mixture of low-, intermediate-, and high-affinity antibodies can be differentiated from sera that only contain high-affinity antibody. In this way, the true status with respect to affinity is determined, and the kinetics of maturation allows conclusions even if the sera are not taken immediately after the onset of disease. It was found that the determination of avidity for the markers p23-IgG , p18-IgG, and p72-IgG was useful for discrimination between acute and past EBV infections, whereas avidity determination of markers from the EA-IgG complex was not suitable due to high variability .

5 Variability of the Serological Response After EBV Infections

The tests of non-preselected sera using a commercial line assay (Mikrogen) showed that the serological responses following EBV infections are defined by a certain basic pattern, but that a high degree of variability can also be observed regularly due to the stochastic processes inherent to the immune reaction. This is summarized in Tables 1 and 2.

Table 1 Main groups within 1577 cases tested in EBV serology using a line assay with recombinant antigens

	Number	Percent
Total number of sera	1577	100
Seronegative for EBV	90	5.7
Borderline	7	0.4
Acute EBV infections	42	2.6
Past EBV infections	1438	91.2

Table 2 Variability of the serological response in past EBV infections determined by a line assay with recombinant antigens

	Number	Percent
Past EBV infections	1438	100
Classical (p72-IgG and p18-IgG > +)	1154	80.2
p72-IgG and p18-IgG +	7	0.5
p72-IgG +, p18-IgG > +	86	6.0
p18-IgG +, p72-IgG > +	29	2.0
p72-IgG neg., p18-IgG > +	106	7.4
p18-IgG neg., p72-IgG > +	11	0.8
p23-IgG neg.	20	1.4
Isolated p23-IgG (high avidity)	5	0.3
Isolated p18-IgG (high avidity)	5	0.3
Isolated p72-IgG (high avidity)	3	0.2
Recent EBV infections (p18-IgG low avidity, p72-IgG neg.)	12	0.8

Using the cutoff band as reference, we differentiated between negative, +, ++, +++, and ++++ positive sera. Sera showing ++ to ++++ reactivity were grouped and named ">+". For simplicity, the term "p18-IgG" has been used for IgG directed against modified p18, which represents a late marker

From 1577 non-preselected sera, which were tested with the line assay, a relatively low percentage was identified as seronegative, and an even lower percentage was identified as acute infection. The majority of sera displayed the picture of a past EBV infection, whereby most sera showed the classical picture with both late markers (p72-IgG and p18-IgG). A very small percentage exhibited one or both late markers in a weakly pronounced way. In 7.4 % of cases, p72-IgG was negative, but the second marker p18-IgG (which exhibited high avidity) allowed the diagnosis of "past EBV infection" in these cases. Conversely, only 0.8 % of past infections exhibited negative p18-IgG and positive p72-IgG . This finding underlines the improvement of diagnostics through combining two late markers and thus preventing inaccurate findings. It shows in particular the stochastic component which plays an important part in serological responses. The finding allows the assumption that the immune system of an affected person incidentally failed to form antibodies against p72 or p18. By accepting this point of view, it can be predicted that, according to the law of probability, a small number of cases should occur in which both late markers are not formed, despite past EBV infection. Five such cases have in fact been found within this study and they confirmed the plausibility of the preceding assumption. Of course, on a first glance, these p18-IgG /p72-IgG-negative cases of past EBV infections resemble acute infections, in which both late markers have not yet been formed. However, a differentiation could be achieved here with the aid of avidity determination, as the rare cases of past infection with missing p72- and p18-IgG showed p23-IgG of high avidity.

The stochastic problem of nonrecognition of epitopes of a certain antigen also arises in the case of p23. It is seen that in 1.4 % of cases with past EBV infections, p23-IgG is not detected. However, these cases could still be identified with certainty as past EBV infection as they showed p72-IgG and p18-IgG of high avidity. The combination of the absence of certain markers in rare cases is the basis for the predictable and actually found constellation in which "isolated p72-IgG" and "isolated p18-IgG" occur. Finding such rare constellations is therefore not a shortcoming of the test system, but rather evidence of the precision with which the stochastic variability of the serological response is measured. It proves that a reliable finding can be derived from it in every single case, despite being different from the basic pattern.

After all, a small fraction of cases exhibit the characteristic of a recent EBV infection in which only one of the two late markers, namely, p18(mod)-IgG, is positive, while p72-IgG is still absent. A differentiation between "recent" and "past (without p72-IgG)" is here achieved through the detection of a low-avidity p18-IgG in combination with an p23-IgG that already shows high avidity.

These cases demonstrate the efficiency of EBV serology by line assays and show the significance of the avidity determination with the aid of this method. The application of the *recom*Line EBV assay (Mikrogen) in avidity determination naturally allows determining the avidity of antibodies against several antigens in parallel. Figure 5 outlines the idealized progression (basic pattern) of the serological response and its avidity maturation following an acute EBV infection. At first, a successive occurrence of the markers BZLF1-IgG, p54-IgG, p138-IgG , and p23-IgG is noticeable in the beginning, before the late markers p18(mod)-IgG and p72-IgG appear. p23-IgG exhibits low avidity early on. The late markers normally appear successively, first p18-IgG and then p72-IgG. They too initially show low avidity, which matures to higher avidity later on. With it the approach to a rational and reliable appraisal is specified: if both late markers are present, an acute EBV infection can be ruled out. An additional investigation of the status with the aid of avidity determination will normally not be necessary in case of these sera. If one of the two late markers is missing, then the detection of the other late marker nevertheless allows, supported by the high avidity of the detected marker and the high avidity of p23-IgG, to reliably diagnose the infection as "past EBV infection." An analogous procedure would be followed when in very rare cases both markers are present, while p23-IgG is missing.
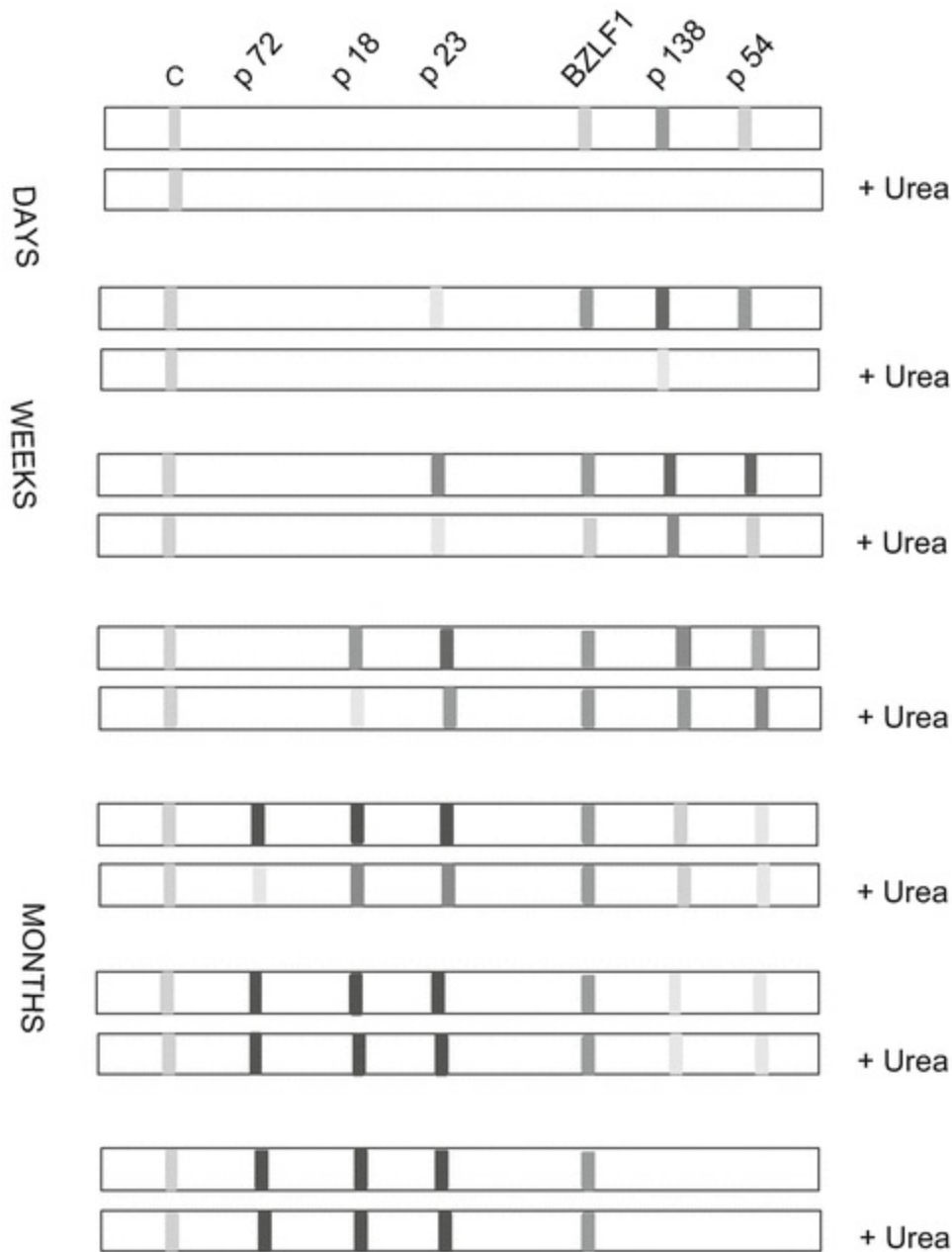
Fig. 5 Basic pattern of appearance of the IgG response after EBV infection measured by the recomLine assay. At the onset of disease, antibodies against BZLF1 (immediate early protein), p138 and p54 (early proteins), are the first ones to be detectable and usually still exhibit low avidity, as demonstrated by the urea-treated parallel test strip. Low-avidity IgG against p23 (viral capsid antigen) appears next. While the avidity of p23-IgG is maturing, the late markers p18-IgG (directed against the modified p18, viral capsid antigen) and p72-IgG (directed against EBNA-1) appear after 3–4 weeks after the onset of disease and show avidity maturation later on. In past infection, p23-IgG, p18-IgG, and p72-IgG exhibit high avidity. IgG directed against p138, p54, and BZLF1 may disappear or remain detectable. In contrast to p72-, p23-, and p18-IgG, IgG against the BZLF1, p54, and p138 may exhibit low avidity even in past infection. This finding is explained by the recognition of new epitopes during silent and clinically irrelevant reactivation of the virus. Therefore, avidity determination for the distinction between acute and past infection has to be restricted to p23-, p18-, and p72-IgG. As shown in Table 2, in a significant percentage of people, certain markers may be missing. This diagnostic problem can be resolved through the determination of two late markers, combined with avidity measurement.

Through the use of line assays with recombinant antigens in combination with avidity measurement in the same test systems, a high diagnostic reliability can be achieved for each individual case. Avidity determination is only necessary in cases which are seropositive for EBV, but have no detectable late markers. The additional time and effort required for an avidity determination is therefore reserved for a selected segment of sera, but then it will ensure an accurate diagnosis in the individual case.

6 Diagnostic Examples

Figure 6 exemplarily demonstrates the use of a commercial line assay with recombinant antigens (Mikrogen) for the serological analysis of acute EBV infection in Case #1. Cases #2–#4 are then discussed without showing the original line assays. *Case #1*: a 17-year-old girl showed the symptoms of infectious mononucleosis . The first serum sample was taken 1 day after the onset of disease. It was positive for p138-IgG and p54-IgG. P23-IgG was below the cutoff. This constellation indicated seropositivity for EBV. Based on our knowledge of the variability of the serological response as outlined in the chapter before, the constellation was in line (1) with the assumption of acute infection and (2) with the less likely assumption that it was a past infection with missing p72- and p18-IgG and very low p23-IgG. Serum #2, taken 4 weeks later, showed the increase in the p23-IgG response that was still of low avidity and thus allowed the conclusive diagnosis of acute EBV infection. A control after 8 additional months confirmed this statement and showed the appearance of the late markers p72- and p18(mod)-IgG that showed high avidity, like p23-IgG.

Fig. 6 Application of a commercial EBV line assay, including avidity determination. Serum #1 was taken at the onset of EBV-related symptoms in a 17-year-old girl and was tested in the line assay with recombinant antigens. The next serum (serum #2) was taken 4 weeks later and final control was taken 8 months later (serum #3). Serums #1–3 are directly compared (positions 1–3). Positions 6–7, 9–10, and 12–13 show the avidity determination for sera #1–3. Positions 6, 9, and 12 are the control tests; positions #7, 10, and 13 are the tests treated with urea after first incubation. Positions 17–30 are repeats of the avidity determination and demonstrate the interassay reproducibility of the test system

In most cases, p23-IgG is present in the first sample and thus avidity determination is possible and useful to secure the serological diagnosis. This is especially relevant in cases where the clinical symptoms are not convincingly clear or the age of the patient is not typical for primary EBV infection.

Case #2 is a 50-year-old male patient with lymphadenitis and fever. He was found positive for VCA-IgG and VCA-IgM using indirect immunofluorescence and anti-EBNA-1 negative in an ELISA test. Though this constellation is typical for acute EBV infection, in light of the untypical age of the patient for primary infection, the task was to exclude that positive VCA-IgM was due to reactivation, and negative anti-EBNA-1 was due to loss of anti-EBNA-1 under immunosuppression . The serum was found positive

for p23-, p138-, and p54-IgG in the line assay with recombinant antigens. All three markers were of low avidity and thus allowed secure diagnosis of acute EBV infection.

Case #3 is a 36-year-old male patient from the oncological ambulance, showing multiple lymphomas. Testing his serum in the line assay with recombinant EBV antigens showed p23- and p54-IgG of low avidity and p138-IgG of high avidity. Low avidity of p23-IgG combined with the absence of late markers was taken as indication for acute EBV infection.

Case #4 is a 22-year-old male patient with symptoms of infectious mononucleosis . The serum showed isolated p23-IgG; thus, the missing late markers were indicative for acute infection, but the absence of p138- and p54-IgG was unusual. Therefore, avidity determination was used for clarification. The isolated p23-IgG was of low avidity and thus allowed the serological diagnosis of acute EBV infection. This case is contrasted by numerous cases (data not shown) where isolated p23-IgG was of high avidity and therefore did not allow the diagnosis acute EBV infection. Rather, they seemed to represent rare cases with both late markers missing despite past infection.

7 Additional Methods for EBV Serology

The section on immunofluorescence techniques has taught us the principles and problems of EBV serology; the subsequent sections have shown us how the use of recombinant antigens in combination with avidity determination can resolve most cases. Thereby the high variability of the serological response has to be kept in mind. Based on these facts, any format of a test system can be used that utilizes defined, purified antigens at sufficient concentration and combines several antigens to allow differentiation between early and late markers and to cope with the stochastics in the immune system that leads to unusual cases. Therefore, the evaluation of any new test system must not be based solely on selected "typical cases" for past and acute EBV infections as these only reflect part of reality (as shown in Table 2).

8 Enzyme Immunoassay (EIA) Testing

EIA tests by several manufacturers with purified recombinant antigens, native antigens, or synthetic peptides have been on the market for many years [33, 34]. Certainly, their advantage is their speed of operation and, especially in the case of robotic systems [35, 36], significantly less hands-on time, compared to the line assay. This fact and the pricing is certainly the reason that most commercial diagnostic virology labs use the EIA format for conducting EBV serology. All EIAs deal with the same restricted set of antibodies, i.e., anti-VCA-IgM , anti-VCA-IgG , and anti-EBNA1-IgG, some of them including also anti-EA [33, 34]. Principally, the three main test parameters should suffice to clearly determine seronegativity as well as past infection with classical

serological markers and thus allow a secure conclusion in about 80 % of routine sera. Due to the variability of the serological response, these three markers are, however, not sufficient to unequivocally discriminate between acute infection on one side and past infection with either missing anti-EBNA-1 or secondary loss of anti-EBNA-1 on the other side. VCA-IgM is not discriminating between these cases, as it may be aberrantly missing during acute infection in some cases and may either persist or become reactivated in cases with past infection but negative anti-EBNA-1. Therefore, up to 20 % of cases from routine diagnosis can be expected to require other methods, like the line assay in combination with avidity determination in addition to EIA testing. In line with these findings, it is not surprising that, in a comparative analysis with IFA as the reference standard of the time, Gärtner et al. concluded that among four manufacturers of EIAs, due to the different composition of antigens and different interpretation criteria, only two of the tests were useful. Therefore, the authors emphasized the need for a standardization of the interpretative criteria between manufacturers [34]. A more recently developed robotic chemiluminescent microparticle assay (CMIA) system, which belongs to the larger EIA test group as well, compared favorably with the IFA and the line assay in two comparative analyses, with sensitivities and specificities for correctly categorizing primary infection, past infection, and seronegativity of well above 90 % [35, 36]. If sequential testing was applied, i.e., anti-EBNA-1 testing was done first, a substantial cost saving was obtained. In cases of positive anti-VCA-IgM, additional anti-CMV -IgM testing was recommended in one study, because cross-reactivity of anti-VCA-IgM in CMV primary infections was frequently observed [36]. The overall favorable performance of the CMIA accords with our own experience when we compared CMIA results for 90 routine sera with the results of the line assay as the reference standard of today. Only less than 5 % of our routine serum panel could not be clearly resolved by the CMIA (unpublished data). Therefore, it is reasonable to use a suitable robotic EIA format for routine testing in the commercial diagnostic virology laboratory. However, a small percentage of more complex or problematic clinical cases which cannot be resolved by EIA tests should be followed up with the line assay which provides a more differentiated conclusion, including the two abovementioned late markers and avidity testing .

9 PCR Testing

Besides CMV , EBV is the major viral pathogen in solid organ or bone marrow transplant patients demanding regular viral load determination in patient groups at high risk of acquiring posttransplant lymphoproliferative disease (PTLD) . The risk to acquire EBV disease is particularly high, when the organ donor and recipient are discordant and the organ recipient is seronegative for EBV. Because serological reactivation, e.g., as documented by anti-VCA-IgM positivity or additional parameters,

does not correlate with the viral load in immune-suppressed patients, EBV serological testing is not useful at all in this patient group, besides for establishing past infection [37]. Thus, while serological testing is applied to differentiating primary infection, past infection or seronegativity in individuals with a functional immune system, EBV testing in patients with immune suppression or EBV-associated malignancies is the domain of PCR testing. Together with quantitative anti-EBV-IgA antibodies as an adjunctive marker, blood viral load testing may be used for screening, for the detection of relapses, and for therapy monitoring of EBV-associated malignancies in high prevalence areas [38, 39].

Numerous commercial and in-house quantitative PCR formats are in use. If utmost sensitivity of virus detection is desired, the internal viral BamHI W-repeat which occurs between 7 and 11 times per viral genome is usually used as PCR target. For exact viral load quantitation, however, a viral single-copy gene must be the target of choice. Because many different viral genes are targeted by PCR assays, international standardization of quantitative PCR results may improve comparability in the future. Regarding the sample of choice, any clinical material may be analyzed for viral load, i.e., serum, plasma, whole EDTA blood, peripheral blood mononuclear cells (PBMCs), or tissue biopsies. Suspicion of EBV-positive PTLD must be raised, when the viral load rises between 10,000 and 100,000 copies/mL serum, plasma, or whole blood or between 1000 and 10,000 copies/million isolated PBMCs. However, it is important to keep in mind that there is considerable variation in viral loads, that also much lower viral loads can signify manifest PTLD, and that no clearly defined threshold and no single preferred type of clinical material exist in diagnosing PTLD. In most laboratories, whole blood is used for initial screening [40]. In case of doubt, more than one type of sample have to be tested, and serial monitoring of the same sample type is helpful to notice dynamic changes also of low viral loads in time and thereby speed up therapeutic intervention [38, 41]. Particularly, PTLD of the central nervous system sometimes coincides with zero viral copies/mL of peripheral blood. In such cases, in situ hybridization for EBV-encoded small nuclear RNAs (EBERs) in tissue sections from brain biopsies is frequently needed to unequivocally diagnose EBV-positive PTLD [42].

In the following, we give a short description of the real-time PCR procedure, as it is used in the Regensburg Clinical Virology lab to quantify EBV DNA [43]:

1. Isolate nucleic acids from clinical material (serum, EDTA blood, EDTA plasma, PBMCs , or tissue biopsies) using an isolation kit according to the instructions of the manufacturer, e.g., QIAamp DNA Blood Mini Kit (Qiagen, Hilden, Germany).

2. Prepare the master mix according to the instructions of the manufacturer. The master mix should contain dNTPs, heat-stable DNA polymerase enzyme, buffer,

salts, primers, and fluorescent probe, according to the instructions of the manufacturer.

3. From a total elution volume of 200 μL, add 5 μL of isolated nucleic acids for each PCR reaction in a 96 well plate, yielding a total volume of 50 μL per reaction.

4. Cover the 96 well plate and start the programmed PCR machine.

5. We use TaqMan probes and Step-One-Plus machines from ABI.

6. Sense primer: 5′-TGACCTCTTGCATGGCCTCT-3′.

7. Antisense primer: 5′-CCTCTTTTCCAAGTCAGAATTTGAC-3′.

8. Probe: FAM-5′-CCATCTACCCATCCTACACTGCGCTTTACA-3′-TAMRA.

9. This primer-probe set amplifies a segment from the alkaline exonuclease gene of EBV (BGLF5) .

10. The PCR profile consists of 45 cycles at 95 °C for 15 s and 60 °C for 60 s, preceded by a denaturation step at 95 °C for 10 min, then cooling to 25 °C, until the machine is opened.

11. Tenfold serial dilutions of plasmids containing the respective target sequence have to be amplified in each run, serving as quantitation standard and positive control. The detection limit of this quantitative EBV assay is at 2.5 plasmid copies per reaction, corresponding to 500 genome equivalents (641 IU/mL) per mL serum.

References

1. Epstein MA, Achong BG, Barr YM (1964) Virus particles in cultured lymphoblasts from Burkitt's lymphoma. Lancet 1:702–703
[CrossRef][PubMed]

2. zur Hausen H, Schulte-Holthausen H, Klein G, Henle W, Henle G, Clifford P, Santesson L (1970) EBV DNA in biopsies of Burkitt tumours and anaplastic carcinomas of the nasopharynx. Nature 228(5276):1056–1058
[CrossRef][PubMed]

3. Wolf H, zur Hausen H, Becker V (1973) EB viral genomes in epithelial nasopharyngeal carcinoma cells. Nat New Biol 244(138):245–247
[CrossRef][PubMed]

4. Cohen JI (2000) Epstein-Barr virus infection. N Engl J Med 343(7):481–492
[CrossRef][PubMed]

5. Cohen JI, Bollard CM, Khanna R, Pittaluga S (2008) Current understanding of the role of Epstein-Barr virus in lymphomagenesis and therapeutic approaches to EBV-associated lymphomas. Leuk Lymphoma 49(Suppl 1):27–34
[CrossRef][PubMed][PubMedCentral]

6. Bornkamm GW (2009) Epstein-Barr virus and its role in the pathogenesis of Burkitt's lymphoma: an unresolved issue. Semin Cancer Biol 19(6):351–365
[CrossRef][PubMed]

7. Niller HH, Szenthe K, Minarovits J (2014) Epstein-Barr virus-host cell interactions: an epigenetic dialog? Front Genet 5:367
[CrossRef][PubMed][PubMedCentral]

8. Niller HH, Salamon D, Ilg K, Koroknai A, Banati F, Bauml G, Rucker O, Schwarzmann F, Wolf H, Minarovits J (2003) The in vivo binding site for oncoprotein c-Myc in the promoter for Epstein-Barr virus (EBV) encoding RNA (EBER) 1 suggests a specific role for EBV in lymphomagenesis. Med Sci Monit 9(1):HY1–HY9
[PubMed]

9. Niller HH, Salamon D, Ilg K, Koroknai A, Banati F, Schwarzmann F, Wolf H, Minarovits J (2004) EBV-associated neoplasms: alternative pathogenetic pathways. Med Hypotheses 62(3):387–391
[CrossRef][PubMed]

10. Gromminger S, Mautner J, Bornkamm GW (2012) Burkitt lymphoma: the role of Epstein-Barr virus revisited. Br J Haematol 156(6):719–729
[CrossRef][PubMed]

11. Rickinson AB (2014) Co-infections, inflammation and oncogenesis: future directions for EBV research. Semin Cancer Biol 26:99–115
[CrossRef][PubMed]

12. Kreck B, Richter J, Ammerpohl O, Barann M, Esser D, Petersen BS, Vater I, Murga Penas EM, Bormann Chung CA, Seisenberger S, Lee Boyd V, Smallwood S, Drexler HG, Macleod RA, Hummel M, Krueger F, Hasler R, Schreiber S, Rosenstiel P, Franke A, Siebert R (2013) Base-pair resolution DNA methylome of the EBV-positive Endemic Burkitt lymphoma cell line DAUDI determined by SOLiD bisulfite-sequencing. Leukemia 27(8):1751–1753
[CrossRef][PubMed][PubMedCentral]

13. Hansen KD, Sabunciyan S, Langmead B, Nagy N, Curley R, Klein G, Klein E, Salamon D, Feinberg AP (2014) Large-scale hypomethylated blocks associated with Epstein-Barr virus-induced B-cell immortalization. Genome Res 24(2):177–184
[CrossRef][PubMed][PubMedCentral]

14. Navari M, Fuligni F, Laginestra MA, Etebari M, Ambrosio MR, Sapienza MR, Rossi M, De Falco G, Gibellini D,

Tripodo C, Pileri SA, Leoncini L, Piccaluga PP (2014) Molecular signature of Epstein Barr virus-positive Burkitt lymphoma and post-transplant lymphoproliferative disorder suggest different roles for Epstein Barr virus. Front Microbiol 5:728
[CrossRef][PubMed][PubMedCentral]

15. Niller HH, Salamon D, Banati F, Schwarzmann F, Wolf H, Minarovits J (2004) The LCR of EBV makes Burkitt's lymphoma endemic. Trends Microbiol 12(11):495–499
[CrossRef][PubMed]

16. Niller HH, Wolf H, Minarovits J (2009) Epigenetic dysregulation of the host cell genome in Epstein-Barr virus-associated neoplasia. Semin Cancer Biol 19(3):158–164
[CrossRef][PubMed]

17. Gruhne B, Sompallae R, Marescotti D, Kamranvar SA, Gastaldello S, Masucci MG (2009) The Epstein-Barr virus nuclear antigen-1 promotes genomic instability via induction of reactive oxygen species. Proc Natl Acad Sci U S A 106(7):2313–2318
[CrossRef][PubMed][PubMedCentral]

18. Cao JY, Mansouri S, Frappier L (2012) Changes in the nasopharyngeal carcinoma nuclear proteome induced by the EBNA1 protein of Epstein-Barr virus reveal potential roles for EBNA1 in metastasis and oxidative stress responses. J Virol 86(1):382–394
[CrossRef][PubMed][PubMedCentral]

19. Frappier L (2012) Contributions of Epstein-Barr nuclear antigen 1 (EBNA1) to cell immortalization and survival. Viruses 4(9):1537–1547
[CrossRef][PubMed][PubMedCentral]

20. Linde A, Fridell E, Dahl H, Andersson J, Biberfeld P, Wahren B (1990) Effect of primary Epstein-Barr virus infection on human herpesvirus 6, cytomegalovirus, and measles virus immunoglobulin G titers. J Clin Microbiol 28(2):211–215
[PubMed][PubMedCentral]

21. Karner W, Bauer G (1994) Activation of a varicella-zoster virus-specific IgA response during acute Epstein-Barr virus infection. J Med Virol 44(3):258–262
[CrossRef][PubMed]

22. Bauer G (1992) Die Aussagemöglichkeiten der Epstein-Barr-Virus-Diagnostik [The diagnostic value of Epstein-Barr virus diagnosis]. Internist (Berl) 33(9):586–592

23. Bauer G (1995) Rationale und rationelle EBV-Diagnostik. Clin Lab 41:623–634

24. Schillinger M, Kampmann M, Henninger K, Murray G, Hanselmann I, Bauer G (1993) Variability of humoral immune response to acute Epstein-Barr virus (EBV) infection: evaluation of the significance of serological markers. Med Microbiol Lett 2:296–303

25. Bauer G (2001) Simplicity through complexity: immunoblot with recombinant antigens as the new gold standard in Epstein-Barr virus serology. Clin Lab 47(5–6):223–230
[PubMed]

26. Motz M, Fan J, Seibl R, Jilg W, Wolf H (1986) Expression of the Epstein-Barr virus 138-kDa early protein in Escherichia coli for the use as antigen in diagnostic tests. Gene 42(3):303–312
[CrossRef][PubMed]

27.

Pottgiesser T, Wolfarth B, Schumacher YO, Bauer G (2006) Epstein-Barr virus serostatus: no difference despite aberrant patterns in athletes and control group. Med Sci Sports Exerc 38(10):1782–1791
[CrossRef][PubMed]

28. Pottgiesser T, Schumacher YO, Wolfarth B, Schmidt-Trucksass A, Bauer G (2012) Longitudinal observation of Epstein-Barr virus antibodies in athletes during a competitive season. J Med Virol 84(9):1415–1422
[CrossRef][PubMed]

29. Reischl U, Gerdes C, Motz M, Wolf H (1996) Expression and purification of an Epstein-Barr virus encoded 23-kDa protein and characterization of its immunological properties. J Virol Methods 57(1):71–85
[CrossRef][PubMed]

30. Wolter T, Gassmann C, Vetter V, Bauer G (1997) Avidity determination: utilization of a basic immunological mechanisms allows to improve serological diagnosis of infections. Clin Lab 43:125–135

31. Andersson A, Vetter V, Kreutzer L, Bauer G (1994) Avidities of IgG directed against viral capsid antigen or early antigen: useful markers for significant Epstein-Barr virus serology. J Med Virol 43(3):238–244
[CrossRef][PubMed]

32. Vetter V, Kreutzer L, Bauer G (1994) Differentiation of primary from secondary anti-EBNA-1-negative cases by determination of avidity of VCA-IgG. Clin Diagn Virol 2(1):29–39
[CrossRef][PubMed]

33. Weber B, Brunner M, Preiser W, Doerr HW (1996) Evaluation of 11 enzyme immunoassays for the detection of immunoglobulin M antibodies to Epstein-Barr virus. J Virol Methods 57(1):87–93
[CrossRef][PubMed]

34. Gärtner BC, Hess RD, Bandt D, Kruse A, Rethwilm A, Roemer K, Mueller-Lantzsch N (2003) Evaluation of four commercially available Epstein-Barr virus enzyme immunoassays with an immunofluorescence assay as the reference method. Clin Diagn Lab Immunol 10(1):78–82
[PubMed][PubMedCentral]

35. Corrales I, Gimenez E, Navarro D (2014) Evaluation of the Architect Epstein-Barr Virus (EBV) viral capsid antigen (VCA) IgG, VCA IgM, and EBV nuclear antigen 1 IgG chemiluminescent immunoassays for detection of EBV antibodies and categorization of EBV infection status using immunofluorescence assays as the reference method. Clin Vaccine Immunol 21(5):684–688
[CrossRef][PubMed][PubMedCentral]

36. Guerrero-Ramos A, Patel M, Kadakia K, Haque T (2014) Performance of the architect EBV antibody panel for determination of Epstein-Barr virus infection stage in immunocompetent adolescents and young adults with clinical suspicion of infectious mononucleosis. Clin Vaccine Immunol 21(6):817–823
[CrossRef][PubMed][PubMedCentral]

37. Gärtner BC, Kortmann K, Schafer M, Mueller-Lantzsch N, Sester U, Kaul H, Pees H (2000) No correlation in Epstein-Barr virus reactivation between serological parameters and viral load. J Clin Microbiol 38(6):2458
[PubMed][PubMedCentral]

38. Gärtner B, Preiksaitis JK (2010) EBV viral load detection in clinical virology. J Clin Virol 48(2):82–90
[CrossRef][PubMed]

39. Adham M, Greijer AE, Verkuijlen SA, Juwana H, Fleig S, Rachmadi L, Malik O, Kurniawan AN, Roezin A, Gondhowiardjo S, Atmakusumah D, Stevens SJ, Hermani B, Tan IB, Middeldorp JM (2013) Epstein-Barr virus DNA load in nasopharyngeal brushings and whole blood in nasopharyngeal carcinoma patients before and after

treatment. Clin Cancer Res 19(8):2175–2186
[CrossRef][PubMed]

40. Styczynski J, Reusser P, Einsele H, de la Camara R, Cordonnier C, Ward KN, Ljungman P, Engelhard D, Second European Conference on Infections in L (2009) Management of HSV, VZV and EBV infections in patients with hematological malignancies and after SCT: guidelines from the Second European Conference on Infections in Leukemia. Bone Marrow Transplant 43(10):757–770

41. Kimura H, Ito Y, Suzuki R, Nishiyama Y (2008) Measuring Epstein-Barr virus (EBV) load: the significance and application for each EBV-associated disease. Rev Med Virol 18(5):305–319
[CrossRef][PubMed]

42. Kittan NA, Beier F, Kurz K, Niller HH, Egger L, Jilg W, Andreesen R, Holler E, Hildebrandt GC (2011) Isolated cerebral manifestation of Epstein-Barr virus-associated post-transplant lymphoproliferative disorder after allogeneic hematopoietic stem cell transplantation: a case of clinical and diagnostic challenges. Transpl Infect Dis 13(5):524–530
[CrossRef][PubMed]

43. Plentz A, Jilg W, Kochanowski B, Ibach B, Knoll A (2008) Detection of herpesvirus DNA in cerebrospinal fluid and correlation with clinical symptoms. Infection 36(2):158–162
[CrossRef][PubMed]

3. Establishment of EBV-Infected Lymphoblastoid Cell Lines

Noemi Nagy[1] ✉

(1)   Department of Microbiology, Tumor and Cell Biology, Karolinska Institutet, Nobels väg 16, SE-171 77 Stockholm, Sweden

✉ **Noemi Nagy**
  Email: noemi.nagy@ki.se

Abstract
Lymphoblastoid cell lines (LCLs) can be generated easily by in vitro EBV infection of B lymphocytes collected from any individual. In vitro, these EBV-infected B cell cultures yield proliferating, transformed lines referred to as lymphoblastoid cell lines (LCLs).

Key words Mononuclear cells – B95-8 – Akata – LCL – Cyclosporin A

1 Introduction

EBV shows a high degree of B cell tropism. Human B cells can easily be infected with EBV in vitro. Its receptor is the B-lymphocyte-specific surface molecule, CD21 (receptor for the C3d fragment of complement), and it uses HLA class II molecules as co-receptors. Proliferation of B cells is induced by the complex interaction of EBV-encoded proteins with cellular proteins. Latent infection of B cells leads to transformation and generation of LCLs with unlimited growth capacity in vitro [1, 2].

Expression of the full set of EBV-encoded proteins detected in the LCLs is designated as "growth program" [3] or is referred to as type III latency [2]. The set of EBV-encoded proteins expressed in these cells comprises six proteins localized in the nucleus, EBNA 1–6 (alternatively called EBNA-1, EBNA-2, EBNA-3A, EBNA-3B,

EBNA-3C, and EBNA-LP), and three cell membrane-associated proteins, LMP-1, LMP-2A, and LMP-2B [4]. LCLs also express two small untranslated nuclear RNAs (EBER1 and EBER2) and the BART (BamHI-A region rightward transcript) RNAs [4]. The functions of the different EBV-encoded proteins in the transformation process and in the maintenance of proliferation have been characterized in LCLs.

LCLs have the phenotype of lymphoblasts, of activated B cells: they express at high level activation markers (CD23), adhesion molecules (LFA1, LFA3, ICAM1), and MHC class I and II molecules [5].

In addition to the in vitro infection of B cells with EBV, LCLs can also emerge spontaneously from the blood of EBV-positive individuals or their tissue explants that contain EBV genome-carrying B lymphocytes when the in vitro condition modifies or eliminates the immunological cell-mediated controls [6].

The EBV strain that is most commonly used in the laboratory for generation of LCLs is derived from the marmoset cell line B95-8 [7]. Another EBV strain that is used for generation of LCLs is derived from the Burkitt lymphoma line Akata [8]. Recombinant variants of both EBV strains, e.g., carrying antibiotic-resistant genes or GFP, have been generated (reviewed in [9]).

---

2 Materials

2.1 Isolation of Mononuclear Cells from Blood

1. Heparinized blood (peripheral or cord blood) or buffy coat.

2. Ficoll-Paque or Lymphoprep.

3. Sterile 15 or 50 mL tubes.

4. Sterile PBS.

5. Pipettes.

6. Complete RPMI medium: RPMI 1640 with 10 % fetal calf serum (FCS), 100 µg/mL penicillin, and 100 µg/mL streptomycin.

7. Ammonium chloride lysing solution (commercial).

2.2 Virus Production

1. B95-8 or Akata cell lines.

2. Complete RPMI medium: RPMI 1640 with 10 % FCS, 100 U/mL penicillin, and 100 µg/mL streptomycin.

3. RPMI 1640 medium with 2 % FCS, 100 U/mL penicillin, and 100 µg/mL streptomycin.

4. Affinity purified antihuman immunoglobulin G (IgG) antibody.

5. Sterile 0.45 µm pore filter.

2.3 In Vitro Infection with EBV

1. Sterile tubes (15 mL) with a round bottom.

2. Cell culture plates with 24 or 48 wells and 75 cm^2 culture flasks.

3. Complete RPMI medium: RPMI 1640 with 10 % FCS, 100 U/mL penicillin, and 100 µg/mL streptomycin.

4. 1 mg/mL cyclosporin A (CsA) solution.

3 Methods

3.1 Isolation of Mononuclear Cells from Blood

The method is based on differences in density of the different cell types. Granulocytes and erythrocytes have a higher density than mononuclear cells and therefore sediment through the density gradient of Ficoll-Paque or Lymphoprep layer during centrifugation. Lymphocytes, monocytes, and platelets are not dense enough to penetrate into the Ficoll-Paque layer. These cells therefore collect as a concentrated band at the interface between the original blood sample and the Ficoll-Paque (*see* **Note 1**).

1. Dilute blood with an equal volume of PBS (*see* **Notes 2** and **3**).

2. Carefully layer the blood on Ficoll-Paque (*see* **Note 4**). When layering the sample, do not mix the Ficoll-Paque and the diluted blood sample (*see* **Notes 5** and **6**).

3. Centrifuge the samples in a swing-out rotor at 18–20 °C with $400 \times g$ for 20 min. The brake of the centrifuge must be set at zero to avoid disturbing the mononuclear cell layer that forms during centrifugation.

4. The mononuclear cells are found in the layer ("ring") that is formed at the interface. Collect them into a clean tube (*see* **Note 7**).

5. Add at least three volumes of PBS to the cells and centrifuge for 10 min with $200 \times g$.

6. Discard supernatant and repeat the washing step by filling up the tube with PBS and centrifuging it again for 10 min with $200 \times g$ (*see* **Note 8**).

7. Resuspend the cells in complete RPMI medium and count them. This cell suspension contains highly purified, viable lymphocytes (T and B cells) and monocytes (*see* **Note 9**).

8. At this point, purified mononuclear cells are ready to be exposed to EBV, leading to infection of B cells. Alternatively, cells can be frozen, kept in liquid nitrogen, and infected at a later time point (*see* **Note 10**).

3.2 Virus Production

3.2.1 Production of Virus-Containing Supernatant from the B95-8 Cell Line

The B95-8 marmoset cell line [5] is used to produce supernatant which contains transforming, infectious virus particles. B95-8 is the prototype laboratory EBV strain and, in the majority of cases, it is the EBV strain of choice for generation of LCLs. The virus is derived from a mononucleosis patient. It was passed to the marmoset cell line trough the supernatant of the LCL established from the patient's blood cells. Under normal culture conditions, a small percentage of B95-8 cells can be found in the lytic

cycle. However, the cell line can produce a significant amount of infectious viral particles when it is cultured in medium with low serum concentration. This culture condition triggers the lytic cycle in a considerable number of cells:

1. Culture B95-8 cells in complete RPMI medium containing 10 % FCS (*see* **Note 11**). When a sufficient number of cells grow in the logarithmic phase (*see* **Note 12**), centrifuge the cells and start a new culture at 2×10^5/mL density in complete RPMI medium that contains 2 % FCS (instead of 10 %). Culture the cells for 2 weeks at 37 °C in a 5 % CO_2 humidified incubator without changing the medium.

2. At the end of the 2-week period, collect culture media and centrifuge it at $300 \times g$ to sediment cells and cell debris.

3. Collect the supernatant without disturbing the pellet. Next, filter the supernatant through a sterile 0.45 μm pore filter to eliminate all cells and store it at 4 °C. The supernatant produced in this way has a virus titer high enough to be used directly, without concentration, for generation of LCLs.

3.2.2 Production of Virus from the Akata Cell Line

Akata is a Burkitt lymphoma cell line that can be induced to produce infectious virus by surface immunoglobulin cross-linking [6]:

1. Culture Akata cells in complete RPMI medium, according to standard protocols. For lytic cycle induction, pellet the cells by centrifugation and resuspend them in a fresh medium at a density of 4×10^6 cells/mL. Add antihuman IgG antibody at a concentration of 50 μg/mL to the medium (*see* **Note 13**), and incubate the cells at 37 °C for 4 h.

2. Add an equal volume of fresh complete RPMI medium, diluting the cells at 2×10^6/mL density. Culture them for 5 additional days in this medium.

3. On day 5 collect the culture media and centrifuge it at $300 \times g$ to sediment the cells and the cell debris.

4. Collect the supernatant without disturbing the pellet. Next, filter the supernatant

through a sterile 0.45 μm pore filter to eliminate all remaining cells and store it at 4 °C. The virus supernatant produced in this way can be used directly, without concentration, for generation of LCLs. Usually, the supernatant produced from Akata by this method has a higher titer than the one produced from B95-8 cells.

3.3 Generation of LCL from Mononuclear Cells

3.3.1 In Vitro-Transformed LCLs

1. Expose the purified mononuclear cells (described at Subheading 3.1) to virus-containing supernatant. Pellet $3-5 \times 10^6$ cells by centrifugation, discard the medium, and resuspend the cells in 3–5 mL B95-8 supernatant or 1–2 mL supernatant obtained from Akata. If the virus titer is high, cell numbers can be increased.

2. Incubate cells with the virus-containing supernatant at 37 °C for 2 h (*see* **Note 14**).

3. Pellet the cells by centrifugation, discard the supernatant, and resuspend the cells at 5×10^5/mL density in complete RPMI medium that contains 0.4 μg/mL cyclosporin A (*see* **Note 15**).

4. Distribute 1 mL of cell suspension/well of a 48-well plate, thus each well will contain 5×10^5 cells. If higher numbers of mononuclear cells are available, 2 mL of cell suspension/well can be distributed to a 24-well plate (10^6 cells/well). Maintain the cultures in a humidified incubator at 37 °C with 5 % CO_2.

5. Feed the cultures weekly by replacing half of the medium with fresh medium containing CsA .

6. After about 3 weeks, foci of EBV-transformed B cells will start to grow. When the cultures grow well, cells can be transferred first to a 24-well plate, then to a 12-well plate, and later to 75 cm^2 flasks (*see* **Note 16**). After about 5–6 weeks, LCLs are stable and will grow continuously.

3.3.2 Spontaneous LCL from Blood of EBV-Seropositive

Donors

LCLs can be generated from the mononuclear cells of an EBV-seropositive donor without infecting the cells in vitro. In this case, the LCL will grow out from the B cells that were infected in vivo with EBV. These LCLs will thus carry a unique EBV strain:

1. Purify mononuclear cells from the blood of an EBV-seropositive donor as described at Subheading 3.1. Resuspend the cells at $5\text{--}10 \times 10^5$/mL density in complete RPMI medium that contains 0.4 μg/mL CsA .

2. Distribute 1 mL of cell suspension to wells of a 48-well plate. Maintain cultures in a humidified incubator at 37 °C with 5 % CO_2.

3. After about 5–6 weeks, small foci of EBV-transformed B cells will appear (*see* **Note 17**). When the cultures grow well, cells can be transferred first to a 24-well plate, then to a 12-well plate, and later to 75 cm^2 flasks (*see* **Note 16**).

---

4 Notes

1. The temperature of Ficoll-Paque should be at 18–20 °C, at which temperature its density is optimal for the separation. At lower temperature, the density of Ficoll-Paque is greater, so granulocytes and red blood cells are prevented from entering the Ficoll-Paque layer.

2. Anticoagulated blood from different sources may be used. Peripheral blood can be used undiluted, while cord blood and buffy coat should be diluted. At high densities, erythrocytes aggregate and lymphocytes get trapped within the clumps, thus sedimenting together with the erythrocytes. Dilution of blood reduces the size of the red cell clumps and their trapping tendency and allows a better lymphocyte yield. Since erythrocyte numbers are especially high in cord blood and buffy coat, dilution of those samples is particularly important.

3. 10–20 mL of blood is sufficient to isolate enough mononuclear cells for generation of LCLs. Even smaller volumes can be used, but extra care should be taken not to lose cells during the separation process.

4. Ficoll-Paque can be substituted with Lymphoprep in this protocol.

5. For smaller volumes of blood, use 15 mL tubes with 3 mL Ficoll-Paque and overlay 5 mL diluted blood. For bigger volumes of blood, use 50 mL tubes containing 10 mL Ficoll-Paque on which you overlay 25 mL diluted blood.

6. To avoid mixing the blood with the Ficoll-Paque layer, overlay the blood by letting it run down slowly on the wall of a tube tilted at approximately 45 angular degrees.

7. First discard the upper layer (diluted plasma) without disturbing the mononuclear cells. In this way, collection of the mononuclear cells is easier and leads to less contamination with thrombocytes. Care should be taken to avoid the lower, Ficoll-Paque layer, since that will result in contamination with red blood cells.

8. This washing procedure will yield efficient removal of platelets from the lymphocytes in the majority of cases.

9. Contamination with erythrocytes (red blood cells) is common, if cord blood was used as a starting material. Even though the presence of some erythrocytes would not interfere with transformation , heavy contamination, i.e., when the cell pellet is basically red, could have negative effects on transformation. In this latter case, we recommend either repeating the Ficoll-Paque separation again (Subheading 3.1, **steps 2–7**) or lysing the erythrocytes with ammonium chloride lysis buffer (commercially available). From these two possibilities, lysis is more efficient in eliminating the contamination with red blood cells. In order to lyse red blood cells, resuspend the cell pellet in 5 mL lysis buffer (in a 50 mL tube) and keep the cell suspension on ice for 5 min after which 45 mL of PBS is added and cells are centrifuged. Wash the cells one more time with PBS. Resuspend cells in complete RPMI medium and count them. Contamination with erythrocytes should be greatly reduced now, and cells are ready for infecting them with EBV.

10. Mononuclear cells can be frozen in 10 % DMSO in fetal calf serum using a controlled rate freezer and thawed on the day of EBV infection.

11. Work with the virus producer cell lines and virus-containing supernatant should be performed in biosafety level 2 cabinets.

12. If LCLs will be regularly established, it is convenient to produce a larger (200–500 mL) volume of virus-containing supernatant. For this volume, a starting number of 40–100×10^6 B95-8 cells are needed.

13. Make sure that the antihuman IgG antibody is functional grade, i.e., it should not contain sodium azide that is toxic to cells. This compound is frequently added to antibody products in order to prevent microbial contamination.

14. This incubation step can be done in 10 mL round-bottom tubes, in which the cells were pelleted.

15. Cyclosporin A (CsA) is added to the culture to inhibit the function of EBV-specific T cells that are present in case that the blood donor is EBV positive. If CsA is not added, these EBV-specific memory T cells get activated by the freshly infected B cells and inhibit the outgrowth of LCLs [10]. Adding CsA to cultures derived from all donors is recommended, because it eliminates the necessity to determine the EBV status. However, if the mononuclear cells were purified from cord blood, CsA may be omitted, since these cultures lack EBV-specific memory T cells.

16. The gradual transition of cultures to larger wells is important, because the cell density is important for growth. At early time points, just change half of the medium with fresh one and disperse the cells present in clumps by pipetting. Transfer cells to bigger wells only after many, big clumps are formed and the medium turns yellow due to metabolic activity and proliferation.

17. When spontaneous LCLs are generated, the presence of growing EBV-transformed B cells in the cultures becomes evident after a longer culture time than during the establishment of LCLs with in vitro infection (Subheading 3.3.1). This is due to the low frequency of B cells that carry EBV in a healthy donor.

References

1. Pope JH, Horne MK, Scott W (1968) Transformation of foetal human leukocytes *in vitro* by filtrates of a human leukaemic cell line containing herpeslike virus. Int J Cancer 3:857–866
[CrossRef][PubMed]

2. Rickinson AB, Kieff E (2001) Epstein–Barr virus. In: Knipe DM, Howley PM (eds) Fields virology, vol 2, 4th edn. Lippincott Williams and Wilkins, Philadelphia, pp 2575–2627

3. Thorley-Lawson DA (2001) Epstein-Barr virus: exploiting the immune system. Nat Rev Immunol 1:75–82
[CrossRef][PubMed]

4. Kang MS, Kieff E (2015) Epstein–Barr virus latent genes. Exp Mol Med 47:e131
[CrossRef][PubMed][PubMedCentral]

5. Kieff E, Rickinson AB (2001) Epstein-Barr virus and its replication. In: Knipe DM, Howley PM (eds) Fields virology, vol 2, 4th edn. Lippincott Williams and Wilkins, Philadelphia, pp 2511–2574

6. Bird AG, McLachlan SM, Britton S (1981) Cyclosporin A promotes spontaneous outgrowth *in vitro* of Epstein-Barr virus-induced B-cell lines. Nature 289:300–301
[CrossRef][PubMed]

7. Miller G, Lipman M (1973) Release of infectious Epstein-Barr virus by transformed marmoset leukocytes. Proc Natl Acad Sci U S A 70:190–194
[CrossRef][PubMed][PubMedCentral]

8. Daibata M, Humphreys RE, Takada K, Sairenji T (1990) Activation of latent EBV via anti-IgG-triggered, second messenger pathways in the Burkitt's lymphoma cell line Akata. J Immunol 144:4788–4793
[PubMed]

9. Delecluse HJ, Feederle R, Behrends U, Mautner J (2008) Contribution of viral recombinants to the study of the immune response against the Epstein-Barr virus. Semin Cancer Biol 18:409–415
[CrossRef][PubMed]

10. Rickinson AB, Rowe M, Hart IJ, Yao QY, Henderson LE et al (1984) T-cell-mediated regression of spontaneous and of Epstein-Barr virus-induced B-cell transformation *in vitro*: studies with cyclosporin A. Cell Immunol 87:646–658
[CrossRef][PubMed]

4. Generation and Infection of Organotypic Cultures with Epstein–Barr Virus

Rachel M. Temple[1, 2], Craig Meyers[1, 3] and Clare E. Sample[1, 3] ✉

(1) Department of Microbiology and Immunology, H107, The Pennsylvania State University College of Medicine, 500 University Drive, Hershey, PA 17033, USA
(2) Department of Microbiology and Immunology, Geisel School of Medicine at Dartmouth, Hanover, NH 03755, USA
(3) The Penn State Hershey Cancer Institute, Hershey, PA 17033, USA

✉ **Clare E. Sample**
  Email: csample@hmc.psu.edu

Abstract
While numerous model systems are available to study EBV latency in B cells and have contributed greatly to our understanding of the role of these cells in the viral life cycle, models to study the EBV life cycle in epithelial cells in vitro are lacking. Epithelial cells are poorly infected in vitro, and EBV-infected cell lines have not been successfully obtained from epithelial tumors. Recently, we have demonstrated that organotypic cultures of oral keratinocytes can be used as a model to study EBV infection in the epithelial tissue. These "raft" cultures generate a stratified tissue resembling the epithelium seen in vivo with a proliferating basal layer and differentiating suprabasal layers. Here, we describe generation of EBV-infected raft cultures established from primary oral mucosal epithelial cells, which exhibit high levels of productive replication induced by differentiation, as well as methods to analyze EBV infection.

Key words Epstein–Barr virus – Organotypic culture – Epithelial cells – Stratified epithelium – Lytic replication – Virus production – qPCR

1 Introduction

The Epstein–Barr virus (EBV) life cycle in epithelial cells is not as well understood as that in B cells due to the difficulty infecting epithelial cells in vitro and the inability to establish EBV-infected epithelial cell lines from cells infected in vitro or from tumors. While epithelial tumors express latency gene products, productive cycle viral proteins are observed in the oral epithelium from HIV -infected individuals [1], in contrast to studies in vitro. In all in vitro systems studied thus far, EBV initially establishes a latent infection. Productive replication rarely occurs spontaneously but can be induced by experimental manipulation using various chemicals, cross-linking the B-cell receptor, or exogenous expression of the immediate-early protein Zta [2–5]. With each of these methods, only a subset of the infected cells reactivate, and it is difficult to generate high-titer virus, making the study of productive EBV replication and virion structure difficult. Organotypic cultures produce a more biologically relevant three-dimensional tissue that closely resembles that seen in vivo: a basal layer containing mitotically active stem cells in contact with the basement membrane and suprabasal layers (the spinosum, granulosum, and corneum layers) in which epithelial cells follow a programmed pattern of gene expression resulting in spontaneous terminal differentiation. These cultures are generated from epithelial cells grown to confluence on a dermal equivalent, leading to formation of tight junctions between the individual cells and cell polarization. When placed at an air–liquid interface (referred to as "raft" cultures), a portion of the cells leave the basal layer and begin to terminally differentiate, eventually forming a multilayered epithelial tissue resembling that found in vivo (Fig. 1) [6]. Using organotypic or "raft" cultures generated from primary gingival and tonsillar keratinocytes, our laboratory demonstrated that EBV infection of stratified epithelium results in high levels of productive replication restricted to terminally differentiating cells, generally resulting in viral titers of 5×10^9 to 5×10^{10} genome equivalents per raft by 6–8 days postinfection [7]. Unlike B cells or epithelial cells in monolayer culture, productive replication is induced by differentiation alone without the addition of exogenous agents, providing an important in vitro model of naturally induced highly productive EBV replication. Most importantly, the EBV productive replication observed is similar to that observed in vivo in terminally differentiated epithelial cells of oral epithelial tissue naturally infected with EBV [8–10].
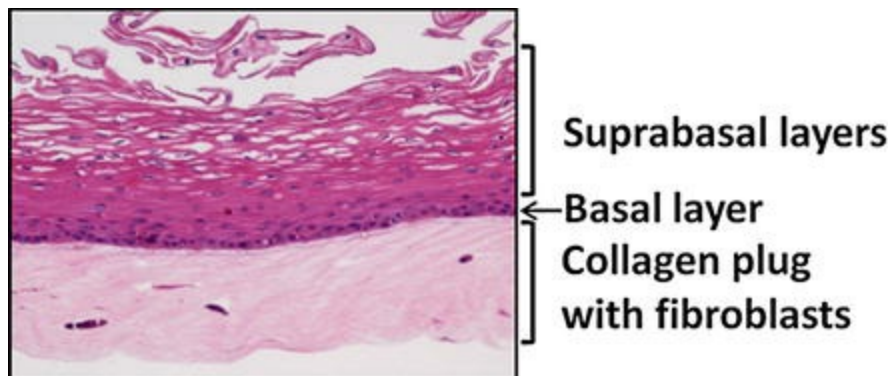
Fig. 1 Hematoxylin and eosin staining of a section of an uninfected organotypic raft generated from primary oral keratinocytes. The section shows the dermal equivalent (the collagen plug containing fibroblasts), the basal layer (where proliferating cells reside), and the suprabasal layers, which begin to differentiate, ultimately losing their nuclei and disassociating from the raft

Thus, EBV-infected raft cultures are likely to facilitate the study of the life cycle of EBV in the epithelium, with particular relevance to the study of the EBV productive cycle and molecular and biochemical analysis of the virion. In this chapter, we describe how to isolate primary oral mucosal epithelial cells and generate EBV-infected organotypic cultures. Given the importance of being able to isolate high-titer EBV, we also describe protocols to isolate and quantify infectious virus from raft cultures. Finally, we describe methods to analyze EBV gene expression by immunofluorescence .

2 Materials

2.1 Reagents for Isolation and Culture of Primary Epithelial Cells

1. Epithelial tissue (*see* **Note** [1]).

2. Wash buffer: PBS, 67 μg/mL gentamicin sulfate and 100 U/mL nystatin; make day of use.

3. 0.05 % trypsin–EDTA.

4. Adenine stock solution (180 mM): to dissolve adenine, add 486 mg adenine to 15 mL dH$_2$O. Add approximately ten drops of concentrated HCl until dissolved, and then adjust volume to 20 mL with dH$_2$O.

5. 3,3′,5-Triiodo-L-thyronine (T3) stock solution: dissolve 13.6 mg T3 in 100 mL 0.02 N NaOH. Make two 100-fold serial dilutions in sterile PBS to obtain final stock solution.

6. Hydrocortisone stock solution: dissolve 25 mg hydrocortisone in 5 mL 100 % ethanol. To generate stock solution, add 4.8 mL of the hydrocortisone solution to 55.2 mL 1 M HEPES, pH 7.

7. To make 10 L E-medium, dissolve 100.3 g powdered DMEM (DMEM with 4.5 g/L D-glucose and L-glutamine without sodium pyruvate and sodium bicarbonate) and 26.6 g powdered Ham's medium (F12 nutrient mixture with L-glutamine, without sodium bicarbonate) in 6 L of dH$_2$O, and then add 30.69 g sodium bicarbonate, 100 mL penicillin–streptomycin solution (10,000 U/mL penicillin and 10,000 μg/mL streptomycin stock solution), 10 mL cholera toxin (10 μg/mL stock dissolved in dH$_2$O), 10 mL adenine stock solution, 10 mL transferrin (5 mg/mL stock dissolved in PBS), 10 mL T3 stock solution, 10 mL hydrocortisone stock solution, and 10 mL insulin (5 mg/mL dissolved in 0.1 N HCl). Adjust volume to 10 L with dH$_2$O, and adjust pH to 7.1–7.15. Filter sterilize with a 0.2 μm pore-size low-protein-binding filter, divide into 940 mL aliquots, and store at 4 °C in the dark. Prior to use, add 10 mL nystatin (10,000 U/mL suspension) and 50 mL FBS.

8. K-154 medium supplemented with Keratinocyte Growth Supplement Kit (Cascade Biologics).

2.2 Reagents for Generation of Raft Culture

1. J2 3T3 mouse fibroblasts: use low-passage fibroblasts maintained in DMEM containing 10 % heat-inactivated newborn calf serum and 25 μg/mL gentamicin sulfate.

2. 10× reconstitution buffer: 62 mM NaOH, 260 mM NaHCO$_3$, 200 mM Hepes, and pH 8.2.

3. 10× DMEM (made from powdered DMEM with 4.5 g/L D-glucose and L-glutamine without sodium pyruvate and sodium bicarbonate).

4. Type 1 collagen from rat tails, approximately 4 mg/mL.

5. 10 M NaOH.

6. Epidermal growth factor (EGF; 1 µg/mL EGF stock solution dissolved in dH_2O supplemented with 1 mg/mL BSA).

2.3 Reagents for Infecting Raft Culture with EBV

1. Akata medium: RPMI containing 10 % FBS.

2. Akata cells (*see* **Note 2**).

3. Goat anti-human IgG F(ab)^2.

4. PBS.

2.4 Reagents for Harvesting Infectious Virus from Raft Culture

1. Homogenization buffer: 0.05 M Na–phosphate, pH 8. To make 500 mL homogenization buffer, first combine 13.25 mL 0.2 M NaH_2PO_4, 236.75 mL 0.2 M Na_2HPO_4, and 250 mL dH_2O to make 0.1 M Na–phosphate buffer. Dilute 250 mL chilled 0.1 M Na–phosphate buffer with 250 mL dH_2O. Sterilize by filtration through a 0.2 µm pore-size filter and store at 4 °C.

2. Dry ice–ethanol slurry.

3. Benzonase nuclease (250 U/µL stock solution).

4. 1 M $MgCl_2$.

5. 5 M NaCl.

2.5 Reagents for Quantification of Viral Genomes Using qPCR

1. Hirt extraction buffer: 400 mM NaCl, 10 mM Tris–HCl, pH 7.4, and 10 mM EDTA.

2. Proteinase K (20 mg/mL dissolved in dH$_2$O).

3. 10 % sodium dodecyl sulfate (SDS).

4. Phenol–chloroform–isoamyl alcohol (25:24:1).

5. Chloroform.

6. 3 M sodium acetate.

7. 100 % and 70 % ethanol.

8. dH$_2$O.

9. PCR strips and PCR caps.

10. Taqman Universal PCR master mix.

11. BALF5 PCR primers: 20 μM BALF5 forward primer (5′-AGTCCTTCTTGGCTAGTCTGTTGAC-3′), 20 μM BALF5 reverse primer (5′-CTTTGGCGCGGATCCTC-3′).

12. BALF5 PCR probe: 5 μM Taqman dual-labeled fluorogenic probe (5′-(FAM)-CATCAAGAAGCTGCTGGCGGCCT (TAMRA)-3′).

13. Sample with known copy number of EBV DNA for generation of standard curve.

2.6 Reagents for Harvesting Raft Cultures for Immunohistology

1. Tissue cassette with lid.

2. Biopsy sponge.

3. 10 % buffered formalin phosphate.

4. 70 % ethanol.

2.7 Equipment

1. Sterile scalpel.

2. Sterile glass universal with stir bar.

3. 40 31/16″ mesh (0.010 SS) wire cloth circles. Bend the edges in several spots (we used three bends) to create "legs" that raise the grid ~2 mm from the bottom of a 100 mm plate (*see* Fig. 2a and **Note 3**).
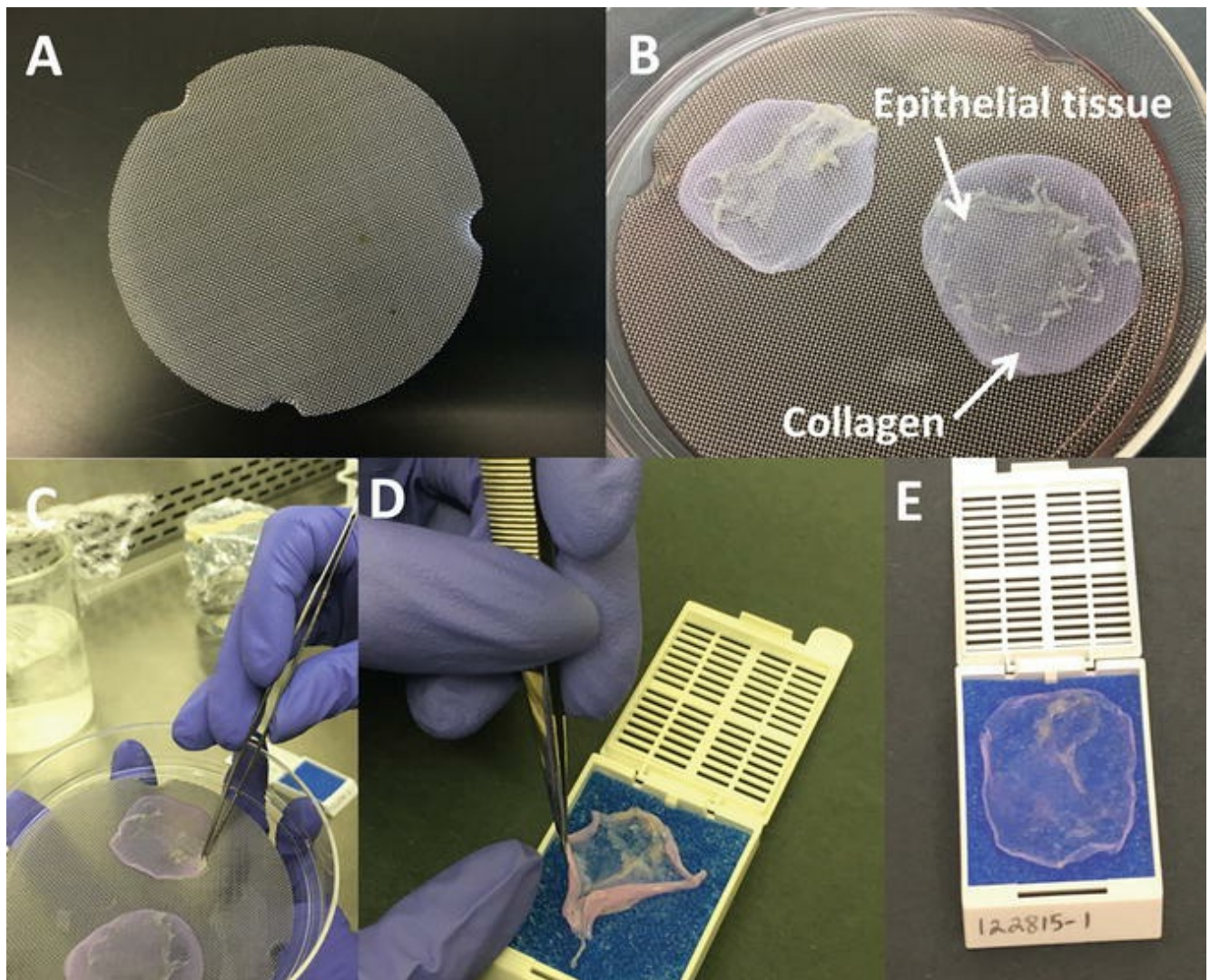
Fig. 2 Organotypic raft procedures. Stainless steel grids (**a**) support the rafts (**b**) that consist of a tissue layer (*white*) growing on a collagen support (*pink*). To remove the raft, the edges are scraped to detach the tis sue from the grid (**c**). The raft can then be placed in a biopsy cassette, where the tissue is spread out using forceps (**d** and **e**) prior to sectioning for downstream applications such as immunofluorescence

4. Dissection kit: forceps and microdissection scissors.

5. 100 mm treated tissue culture plates.

6. Spatula.

7. Disposable plastic pellet pestle.

8. Microcentrifuge.

9. Real-time qPCR machine (DNA Engine Opticon system from Bio-Rad or equivalent) with appropriate software.

---

3 Methods

The experimental procedures outlined below describe how to isolate primary gingival mucosal epithelial cells (Subheading 3.1). The techniques used to generate stratified and terminally differentiated primary epithelial cells are based on those used to generate similar tissue from human papillomavirus (HPV)-immortalized cell lines [11, 12] with minor, but essential, modifications for the use of primary epithelial cells capable of replicating EBV (Subheading 3.2) [7, 13, 14]. Next, we outline how to inoculate these cultures with EBV-producing B cells (Subheading 3.3), how to harvest and quantify infectious virus from the cultures (Subheadings 3.4–3.5), and how to prepare the tissue for histological and immunofluorescence analysis (Subheading 3.6).

3.1 Isolation and Culture of Primary Epithelial Cells

1. Remove tissue from buffer (*see* **Note 4**), and completely submerge in cold wash buffer for at least 20–30 min at room temperature, changing the buffer three times.

2. Move the tissue to a clean 100 mm plate containing ~5 mL cold wash buffer. Hold the tissue with sterile forceps and scrape away the connective tissue and dermis (soft white tissue) using a clean scalpel (*see* **Note 5**).

3. Move the epithelial tissue to a clean 100 mm plate containing ~5 mL wash buffer.

4. Aspirate the wash buffer, and mince the tissue using a scalpel and microdissection scissors.

5. To disassociate the epithelial cells from the tissue, place the minced tissue into a sterile glass universal containing a stir bar with 25 mL 0.05 % trypsin–EDTA.

6. Incubate at 37 °C for 1 h, with slow rotation of the stir bar.

7. Following the 1 h incubation, allow the tissue to settle to the bottom of the glass universal. Remove ~20 mL of the supernatant fraction and neutralize with ~30 mL E-media.

8. To obtain additional epithelial cells, add 20 mL fresh 0.05 % trypsin–EDTA to the glass universal and repeat **steps 7** and **8**.

9. Pellet the cells at $2100 \times g$ for 7 min, and remove the supernatant fraction. Resuspend the cells in K-154 medium (normally 20 mL per gingiva) and add 10 mL to each 100 mm tissue culture plate.

10. Incubate the cells at 37 °C and 5 % CO_2 for 3 days without disturbing, and change the media every other day thereafter.

11. At 2 weeks or when cells reach 70 % confluence, passage or freeze the cells.

3.2 Generation of Raft Culture

1. Trypsinize sub-confluent J2 3 T3 fibroblasts with 0.05 % trypsin–EDTA (*see* **Note 6**).

2. Neutralize trypsin with J2 3T3 medium.

3. Pellet cells at $2100 \times g$ for 7 min, and for each raft culture, resuspend 6.25×10^5 J2 3T3 cells in 0.25 mL 10× reconstitution buffer. All work from this point forward should be performed on ice to prevent the cells from clumping excessively and to prevent the collagen from solidifying prematurely.

4. Add 0.25 mL 10× DMEM per raft culture and mix well by pipetting up and down.

5. Keeping tube on ice, add 2 mL collagen per raft culture, and adjust the pH with 2.4

μL 10 N NaOH per mL of collagen. Mix by inverting the tube for at least 2 min.

6. For each raft, aliquot 2.5 mL of the collagen containing the J2 fibroblasts in one well of a six-well plate to form the collagen plug. Tilt the plate to evenly distribute the collagen, and remove any air bubbles with a sterile pasture pipet.

7. Incubate the collagen plugs at 37 °C and 5 % CO_2 for 1–2 h to allow the collagen to solidify.

8. Once the collagen has solidified, add 2 mL of E-medium supplemented with 5 ng/mL EGF (5 mL of EGF stock per liter E-media) to each well and allow to equilibrate for at least 10 min at room temperature.

9. While the collagen is equilibrating, harvest the primary keratinocytes with 0.05 % trypsin–EDTA (*see* **Note 7**). Neutralize the trypsin with E-medium supplemented with 5 ng/mL EGF.

10. Pellet the cells at 2100 × *g* for 7 min and resuspend at a final concentration of 2 × 10^6 cells/mL in E-medium supplemented with 5 ng/mL EGF. Make sure cells are completely resuspended, and add 1 mL of cell suspension to each collagen plug. Incubate at 37 °C, 5 % CO_2 for ~4 h, to allow the epithelial cells to adhere to the collagen matrix (*see* **Note 8**).

11. To lift the collagen matrices, gently loosen the collagen plug from the six-well plate by running a sterile spatula around the perimeter of the collagen matrix. Carefully lift the collagen matrix with the spatula and lay on sterile wire grid in a 100 mm plate so that the epithelial cells are on the upper surface. Gently spread out the collagen matrix evenly on the wire grid, ensuring there are no folds or air bubbles beneath it.

12. Aspirate any residual medium from the raft cultures, wash the raft and grid with PBS, and apply E-medium at the edge of the plate until it contacts the bottom surface of the raft. Do not allow any portion of the raft culture to be submerged in medium as this will prevent the cells from differentiating. Incubate the raft cultures at 37 °C, 5 % CO_2.

13. Change the medium for the raft cultures every other day. Be careful not to allow

medium to splash onto the surface of the raft culture as this will interfere with epithelial cell differentiation.

3.3 Infecting Raft Cultures with EBV

One Day Prior to Infection (Generally, Day 3 Post Airlifting), Induce Akata Cells

1. Resuspend Akata cells at a density of 5×10^5 cells/mL in RPMI supplemented with 10 % FBS (*see* **Note 9**).

2. Add 100 µg/mL goat anti-human IgG F(ab)^2 and mix well.

3. Incubate the cells at 37 °C and 5 % CO_2 for 24 h.

On Day of Infection (Day 4 Post Airlifting) (See Note 10)

4. Harvest the induced Akata cells and wash once in PBS.

5. Resuspend cells in PBS at a final concentration of 1.25×10^7 cells/mL.

6. Aspirate medium from the raft culture immediately prior to inoculation.

7. Score the top of the raft tissue by slicing through the raft repeatedly with a sterile scalpel (*see* **Note 11**).

8. Inoculate the raft culture with 200 µL of the Akata cell suspension (2.5×10^6 cells/200 µL) using a 200 µL pipet, and gently distribute the inoculum across the surface of the tissue with the pipet tip (*see* **Note 12**). It is not uncommon for a portion of the inoculum to spread between the collagen matrix and the basal surface of the tissue forming a small bubble. This will not damage the tissue.

9. Allow the inoculum to absorb into the surface of the tissue for a few minutes, then replace the medium in the bottom of the culture dish, and incubate at 37 °C and 5 % CO_2 for desired length of time (*see* **Note 13**).

3.4 Harvesting Raft Cultures for Virus Isolation

Harvesting Raft Tissue

1. Remove the medium from the raft culture prior to harvesting the tissue.

2. Using a sterile scalpel, gently scrap the edges of the tissue toward the center of the grid to detach the edge of the epithelial tissue from the grid.

3. Separate the tissue (white) from the collagen matrix (pink) using sterile forceps. Move the tissue to a 1.5 mL microfuge tube and store immediately at −80 °C. Store the raft tissue at −80 °C until isolation of infectious virus.

Isolating Infectious EBV from the Raft Tissue

4. Thaw the raft tissue on ice and add 500 μL homogenization buffer (*see* **Note 14**).

5. Freeze–thaw the tissue by incubation in a dry ice–ethanol bath for 15 min followed by incubation in a 37 °C water for 15 min. Repeat freeze–thaw two more times, and cool samples on ice.

6. Using a disposable plastic pellet pestle, grind the tissue 30 times.

7. Move the supernatant fraction to a clean microfuge tube.

8. Wash the pestle and tissue with an additional 250 μL homogenization buffer and combine with the 500 μL homogenate. Discard any remaining tissue.

Benzonase Treatment to Degrade Non-encapsidated Genomes

9. To the supernatant from each raft (~750 μL), add 1.5 μL benzonase and 1.5 μL 1 M $MgCl_2$. Mix well.

10. Incubate at 37 °C for 1 h, inverting the tube every 20 min.

11. To inactivate the benzonase, add 195 µL 5 M NaCl to each tube and mix.

12. Pellet cell debris by centrifugation at 2500 × *g* at 4 °C for 10 min.

13. Remove the supernatant fraction, which is the virus stock. Aliquot in cryovials in single-use aliquots to prevent multiple freeze–thaw cycles of the virus. Store at −80 °C (*see* **Note 15**).

3.5 Quantification of Viral Genomes by qPCR

*Extracting the Viral DNA (See **Note 16**)*

1. To extract viral DNA, combine 10 µL virus stock with 166 µL Hirt buffer, 2 µL of 20 mg/mL proteinase K, and 10 µL of 10 % SDS. Incubate for 2 h at 37 °C with constant agitation. Extractions are generally performed in duplicate or triplicate.

2. Following incubation, add equal volume (188 µL) of phenyl–chloroform–isoamyl alcohol (25:24:1) to each sample and vortex.

3. Centrifuge for 10 min at maximum speed in microcentrifuge at room temperature.

4. Remove the aqueous phase (top layer) and place in new microfuge tube.

5. Add 188 µL chloroform to the extracted aqueous phase from **step 4**, mix well, and centrifuge at maximum speed in microcentrifuge at room temperature.

6. Remove the aqueous phase (top portion) and place in new microfuge tube.

7. To precipitate the DNA, add 0.1 volume (18.8 µL) 3 M sodium acetate and 2.5 volumes (470 µL) 100 % ethanol. Vortex to mix the samples. Incubate at −20 °C overnight.

8. Pellet the DNA by centrifugation at maximum speed at 4 °C in a microcentrifuge for 10 min. Decant the supernatant fraction, and carefully wash the DNA pellet with 300 μL 70 % ethanol. Pellet the DNA at maximum speed at 4 °C in a microcentrifuge.

9. Decant the supernatant fraction, and dry the DNA samples (*see* **Note 17**).

10. Resuspend the DNA in 20 μL dH$_2$O for ~30 min at 37 °C.

Quantification of Viral DNA Genome Copy Number

11. The PCR is performed using a 25 μL reaction and is adapted from that previously described [15]. While the DNA is being resuspended, prepare qPCR master mix containing 12.5 μL Taqman Universal PCR master mix, 0.25 μL of 20 μM BALF5 forward primer, 0.25 μL of 20 μM BALF5 reverse primer, 0.5 μL of 5 μM Taqman dual-labeled fluorogenic probe, and 10.5 μL dH$_2$O for each sample.

12. Pipet 24 μL of the qPCR master mix into each well of appropriate qPCR strips.

13. Add 1 μL sample DNA to each well. Cover the wells with cover strips.

14. Each sample should be assayed in duplicate or triplicate. For negative controls, use 1 μL dH$_2$O in place of DNA. To generate a standard curve, prepare a DNA stock with 1×10^9 genome equivalents per μL in distilled H$_2$O (*see* **Note 18**). Generate a standard curve ranging from 1×10^8 to 1×10^2 genome equivalents using ten-fold serial dilutions of the DNA standard master stock diluted in dH$_2$O. Use 1 μL of standard DNA per reaction, and perform the standard curve in triplicate.

15. To activate the uracil-N-glycosylase, incubate the reaction mixture at 50 °C for 2 min, followed by activation of the AmpliTaq Gold at 95 °C for 10 min. Amplify the DNA for 40 cycles consisting of 15 s denaturation at 95 °C and 60 s extension at 60 °C, detecting the fluorescence signal generated at the end of each cycle.

16. Use the qPCR software to generate a standard curve, for which the R^2 should be

≥0.99, and estimate the number of genomes in each sample based on its fit to the standard curve. The number of EBV genomes per raft culture can then be calculated. Using the procedure given here, the number of genomes per raft culture can be determined by multiplying the number of EBV genomes per PCR reaction (this equates to the number of genomes per 0.5 μL virus stock) by the dilution factor.

3.6 Harvesting Raft Cultures for Histology and Immunostaining

1. Soak biopsy sponge in PBS. Drain excess PBS from sponge and place in bottom portion of tissue cassette.

2. Remove media from the raft culture prior to harvesting the tissue.

3. Using a sterile scalpel, gently scrap the edges of the tissue toward the center to detach the edge of the epithelial tissue from the grid.

4. Lift the raft tissue and collagen matrix from the wire grid with forceps and place tissue side down on the biopsy sponge. Use the forceps to spread the tissue evenly across the sponge.

5. Close the tissue cassette lid and drop the cassette into a beaker filled with 10 % buffered formalin phosphate. Incubate at room temperature 2–4 h.

6. Use tweezers to transfer tissue cassettes from formalin to 70 % ethanol where they can be stored at room temperature prior to sectioning. Sections can then be deparaffinized and processed for staining with hematoxylin and eosin or immunofluorescence staining (*see* **Note 19**).

4 Notes

1. We obtained the gingival tissue from an oral surgeon performing wisdom tooth extractions and the tonsil tissue from patients undergoing surgical treatment for

chronic tonsillitis. Tissue can be held in tissue storage buffer (Minimal Eagle's Medium containing 0.01 M Hepes, 9 mM sodium bicarbonate, 100 U/mL penicillin, 100 µg/mL streptomycin, 2.3 µg/mL Fungizone, and 0.37 mg/mL gentamycin) at 4 °C until processing.

2. Our laboratory uses wild-type Akata virus to infect raft cultures. We have also successfully infected raft cultures with recombinant EBV generated from EBV BACs, though productive replication of strains that lack a functional thymidine kinase gene is attenuated.

3. Prior to use, clean the wire grids with dichromate acid cleaning solution composed of 2.5 L concentrated sulfuric acid and 25 mL Chromerge. Make cleaning solution at least 24 h before use. Soak grids in cleaning solution for 2 h, and then rinse copiously with running tap water followed by a final rinse in dH$_2$O for at least 1 h. Autoclave before use.

4. We pooled the tissue from multiple patients beginning at the wash step to ensure a heterogeneous cell harvest.

5. To reduce the risk of contamination, it is advisable to perform multiple rounds of scraping the connective tissue and dermis from the epithelium, moving the tissue to clean 100 mm plates containing fresh wash buffer after each round. We typically use three sets of plates during the harvesting process.

6. J2 3T3 fibroblasts should be low passage (we use cells below passage 15). Collagen plugs can be made up to 2 days in advance. Once solidified, add 2 mL of E-medium and maintain at 37 °C. Prior to seeding epithelial cells, change medium in dish.

7. For optimal results, use gingival keratinocytes at passage 0–2 and tonsil keratinocytes at passage 0 or 1.

8. EGF is required to facilitate adherence and growth of primary epithelial cells on the collagen, but it is toxic to the J2 3 T3 feeder cells. For optimal results, the entire process (from making the collagen matrix to lifting the raft culture) should

be accomplished in a single day.

9. This cell density tends to result in the highest number of infectious viral particles per induced cell, though it does not result in the highest number of infectious viral particles in the supernatant.

10. We generally infect raft cultures on day 4 post airlifting, though we successfully inoculated the cultures at both earlier and later time points.

11. Scoring (or wounding) the tissue is not necessary for successful infection. However, it increases the rate of absorption of the liquid into the collagen, helping to minimize the loss of the inoculum during handling.

12. Raft cultures can be infected using high-titer cell-free virus. Volumes up to 400 μL can also be used to inoculate raft cultures when necessary.

13. Antiviral compounds or other compounds can be added to the medium used to feed the raft cultures and will gain access to the raft tissue by diffusion through the collagen.

14. Virus can be extracted from the raft tissue in PBS if the removal of unencapsidated genomes is not necessary. This change may be particularly important when using virus for downstream applications that might be sensitive to the high concentration of salts present in the homogenization buffer.

15. We found it convenient to extract viral DNA at the same time we harvested the virus, prior to freezing the virus stocks.

16. If total DNA is desired, including cellular DNA and all forms of viral DNA, a commercially available DNA extraction kit such as QIAamp DNA mini kit can be used.

17. The DNA pellets can be air-dried at room temperature for ~2–5 h or dried in a vacuum centrifuge at 3 °C for 30–60 min.

18. We used purified recombinant EBV Akata BAC DNA, which has an estimated genome size of 180.5 kb [16]. Thus, 197.828 ng/mL is 1×10^9 genome equivalents per μL. Others have used DNA from cells with a known EBV DNA copy number.

19. We have successfully used antibodies to BZLF1 (BZ1, Santa Cruz), EBNA2 (PE2, Dako), LMP1 (S12, [17] or CS1-4, Dako), BHRF1 (Millipore), gp350 (2 L10, Millipore), gp110 (Chemicon), and EA-D (Capricorn).

Acknowledgment

References

1. Niedobitek G, Young LS, Lau R, Brooks L, Greenspan D, Greenspan JS, Rickinson AB (1991) Epstein-Barr virus replication in oral hairy leukoplakia: virus replication in the absence of a detectable latent phase. J Gen Virol 72:3035–3046
[CrossRef][PubMed]

2. Takada K (1984) Cross-linking of cell surface immunoglobulins induces Epstein-Barr virus in Burkitt lymphoma cell lines. Int J Cancer 33:27–32
[CrossRef][PubMed]

3. zur Hausen H, O'Neill FJ, Freese UK, Hecker E (1978) Persistent oncogenic herpesvirus induced by the tumor promotor TPA. Nature 272:373–375
[CrossRef][PubMed]

4. Luka J, Kallin B, Klein G (1979) Induction of the Epstein-Barr virus (EBV) in latently infected cells by n-butyrate. Virology 94:228–231
[CrossRef][PubMed]

5. Countryman J, Jenson H, Seibl R, Wolf H, Miller G (1987) Polymorphic proteins encoded within BZLF1 of defective and standard Epstein-Barr viruses disrupt latency. J Virol 61:3672–3679
[PubMed][PubMedCentral]

6. Kopan R, Traska G, Fuchs E (1987) Retinoids as important determinants of terminal differentiation: examining keratin expression in individual epidermal cells at various stages of keratinization. J Cell Biol 105:427–440
[CrossRef][PubMed]

7. Temple RM, Zhu J, Budgeon L, Christensen ND, Meyers C, Sample CE (2014) Efficient replication of Epstein-Barr virus in stratified epithelium in vitro. Proc Natl Acad Sci U S A 111(46):16544–16549
[CrossRef][PubMed][PubMedCentral]

8. Frangou P, Buettner M, Niedobitek G (2005) Epstein-Barr virus (EBV) infection in epithelial cells in vivo: rare

detection of EBV replication in tongue mucosa but not in salivary glands. J Infect Dis 191:238–242
[CrossRef][PubMed]

9. Young LS, Lau R, Rowe M, Niedobitek G, Packham G, Shanahan F, Rowe DT, Greenspan D, Greenspan JS, Rickinson AB (1991) Differentiation-associated expression of the Epstein-Barr virus BZLF1 transactivator protein in oral hairy leukoplakia. J Virol 65:2868–2874
[PubMed][PubMedCentral]

10. Walling DM, Flaitz CM, Nichols CM, Hudnall SD, Adler-Storthz K (2001) Persistent productive Epstein-Barr virus replication in normal epithelial cells in vivo. J Infect Dis 184:1499–1507
[CrossRef][PubMed]

11. Biryukov J, Cruz L, Ryndock EJ, Meyers C (2015) Native human papillomavirus production, quantification and infectivity analysis. Methods Mol Biol 1249:317–331
[CrossRef][PubMed]

12. Meyers C, Frattini MG, Hudson JB, Laimins LA (1992) Biosynthesis of human papilloma virus from a continuous cell line upon epithelial differentiation. Science 257:971–973
[CrossRef][PubMed]

13. Schweinfurth JM, Meyers C (2006) Organotypic (raft) culture of biopsy-derived upper respiratory epithelium. Laryngoscope 116:1600–1602
[CrossRef][PubMed]

14. Israr M, Mitchell D, Alam S, Dinello D, Kishel JJ, Meyers C (2010) Effect of the HIV protease inhibitor amprenavir on the growth and differentiation of primary gingival epithelium. Antivir Ther 15:253–265
[CrossRef][PubMed][PubMedCentral]

15. Junying J, Herrmann K, Davies G, Lissauer D, Bell A, Timms J, Reynolds GM, Hubscher SG, Young LS, Niedobitek G, Murray PG (2003) Absence of Epstein-Barr virus DNA in the tumor cells of European hepatocellular carcinoma. Virology 306:236–243
[CrossRef][PubMed]

16. Kanda T, Yajima M, Ahsan N, Tanaka M, Takada K (2004) Production of high titer Epstein-Barr virus recombinants from Akata cells by using a bacterial artificial chromosome. J Virol 78:7004–7015
[CrossRef][PubMed][PubMedCentral]

17. Mann KP, Staunton D, Thorley-Lawson DA (1985) Epstein-Barr virus-encoded protein found in plasma membranes of transformed cells. J Virol 55:710–720
[PubMed][PubMedCentral]

5. Affinity Purification–Mass Spectroscopy Methods for Identifying Epstein–Barr Virus–Host Interactions

Anna A. Georges[1] and Lori Frappier[1] ✉

(1) Department of Molecular Genetics, University of Toronto, 1 Kings College Circle, Toronto, ON, Canada, M5S 1A8

✉ **Lori Frappier**
  Email: lori.frappier@utoronto.ca

Abstract
Considerable insight into the function and mechanism of action of viral proteins has come from identifying the cellular proteins with which they interact. In recent years, mass spectrometry-based methods have emerged as the method of choice for protein interaction discovery due to their comprehensive and unbiased nature. Methods involving single affinity purifications of epitope-tagged viral proteins (AP–MS) and tandem affinity purifications of viral proteins with two purification tags (TAP tagging) have both been used to identify novel host interactions with EBV proteins. However, to date these methods have only been applied to a small number of EBV proteins. Here we provide detailed methods of AP–MS and TAP tagging approaches that can be applied to any EBV protein in order to discover its host interactions.

Key words Epstein–Barr virus – Affinity purification – Mass spectrometry – Proteomics – TAP tag – SPA tag – FLAG tag – Protein interactions

1 Introduction

Epstein–Barr virus (EBV) encodes over 80 proteins, many of which interact with specific cellular proteins as part of the mechanism by which they manipulate cellular
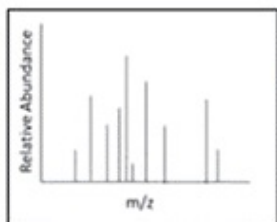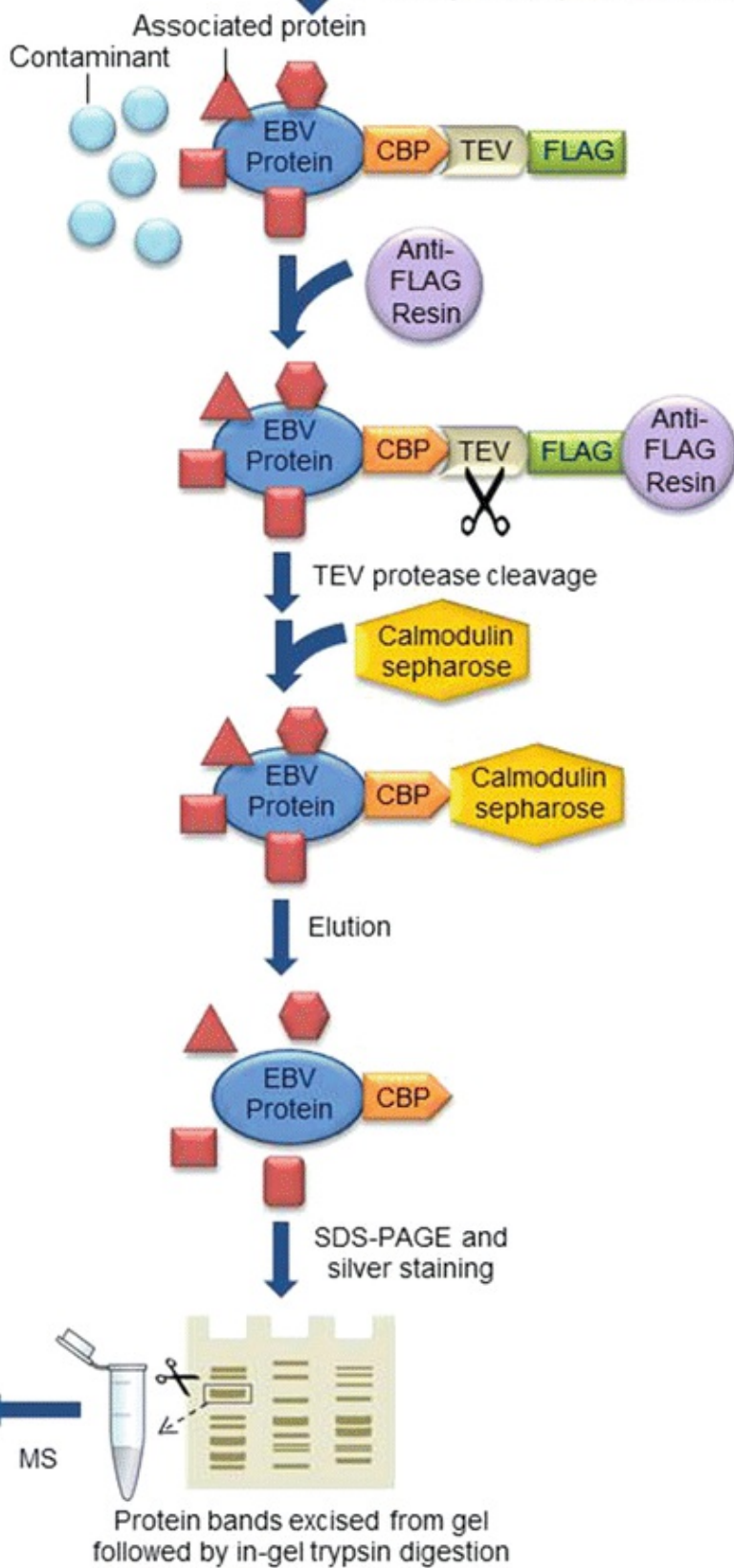
processes and/or fulfill their roles in viral infection. Therefore, identifying the cellular proteins with which an EBV protein interacts can provide considerable insight into the function and mechanism of action of that protein. Proteomics methods involving protein identification by mass spectroscopy (MS) are particularly valuable in this regard, because they can reveal interactions for which there were no previously known connections, they allow for detection of cellular proteins for which there are no suitable antibodies, and they provide an unbiased view of the relative frequency with which interactions occur. Here we will describe two MS-based approaches for identifying viral–host protein interactions that have proven to be most useful: affinity purification coupled with mass spectrometry (AP–MS) and tandem affinity purification (TAP) tagging. For more detailed comparison of these methods and their applications to viruses, *see* Georges and Frappier [1].

In TAP tagging, the viral protein of interest is expressed fused to two tandem affinity tags separated by a TEV (tobacco etch virus) protease cleavage site. The original TAP tag, which was developed for use in yeast, is composed of two protein A IgG -binding domains and a calmodulin-binding peptide (CBP) separated by a TEV protease cleavage site [2]. TAP-tagged proteins are recovered from cell extracts on IgG resin (agarose or Sepharose), eluted by TEV cleavage, and then further purified on calmodulin resin. Eluted proteins are typically analyzed by SDS–PAGE and silver staining, prior to tryptic digestion of excised bands and protein identification by matrix-assisted laser desorption/ionization (MALDI) MS (however direct trypsinization and identification of eluted proteins by tandem MS as described for AP–MS are also possible). The two purification steps in tandem affinity approaches limit the recovery of nonspecific protein interactions (as compared to single affinity purifications). However, a caveat of this method is that specific interactions that are weak or transient tend not to survive the two-step purification and therefore are not detected. In addition to the classic TAP tag, tandem tags that include 3×FLAG or Strep tags have also been described and tend to give more efficient protein recovery [3–5]. In Subheading 3.3, we describe the use of a sequential purification affinity (SPA) tag developed by Zeghouf et al. [3], which combines 3×FLAG and CBP tags (Fig. 1) and has been used for a variety of applications including viral–host interactions [6–8].

Cells expressing tagged EBV protein

- Harvest cells
- Cell lysis and protein extraction

Associated protein

Contaminant

EBV Protein | CBP | TEV | FLAG

Anti-FLAG Resin

EBV Protein | CBP | TEV | FLAG | Anti-FLAG Resin

TEV protease cleavage

Calmodulin sepharose

EBV Protein | CBP | Calmodulin sepharose

Elution

EBV Protein | CBP

SDS-PAGE and silver staining

MS

Relative Abundance

m/z

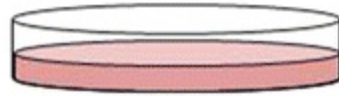Protein bands excised from gel followed by in-gel trypsin digestion

Fig. 1 Representation of a TAP tagging experiment using a SPA tag. A tandem affinity purification is shown using the FLAG and calmodulin-binding peptide (CBP) tags that comprise a SPA tag

TAP tagging methods have been applied to several EBV proteins. This method was first used by Holowaty et al. [6] to identify interactions between the EBV EBNA1 protein and host proteins, revealing strong, direct interactions with ubiquitin-specific protease 7 (USP7) and CK2 kinase. These interactions were later shown to be important for p53 destabilization and promyelocytic leukemia (PML) nuclear body disruption by EBNA1 [9–11]. Subsequently, TAP tagging was used by Forsman et al. [12] to identify cellular interactors with EBNA5 (also called EBNA-LP) and by Bailey et al. [13] to identify host interactions with the BZLF1 immediate-early protein. The latter led to the identification of the 53BP1 DNA damage response protein as a BZLF1 target, an interaction that appears to be important for lytic viral replication. While the above experiments were conducted by expressing the TAP-tagged viral protein in the absence of the virus, Ohashi et al. [14] recently constructed recombinant EBV genomes expressing tandemly tagged (FLAG and HA) EBNA3A , EBNA3B, or EBNA3C proteins and used them to generate lymphoblastoid cell lines. Tandem affinity purification of the EBNA3s confirmed their interaction with RBPJ and revealed novel interactions of EBNA3A and EBNA3B with complexes containing WDR48 and USP46 or USP12 deubiquitinating enzymes.

AP–MS differs from TAP tagging in that it involves a single affinity purification of a protein containing one epitope tag, most commonly 3×FLAG (Fig. 2), followed by green fluorescent protein (GFP) and HA. The tagged protein is recovered from the cell extract using a tag-specific antibody coupled to column resin. After elution, recovered proteins are typically digested with trypsin and then identified by liquid chromatography (LC) coupled to tandem MS (MS/MS). For details on this and other MS methods, *see* reviews by Chen and Gingras, Kean et al., and Owen et al. [15–17]. AP–MS is a more sensitive method for detecting protein interactions than TAP tagging, as it can detect both stable and transient interactions. As a result, it is also more prone to identifying nonspecific interactions, and measures must be taken to limit and/or filter these interactions in order to obtain meaningful data. This includes increasing the salt concentration of the extract above physiological levels, which interferes with nonspecific interactions to a greater degree than specific interactions, giving cleaner results. In addition, nucleic acid-mediated interactions frequently occur and can be limited by incubating the lysates with Benzonase prior to affinity purification. Despite these measures, some nonspecific interactions will still occur. These can be identified by the frequency and efficiency (according to total spectral counts) with which the interacting protein is recovered in AP–MS experiments with unrelated proteins. A comprehensive database of AP–MS data from 293 cells, called the contaminant

repository for affinity purification data or CRAPome, has been established for this purpose (http://www.crapome.org/) [18] and is an excellent resource for identifying background contaminants in a data set. The most common nonspecific contaminants include heat shock proteins, keratins, tubulins, actins, histones , translation elongation factors, ribosomal proteins, and ribonucleoproteins [18].

Cells expressing tagged EBV protein

- Harvest cells
- Cell lysis and protein extraction

Associated protein

Contaminant
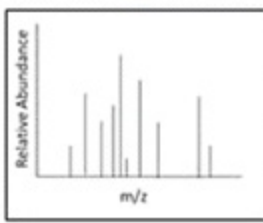
EBV Protein FLAG

Anti-FLAG Resin

EBV Protein FLAG Anti-FLAG Resin

Elution

EBV Protein FLAG
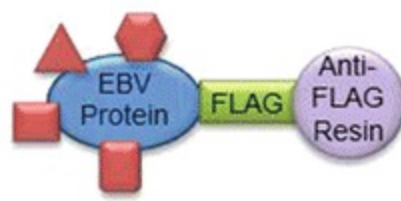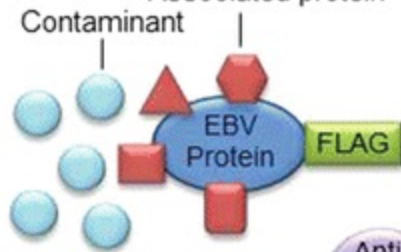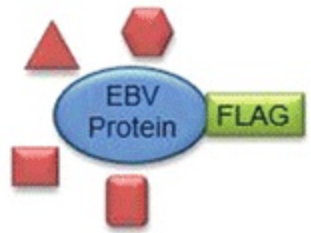
In-solution trypsin digestion

RAWTMR RTLMK
RTAK KLPTDSK
KHFAMQR KLVK
KIWYK RYQDLVR

LC-MS/MS

Relative Abundance

m/z

Fig. 2 Representation of an AP–MS experiment using a FLAG tag. A typical single affinity purification experiment with a FLAG -tagged viral protein is shown

A few studies have used AP–MS to investigate host interactions of EBV proteins. AP–MS performed on FLAG–BZLF1 expressed in 293 T cells by transient transfection identified an interaction with mitochondrial single-stranded DNA-binding protein (mtSSB) that contributes to EBV lytic DNA replication while inhibiting mitochondrial DNA replication [19]. Similar transient expression of the FLAG-tagged EBV tegument protein BGLF2 in CNE2Z nasopharyngeal carcinoma cells identified interactions with GMIP and NEK9 kinase that appear to be important for cell cycle regulation [20]. BGLF2 was shown to induce the G1/S phase of the cell cycle by increasing p21 levels, and silencing of either GMIP or NEK9 mimicked BGLF2 expression in inducing p21 and abrogated the ability of BGLF2 to further induce p21. AP–MS a pproaches have also been applied to EBNA1, in both cases by expressing EBNA1 at low levels in order to limit nonspecific interactions that can arise due to overexpression. Malik-Soni et al. [21] used an adenovirus delivery system to express FLAG-tagged EBNA1 in both EBV-negative and EBV-positive nasopharyngeal and gastric carcinoma cell lines and compared protein interactions in EBV latent and lytic infection to uninfected cells. The results showed that previously identified EBNA1 interactions with USP7, CK2, PRMT5, NAP1, and TAF-Iβ occur in the context of both latent and lytic infection. This study also identified an interaction with nucleophosmin, which was subsequently shown to be important for the transcriptional activation function of EBNA1 [22]. Chen et al. [23] conducted an AP–MS experiment with FLAG-tagged EBNA1 stably expressed in BJAB Burkitt lymphoma cells and identified interacting host proteins that were excised from Coomassie-stained polyacrylamide gels. This identified EBNA1 interactions with nucleolin and ribosome protein L4, which appear to cooperate in promoting EBNA1 binding to *oriP* in B cells [24].

An important consideration in AP–MS or TAP tagging experiments is the buffer conditions used for cell lysis and subsequent protein recovery. Higher salt and detergent concentrations tend to improve protein recovery but decrease protein interactions. Prior to the proteomic experiment, the buffer conditions required to efficiently extract the viral protein from the cell in soluble form should be determined. Proteins that are associated with insoluble structures (e.g., chromatin and nuclea r matrix) often require high salt concentrations for efficient extraction. In such cases, the high-salt extraction method described below (Subheadings 2.1 and 3.1) can be used, followed by dialysis to physiological salt to allow restoration of protein interactions. If the viral protein is efficiently recovered in soluble form when cells are lysed in physiological to moderate salt conditions, then the extraction methods in Subheadings 2.2 and 3.2 are recommended, as interacting proteins can be recovered directly without the need for dialysis.

2 Materials

2.1 High-Salt Extraction

1. TpA buffer: 10 mM HEPES, pH 7.9, 1.5 mM $MgCl_2$, 10 mM KCl, 1 mM DTT, and P8340 protease inhibitor cocktail (Sigma). Add about 400 mL water to a 1 L glass beaker. Weigh 2.36 g HEPES, 0.304 g $MgCl_2$, and 0.748 g KCl and transfer to the beaker. Add water to a volume of 900 mL. Mix with a stir bar and adjust pH with HCl (*see* **Note 1**). Make up to 1 L with water. Sterilize by vacuum filtration and store at 4 °C. Add the DTT and protease inhibitor just before using (*see* **Note 2**).

2. TpB buffer: 50 mM HEPES, pH 7.5, 1.5 mM $MgCl_2$, 1.26 M potassium acetate, and 75 % glycerol. Sterilize by vacuum filtration and store at 4 °C (*see* **Note 3**).

3. Spectra/Por® 18 mm dialysis tubing.

4. Dialysis buffer: 10 mM HEPES, pH 7.9, 0.1 mM EDTA, 0.1 mM DTT, 0.1 M potassium acetate, and 10 % glycerol. Make up two 2 L solutions of dialysis buffer (*see* **Note 4**).

2.2 Physiological or Moderate Salt Extraction

1. Physiological or moderate salt lysis buffer: 50 mM HEPES (pH 8.0), 100 mM–300 mM KCl, 2 mM EDTA, 0.1 % NP40, 10 % glycerol, 1 mM PMSF, and 1 mM DTT and protease inhibitor cocktail (*see* **Note 5**).

2. 25 U Benzonase (Novagen).

2.3 Recovery of FLAG- Tagged Proteins for AP– MS

1. Anti-FLAG M2 resin (Sigma-Aldrich).

2. Rinsing buffer: 50 mM ammonium bicarbonate, pH 8, and 75 mM KCl (*see* **Note 6**).

3. 0.5 M ammonium hydroxide: Ensure the pH is 11–12 (*see* **Note 7**).

4. 0.1 μg/μL mass spectrometry grade trypsin: Dissolve 20 μg of lyophilized proteomics grade trypsin (Sigma) in 1 mL of 1 mM HCl.

2.4 Tandem Affinity Purification Using a SPA Tag

1. TEV buffer: 10 mM Tris–HCl, pH 8, 100 mM NaCl, 0.1 % Triton X-100, 10 % glycerol, and 1 mM DTT.

2. Calmodulin Sepharose 4B resin (GE Healthcare).

3. Calmodulin binding buffer (CBB): 10 mM Tris, pH 8, 100 mM NaCl, 1 mM imidazole, 1 mM magnesium acetate, 2 mM $CaCl_2$, 0.1 % Triton X-100, 10 % glycerol, and 10 mM β-mercaptoethanol.

4. Calmodulin column: Bend the end of a 200 μL pipette tip using forceps and add 10 μL of glass beads to the bent tip. Place the tip in an Eppendorf tube on ice and wash the glass beads with 50 μL of CBB. Drain by gravity flow (*see* **Note 8**).

5. Calmodulin elution buffer: 10 mM Tris, pH 8, 100 mM NaCl, 1 mM imidazole, 1 mM magnesium acetate, 5 mM EGTA, 0.1 % Triton X-100, and 10 mM β-mercaptoethanol.

6. 5× Laemmli sample buffer: 60 mM Tris–Cl, pH 6.8, 2 % SDS, 10 % glycerol, 5 % β-mercaptoethanol, and 0.01 % bromophenol blue. Add 1 mL of 1 % bromophenol blue to 4 mL of 1.5 M Tris–Cl and pH 6.8. Add 10 mL of glycerol and mix. Add 2 g of SDS and mix until dissolved. Add 5 mL of β-mercaptoethanol and mix. Aliquot and store at −20 °C.

3 Methods

3.1 AP–MS of FLAG-Tagged Proteins: High-Salt Extraction Method

The following protocol is one we have used to profile the host interactions of the EBV EBNA1 protein in multiple cell lines [21]. The extraction method is adapted from Zeghouf et al. [3] and Coulombe et al. [25]. The elution method is adapted from Chen and Gingras 2007 [15]:

1. Harvest cells from 10 to 20 150 cm^2 plates expressing the FLAG-tagged viral protein of interest, collect by centrifugation at 1000 × g for 5 min at 4 °C, and wash cell pellet three times in 10 mL PBS (*see* **Note 9**).

2. Add 1.33 pellet volumes of TpA buffer followed by ten strokes in a dounce homogenizer at 4 °C (*see* **Note 10**).

3. Add 1 pellet volume of TpB buffer to the lysate, followed by ten (additional) strokes in the homogenizer (*see* **Note 11**).

4. Incubate lysate at 4 °C or on ice for an additional 30 min.

5. Transfer the lysate from the glass homogenizer to tubes suitable for the Beckman 50 Ti rotor. Clarify the lysate by centrifugation at 37,000 rpm (125,000 × g) in a Beckman 50 Ti rotor for 2–3 h.

6. Transfer the supernatant to 18 mm dialysis tubing and seal both ends (*see* **Note 12**). Dialyze for 1 h at 4 °C in 2 L dialysis buffer. Transfer to the second 2 L of dialysis buffer and continue dialysis for several hours to overnight at 4 °C with slow stirring with a magnetic stir bar.

7. After dialysis, transfer the lysate to an Eppendorf tube and spin in a microcentrifuge at 15,000 rpm (20,000 × g) for 5 min at 4 °C (*see* **Note 13**).

8. Meanwhile, for each sample, wash a 50 μL bed volume of anti-FLAG M2 resin with 1 mL IPP buffer and pellet the beads by centrifugation at 1500 × g for 3 min (*see* **Note 14**). Repeat twice.

9. Add the clarified lysate from **step 7** to the pre-washed resin and rotate end over end for 4 h at 4 °C.

10. After the incubation, pellet the resin by centrifugation as in **step 8** and discard the supernatant. Wash the beads twice with 1 mL IPP buffer, followed by three washes with 1 mL rinsing buffer (*see* **Note 15**).

11. After the last wash with rinsing buffer, remove most of the liquid, centrifuge the sample at 3000 rpm ($800 \times g$) for 5 s, and then remove the remaining liquid with a narrow-tip pipette.

12. To elute the protein, add 400 μL of 0.5 M ammonium hydroxide to the beads and rotate end over end for 15 min at 4 °C. Pellet the beads by brief centrifugation and remove the supernatant (*see* **Note 16**). Repeat two more times.

13. Pool eluates and lyophilize in a SpeedVac overnight or until ammonium hydroxide has completely evaporated. A white powder should be evident.

14. Wash the dried pellet in 200 μL HPLC grade H_2O, and then lyophilize again. Store at −80 °C or proceed to tryptic digestion.

15. For tryptic digestion, first dissolve the lyophilized pellet in 100 μL of 50 mM ammonium bicarbonate. Then add 7.5 μL of 0.1 μg/μL of mass spectrometry grade trypsin and incubate overnight at 37 °C. The next day, add 2.5 μL of 0.1 μg/μL trypsin to the sample, incubate for another 2 h at 37 °C, and then lyophilize.

16. Resuspend the lyophilized peptides in 20 μL of 2 % acetonitrile and 0.1 % formic acid. Clarify the sample by 10 min centrifugation in a microcentrifuge, and then transfer the supernatant to a fresh tube. The sample can now be loaded on a reverse phase column for LC–MS or stored at −20 °C.

3.2 AP–MS of FLAG-Tagged Proteins: Physiological/Moderate Salt Extraction Method

Extraction methods using physiological or moderate salt concentrations can be conducted with fewer plates of cells, since no dialysis step is required.

1. Harvest five 150 cm^2 plates of cells expressing the protein of interest as per **step 1**

in Subheading 3.1 above.

2. Resuspend the cell pellet in 1:4 pellet weight–volume of physiological or moderate salt lysis buffer (*see* **Note 5**). Incubate on ice for 10 min.

3. Freeze the sample in liquid nitrogen or dry ice for 5 min, and then thaw at 37 °C with agitation (*see* **Note 17**).

4. When thawed, transfer the lysate to a 2 mL Eppendorf tube and spin in a microcentrifuge at 14,000 rpm (18,000 × g) for 20 min at 4 °C. Transfer the supernatant to a fresh 15 mL conical tube.

5. Meanwhile wash 30 µL packed FLAG M2 resin four times in lysis buffer (*see* **Note 14**).

6. Add 25 U Benzonase and the pre-washed FLAG M2 resin to the supernatant and incubate for 2 h at 4 °C with end-over-end rotation (*see* **Note 18**).

7. Pellet the resin by centrifugation at 1000 × g for 1 min and discard the supernatant. Add 1 mL lysis buffer to the resin and transfer the resin lysis solution to a fresh 1.5 mL Eppendorf tube.

8. Wash the beads with rinsing buffer, followed by protein elution and trypsinization as described in **steps 11–16** in Subheading 3.1 above.

3.3 Tandem Affinity Purification Using a SPA Tag

Tandem affinity purification methods are useful for revealing stable complexes and can be used in conjunction with either of the above lysis methods. We have used the following method (adapted from Zeghouf et al. [3]) to identify interactors with SPA-tagged viral and cellular proteins [6, 8]:

1. Lyse the cells and incubate the lysate with pre-washed FLAG M2 resin using one of the above methods.

2. Harvest the resin by centrifugation and wash three times with 500 µL TEV buffer. Remove all of the buffer from the beads after the last wash.

3. Add 200 µL of TEV buffer and 30 units of TEV protease to the resin and mix by end-over-end rotation overnight at 4 °C. TEV will cleave off the FLAG tag, resulting in elution of the calmodulin-tagged bait protein.

4. Meanwhile, prepare the calmodulin resin by washing 50 µL of calmodulin Sepharose 4B (GE Healthcare) twice with 500 µL of calmodulin-binding buffer (CBB) (*see* **Note 14**). After the second wash, remove all the buffer from the resin, and then add 50 µL of CBB (*see* **Note 19**).

5. Pellet the FLAG M2 resin from **step 3** by centrifugation at $1500 \times g$ for 3 min, and transfer the supernatant (eluate) to a new tube. Add 400 µL of CBB, 0.8 µL of 1 M $CaCl_2$ (final concentration approximately 1 µM), and 25 U of micrococcal nuclease or Benzonase to the eluate. Incubate for 20 min at room temperature.

6. Add 200 µL of cold CBB and the 100 µL slurry of calmodulin Sepharose (prepared in **step 4**) to the eluate and mix by end-over-end rotation for 2 h at 4 °C.

7. Collect the calmodulin Sepharose in **step 6** by brief centrifugation and remove the supernatant. Wash the resin twice with 500 µL CBB. After the second wash, pellet the resin and remove all but 200 µL of the supernatant. Resuspend the resin in the remaining supernatant and transfer it to the calmodulin pipette tip column containing glass beads (*see* **Note 20**). Rinse the Eppendorf tube with 500 µL CBB and transfer to the column. Wash the column two more times with 500 µL CBB.

8. If the sample is to be analyzed by SDS–PAGE coupled to MALDI–TOF MS, elute the bound protein in a siliconized (low retention) Eppendorf tube by adding 100 µL calmodulin elution buffer to the column. Repeat five times and pool eluates. Perform an additional elution with 200 µL of 1 % SDS at room temperature, which can be pooled with the other eluates or processed separately (*see* **Note 21**). The SDS elution is only used if the sample is to be analyzed by SDS–PAGE prior to MALDI–TOF or other MS. If samples are to be analyzed by LC–MS/MS, elute with

50 mM ammonium bicarbonate, pH 8, and 25 mM EGTA, and then proceed as in **step 12** in Subheading 3.1 (*see* **Note 22**).

9. Cap the Eppendorf tube containing the eluate and pierce the cap several times with a needle. Freeze in liquid nitrogen and then desiccate in a SpeedVac to reduce the volume to ~60 μL. Add Laemmli sample buffer, and boil and analyze the whole sample by SDS–PAGE followed by silver staining. Excise silver-stained bands, reduce, alkylate, and perform in-gel trypsinization as in Shevchenko et al. [26]. Analyze the peptides by MALDI–TOF MS.

---

4 Notes

1. Having the magnetic stir bar stirring in the water prior to adding the solids will help them to dissolve more easily.

2. DTT has a half-life of only 11 h when stored at refrigerated temperatures (0–4 °C) at pH 8 and therefore should always be added to the buffer immediately before use. Aliquots of 100× protease inhibitor are stored at −20 °C and, like DTT, should be added to the buffer just before using.

3. The solution will be viscous, so the vacuum filtration process will take much more time than that for TpA. Since it will be difficult to mix the protease inhibitor into the TpB buffer, we recommend adding a 2× concentration of P8340 to the TpA buffer, which will be diluted to 1× once the TpB is added.

4. Make the dialysis buffer ahead to allow time for it to cool to 4 °C in the cold room. DTT should be added immediately before use.

5. The higher the salt concentration, the more protein interactions tend to be disrupted. However, since nonspecific interactions are disrupted more easily than specific interactions, the salt concentration can be adjusted to strike the best balance between reducing nonspecific interactions and retaining detectable specific interactions. It is also important to verify that the bait viral protein is extracted in soluble form using the selected buffer conditions.

6. It is essential that HPLC grade H_2O is used to make up both the rinsing and elution

buffers.

7. We recommend making the elution buffer right before use.

8. The flow of CBB through the column can be initiated by pushing on the top of the tip, if necessary.

9. The lower the expression level of the bait protein, the more plates of cells are required. The cell pellets washed in PBS can be stored at −80 °C or lysed immediately.

10. It is easiest to determine the amount of TpA to use based on the weight of the pellet. Assume 1 g of cell pellet is 1 mL. Therefore, for every 1 g of cell pellet, use 1.33 mL of TpA.

11. Add 1 mL of TpB for every 1 g of cell pellet.

12. Begin by sealing one end of the dialysis tube with a dialysis tube closure. Then add all of the supernatant slowly to the tubing using a long pipette tip. Seal the open end with a second dialysis tube closure. During dialysis, the volume of the dialysate will increase. Therefore, to avoid rupture of the tubing, do not completely fill the tubing, but rather, use enough tubing so that it is only half full with the extract.

13. Some proteins may come out of solution during dialysis resulting in a white precipitate. The precipitated proteins are pelleted by centrifugation in this step.

14. To transfer the resin, use a pipette tip in which the narrow end has been trimmed off to give a larger opening.

15. It is important that the beads are handled gently from this point forward, to avoid losses of the resin or disruption of bound proteins. To wash the beads, invert the tube end over end very gently for 30 s.

16. It is important to avoid collecting any of the resin with the supernatant, as it will block the column used in LC–MS/MS. One way to avoid transferring any resin is to remove the eluate using gel loading tips. Additionally, once all the eluate has

been collected and pooled, spin the tube in a tabletop centrifuge on maximum speed for 1 min to pellet any resin that may have been transferred with the eluate. Then transfer the supernatant to a fresh tube leaving behind a ~20 µl volume so as not to disturb the pellet.

17. Remove the sample from the 37 °C bath as soon as it is thawed to avoid protein degradation.

18. Many proteins bind RNA or DNA nonspecifically, and hence two such proteins may co-purify because they are both bound to the same nucleic acid fragment. RNA-mediated interactions are especially a problem due to the high abundance of RNA-binding proteins in the cell. Benzonase digests RNA and DNA and therefore adding it at this stage helps to limit nucleic acid-mediated interactions.

19. Use siliconized (low retention) Eppendorf tubes and pipette tips when handling the calmodulin resin to reduce losses of the resin.

20. While the calmodulin resin can be recovered by centrifugation, the recovery, washing, and elution of the resin are greatly facilitated by pouring a column.

21. The EGTA in this buffer gradually results in elution by chelating calcium; however, this elution can be inefficient. Therefore it is recommended to perform an additional elution with 200 µL of 1 % SDS at room temperature, to recover any remaining bound protein.

22. If samples are to be analyzed by LC–MS/MS, then no detergents can be used during the elution step.

References

1. Georges AA, Frappier L (2015) Proteomics methods for discovering viral-host interactions. Methods 90:21–27
[CrossRef][PubMed]

2. Rigaut G, Shevchenko A, Rutz B, Wilm M, Mann M, Seraphin B (1999) A generic protein purification method for protein complex characterization and proteome exploration. Nat Biotechnol 17:1030–1032
[CrossRef][PubMed]

3. Zeghouf M, Li J, Butland G, Borkowska A, Canadien V, Richards D, Beattie B, Emili A, Greenblatt JF (2004)

Sequential Peptide Affinity (SPA) system for the identification of mammalian and bacterial protein complexes. J Proteome Res 3:463–468
[CrossRef][PubMed]

4. Burckstummer T, Bennett KL, Preradovic A, Schutze G, Hantschel O, Superti-Furga G, Bauch A (2006) An efficient tandem affinity purification procedure for interaction proteomics in mammalian cells. Nat Methods 3:1013–1019
[CrossRef][PubMed]

5. Gloeckner CJ, Boldt K, Schumacher A, Roepman R, Ueffing M (2007) A novel tandem affinity purification strategy for the efficient isolation and characterisation of native protein complexes. Proteomics 7:4228–4234
[CrossRef][PubMed]

6. Holowaty MN, Zeghouf M, Wu H, Tellam J, Athanasopoulos V, Greenblatt J, Frappier L (2003) Protein profiling with Epstein-Barr nuclear antigen-1 reveals an interaction with the herpesvirus-associated ubiquitin-specific protease HAUSP/USP7. J Biol Chem 278:29987–29994
[CrossRef][PubMed]

7. Cochrane A, Murley LL, Gao M, Wong R, Clayton K, Brufatto N, Canadien V, Mamelak D, Chen T, Richards D, Zeghouf M, Greenblatt J, Burks C, Frappier L (2009) Stable complex formation between HIV Rev and the nucleosome assembly protein, NAP1, affects Rev function. Virology 388:103–111
[CrossRef][PubMed]

8. Sakwe AM, Nguyen T, Athanasopoulos V, Shire K, Frappier L (2007) Identification and characterization of a novel component of the human minichromosome maintenance complex. Mol Cell Biol 27:3044–3055
[CrossRef][PubMed][PubMedCentral]

9. Saridakis V, Sheng Y, Sarkari F, Holowaty MN, Shire K, Nguyen T, Zhang RG, Liao J, Lee W, Edwards AM, Arrowsmith CH, Frappier L (2005) Structure of the p53 binding domain of HAUSP/USP7 bound to Epstein-Barr nuclear antigen 1 implications for EBV-mediated immortalization. Mol Cell 18:25–36
[CrossRef][PubMed]

10. Sivachandran N, Sarkari F, Frappier L (2008) Epstein-Barr nuclear antigen 1 contributes to nasopharyngeal carcinoma through disruption of PML nuclear bodies. PLoS Pathog 4:e1000170
[CrossRef][PubMed][PubMedCentral]

11. Sivachandran N, Cao JY, Frappier L (2010) Epstein-Barr virus nuclear antigen 1 Hijacks the host kinase CK2 to disrupt PML nuclear bodies. J Virol 84:11113–11123
[CrossRef][PubMed][PubMedCentral]

12. Forsman A, Ruetschi U, Ekholm J, Rymo L (2008) Identification of intracellular proteins associated with the EBV-encoded nuclear antigen 5 using an efficient TAP procedure and FT-ICR mass spectrometry. J Proteome Res 7:2309–2319
[CrossRef][PubMed]

13. Bailey SG, Verrall E, Schelcher C, Rhie A, Doherty AJ, Sinclair AJ (2009) Functional interaction between Epstein-Barr virus replication protein Zta and host DNA damage response protein 53BP1. J Virol 83:11116–11122
[CrossRef][PubMed][PubMedCentral]

14. Ohashi M, Holthaus AM, Calderwood MA, Lai CY, Krastins B, Sarracino D, Johannsen E (2015) The EBNA3 family of Epstein-Barr virus nuclear proteins associates with the USP46/USP12 deubiquitination complexes to regulate lymphoblastoid cell line growth. PLoS Pathog 11:e1004822

[CrossRef][PubMed][PubMedCentral]

15. Chen GI, Gingras AC (2007) Affinity-purification mass spectrometry (AP-MS) of serine/threonine phosphatases. Methods 42:298–305
[CrossRef][PubMed]

16. Kean MJ, Couzens AL, Gingras AC (2012) Mass spectrometry approaches to study mammalian kinase and phosphatase associated proteins. Methods 57:400–408
[CrossRef][PubMed]

17. Owen CB, Hughes DJ, Baquero-Perez B, Berndt A, Schumann S, Jackson BR, Whitehouse A (2014) Utilising proteomic approaches to understand oncogenic human herpesviruses (Review). Mol Clin Oncol 2:891–903
[PubMed][PubMedCentral]

18. Mellacheruvu D, Wright Z, Couzens AL, Lambert JP, St-Denis NA, Li T, Miteva YV, Hauri S, Sardiu ME, Low TY, Halim VA, Bagshaw RD, Hubner NC, Al-Hakim A, Bouchard A, Faubert D, Fermin D, Dunham WH, Goudreault M, Lin ZY, Badillo BG, Pawson T, Durocher D, Coulombe B, Aebersold R, Superti-Furga G, Colinge J, Heck AJ, Choi H, Gstaiger M, Mohammed S, Cristea IM, Bennett KL, Washburn MP, Raught B, Ewing RM, Gingras AC, Nesvizhskii AI (2013) The CRAPome: a contaminant repository for affinity purification-mass spectrometry data. Nat Methods 10:730–736
[CrossRef][PubMed][PubMedCentral]

19. Wiedmer A, Wang P, Zhou J, Rennekamp AJ, Tiranti V, Zeviani M, Lieberman PM (2008) Epstein-Barr virus immediate-early protein Zta co-opts mitochondrial single-stranded DNA binding protein to promote viral and inhibit mitochondrial DNA replication. J Virol 82:4647–4655
[CrossRef][PubMed][PubMedCentral]

20. Paladino P, Marcon E, Greenblatt J, Frappier L (2014) Identification of herpesvirus proteins that contribute to G1/S arrest. J Virol 88:4480–4492
[CrossRef][PubMed][PubMedCentral]

21. Malik-Soni N, Frappier L (2012) Proteomic profiling of EBNA1-host protein interactions in latent and lytic Epstein-Barr virus infections. J Virol 86:6999–7002
[CrossRef][PubMed][PubMedCentral]

22. Malik-Soni N, Frappier L (2014) Nucleophosmin contributes to the transcriptional activation function of the Epstein-Barr virus EBNA1 protein. J Virol 88:2323–2326
[CrossRef][PubMed][PubMedCentral]

23. Chen YL, Liu CD, Cheng CP, Zhao B, Hsu HJ, Shen CL, Chiu SJ, Kieff E, Peng CW (2014) Nucleolin is important for Epstein-Barr virus nuclear antigen 1-mediated episome binding, maintenance, and transcription. Proc Natl Acad Sci U S A 111:243–248
[CrossRef][PubMed]

24. Shen CL, Liu CD, You RI, Ching YH, Liang J, Ke L, Chen YL, Chen HC, Hsu HJ, Liou JW, Kieff E, Peng CW (2016) Ribosome Protein L4 is essential for Epstein-Barr Virus Nuclear Antigen 1 function. Proc Natl Acad Sci U S A 113:2229–2234
[CrossRef][PubMed][PubMedCentral]

25. Coulombe B, Killeen M, Liljelund P, Honda B, Xiao H, Ingles CJ, Greenblatt J (1992) Identification of three mammalian proteins that bind to the yeast TATA box protein TFIID. Gene Expr 2:99–110
[PubMed]

26. Shevchenko A, Tomas H, Havlis J, Olsen JV, Mann M (2006) In-gel digestion for mass spectrometric characterization of proteins and proteomes. Nat Protoc 1:2856–2860
[CrossRef][PubMed]

6. The Use of 3D Telomere FISH for the Characterization of the Nuclear Architecture in EBV-Positive Hodgkin's Lymphoma

Hans Knecht[1]✉ and Sabine Mai[2]

(1)   Division of Hematology, Department of Medicine, Jewish General Hospital, McGill University, 3755, Chemin de la Côte Ste-Catherine, Montréal, Québec, Canada, H3T 1E2
(2)   Genomic Center for Cancer Research and Diagnosis, Cell Biology, Univeristy of Manitoba, CancerCare Manitoba, Winnipeg, MB, Canada

✉ **Hans Knecht**
   Email: hans.knecht@mcgill.ca

Abstract
The 3D nuclear architecture is closely related to cellular functions and chromosomes are organized in distinct territories. Quantitative 3D telomere FISH analysis (3D Q-FISH) and 3D super-resolution imaging (3D-SIM) at a resolution up to 80 nm as well as the recently developed combined quantitative 3D TRF2-telomere immune FISH technique (3D TRF2/Telo-Q-FISH) have substantially contributed to elucidate molecular pathogenic mechanisms of hematological diseases. Here we report the methods we applied to uncover major molecular steps involved in the pathogenesis of EBV-associated Hodgkin's lymphoma. These methods allowed us to identify the EBV-encoded oncoprotein LMP1 as a key element in the formation of Hodgkin (H-cell) and multinucleated Reed-Sternberg cells (RS-cell), the diagnostic tumor cell of classical Hodgkin's lymphoma (cHL). LMP1 mediates multinuclearity through downregulation of shelterin proteins, in particular telomere repeat binding factor 2 (TRF2).

Key words Telomere – 3D Q-FISH – Three-dimensional (3D) imaging – 3D TRF2/Telo-Q-FISH – Hodgkin's lymphoma – Hodgkin cell – Reed-Sternberg cell –

1 Introduction

Telomeres are the nucleoprotein complexes at the ends of chromosomes. Telomeric DNA consists of multiple double-stranded TTAGGG repeats and ends in a single-stranded overhang of the G rich 3′ strand [1]. Furthermore, a number of specific proteins, either binding telomeric DNA directly or being associated with telomeric chromatin, called the shelterin complex, are found on telomeres [2, 3]. Many cancer cells display chromosomal aberrations that are the direct result of telomere dysfunction [4, 5], and the 3D organization of telomeres is altered in cancer cells [6, 7].

This basic finding led to an advanced understanding of genetic changes in early cancer cells and proved that telomere organization is key to genome stability vs. instability [8, 9]. We have shown that each nucleus has a specific three-dimensional (3D) telomeric signature that defines it as normal or aberrant. Four criteria define this difference: (1) nuclear telomere distribution, (2) the presence/absence of telomere aggregate(s), (3) telomere numbers per cell, and (4) telomere sizes [10, 11].

The bi- or multinuclear Reed-Sternberg cells (RS-cells), the diagnostic element of Hodgkin's lymphoma (HL), are derived from mononuclear precursors called Hodgkin cells (H-cell), via endo-reduplication and have a limited capacity to divide further [12–14]. H-cells originate from germinal center B cells [15], and small circulating clonotypic B cells, putative precursors of H-cells, have been identified by flow cytometry [16]. H- and RS-cells show high telomerase activity [17, 18] and express abundant telomerase RNA [19].

Using a three-dimensional quantitative fluorescent in situ hybridization technique to visualize telomeres in cultured cells and biopsies (3D telomere Q-FISH) [8], we recently characterized the transition from mononuclear H- to multinuclear RS-cells at the molecular level [20–22]. We demonstrated that RS-cells are true end-stage tumor cells in both classical Epstein-Barr virus (EBV)-negative and EBV-positive HL. The number of nuclei in these RS-cells correlates closely with the 3D organization of telomeres, and further nuclear divisions are hampered by sustained telomere shortening or loss and telomere aggregation. The increase of very short telomeres and aggregates in these RS-cells compared to their mononuclear precursor H-cells is highly significant ($p < 0.01$). Such RS-cells contain telomere/DNA-poor "ghost" nuclei and giant "zebra" chromosomes including up to seven different chromosomal partners as revealed by spectral karyotyping (SKY). These molecular changes are the result of multiple breakage-bridge-fusion (BBF) cycles [22].

Analogous findings are observed in an in vitro model for post-germinal center B - cell, Epstein-Barr-virus (EBV)-associated cHL [23]. In this experimental system, the EBV-encoded oncogene latent membrane protein 1 (LMP1) mediates multinuclearity

and complex chromosomal abnormalities primarily through downregulation of telomere repeat binding factor 2 (TRF2) [23]. To further analyze these LMP1-mediated changes, we developed a combined quantitative 3D TRF2-telomere immune FISH technique (3D TRF2/Telo-Q-FISH) protocol and applied it to primary H- and RS-cells of EBV-associated and EBV-negative cHL. TRF2 has recently emerged as a key element of the shelterin complex [24] and also interacts with lamin A/C in the maintenance of the 3D genome organization [25].

---

2 Materials and Methods

Every step has to be carefully performed to guarantee the success of the hybridization.

2.1 3D Telomere Hybridization for Cell Cultures

1. Fix cells in 3.7 % formaldehyde/1× PBS for 20 min.

2. Wash 3× in 1× PBS for 5 min.

3. Incubate in 0.5 % Triton X-100 for 10 min.

4. Incubate in 20 % glycerol for 1 h or overnight.

5. Freeze-thaw treatment: Take the slide with forceps; dip the slide into liquid nitrogen, until the sound "click" is heard. Place the slide on paper towel and wait until glycerol thaws (if you have more than one slide, process them one by one).

6. Briefly soak slide in 20 % glycerol and then repeat freeze-thaw treatment three more times.

7. Wash 3× in 1× PBS for 5 min.

8. Incubate in fresh 0.1 M HCl for 5 min.

9. Wash 2× in 1× PBS for 5 min.

10. Equilibrate slides in 70 % formamide/2× SSC pH 7.0 for 1–2 h RT before

hybridization (*see* **Note 1**).

11. Pull the slide out of the Coplin jar and quickly drain excess liquid. Cover the coverslip with probe with the selected area of the slide (upside down). Wipe excess fluid around the coverslip and seal with rubber cement.

12. Apply ≤8 μL PNA-telomere probe (DAKO) [amount of probe depends on size of area to be hybridized] in the dark, add 25 × 25 mm coverslip, and apply rubber cement to seal.

13. Denature 3 min 80 °C, and hybridize 2 h at 30 °C (Hybrite™, Vysis/Abbott).

14. Remove rubber cement carefully and *work in the dark* (*see* **Note 2**).

15. Place slides including coverslips in 70 % formamide/10 mM Tris (pH = 7.4) shaking until coverslip floats off; wash twice for 15 min in this solution after coverslip is removed, RT, shaking.

16. Wash in 1× PBS, RT, one min, shaking.

17. Wash 5 min at 55 °C in 0.1× SSC, shaking.

18. Wash 2 × 5 min in 2× SSC/0.05 % Tween 20, RT, shaking.

19. Stain with DAPI (0.1 μg/mL stock), apply 50 μL, cover with coverslip, and incubate in the dark for 3 min.

20. Mount in Vectashield.

21. Clean Hybrite™ from water and rubber cement.

22. Image (*see* Fig. 1).
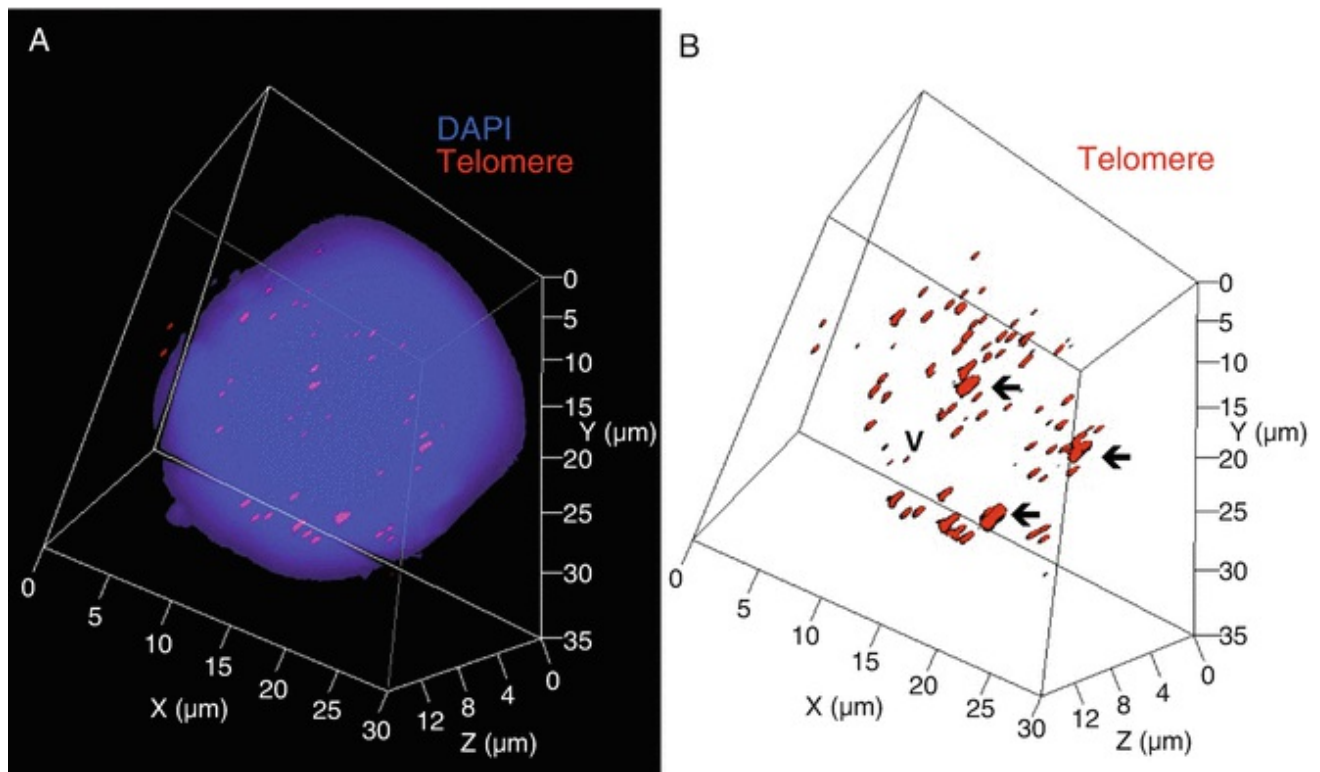
Fig. 1 Large mononuclear LMP1 -expressing BJAB-tTA-LMP1 cell at day 7 of culture. (**a**) Combined 3D nuclear staining (DAPI: *blue*; Telomere: *red*) in transparency mode reveals very short, short, and midsized telomeres as well as three aggregates (large *red dots*). (**b**) 3D telomere (*red*) reconstruction against white background increases contrast and enhances visibility of very short telomeres (*arrowhead*) and the three aggregates (*arrows*)

2.2 Paraffin Removal from Hodgkin's Tissue Sections (5 μm Lymph Nodes Sections)

To remove paraffin: three times 15 min each soak in xylene; wash longer or repeat if the paraffin is still visible on the slides; then clear the greasy xylene by soaking in a reverse-graded series of ethanol (start with 100 % and then 75, 70, and 50, 2–10 min each; usually 5 min each is sufficient for 5 μm thick sections); dip briefly in ddH2O water (*see* **Notes 3** and **4**).

2.3 Telomere Hybridization–Hodgkin Tissue Sections

2.3.1 Prepare First

80 °C NaSCN
1. Turn water bath to 80 °C. Put 150 mL of 1 M NaSCN into glass Coplin jar and put

in water bath to warm up. 1 M NaSCN is stored in the hazardous chemical cupboard below the fume hood.

3.7 % Formaldehyde

1. Mix together 90 mL of 1× PBS and 10 mL 37 % formaldehyde in 100 mL glass bottle. Set aside in the fume hood.

37° Pepsin

1. Mix in a glass Coplin jar 150 mL ddH2O and 0.75 mL (750 μL) 2 M HCl (50 mL tube of it on my bench). Put this into the 37 °C water bath.

2. Remove the vial of pepsin from the freezer and put into ice bucket to thaw.

3. Add the 75 μL of pepsin (frozen vial) right before the slides go into that Coplin jar (*see* **Note 5**).

70 % Formamide/10 mM Tris Wash Solution

1. Mix in a brown glass bottle:

   (a) 210 mL of deionized formamide (brown bottle in the fridge).

   (b) 87 mL ddH$_2$O.

   (c) 3 mL 1 M Tris pH 7.4 (50 mL tube of it on my bench).

2.3.2 Hybridiztion Steps

*2× SSC/0.05 % Tween Wash Solution*

1. Mix in a 500 mL glass bottle:

(a) 268.5 mL ddH$_2$O.

(b) 30 mL 20× SSC.

(c) 1.5 mL 10 % Tween.

(a) Deparaffinize the slides in 2 × 15 min xylene washes; put xylene in glass upright Coplin jars. *This incubation is done in the fume hood.* Can use xylene twice before discarding into xylene waste container. After one use, put used xylene into glass bottle and back into yellow flammable cabinet.

(b) Hydrate the slides in descending alcohol: 5 min each of 100, 70, and 50 % ethanol.

(c) Put slides into water Coplin jar for 3 min.

(d) Incubate slides at RT in 1× PBS for 5 min, *do not* shake (*see* **Note 6**).

(e) Put slides into the 80 °C NaSCN jar for exactly 20 min (*see* **Note 7**).

(f) Incubate slides at RT in 1× PBS for 5 min, *do not* shake.

(g) Put half of the volume, i.e., 50 mL of the 3.7 % formaldehyde/1× PBS solution into a vertical Coplin jar. Transfer slides into this vertical Coplin jar and incubate for 30 min, for 5 µm tissue sections). This incubation is done in the fume hood!

(h) 3 × 5 min 1× PBS, RT, shaking platform.

(i) 10 min 37°C pepsin treatment: at this point, add the 75 µL of pepsin (10 mg/mL) to the 37 °C jar (150 mL), mix with the pipette tip, and then put the slides in (*see* **Note 5**).

(j) 1 × 5 min in 1× PBS, RT, shaking platform.

(k) 10 min RT, 3.7 % formaldehyde/1× PBS, *do not* shake.

(l) Apply 8 µL PNA-telomere probe (DAKO) in the dark, add 25 × 25mm coverslip, and apply rubber cement to seal.

Hybrite Program: Need 3 min 80 °C, 2 h 30 °Cs

1. Put water into little side troughs of the Hybrite machine prior to use.

2. Denature 3 min 80 °C, hybridize 2 h at 30 °C (Hybrite™, Vysis/Abbott).

3. Put 0.1× SSC into glass Coplin jar and put into 55 °C water bath to warm up.

4. Remove rubber cement carefully and work in the dark (*see* **Note 2**).

5. Place slides with/without coverslips in 70 % formamide/10 mM Tris (pH = 7.4) shaking until coverslip floats off; wash twice for 15 min in this solution after coverslip is removed, RT, shaking.

6. Wash in 1× PBS, RT, 1 min, shaking.

7. Wash 5 min at 55 °C in 0.1× SSC, shaking.

8. Wash 2 × 5 min in 2× SSC/0.05 % Tween 20, RT, shaking.

9. Stain with DAPI (0. 1 µg/mL stock), apply 50 µL, cover with coverslip, and incubate in cardboard slide holder (dark) for 3 min.

10. Rinse with ddH$_2$O; put slides into holder and dip 3× in water Coplin jar.

11. Mount in Vectashield; 1 small drop; cover with coverslip. Clean up Hybrite.

12. Image slide (*see* Fig. 2).
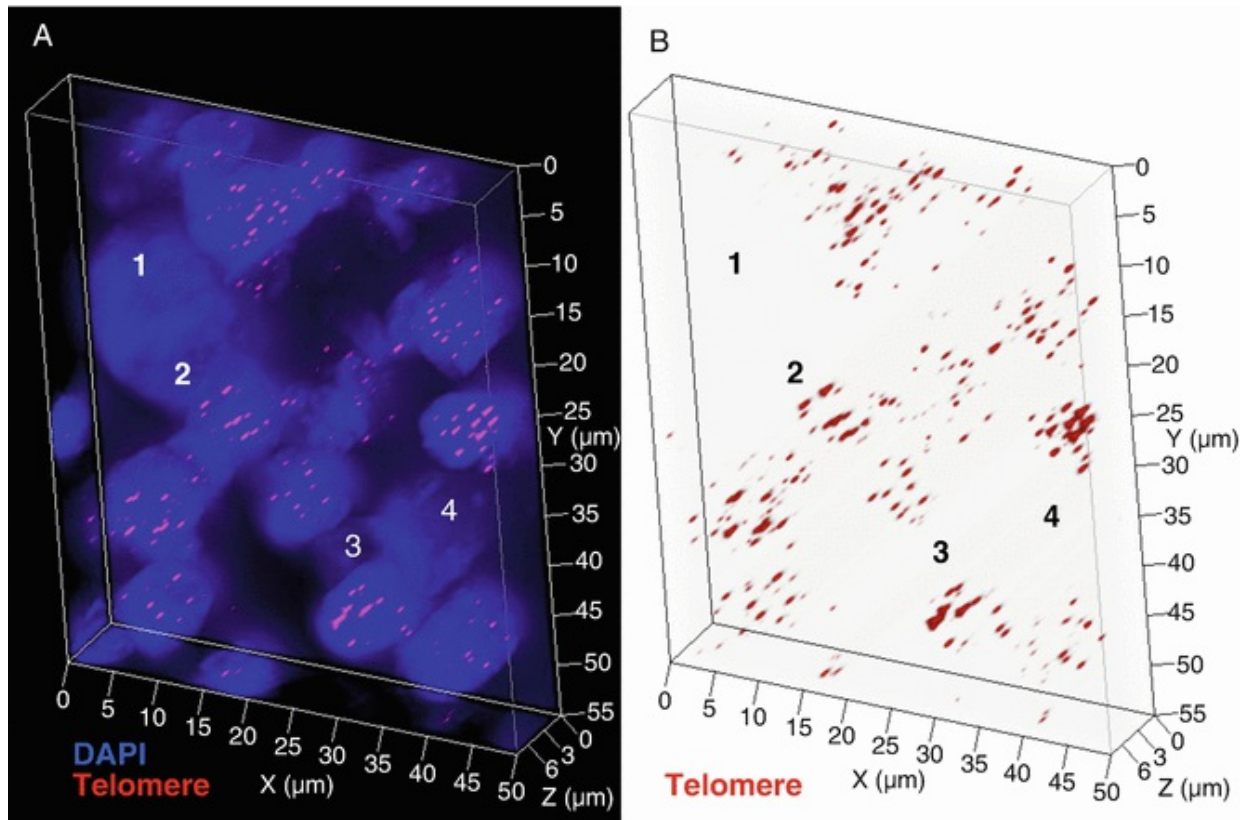
Fig. 2 3D identification of disturbed nuclear telomere organization in two binuclear LMP1 -expressing Reed-Sternberg cells. Upper Reed-Sternberg cell (1, 2) is endoreplicating, whereas lower Reed-Sternberg cell (3, 4) is clearly binucleated. (**a**) Combined 3D nuclear staining demonstrates telomere poor nuclei (blue) and identifies both Reed-Sternberg cells as nearly telomere-free. These "ghost" Reed-Sternberg cells may still contain "t-stumps" only identifiable with 3D-SIM technology [26]. (**b**) 3D telomere reconstruction in surface mode confirms virtually telomere-free "ghost" Reed-Sternberg cells (1, 2; 3, 4) surrounded by mainly midsized telomeres belonging to reactive lymphocytes

2.4 TRF2 -Telomere Immuno-FISH Protocol

Rabbit polyclonal TRF2 (1 mg/mL), Novus (NB110 57130) 1:500 dilution.

Secondary antibody: Goat anti-rabbit Alexa 488 (Molecular Probes).1:1000 dilution.

1. Fix cells in 3.7 % formaldehyde/1× PBS, 10 min, RT.

2. Wash in PBS twice, 5 min, RT, shaking.

3. Permeabilize with 0.1 % Triton X-100 (in ddH$_2$O), 12 min, no shaking, RT (*see* **Note 6**).

4. Wash in PBS three times, 5 min, RT, shaking.

5. Block in 4 % BSA/4× SSC for 5 min, RT.

6. Add antibody in 4 % BSA/4× SSC, 45 min, 37 °C, humidified atmosphere.

7. Wash in PBS three times, 5 min, RT, shaking.

8. Add secondary antibody in 4 % BSA/4× SSC, 30 min, 37 °C, humidified atmosphere.

9. Three washes in PBS, 5 min, RT, shaking:

   10. Apply 8 μL PNA-telomere probe (DAKO) in the dark, add 25 × 25 mm coverslip, and apply rubber cement to seal.

   11. Denature 3 min 80 °C, and hybridize 2 h at 30 °C (Hybrite™, Vysis/Abbott).

   12. Remove rubber cement carefully and work in the dark, from now until the end of the protocol (*see* **Note 2**).

   13. Place slides including coverslips in 70 % formamide/10 mM Tris (pH = 7.4) shaking.

   14. Until coverslip floats off; wash twice for 15 min in this solution after coverslip is removed, RT, shaking.

   15. Wash in 1× PBS, RT, 1 min, shaking.

   16. Wash 5 min at 55 °C in 0.1× SSC, shaking.

17. Wash 2 × 5 min in 2× SSC/0.05 % Tween 20, RT, shaking.

18. Reapply primary and secondary antibodies as described above.

19. Wash three times in 1× PBS.

20. Stain with DAPI (0.1 µg/mL stock), apply 50 µL, cover with coverslip, and incubate in the dark for 3 min.

21. Mount in Vectashield.

22. Image (*see* Fig. 3).
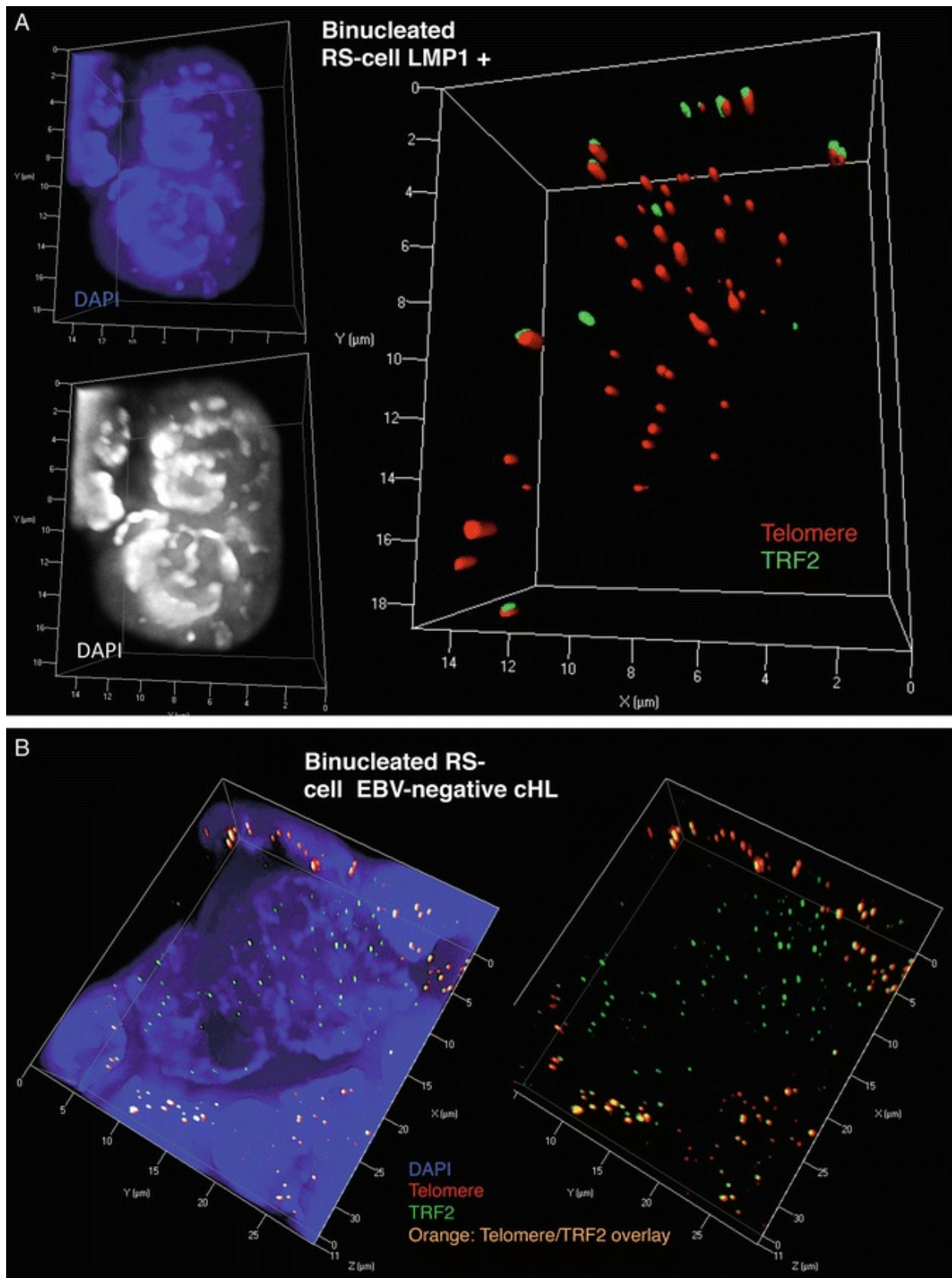
Fig. 3 3D TRF2 /Telo-Q-FISH detects two different (opposite) mechanisms of telomere de-protection. (**a**) Binucleated LMP1 -expressing Reed-Sternberg cell (*upper left*: DAPI blue; *lower left* DAPI gray for better contrast) contains mainly de-protected, small to midsized telomeres without physical link to the remaining TRF2 signals (*right*). (**b**) On the contrary, many EBV-negative cHL contain RS-cells with

upregulated free TRF2 signals and nearly no more identifiable telomeres as shown in transparency mode. The reactive, surrounding lymphocytes act as an endogenous control, showing as expected telomere/TRF2 overlay (*orange*) in a 1:1 ratio [27] as demonstrated by surface mode

2.5 3D Image Acquisition of Interphase Nuclei

AXIOVISION 4.8 with deconvolution module and rendering module are used. For every fluorochrome, the 3D image consists of a stack of 80 images for cell lines (50 images for 5 µm histology sections) with a sampling distance of 200 nm along the z and 102 nm in the x, y direction. The constrained iterative algorithm option is used for deconvolution [28]. For statistical analysis the number of telomeres is plotted against the intensity of telomere signals (telomere length) and the number of TRF2 signals against the intensity of TRF signals. A minimum of 30 interphase nuclei is analyzed (*see* **Notes 4** , **8** , and **9**).

2.6 3D Image Analysis for Telomeres

Telomere measurements are done with TeloView™ [29]. By choosing a simple threshold for the telomeres, a binary image is found. Based on that, the center of gravity of intensities is calculated for every object resulting in a set of coordinates (x, y, z) denoted by crosses on the screen. The integrated intensity of each telomere is calculated, because it is proportional to the telomere length [29].

2.7 Telomere Aggregates

Telomere aggregates are defined as clusters of telomeres that are found in close association and cannot be further resolved as separate entities at an optical resolution limit of 200 nm [30].

2.8 Telomere Length

Telomeres with a relative fluorescent intensity (x-axis) ranging from 0-5000 units are classified as very short, with an intensity ranging from 5,000-15,000 units defined as short, with an intensity ranging from 15,000–30,000 units defined as midsized, and with an intensity >30,000 units defined as large [21].

2.9 Telomere Volume

Total telomere volume is the sum of all very short, short, midsized, and large telomeres

and aggregates within one mononuclear or multinucleated cell. TeloView loads the 3D image and displays a maximum projection along the three main optical axes. Although thresholds and other parameters can be adjusted for display purposes, the analysis is performed on the original 3D data. The detailed physics of these measurements [29] are not in the scope of this chapter.

2.10 Nuclear Volume

The nuclear volume is calculated according to the 3D nuclear 4′, 6-diamidino-2-phenylindoline staining and corresponds to the integral of all DAPI-stained regions of the 80 images for cell lines (50 images for 5 μm histology sections) with a sampling distance of 200 nm along the z-axis [29, 30].

2.11 3D Image Analysis TRF2 Spots

The measurement parameters applied for the TRF2 length and TRF2 volume are identical to those established for telomeres (*see* **Note 9**).

2.12 Statistical Analysis

For each situation, where 30 cells (lymphocytes, H-cells, RS-cells) are analyzed, normally distributed parameters are compared between the two types of cells using nested ANOVA or two-way ANOVA. Multiple comparisons using the least square means tests followed, in which interaction effects between two factors were found to be significant. Other parameters that were not normally distributed were compared using a nonparametric Wilcoxon rank sum test. Significance level was set at $P = 0.05$. Analyses are carried out using SAS v9.1 programs (*see* Fig. 4).
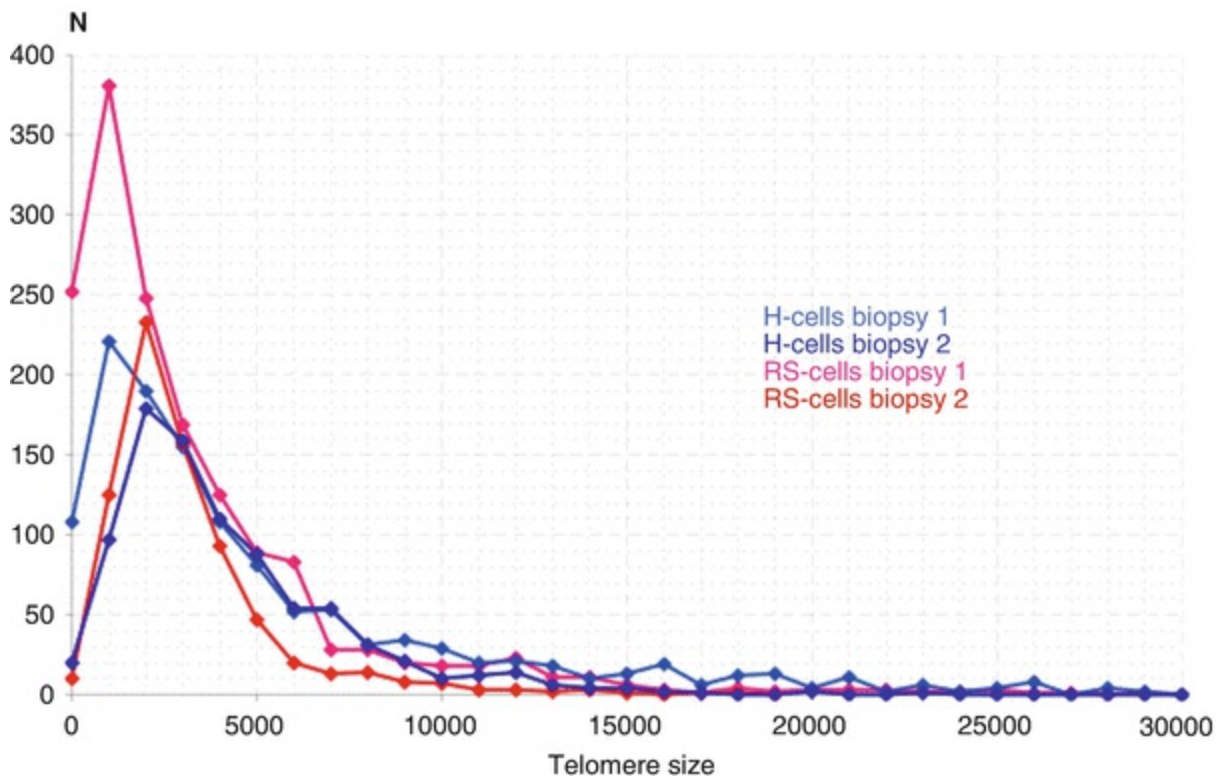
Fig. 4 Typical telomere profiles associated with refractory LMP1 -expressing nodular sclerosis cHL. Telomere distribution according to size in mononuclear H- (*blue*) and at least binuclear RS-cells (*red*). Results of two biopsies are based on 3D analysis of at least 30 Hodgkin and 30 Reed-Sternberg cells in each biopsy. Frequency (*x*-axis) and relative fluorescent intensity, i.e., size of telomeres (*y*-axis) in a diagnostic 5 μm lymph node section. Importantly, already the mononuclear H-cells exhibit a 3D telomere profile usually identified only in RS-cells. H-cells in aggressive disease do, contrary to H-cells in cases entering persistent remission, already contain multiple very short telomere consistent with having passed multiple rounds of mitosis without ending up in multinuclear end-stage RS-cells [31]

3 Notes

1. Slides may be stored in that solution for up to 3 months at 4 °C.

2. From this point of the protocol onward, work has to be performed in the dark.

3. Use xylene-proof dish, e.g., glass or green-colored standard histology dish. The tissue should appear transparent after the 3× xylene washes. If tissue still appears whitish, do a fourth xylene soak.

4. The quality of the 5 μm sections is crucial for a good hybridization and 3D analysis.

5. Pepsin has to be added immediately before use.

6. Subsequently, it is important not to mix up steps where a shaking platform is required and where shaking is prohibited.

7. After this incubation, turn the water bath down to 55 °C, or another one is needed.

8. The 3D imaging has to be performed the day after the hybridization in order to account for all signals present in the same way for each section; this is specifically important for low-intensity signals.

9. The bulb of the fluorescence microscope should be calibrated using fluorescent beads and should be at its peak performance in order to avoid too long exposition times and bleaching, especially if the TRF2 -telomere immuno-FISH protocol is used, i.e., three subsequent 3D z-stacks for each of the fluorochromes.

References

1. LeBel C, Wellinger RJ (2005) Telomeres: what's new at your end? J Cell Sci 118:2787–2788
   [CrossRef]

2. De Lange T (2005) Shelterin: the protein complex that shapes and safeguards human telomeres. Gene Dev 19:2100–2110
   [CrossRef][PubMed]

3. Hug N, Lingner J (2006) Telomere length homeostasis. Chromosoma 115:413–425
   [CrossRef][PubMed]

4. DePinho RA, Polyak K (2004) Cancer chromosomes in crisis. Nat Genet 36:932–934
   [CrossRef][PubMed]

5. Landsdorp PM (2009) Telomeres and disease. EMBO J 28:2543–2540

6. Chuang TC, Moshir S, Garini Y et al (2004) The three-dimensional organization of telomeres in the nucleus of mammalian cells. BMC Biol 2:12
   [CrossRef][PubMed][PubMedCentral]

7. Mai S, Garini Y (2005) Oncogenic remodeling of the three-dimensional organization o the interphase nucleus: c-Myc induces telomeric aggregates whose formation precedes chromosomal rearrangements. Cell Cycle 4:1327–1331
   [CrossRef][PubMed]

8. Louis SF, Vermolen BJ, Garini Y et al (2005) C-Myc induces chromosomal rearrangements through telomere and

chromosome remodeling in the interphase nucleus. Proc Natl Acad Sci U S A 102:9613–9618
[CrossRef][PubMed][PubMedCentral]

9. Mai S, Garini Y (2006) The significance of telomeric aggregates in the interphase nuclei of tumor cells. J Cell Biochem 97:904–915
[CrossRef][PubMed]

10. Mai S (2010) Initiation of telomere-mediated chromosomal rearrangements in cancer. J Cell Biochem 109:1095–1102
[PubMed]

11. Knecht H, Mai S (2011) 3D imaging of telomeres and nuclear architecture: an emerging tool of 3D nano-morphology based diagnosis. J Cell Physiol 226:859–867
[CrossRef][PubMed]

12. Hsu SM, Zhao X, Chakraborty S et al (1988) Reed- Sternberg cells in Hodgkin's cell lines HDLM, L-428, and KM-H2 are not actively replicating: lack of bromodeoxyuridine uptake by multinuclear cells in culture. Blood 71:1382–1389
[PubMed]

13. Drexler HG, Gignac SM, Hoffbrand AV et al (1989) Formation of multinucleated cells in a Hodgkin's-disease-derived cell line. Int J Cancer 43:1083–1090
[CrossRef][PubMed]

14. Newcom SR, Kadin ME, Phillips C (1988) L-428 Reed-Sternberg cells and mononuclear Hodgkin's cells arise from a single cloned mononuclear cell. Int J Cell Cloning 6:417–431
[CrossRef][PubMed]

15. Küppers R (2009) The biology of Hodgkin's lymphoma. Nat Rev Cancer 9:15–27
[CrossRef][PubMed]

16. Jones RJ, Gocke CD, Kasamon YL et al (2009) Circulating clonotypic B cells in classic Hodgkin lymphoma. Blood 113:5920–5926
[CrossRef][PubMed][PubMedCentral]

17. Brousset P, Al Saati T, Chaouche N et al (1997) Telomerase activity in reactive and neoplastic lymphoid tissue: infrequent detection of activity in Hodgkin's disease. Blood 89:26–31
[PubMed]

18. Norrback KF, Enblad G, Erlanson M et al (1998) Telomerase activity in Hodgkin's disease. Blood 92:567–573
[PubMed]

19. Heine B, Hummel M, Demel G et al (1999) Hodgkin and Reed-Sternberg cells of classical Hodgkin's disease overexpress the telomerase RNA template (hTR). J Pathol 188:139–145
[CrossRef][PubMed]

20. Knecht H, Sawan B, Lichtensztejn D et al (2009) The 3D nuclear organization of telomeres marks the transition from Hodgkin to Reed-Sternberg cells. Leukemia 23:565–573
[CrossRef][PubMed]

21. Knecht H, Sawan B, Lichtensztejn Z et al (2010) 3D telomere FISH defines LMP1 expressing Reed-Sternberg cells as end-stage cells with telomere-poor "ghost" nuclei. Lab Invest 90:611–619
[CrossRef][PubMed]

22. Guffei A, Sarkar R, Klewes L et al (2010) Dynamic chromosomal rearrangements in Hodgkin's lymphoma are due to ongoing three-dimensional nuclear remodeling and breakage-bridge-fusion cycles. Haematologica 95:2038–2046
[CrossRef][PubMed][PubMedCentral]

23. Lajoie V, Lemieux B, Sawan B et al (2015) LMP1 mediates multinuclearity through downregulation of shelterin proteins and formation of telomeric aggregates. Blood 125:2101–2110
[CrossRef][PubMed][PubMedCentral]

24. Feuerhahn S, Chen LY, Luke B et al (2015) No DDRama at chromosome ends: TRF2 takes centre stage. Trends Biochem Sci 40:275–285
[CrossRef][PubMed]

25. Wood AM, Rendtlew Danielsen JM et al (2014) TRF2 and lamin A/C interact to facilitate the functional organization of chromosome ends. Nat Commun 5:5467
[CrossRef][PubMed][PubMedCentral]

26. Knecht H, Righolt C, Mai S (2013) Genomic instability: the driving force behind refractory/relapsing Hodgkin's lymphoma. Cancers 5:714–725
[CrossRef][PubMed][PubMedCentral]

27. Knecht H, Johnson N, Haliotis T, et al. (2015) Disruption of Direct 3-Dimensional (3D) Telomere-TRF2 (Telomere Related Factor 2) interaction is a hallmark of primary Hodgkin (H) and Reed-Sternberg (RS) cells. Abstract #177. 57th ASH Annual Meeting, Orlando, FL, December 5–8, 2015

28. Schaefer LH, Schuster D, Herz H (2001) Generalized approach for accelerated maximum likelihood based image restoration applied to three-dimensional fluorescence microscopy. J Microsc 204:99–107
[CrossRef][PubMed]

29. Vermolen BJ, Garini Y, Mai S et al (2005) Characterizing the three-dimensional organization of telomeres. Cytometry A 67:144–150
[CrossRef][PubMed]

30. Sarkar R, Guffei A, Vermolen BJ et al (2007) Alterations of centromere positions in nuclei of immortalized and malignant mouse lymphocytes. Cytometry A 71:386–392
[CrossRef][PubMed]

31. Knecht H, Kongruttanachok N, Sawan B et al (2012) 3D telomere signatures of Hodgkin- and Reed-Sternberg cells at diagnosis identify patients with poor response to conventional chemotherapy. Transl Oncol 5:269–277
[CrossRef][PubMed][PubMedCentral]

7. Analysis of EBV Transcription Using High-Throughput RNA Sequencing

Tina O'Grady[1], Melody Baddoo[1, 2] and Erik K. Flemington[1, 2] ✉

(1) Department of Pathology, Tulane University School of Medicine, 1430 Tulane Avenue, Box SL-79, New Orleans, LA 70112, USA
(2) Tulane Cancer Center, New Orleans, LA, USA

✉ **Erik K. Flemington**
   Email: erik@tulane.edu

Abstract
High-throughput sequencing of RNA is used to analyze the transcriptomes of viruses and cells, providing information about transcript structure and abundance. A wide array of programs and pipelines has been created to manage and interpret the abundance of data generated from high-throughput RNA sequencing experiments. This protocol details the use of free and open-source programs to align RNA-Seq reads to a reference genome, visualize read coverage and splice junctions, estimate transcript abundance, and evaluate differential expression of transcripts in different conditions. Particular concerns related to EBV and viral transcriptomics are addressed and access to EBV reference files is provided.

Key words RNA-Seq – Epstein-Barr virus – Transcriptomics – Differential expression – STAR – Integrative genomics viewer – IGV – RSEM – EBSeq

1 Introduction

High-throughput RNA sequencing has become a powerful tool in virus research. The parallel sequencing of millions of short reads has allowed transcriptome-wide analysis of cellular and viral gene expression , not to mention discovery of novel genes, splice

junctions, and isoforms. Translational research makes use of high-throughput RNA sequencing to detect known and novel viruses in clinical samples and to analyze both transcript- and transcriptome-level changes as viruses interact with their hosts. In addition, high-throughput RNA sequencing can be combined with other techniques for specialized tasks such as transcription start site annotation, identification of RNA-protein partners, and examination of active transcription and translation genome wide [1–4].

While several high-throughput RNA sequencing technologies have been developed, Illumina RNA-Seq has become the de facto standard. Variations in protocols allow researchers to ask different questions of the transcriptomes under study. One important consideration is the treatment of the RNA before sequencing. Poly(A)-selection extracts mRNA and polyadenylated long noncoding RNA for sequencing. Ribodepletion removes most ribosomal RNA before sequencing, leaving polyadenylated RNAs, RNA species without poly(A) tails such as EBV's EBERs , and some unprocessed mRNA transcripts. At the RNA library preparation step, researchers can choose to use a stranded protocol to preserve information about which DNA strand the sequenced RNA arose from. This approach has revealed significant previously unknown antisense and intergenic transcription in EBV and other herpesviruses [5–8] and is recommended, especially, for cases in which the virus is expected to be in a replicative phase. Researchers can also choose between single-end and paired-end sequencing. In single-end sequencing a single read is generated from one end of each RNA fragment. In paired-end sequencing two reads are produced from each RNA fragment: one from each end. Single-end sequencing is useful for expression quantification, and with sufficient read length, it can provide meaningful information on structural features such as splice junctions and fusion transcripts. Paired-end sequencing offers more transcript structure information, especially for cases of fusion transcripts, circular RNA, and other unannotated variants, but comes at a greater time and financial cost. The read lengths obtainable with RNA-Seq have increased substantially in recent years. High-quality 100 bp reads are now readily obtainable on the Illumina platform, and this length is sufficient to allow sensitive detection of splice junctions. Finally, a common option to reduce RNA-Seq costs is multiplexing: adding unique "barcode" sequences to samples, allowing them to be sequenced together and informatically separated after sequencing. In general, multiplexing still allows sufficient read depth to study EBV genes that are expressed at relatively low levels.

There are some special considerations when applying RNA-Seq to EBV research. Most plainly, EBV is studied within the context of the human cellular environment. RNA-Seq experiments from EBV-infected cells mostly produce reads that map to the human genome, with the proportion of EBV reads ranging from up to about 25 % (after a highly robust lytic induction in a cell line) down to a few reads (e.g., in a weakly EBV-positive tumor sample with a latent gene expression profile). Generally, higher read

counts allow more effective transcriptome analysis. However, analysis of EBV-mapping reads is more straightforward under latency conditions, when the viral transcriptome is substantially simpler and it is easier to discern individual transcripts.

This protocol describes analysis steps performed in nearly any RNA-Seq experiment. First, RNA-Seq reads are aligned to a reference genome. Many alignment programs, both open source and commercial, are available; this protocol uses the fast and sensitive STAR aligner [9]. Output from STAR is used to examine RNA-Seq coverage of the genome as well as to identify splice junctions. The data is visualized on a genome browser, in this case IGV, the Integrative Genomics Viewer [10]. Finally, transcript expression levels are quantified and compared between samples in a statistically meaningful way. This protocol uses the program RSEM [11] and its accompanying EBSeq [12] module for quantification and the evaluation of differential expression.

2 Materials

1. RNA-Seq data: fastq or fasta files acquired from a sequencing facility or downloaded from a data repository.

2. Hardware: a computer with X86-64 compatible processors running a 64-bit UNIX/Linux-based operating system (e.g., Mac OS, Ubuntu, or Cygwin) with at least 30 GB of RAM and enough storage space to accommodate sequence and reference files. Estimate at least 60 GB of storage for reference/index files and another 50 GB per single-end RNA-Seq sample (*see* **Note 1**).

3. A terminal program to interface with the operating system, (e.g., Terminal in Mac OS) (*see* **Note 2**).

4. STAR aligner : the most recent version of STAR aligner is available at https://github.com/alexdobin/STAR. The site provides the necessary files and instructions for installation.

5. Fasta files for reference genomes: fasta-format files (with file extension .fa) are available for several strains of EBV at https://github.com/flemingtonlab/public/tree/master/annotation (*see* **Notes 3** and **4**). Fasta-format files for the human genome may be downloaded from Ensembl at http://www.ensembl.org/info/data/ftp/index.html. Fasta-format files for many more genomes can be obtained from the

NCBI Nucleotide database at http://www.ncbi.nlm.nih.gov/nuccore.

6. A text editor program (e.g., TextEdit, pre-loaded on most Macs).

7. Integrative Genomics Viewer (IGV) : the most recent version of IGV is available, along with instructions for installation, at http://www.broadinstitute.org/software/igv/download.

8. Genome annotation files: BED-format (with file extension .bed) and GTF-format (with file extension .gtf) files are available for several strains of EBV at https://github.com/flemingtonlab/public/tree/master/annotation. GTF-format files for the human genome may be downloaded from Ensembl at http://www.ensembl.org/info/data/ftp/index.html.

9. Perl: the current version of Perl is available at https://www.perl.org/ (*see* **Note 5**).

10. The Perl script *junctions_to_introns_STAR.pl*, available from https://github.com/flemingtonlab/public/tree/master/code.

11. RSEM : the latest version of RSEM can be obtained from http://deweylab.biostat.wisc.edu/rsem/. The site provides the necessary files and instructions for installation.

3 Methods

3.1 Creating Genome Index Files for STAR Aligner

Aligners require that the genomes first be "indexed" to facilitate quicker and less computationally intensive sequence matching. Genome indexes are generated from fasta files containing each chromosome of the genome of interest and only need to be generated once. This example creates a genome index containing both the human genome and the EBV genome, using a human reference fasta file downloaded from Ensembl and the EBV reference fasta file *chrEBV_Akata_inverted.fa* [13] downloaded from https://github.com/flemingtonlab/public/tree/master/annotation (*see* **Notes 6** and **7**):

1. Create a new, empty directory to which the STAR genome index will be written (for the example below, the directory must be named *GenomeDirectory*). The path

to this directory will need to be entered below, after --genomeDir.

2. Run the following command in Terminal:

```
$ STAR --runMode genomeGenerate --genomeDir
/PATH/TO/GenomeDirectory --runThreadN 4 --
genomeFastaFiles /PATH/TO/chrEBV_Akata_inverted.fa
/PATH/TO/Homo_sapiens.GRCh38.dna.primary_assembly.fa
```

The runThreadN number, in this case 4, should be equal to or less than the number of processor cores available. Run time for this procedure is about 1 h using a computer with 12 cores.

STAR will generate multiple files in the genome directory. These files should not be modified .

3.2 Aligning Sequence Reads to the Reference Genome

In this step the fastq/fasta files containing sequence data are mapped to the reference genome index that was generated in the previous step (*see* **Note 8**). The following command uses STAR to align single-end sequence reads and report their alignments in a SAM-format text file and their splice junctions in another text file. Sequence reads that map to fewer than ten different genomic locations with fewer than ten mismatches to the genome are reported (*see* **Note 9**):

1. In Terminal, use *cd* to move to the desired output directory.

2. Run the following command:

```
$ STAR --genomeDir /PATH/TO/GenomeDirectory --
readFilesIn /PATH/TO/reads.fastq --runThreadN 4 --
outSAMprimaryFlag AllBestScore
   The runThreadN number, in this case 4, should be
equal to or less than the number of processor cores
available. The argument --outSAMprimaryFlag
AllBestScore determines output for the reads that map
to multiple places in the genome. With this option set,
if multiple genomic locations tie for the best score,
all of those locations will be reported as primary
alignments with the same score. Run time for this
procedure, assuming a fastq file 6 GB in size, is about
```

```
6 min using a computer with 12 cores.
```

STAR will generate multiple output files into the current working directory. The file containing the aligned reads is *Aligned_out.sam*, and the file containing identified splice junctions is *SJ.out.tab* (*see* **Notes 10** and **11**).

3.3 Visualizing the Data

The alignment and splice junction files are, to a certain extent, human readable and may potentially be inspected by opening them in a text editor. Often the alignment file in particular is very large and difficult or impossible (due to RAM limitations) to open in a text editor. An alternative is to open a small portion of the file in Terminal using the command:

```
$ less Aligned_out.sam
```

The file can then be scrolled through a line at a time using the keyboard arrow keys (*see* **Note 12**). To exit the *less* view and return to terminal, type *q*. Examining these text files in this way is a limited and difficult way to interpret the data however. To better view and analyze alignment data, it can be loaded onto a genome browser. The steps below outline the use of the Integrative Genomics Viewer (IGV) to view RNA-Seq read coverage across the entire viral genome. Prior to loading alignment data however, the reference genome must be formatted by IGV. The human genome is pre-loaded, but a reference genome must be created for EBV. This example creates a reference genome for the Akata strain of EBV, using the files *chrEBV_Akata_inverted.fa* (genome sequence file) and *chrEBV_Akata_inverted.bed* (genome feature annotation file), both downloaded from https://github.com/flemingtonlab/public/tree/master/annotation. The .genome file created through this process need only be created once.

1. In IGV , from the *Genomes* menu select *Create .genome File*.

2. Enter a user-specified ID for the genome (this will be displayed in the IGV Genomes list) and a descriptive name.

3. Using the fasta file *Browse* button, select *chrEBV_Akata_inverted.fa*.

4. Using the genome annotation *Browse* button, select *chrEBV_Akata_inverted.bed*. Leave the cytoband file box blank.

5. Save the file with a .genome file extension in the directory of your choice. The new

genome will be loaded onto the IGV genomes list automatically.

In order to view the alignment file on IGV, it must first be sorted. Sort the alignment file using the following command in Terminal:

```
$ sort –k4,4n Aligned_out.sam > Aligned_out_sorted.sam
```

Full alignment files are frequently too large to be loaded onto IGV (because of RAM limitations). To create an alignment file of EBV-mapped reads only, run the following command in Terminal:

```
$ awk '$3=="chrEBV_Akata_inverted"'
Aligned_out_sorted.sam > Aligned_out_sorted_EBV_only.sam
```
(*see* **Note 13**).

The sorted alignment file can be loaded onto IGV by selecting the *File* menu, then *Load from File*, and browsing to the file. IGV will prompt you to create an index file (necessary for display of the data): reply *OK* to the prompt to allow IGV to create the index file automatically.

For strand-specific RNA-Seq, reads in the display are color-coded according to strand (Fig. 1). Above the track displaying the reads, IGV displays an automatically generated coverage track that contains a histogram of read depth for each coordinate across the genome. This coverage track combines reads from both strands. To look at each strand separately, create an alignment file for each strand using the following Terminal commands (*see* **Notes 14 – 16**):
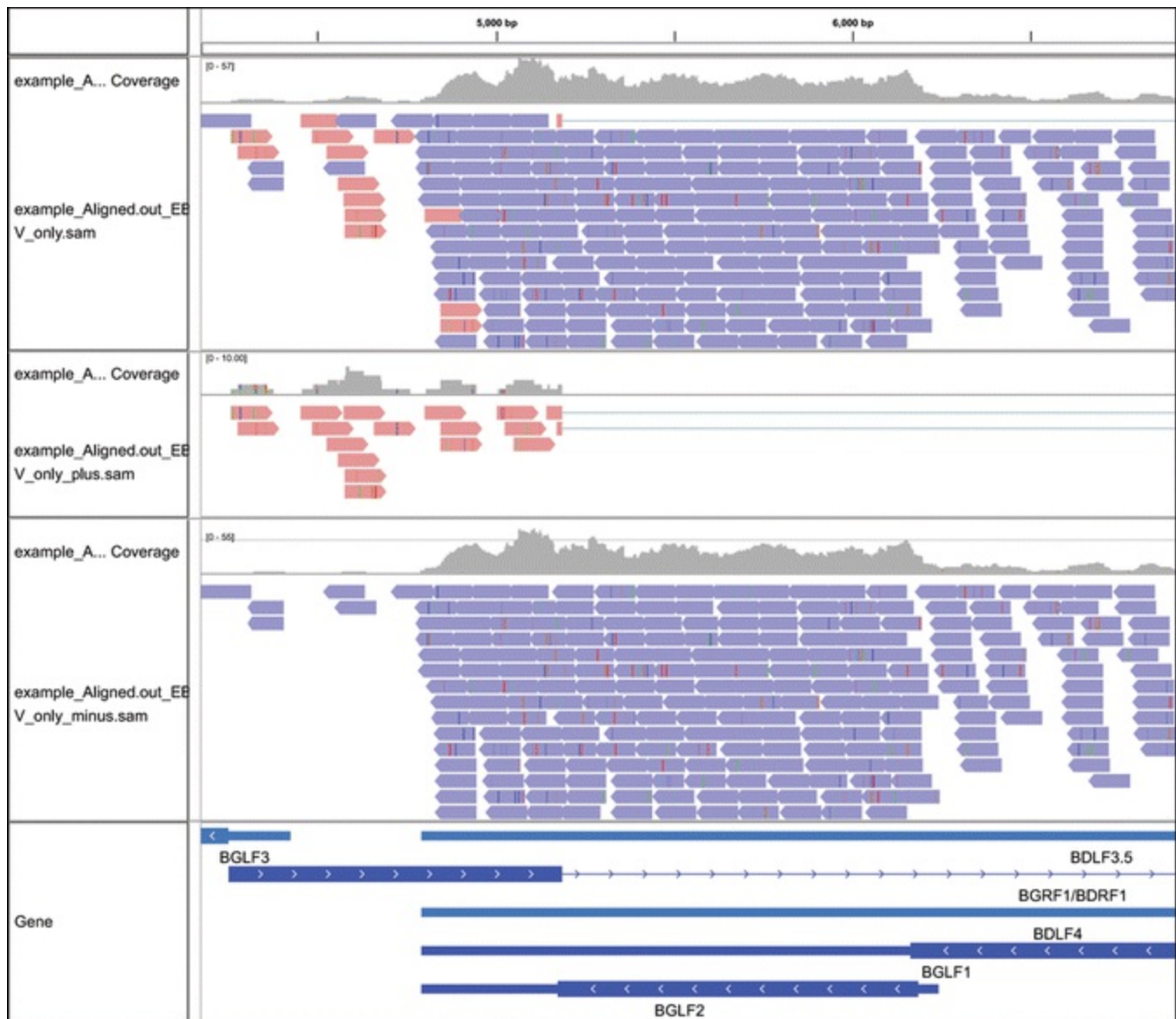
Fig. 1 SAM-format alignment files displayed on IGV . From *top* to *bottom*: RNA-Seq coverage and reads from both strands, RNA-Seq coverage and reads from the plus strand, RNA-Seq coverage and reads from the minus strand, and gene annotation (*chrEBV_Akata_inverted.bed*)

```
$ awk '$2==0' Aligned_out_sorted_EBV_only.sam >
Aligned_out_sorted_EBV_only_0_plus.sam
  $awk '$2==16' Aligned_out_sorted_EBV_only.sam >
Aligned_out_sorted_EBV_only_16_minus.sam
```

Then load each track separately onto the genome browser. Additionally, it is possible to create a standalone coverage track for each strand (or both strands together) using IGV's IGVtools feature with the following steps:

1. Select the *Tools* menu and then *Run igvtoools*.

2. Make sure the *Command* drop-down menu is set to *Count*.

3. Use the *Input File* browse button to locate the desired alignment file (e.g., *Aligned_out_sorted_EBV_only_0_plus.sam*).

4. An output filename is automatically generated, with the file extension .tdf. This creates a binary file; if you prefer a human-readable output file, change the file extension to .wig.

5. Change the *Window Size* to *1* to get an accurate read depth count for each genomic position.

6. Click *Run.*

3.4 Examining Splice Junctions

Like the alignment file, the splice junctions output file (*SJ.out.tab*) is human readable but is easier to visualize on a genome browser. To view the text, use the Terminal *less* command as in Subheading 3.3:

```
$ less SJ.out.tab
```

In order to visualize the splice junctions file on IGV , it must first be converted to BED format. To do this, use the Perl script *junctions_to_introns_STAR.pl*:

1. In Terminal, use *cd* to move to the directory that contains the *SJ.out.tab* file.

2. Use the following Terminal command:

```
$ perl /PATH/TO/junctions_to_introns_STAR.pl
SJ.out.tab
```

The output file *SJ.out.tab.bed* will be located in the same directory.

3. Like the alignment file, the full splice junctions file may be too large to load on IGV

due to RAM limitations. Create a file of EBV splice junctions by using the Terminal command:

```
$ awk '$1=="chrEBV_Akata_inverted"'SJ.out.tab.bed >
SJ.out.tab_EBV_ only.bed (see Note 17 )
```

4. In IGV, load the splice junctions file by selecting *Load from File* from the *File* menu and browsing to *SJ.out.tab_EBV_only.bed*.

When loaded on IGV, the *SJ.out.tab_EBV_only.bed* file displays features corresponding to spliced-out introns, with the first base of the feature representing the first base of the intron and the last base of the feature representing the last base of the intron (Fig. 2, *see* **Note 18**). The default view on IGV is *Collapsed*: to view any overlapping introns with greater detail, right click on the track name (*SJ.out.tab_EBV_only.bed*, to the left of the display) and select *Expanded*. Mouse over an individual splice junction feature to see its *Score*: this is the number of uniquely mapping RNA-Seq reads that span this junction.
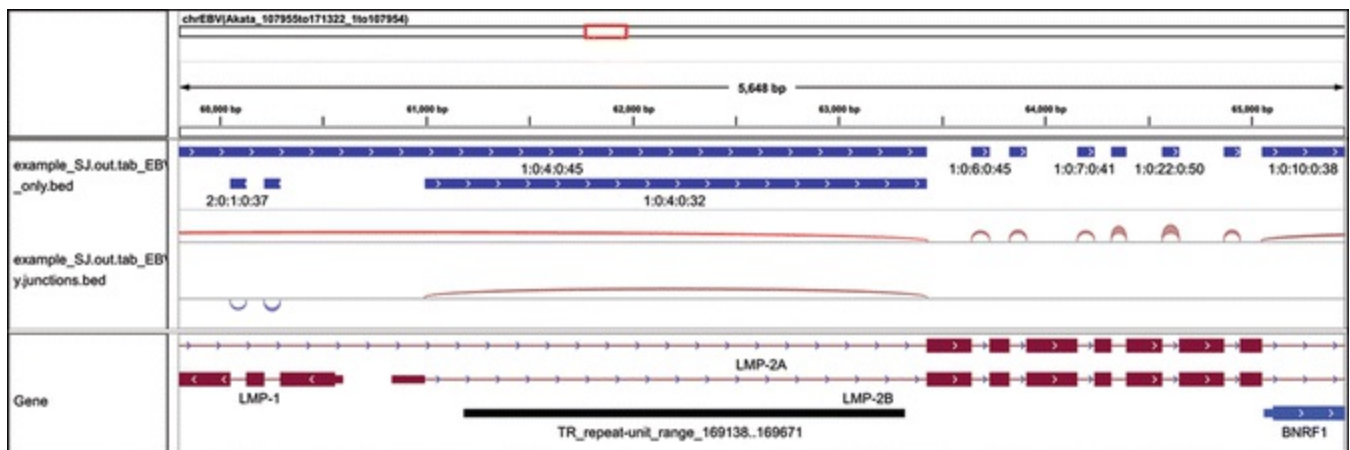
Fig. 2 BED-format splice junction files displayed on IGV. From *top* to *bottom*: introns displayed as BED features, introns displayed as splice junction arcs, and gene annotation (*chrEBV_Akata_inverted.bed*)

3.5 Creating Transcriptome Reference Files for RSEM

The RSEM package works well to quantify transcript expression, even for overlapping transcripts that have ambiguous read mappings. It uses STAR to align reads to a reference transcriptome and then estimates the abundance of each transcript using the expectation-maximization algorithm. Because abundance estimation involves normalization to total read depth, abundance estimates for EBV genes are better represented when RSEM reference transcriptome files include both viral and cellular genes (*see* **Notes 19** and **20**). In this step, RSEM prepares transcriptome reference files by using transcript coordinates in a .gtf-format annotation file to extract transcript

sequences from a genome fasta file and indexes those transcripts to serve as reference sequences for alignment. Transcriptome reference files need only be generated once for each transcriptome. To prepare all the necessary reference files for RSEM:

1. Create a directory called, e.g., *human_and_EBV_references*, and move all human and EBV genome fasta files and annotation GTF files to it.

2. In Terminal, use *cd* to move to the newly created directory.

3. Combine the human and EBV GTF-format files into a single file by using the following command:

```
$ cat Homo_sapiens.GRCh38.81.gtf
chrEBV_Akata_inverted_for_EBV.gtf >
human_38.81_and_Akata_inverted.gtf
```

4. Create a new, empty directory to contain the RSEM transcriptome index.

5. In Terminal, use *cd* to move to the new directory.

6. Run the following command:

```
$ rsem-prepare-reference
/PATH/TO/human_and_EBV_references --gtf
/PATH/TO/human_38.81_and_Akata_inverted.gtf -p 4 --star
human_and_EBV_RSEM_reference (see Note 21 )
```

The final argument is the user-defined name of the reference genome and should be informative. The -p number, in this case 4, should be equal to or less than the number of processor cores available. The --star argument creates STAR transcriptome index files for the next step. RSEM will generate multiple files in the transcriptome directory. Run time for this procedure is about 4.5 h using a computer with 12 cores.

3.6 Quantifying Transcript Expression

In this step the fastq/fasta files containing sequence data are mapped to the transcriptome reference that was generated in the previous step, and transcript abundance is estimated. The following steps use RSEM and STAR to align single-end sequence reads and produce a text file containing abundance estimates for all transcripts in the transcriptome reference.

1. In Terminal, use *cd* to move to the desired output directory.

2. Run the following command:

```
$ rsem-calculate-expression -p 4 --star --no-bam-
output /PATH/TO/reads.fastq
/PATH/TO/human_and_EBV_RSEM_reference
human_and_EBV_RSEM (see Notes 21 – 23 )
```

The -p number, in this case 4, should be equal to or less than the number of processor cores available. The --star argument instructs RSEM to perform the alignment step with STAR, using predetermined parameters optimizing the alignment for expression quantification. The --no-bam-output argument prevents RSEM from producing an alignment file: this argument can be left out of the command if alignment files are desired, though for most purposes this alignment file will not be as useful as that produced in step 3.2 as it presents reads aligned to individual transcripts rather than the genome. Run time for this procedure, assuming a fastq file 6 GB in size, is about 15 min using a computer with 12 cores.

RSEM will generate three files in the current working directory. Human_EBV_RSEM.genes.results is a tab-delimited text file containing abundance estimates for all genes in the transcriptome file. It can be opened with a text editor or with Microsoft Excel (*see* **Notes 24** and **25**). The column labeled *expected_count* contains the number of reads estimated to map to that transcript after taking into account background noise and overlapping genes (*see* **Note 26**). *TPM* (Transcripts Per Million) and *FPKM* (Fragments Per Kilobase of transcript per Million mapped reads) are two different normalized abundance measures that take into account transcript length and overall read depth.

3.7 Comparing Transcript Expression

EBSeq is an empirical Bayesian differential expression analysis tool that is built into the RSEM package. It is used to find statistically significant differential expression of transcripts between two or more groups of one or more samples each. If EBseq has not yet been used after RSEM installation, use the Terminal command:

```
$ make ebseq
```

to compile the necessary codes. This need only be done once. The following steps use EBSeq to compare transcript expression in two treatments with three replicates

each:

1. In Terminal, use *cd* to move to the desired output directory.

2. Create a matrix of genes and their read counts in the samples to be compared by runni
   command:

```
$ rsem-generate-data-matrix
/PATH/TO/first_sample_first_replicate_human_and_EBV_RSEM
/PATH/TO/first_sample_second_replicate_human_and_EBV_RSE
/PATH/TO/first_sample_third_replicate_human_and_EBV_RSEM
/PATH/TO/second_sample_first_replicate
_human_and_EBV_RSEM.genes.results
/PATH/TO/second_sample_second_replicate
_human_and_EBV_RSEM.genes.results
/PATH/TO/second_sample_third_replicate
_human_and_EBV_RSEM.genes.results >
condition_one_condition_two.counts.matrix
```

   Ensure that input files in this command are grouped in an appropriate order to do
   from each group to be compared must be adjacent to each other in the command. RSE
   matrix file of read counts for each transcript, which will be used by EBSeq in the nex

3. Indicate to EBseq how to group and compare the samples, and run EBSeq's algorithm
   command:

```
$ rsem-run-ebseq /PATH/TO/condition_one_condition_two.
3,3 condition_one_condition_two_ebseq.results
```

   In this case, 3,3 indicates two samples, each with triplicates. 2,2 would indicate t
   duplicates, 3,3,3 would indicate 3 samples each with triplicates, and so on. The orde
   must correspond to the order of the samples in the counts.matrix file, i.e., in
   condition_one_condition_two.counts.matrix produced in the previous step, the three s
   are listed and then the three sample two replicates. The final argument is the user-def
   file, which is a text file of the posterior probability of differential expression.

4. Determine which transcripts are statistically significantly differentially expressed by
   command:

```
$rsem-control_fdr /PATH/TO/condition_one_condition_two
```

```
0.05 condition_one_condition_two_DE.txt
```

This will produce a text file listing the genes that are statistically significantly dif at a false discovery rate (FDR) of 0.05. The FDR can be altered as desired by replac the command.

Run time for this procedure is about 10 min using a computer with 12 cores.

The file produced (in this example named *condition_one_condition_two_DE.txt*) is a tab-delimited text file that can be opened in a Text Editor or Microsoft Excel (*see* **Notes 24** and **25**). In the above case of two groups being compared, this output file contains four columns: *PPEE* is the posterior probability of equal expression, ranging from 0 to 1; *PPDE* is the posterior probability of differential expression, ranging from 0 to 1; *posterior fold change* is the ratio of the posterior mean expression estimate of the gene in sample one to that in sample two; and *real fold change* is the ratio of the gene's normalized mean count in sample one to that in sample two. Genes with fold change greater than one are expressed more highly in condition one; genes with fold change less than one are expressed more highly in condition two.

When more than two samples are compared, EBSeq produces a file that indicates the posterior probability that the gene is expressed in any of a number of "patterns." An additional file with the suffix .pattern is the key to these patterns, indicating the samples in which the gene shows differential expression.

---

4 Notes

1. The first steps of this protocol (up to *Examining Splice Junctions*) may be completed on a computer with 16 GB of RAM. However, quantifying and comparing transcript expression levels using these methods will require up to 30 GB of RAM.

2. For those new to Unix/Linux or command line interfaces, an excellent tutorial is Ian Korf and Keith Bradnam's *Unix & Perl Primer for Biologists*, available at http://korflab.ucdavis.edu/unix_and_Perl/.

3. For the best alignments, it is best to use a reference genome that matches the strain of EBV in the sample. For samples containing the type I EBV strain (the most common), the Akata genome should provide good results. For samples containing the type II EBV strain, the AG876 genome can be used.

4. Several files at https://github.com/flemingtonlab/public/tree/master/annotation are

available in "inverted" format. This format splits the EBV genome between the BBRF3 and BGLF3 genes (between positions 107954 and 107955) rather than the terminal repeats to allow better detection of LMP2 transcripts, which span the terminal repeats, where EBV genomes are normally split (as in Genbank).

5. Perl may already be installed on your system. A quick way to check is to run the Terminal command.
   $ perl -v
   This will report the version of Perl, if any, that is installed.

6. Genome index files that contain multiple genomes, e.g., human and EBV, may be created; however, genome indexes from multiple strains of EBV should be created separately and not combined into a single index.

7. If only the EBV transcriptome is of interest, an index of the EBV genome (only) may be created by leaving out the human genome fasta files from the command. The argument *--genomeSAindexNbases 8* should be added to the command to adjust for the much smaller genome size. The index creation and read alignment steps will be faster and less computationally intensive when using the EBV genome only.

8. This protocol assumes that quality control and filtering steps have already been performed, e.g., by the sequencing center. If not, or if this is unclear, FastQC (http://www.bioinformatics.babraham.ac.uk/projects/fastqc/) is a quick and user-friendly program to check data quality.

9. Many STAR parameters can be altered to meet the requirements of different experiments. Some common variations are listed here; many others can be found in the STAR manual at https://github.com/alexdobin/STAR/blob/master/doc/STARmanual.pdf.
   For paired-end RNA-Seq data, simply list both read files after the --readFilesIn argument, i.e., --readFilesIn /PATH/TO/reads_1.fastq /PATH/TO/reads_2.fastq
   To only report alignments for reads that map uniquely to one genomic location, add the argument *--outFilterMultimapNmax 1*. Or change this number to report alignments for reads that map to multiple locations in the genome. The default (as used in step 3.2) is 10: reads aligning to more than 10 genomic locations will not

be reported.

Use the argument *--genomeSAsparseD 2* to reduce the RAM usage. This will result in a longer run time.

10. The names of output files can be specified by adding the argument *--outFileNamePrefix* to the command line statement followed by the desired name, which will be used as a prefix for the standard output names (*Aligned.out*, *Log.out*, etc.). It is good practice to make the file name prefix as informative as reasonably possible, e.g., *--outFileNamePrefix sample_one_repeat_one_STAR_chrEBV_Akata_inverted.*

11. To check what parameters were used for previous STAR alignments, open the *Log.out* file with a text editor. The default parameters are listed at the top. Scroll down to see the arguments entered on the command line, which defaults were changed and the new values used in the alignment.

12. *Less* has additional functionality that is often useful, for example, patterns may be searched using the format */pattern < enter>*. To learn more about *less*, bring up the manual in Terminal with the command

    ```
    $ man less
    ```

13. You must ensure that the chromosome name in the command matches the desired chromosome name in the alignment file. In this example, all reads that align to the chromosome called *chrEBV_Akata_inverted* will be extracted and written to the EBV only file. To inspect the names of chromosomes in the alignment file, use

    ```
    $less Aligned_out.sam
    ```

    to open the alignment file, and look in the header lines after *@SQ SN:* for the names of chromosomes.

14. Depending on whether the cDNA protocol used first-strand or second-strand synthesis, the numbers 0 and 16 may be reversed. For example, using the TruSeq stranded protocol, reads corresponding to the plus strand have a FLAG code of 16, and reads corresponding to the minus strand have a FLAG code of 0.

15. Some reads may align to multiple parts of the genome. These commands return

only the primary alignments, that is, the location with the best alignment score. In order to return both primary and secondary alignments, use the following commands:

```
    $ awk '$2==0||$2==256'
Aligned_out_sorted_EBV_only.sam >
Aligned_out_sorted_EBV_only_0_plus.sam
    $awk '$2==16||$2==272'
Aligned_out_sorted_EBV_only.sam >
Aligned_out_sorted_EBV_only_16_minus.sam
```

16. For paired-end sequencing, use the following commands:

```
    $ awk '$2==99||$2==147'
Aligned_out_sorted_EBV_only.sam >
Aligned_out_sorted_EBV_only_plus.sam
    $awk '$2==83||$2==163'
Aligned_out_sorted_EBV_only.sam >
Aligned_out_sorted_EBV_only_minus.sam
    to create files contain only the best-mapping reds.
Use:
    $ awk '$2==99||$2==147 || 2==73|| 2==97||
2==145||2==153' Aligned_out_sorted_EBV_only.sam >
Aligned_out_sorted_EBV_only_plus.sam
    $awk '$2==83||$2==163|| 2==81|| 2==89||
2==137||2==161' Aligned_out_sorted_EBV_only.sam >
Aligned_out_sorted_EBV_only_minus.sam
    to create files containing both primary and
secondary alignments.
```

17. Higher numbers of reads spanning a splice junction provide greater support for that splice junction. *junctions_to_introns_STAR.pl* reports all detected splice junctions. If you would like to specify a minimum read depth to report splice junctions, use a command of the form

```
    $ awk '$5 >= 5'SJ.out.tab_EBV_only.bed >
SJ.out.tab_EBV_only_5.bed
    This example extracts splice junctions supported by
at least five uniquely mapping reads.
```

18. IGV has a built-in option to display splice junctions as visually pleasing arcs rather than the default bed file blocks. To turn on this option, simply rename *SJ.out.tab.bed* to *SJ.out.tab.junctions.bed* and load the new file onto IGV.

19. Note that abundant unannotated transcription has been detected in EBV during reactivation [8]. Annotation files including these new transcripts are available at https://github.com/flemingtonlab/public/tree/master/annotation.

20. If annotation files include features that are not transcripts (e.g., annotated repeat regions, promoters , etc.), these should be removed before using the GTF file to create an RSEM reference. Otherwise, RSEM will interpret these features as annotated transcripts and may erroneously assign reads to them.

21. Depending on the installation, the error message */STAR* : *No such file or directory!* may be encountered. If so, add the argument *--star-path /PATH/TO/directory containing STAR*.

22. Many RSEM parameters can be altered to meet the requirements of different experiments. Some common variations are listed here; many others can be found in the RSEM manual at http://deweylab.biostat.wisc.edu/rsem/README.html.
    For paired-end RNA-Seq data, add the argument *--paired-end* to the *rsem-calculate-expression* command, and add the second file of reads after the first, e.g.,

    ```
    $ rsem-calculate-expression --star -p 4 --no-bam-
    output --paired-end /PATH/TO/reads_1.fastq
    /PATH/TO/reads_2.fastq
    /PATH/TO/human_and_EBV_RSEM_reference human_
    and_EBV_RSEM
    ```

    The last argument in the command (*human_and_EBV_RSEM* in this example) is the name prefix for the output files. It is good practice to make the file name prefix as informative as reasonably possible, e.g., *sample_one_repeat_one_RSEM_human_chrEBV_Akata_inverted*

23. An error that may be encountered is *EXITING because of FATAL ERROR: could not open genome file /PATH/genomeParameters.txt*. If this occurs, rerun the command adding the text */a* to the genome directory argument, i.e.,

24. When using GTF files downloaded from Ensembl, RSEM output may use Ensembl IDs rather than gene names. IDs and gene names may be cross-referenced individually at Ensembl (http://www.ensembl.org), or a complete list for cross-referencing may be downloaded from Ensembl's BioMart (http://www.ensembl.org/biomart).

25. When displaying text files, Excel automatically formats cells based on their content. This is sometimes inappropriate, e.g., converting the gene symbol SEPT7 to the date September 7. To avoid this problem, open text files in Excel using the following steps:

    Open a new Excel worksheet.
    From the *File* menu, select *Import*.
    Select *Text file*, navigate to the desired file and click *Get Data*.
    When the Text Import Wizard opens, select *Delimited* and click *Next*.
    In the *Delimiters* section, select *Tab*.
    The next screen allows selection of the Data Format for each column. Ensure that the column containing gene IDs is set to *Text* and click *Finish*.

26. Note that because the expected count takes into account background noise and overlapping transcripts, its value may not be an integer.

Acknowledgments

References

1. Kurosawa J, Nishiyori H, Hayashizaki Y (2011) Deep cap analysis of gene expression. Methods Mol Biol 687:147–163. doi:10.1007/978-1-60761-944-4_10
   [CrossRef][PubMed]

2. Zhao J, Ohsumi TK, Kung JT, Ogawa Y, Grau DJ, Sarma K, Song JJ, Kingston RE, Borowsky M, Lee JT (2010) Genome-wide identification of polycomb-associated RNAs by RIP-seq. Mol Cell 40(6):939–953. doi:10.1016/j.molcel.2010.12.011, S1097-2765(10)00967-6 [pii]
   [CrossRef][PubMed][PubMedCentral]

3. Core LJ, Waterfall JJ, Lis JT (2008) Nascent RNA sequencing reveals widespread pausing and divergent initiation

at human promoters. Science 322(5909):1845–1848. doi:10.1126/science.1162228, 1162228 [pii]
[CrossRef][PubMed][PubMedCentral]

4. Ingolia NT (2010) Genome-wide translational profiling by ribosome footprinting. Methods Enzymol 470:119–142. doi:10.1016/S0076-6879(10)70006-9, S0076-6879(10)70006-9 [pii]
[CrossRef][PubMed]

5. Gatherer D, Seirafian S, Cunningham C, Holton M, Dargan DJ, Baluchova K, Hector RD, Galbraith J, Herzyk P, Wilkinson GW, Davison AJ (2011) High-resolution human cytomegalovirus transcriptome. Proc Natl Acad Sci U S A 108(49):19755–19760. doi:10.1073/pnas.1115861108, 1115861108 [pii]
[CrossRef][PubMed][PubMedCentral]

6. Concha M, Wang X, Cao S, Baddoo M, Fewell C, Lin Z, Hulme W, Hedges D, McBride J, Flemington EK (2012) Identification of new viral genes and transcript isoforms during Epstein-Barr virus reactivation using RNA-Seq. J Virol 86(3):1458–1467. doi:10.1128/JVI.06537-11, JVI.06537-11 [pii]
[CrossRef][PubMed][PubMedCentral]

7. Arias C, Weisburd B, Stern-Ginossar N, Mercier A, Madrid AS, Bellare P, Holdorf M, Weissman JS, Ganem D (2014) KSHV 2.0: a comprehensive annotation of the Kaposi's sarcoma-associated herpesvirus genome using next-generation sequencing reveals novel genomic and functional features. PLoS Pathog 10(1):e1003847, doi: 10.1371/journal.ppat.1003847 PPATHOGENS-D-13-01657 [pii]
[CrossRef][PubMed][PubMedCentral]

8. O'Grady T, Cao S, Strong MJ, Concha M, Wang X, Splinter Bondurant S, Adams M, Baddoo M, Srivastav SK, Lin Z, Fewell C, Yin Q, Flemington EK (2014) Global bidirectional transcription of the Epstein-Barr virus genome during reactivation. J Virol 88(3):1604–1616. doi:10.1128/JVI.02989-13, JVI.02989-13 [pii]
[CrossRef][PubMed][PubMedCentral]

9. Dobin A, Davis CA, Schlesinger F, Drenkow J, Zaleski C, Jha S, Batut P, Chaisson M, Gingeras TR (2013) STAR: ultrafast universal RNA-seq aligner. Bioinformatics 29(1):15–21. doi:10.1093/bioinformatics/bts635, bts635 [pii]
[CrossRef][PubMed]

10. Thorvaldsdottir H, Robinson JT, Mesirov JP (2013) Integrative Genomics Viewer (IGV): high-performance genomics data visualization and exploration. Brief Bioinform 14(2):178–192. doi:10.1093/bib/bbs017, bbs017 [pii]
[CrossRef][PubMed]

11. Li B, Dewey CN (2011) RSEM: accurate transcript quantification from RNA-Seq data with or without a reference genome. BMC Bioinformatics 12:323. doi:10.1186/1471-2105-12-323, 1471-2105-12-323 [pii]
[CrossRef][PubMed][PubMedCentral]

12. Leng N, Dawson JA, Thomson JA, Ruotti V, Rissman AI, Smits BM, Haag JD, Gould MN, Stewart RM, Kendziorski C (2013) EBSeq: an empirical Bayes hierarchical model for inference in RNA-seq experiments. Bioinformatics 29(8):1035–1043. doi:10.1093/bioinformatics/btt087, btt087 [pii]
[CrossRef][PubMed][PubMedCentral]

13. Lin Z, Wang X, Strong MJ, Concha M, Baddoo M, Xu G, Baribault C, Fewell C, Hulme W, Hedges D, Taylor CM, Flemington EK (2013) Whole-genome sequencing of the Akata and Mutu Epstein-Barr virus strains. J Virol 87(2):1172–1182. doi:10.1128/JVI.02517-12, JVI.02517-12 [pii]
[CrossRef][PubMed][PubMedCentral]

8. Analysis of Viral Promoter Usage in EBV-Infected Cell Lines: A Comparison of qPCR Following Conventional RNA Isolation and Nuclear Run-On Assay

Kalman Szenthe[1] and Ferenc Banati[1] ✉

(1) RT-Europe Nonprofit Research Ltd., Vár 2., Dunacsunyi ut, Szigetköz Building, Mosonmagyaróvár, H-9200, Hungary

✉ **Ferenc Banati**
Email: fbanati@yahoo.co.uk

Abstract
To interpret the results of an epigenetic analysis in gene expression studies, it is essential to characterize the activity of the relevant promoters. According to the literature, real-time PCR assay is the most widely used method for the determination of latent EBV promoter usage. Here we describe two alternative approaches to measure the activity of viral promoters in cell lines carrying latent EBV episomes. The widespread typical approach relies on total cellular RNA isolation, whereas the nuclear run-on assay described here is based on the initial isolation of nuclei, followed by in vitro transcription in the presence of biotinylated-UTP, and purification of RNA transcripts using avidin-coated magnetic beads. Finally, both methods apply reverse transcription-based real-time PCR (i.e., quantitative polymerase chain reaction, qPCR) to quantitatively measure the amount of specific transcripts. We shall describe these methods step by step and demonstrate their use for the determination of EBER1 promoter activity in EBV-positive cell lines.

Key words Gene expression – Reverse transcription – Quantitative PCR – Nuclear run-on assay – Latent EBV promoter

1 Introduction

Similarly to certain cellular genes, Epstein-Barr virus also utilizes alternative promoters called Wp, Cp, and Qp for the generation of transcripts encoding either a single nuclear antigen, EBNA1 , or six nuclear antigens (EBNAs 1-6) (reviewed by [1]). The activity of Wp, Cp, and Qp depends on the host cell phenotype. Similarly, the latency promoters for the viral genes coding for latent membrane proteins (LMPs) also vary in different host cells. In contrast, two nontranslated viral RNAs, EBER1 and EBER2, are invariably expressed in the majority of EBV-carrying cell types. At present, there are many methods for the analysis of promoter activity. Earlier, gene expression studies relied mainly on Northern blot analysis based on hybridization [2] or on the classical reverse transcription polymerase chain reaction (RT-PCR) approach followed by agarose gel electrophoresis [3] or on competitive-quantitative PCR [4]. These methods are slower and may require more laboratory work and manual dexterity than the newer generation methods, e.g., reverse transcription followed by real-time, quantitative polymerase chain reaction (qPCR), mRNA microarray, or transcriptome sequencing. In addition, reverse transcription followed by classical PCR is not quantitative enough, because it is very difficult to stop the reaction in the linear phase (End-point method) to obtain the highest difference between the samples. In addition, the linear range is highly dependent on the starting concentration of the template [3]. Thus, qPCR is currently used in most cases, but mRNA microarray or transcriptome sequencing methods are also very common, because of their high-throughput capacity and lower overall cost per sample.

Notably, nuclear run-on analysis is the most suitable method for the determination of the actual, "real" promoter activity, i.e., the frequency of the generation of nascent transcripts within a certain time interval [5, 6]. The other methods mentioned above reflect rather the steady-state level of transcripts or mRNAs in biological samples, which, besides the promoter activity, depends on post-transcriptional events, e.g., splicing, maturation, or degradation, all influencing mRNA half life. In addition, the nuclear run-on assay can also be coupled with new generation methods.

Because qPCR is the most frequently applied method to determine promoter usage for EBV-infected cells, we shall present it in details, and compare it with a version of the nuclear run-on assay established in our laboratory [7]. We shall demonstrate the use of both methods to quantitate the level of EBER1 , and to determine the activity of the EBER1 promoter (EBER1p) in EBV infected cell lines.

EBV exhibits distinct viral latency gene expression patterns which can be classified into two major different groups: the first one is the C-promoter-off (Cp-off; including latency classes 0, 1, and 2), and the second one is the Cp-on group (containing latency class 3) (reviewed by [8]). The small noncoding RNAs called EBV-encoded RNA 1 and 2 (EBER1 and 2) are expressed in latency class 0 [9] and in latency classes 1, 2,

and 3 [10] as well. Both RNAs are about 170 nucleotides long and transcribed by RNA polymerase III. Their importance in infection and latency programs remains to be exactly clarified. However, because of their high, constitutive expression, both EBERs are useful diagnostic markers of EBV infection.

In the following we shall describe two procedures, conventional RNA isolation and nuclear run-on assay ([6], with modifications) both followed by qPCR as applied to characterize EBER1 transcription in EBV positive cell lines.

2 Materials

2.1 Cell Lines

Cells were cultured in RPMI 1640 medium containing 10 % FCS (fetal calf serum), 2 mM glutamine, 50 units/mL streptomycin at 5 % CO_2 content and 37 °C. Cell lines, and their main characteristics are shown in Table 1.

Table 1 Cell lines and their main characteristics

Cell line	Cell type and developmental stage of B cell maturation	EBV and expression of EBERs	EBV Latency group	Reference
CBM1-Ral-STO	Lymphoblastoid	+	Cp-on	[18, 19]
Rael	Endemic, EBV positive BL; late germinal center B cell [a]	+	Cp-off	[18, 19]
Mutu- BL-I-cl-216				[19, 20]
Mutu-BL-III-cl-99			Cp-on	[19, 20]
Raji[b]			Cp-off[c]	[21]
C666.1	Epithelial cell	+	Cp-off	[12, 22]

[a][23, 24]

[b]Raji carries a virus strain that has a deletion of the EBNA-6 gene

[c]Raji has multiple mutations in region Cp and Wp, so the EBNA transcription is initiated from a distinct and until now unidentified promoter [25]

2.2 Preparation of RNA (Nuclear Run-On Assay)

1. Lysis Solution: 10 mM Tris–HCl pH 7.4, 3 mM $MgCl_2$, 10 mM NaCl, 150 mM sucrose and 0.5 % NP-40.

2. Storage buffer: 50 mM Tris–HCl pH 8.3, 40 % glycerol, 5 mM $MgCl_2$ and 0.1 mM EDTA.

3. Transcription buffer: 200 mM KCl, 20 mM Tris–HCl pH 8.5 mM $MgCl_2$, 200 mM sucrose, 20 % glycerol.

4. Stop buffer: 250 mM $CaCl_2$.

5. 1× BW buffer: 5 mM Tris–HCl pH7.5, 0.5 mM EDTA, 1 M NaCl.

6. 1× SSC buffer: 150 mM NaCl, 15 mM sodium citrate, pH 7 (using 1 M HCl).

7. 1× PBS (phosphate buffered saline): 137 mM NaCl, 2.7 mM KCl, 10 mM Na_2HPO_4, 2 mM KH_2PO_4, adjust pH to 7.4 with HCl.

---

3 Methods
3.1 Nuclear Run-On Assay
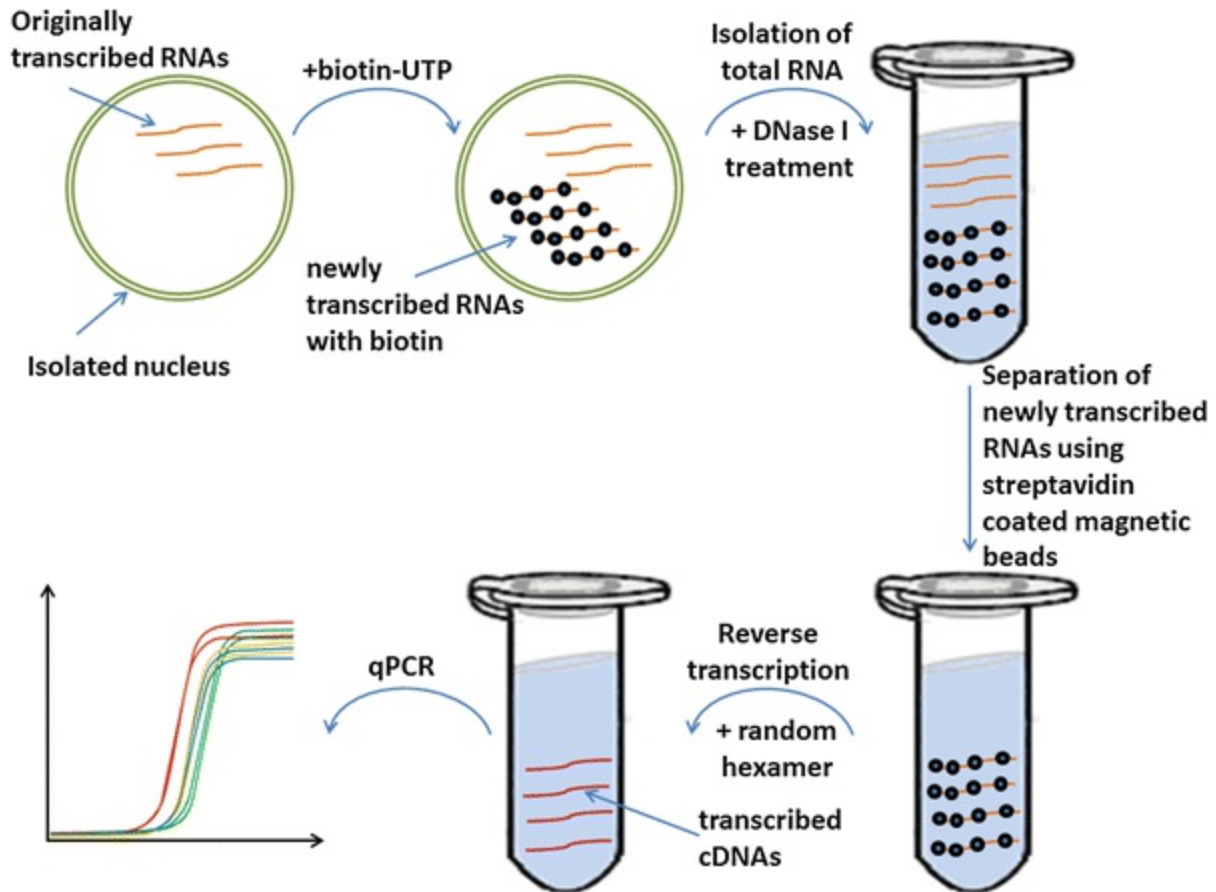
Fig. 1 Short scheme of nuclear run-on analysis according to Patrone and colleagues [6] with modifications

3.1.1 Isolation of Nuclei

1. Centrifuge ca 5×10^7 cells and wash twice in 10 mL $1\times$ PBS.

2. Centrifuge the cells after each wash step with $270 \times g$ at 4 °C for 10 min.

3. Discard the supernatant and resuspend the pellet in 4 mL Lysis Solution and keep on ice for 5 min.

4. Centrifuge the solution with $170 \times g$ at 4 °C for 10 min to pellet the nuclei.

5. Wash the pellet once in 4 mL modified lysis solution (without NP40).

6. Discard the supernatant and suspend the nuclei in 150 μL storage buffer. After this step the nuclei can be stored at −150 °C for a few months.

3.1.2 Labeling with Biotinylated UTP

1. Dilute the nuclei suspended in Storage Buffer with 150 µL 2× transcription buffer containing 1.6 µL 50 mM biotinylated-UTP (biotin-16-UTP).

2. Incubate at 29 °C for 30 min.

3. Add 6 µL stop buffer and 60 U RNase-free DNase I.

4. Isolate RNA using TRI-reagent (see step 2 of Subheading 3.2), finally dissolve the RNA pellet in 120 µL DNase- and RNase-free Ultrapure water.

3.1.3 Isolation of Biotin-Labeled RNA

1. In order to isolate the newly synthetized RNA (biotin labeled), add 120 µL streptavidin-conjugated magnetic beads (Dynabead, Invitrogen) to 120 µL-samples. Before adding the beads, wash 70 µL beads in 1× BW buffer twice and finally dilute with 1× BW to a total of 120 µL.

2. Incubate and rotate slowly for 2 h at 37 °C and separate the beads using a magnetic rack.

3. Wash the pellet twice with 1× SSC containing 15 % formamide.

4. Wash the pellet once in 2× SSC.

5. Dissolve in 30 µL RNase-free water (store at −150 °C until further use).

3.1.4 Reverse Transcription -Reaction and Quantitative PCR
See Subheadings 3.3. and 3.4.

3.2 Isolation of RNA

1. Conventional way: pellet ca 5×10^7 cells and wash twice in 10 mL 1× PBS. Centrifuge the cells after each wash step at 4 °C with 270 × g for 10 min. Discard the supernatant and add 1 mL TRI-reagent to the cells, mix vigorously, incubate at room temperature (RT) for 5 min.

2. Nuclear run-on: add 1 mL LS Tri-reagent to the solution, (see Subheading 3.1.2), mix vigorously, incubate at RT for 5 min.

3. Add 200 μL chloroform to the solution from **steps 1** or **2**, shake well, and incubate at RT for 5 min.

4. Centrifuge the solution with 12,000 × g at 4 °C for 15 min.

5. Transfer upper phase into a new tube and add 500 μL isopropanol, mix, and incubate at −20 °C for 20 min.

6. After the incubation centrifuge the mixture with 12,000 × g at 4 °C for 10 min. The RNA should be visible as a pellet.

7. Wash the pellet once with 800 μL 70 % ethanol.

8. Dissolve the precipitate in 50 μL (for step 1) or 120 μL (for step 2) RNase-free ultrapure water.

3.3 Reverse Transcription (Random Hexamer, Specific Oligos, Oligo-dT)

To reverse transcribe mRNA to cDNA, random hexamers, oligo-dTs, and specific oligos may be used. Using specific oligonucleotide-priming is the most common approach, resulting in the best yield. However, the random hexamer priming-approach has the advantage, that the resulting cDNA comprises all transcribed mRNAs or RNAs. Thus, one cDNA product may be used for different PCR reactions. For normalization of RNA quantity, one suitable housekeeping gene or a couple such genes have to be included in the study (*see* **Note 1**). In general, depending on the kit, a reverse transcription reaction contains specific amounts of dH_2O, oligos (specific, random, or oligo-dT), dithiothreitol (DTT) which in low concentrations helps to stabilize the

enzyme, buffer, dNTPs, template, and RT enzyme (reverse transcriptase). The actual reaction depends on the kit, the enzyme, and the type of oligonucleotides used. Subsequently, we suggest an optional approach using a kit by Invitrogen.

1. Take 5 µg RNA and dilute it to 10 µL. Add 1 µL each (2 µM) of two oligos or 2 µL random hexamer (60 µM), 1 µL dNTP (10 mM) and incubate at 65 °C for 5 min.

2. After this, keep the reaction on ice and add 4 µL 5× SuperScript IV buffer, 1 µL 0.1 M DTT, 1 µL RNaseOUT (40 U/µL), and 1 µL SuperScript IV reverse transcriptase (200 U/µL). The final volume then is 20 µL.

3. The transcription reaction starts with incubation at 45 °C for 50 min in a PCR instrument and is finished with an inactivation step at 70 °C for 20 min. When using random hexamers, there is an additional incubation step at 29 °C for 10 min prior to the reverse transcription reaction at 45 °Cfor 50 min.

   For reverse transcription and the subsequent qPCR there is the alternative possibility of a single-tube one-step qPCR. This is a faster approach with the potential for high-throughput multiwell systems (*see* **Note 2**).

3.4 Real-Time (Quantitative) PCR

In general, a real-time qPCR reaction contains a DNA polymerase, reaction buffer, dNTPs, $MgCl_2$, specific oligonucleotides, and template DNA. Generally, it is also important to select primers and cycling conditions well (*see* **Notes 3** and **4**). However, just as for reverse transcription , the actual qPCR process depends on the system used (qPCR kit and qPCR instrument). Subsequently, we suggest an optional approach, using the Roche LightCycler® 480 Instrument II.

1. Add 1 µL each (5 µM) of two oligos (EBER1 _upper: 5′- cta ggg agg aga cgt gtg tgg-3′; EBER1_lower: 5′- gct ggt act tga ccg agg acg-3′; or GAPDH_upper: 5′- gga agg tga agg tcg gag tca-3′; GAPDH_lower: 5′- atg ggt gga atc ata ttg gaa ca-3′), 5 µL 2× reaction mix (contains buffer, dNTP, $MgCl_2$ and polymerase; SensiFAST SYBR No-ROX kit, Bioline), 2 µL ultrapure dH_2O and 1 µL sample (10× diluted, *see* **Note 5**).

2. The actually used thermal profile has to be adapted to the melting temperature of the oligonucleotide set used: Start with a denaturation step at 95 °C for 2 min, then continue with 95 °C for 10 s and 60 °C for 30 s, alternating for 45 cycles.

3.5 Comparison of EBER1 Expression Using Nuclear Run-On Assay and Conventional RNA Isolation

We used well characterized EBV-positive cell lines including Burkitt lymphoma subclones (MUTU -BL-I-Cl-216, MUTU-BL-III-Cl-99) and cell lines (RAEL, RAJI). Besides these, we used a lymphoblastoid cell line (CBM1-Ral-STO) and a nasopharyngeal carcinoma-derived cell line (C666.1). All cells constantly express EBER1 [11, 12] (Fig. 2).
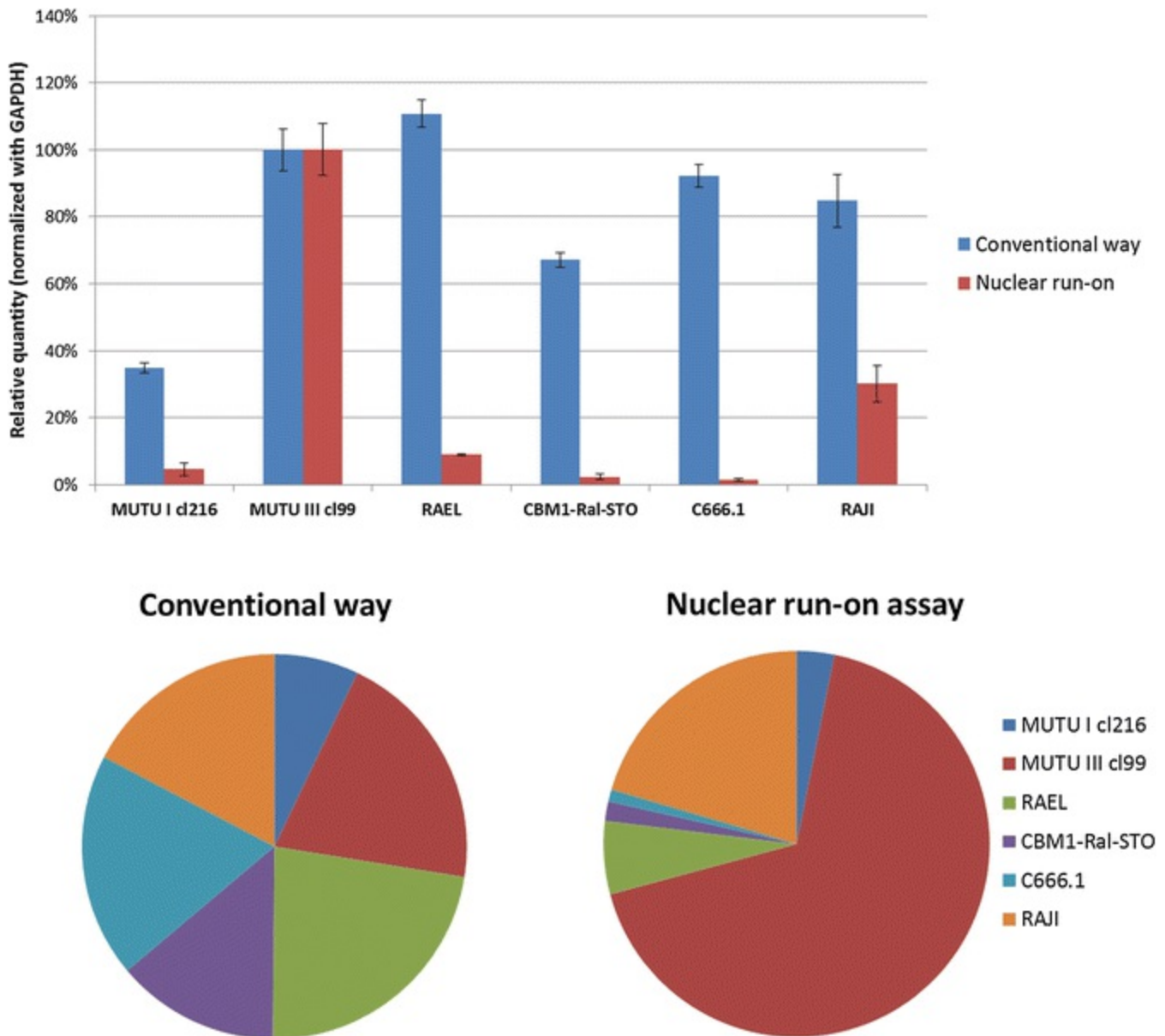
Fig. 2 Results of qPCR assays. Relative EBER1 RNA levels normalized to GAPDH mRNA levels are shown, correlated to the Mutu -BLIII-Clone-99 EBER1 level (100 %). Upper graph: blue mark, qPCR following isolation of total cellular RNA purified by conventional isolation; red mark, qPCR following nuclear run-on assay . *Lower graph,*

the two pie charts show the ratio of the expression values of the examined cell lines

Our results showed that the ratio of EBER1 levels varied between the cell lines, depending on the method applied. The RAEL cell line showed the highest EBER1 expression level using conventional, total cellular RNA isolation, while in the nuclear run-on assay the MUTU-BL-III-Cl-99 clone had the highest expression level. Our results raise the point that the interpretation of an epigenetic analysis may completely differ depending on the specific approach used for analyzing transcription. We suggest to use the nuclear run-on assay in experiments analyzing promoter activity, e.g., in the context of epigenetic studies, because it more closely reflects promoter activity independent of RNA steady-state levels or RNA stability.

4 Notes

1. A house-keeping gene has to be included into a gene expression study to normalize the sampling differences which could disguise the real alterations between the mRNA levels of the gene or genes of interest. Experimentally obtained gene expression levels can be normalized with a single division operation. Theoretically, housekeeping genes have constant expression levels because they are required for the maintenance of essential cellular functions that are elemental for the existence of a cell, to attend the appropriate role in the living tissue or within a one-cell organism [13]. However, housekeeping genes can have distinct expression levels in tissues or organs, depending on the experimental conditions or depending on drug treatment. Specific experimental conditions may influence the selection of a housekeeping gene which is suitable for normalization under the given circumstances. Therefore, it is recommended to try more than one housekeeping gene (actually a minimum of three) in the same study to identify and validate the constantly active ones [14].

2. The one-step qPCR method can be a quick solution for reverse transcription and qPCR in a one-step reaction. The major advantage of the single-tube approach comes into effect at high sample numbers. The one-step reaction uses one of the oligos of the PCR primer-set, i.e., the oligo complementary to the RNA of interest, to transcribe cDNA, and afterwards in the cycle phase of the reaction, the heat-stable DNA polymerase amplifies the DNA in a PCR reaction. The intervening DNase I treatment is avoided in this case by using oligo-primers hybridizing to exon–exon boundaries. Alternatively, oligo primer-sets hybridizing to exons and enclosing a long intronic section which is larger than 1000 nt are suitable for avoiding the DNAse step as well. The disadvantage of the one-step qPCR approach

is that random hexamers cannot be used. Furthermore, because the tube is not opened between reverse transcription and PCR reaction, at the end there is no remaining cDNA which might be used as a template for later or additional experiments.

3. The general oligonucleotide-primer design rules have been described by Dieffenbach and colleagues [15]. We suggest that for optimizing the conditions of the virtual PCR reaction 50 mM Na^+ and 2.5 mM $MgCl_2$ should be used during the design. Under these conditions the Tm of the qPCR oligos should be around 54–60 °C. For the oligos used in the reverse transcription reaction the Tm has to be closer to the working temperature of the reverse transcriptase. This temperature depends on the used kit, but in general is about 45 °C. Because primer binding specificity depends on the Tm and oligo-length, the closest Tm option in case of specific oligos is about 50 °C (and may go as high as 60 °C). Using random hexamers, there is an additional step at 29 °C before the reverse transcription step at about 45–50 °C, because of the lower Tm of the random hexamers.

4. For the real-time PCR design it is recommended to use the MIQE Guidelines [16]. Furthermore, at present there is the possibility to multiplex qPCR using distinct probes [17]: http://www.premierbiosoft.com/tech_notes/multiplex-pcr.html. For multiplex-PCR, inner control reactions, needed to prove the operable reaction conditions in negative samples, and two or three different specific oligo sets for a gene or genes of interest may be combined in a single reaction tube. Thus, a multiplex system combined with the one-step qPCR approach results in an almost high-throughput assay system depending on the number of the samples. For example, three genes of interest in each well of a 384 multiwell plate results in more than one thousand reactions per plate, which comes close to the new generation methods.

5. In most cases 10× diluted cDNAs result in better amplification curves and contain still enough cDNA for quantification. The appropriate dilution depends on the promoter activity of the analyzed gene, i.e., the amount of the isolated RNA, the working efficiency of the oligos and the used real-time PCR kit.

References

1. Niller HH, Szenthe K, Minarovits J (2014) Epstein-Barr virus-host cell interactions: an epigenetic dialog? Front Genet 5:367
[CrossRef][PubMed][PubMedCentral]

2. Manet E, Chevallier A, Zhang CX et al (1985) Construction and use of cDNA clones for the mapping and identification of Epstein-Barr virus early P3HR-1 mRNAs. J Virol 54:608–614
    [PubMed][PubMedCentral]

3. Pfaffl MW (2004) Quantification strategies in real-time PCR. In: Bustin SA (ed) A-Z of quantitative PCR. International University Line, La Jolla, pp 87–112

4. Gattei V, Degan M, De Iuliis A et al (1997) Competitive reverse-transcriptase PCR: a useful alternative to northern blotting for quantitative estimation of relative abundances of specific mRNAs in precious samples. Biochem J 325:565–567
    [CrossRef][PubMed][PubMedCentral]

5. Murphy D (1993) Nuclear run-on analysis of transcription. Methods Mol Biol 18:355–361
    [PubMed]

6. Patrone G, Puppo F, Cusano R et al (2000) Nuclear run-on assay using biotin labeling, magnetic bead capture and analysis by fluorescence-based RT-PCR. BioTechniques 29:1012–1017
    [PubMed]

7. Szenthe K, Koroknai A, Banati F et al (2013) The 5′ regulatory sequences of active miR-146a promoters are hypomethylated and associated with euchromatic histone modification marks in B lymphoid cells. Biochem Biophys Res Commun 433:489–495
    [CrossRef][PubMed]

8. Niller HH, Wolf H, Minarovits J (2007) Epstein-Barr Virus. In: Minarovits J, Gonczol E, Valyi-Nagy T (eds) Latency strategies of herpesviruses. Springer, New York, pp 154–191
    [CrossRef]

9. Hochberg DR, Thorley-Lawson DA (2005) Quantitative detection of viral gene expression in populations of Epstein-Barr virus-infected cells in vivo. Methods Mol Biol 292:39–56
    [PubMed]

10. Niller HH, Wolf H, Minarovits J (2009) Epigenetic dysregulation of the host cell genome in Epstein-Barr virus-associated neoplasia. Semin Cancer Biol 19:158–164
    [CrossRef][PubMed]

11. Minarovits J, Hu LF, Marcsek Z et al (1992) RNA polymerase III-transcribed EBER 1 and 2 transcription units are expressed and hypomethylated in the major Epstein-Barr virus-carrying cell types. J Gen Virol 73:1687–1692
    [CrossRef][PubMed]

12. Cheung ST, Huang DP, Hui AB et al (1999) Nasopharyngeal carcinoma cell line (C666-1) consistently harbouring Epstein-Barr virus. Int J Cancer 83:121–126
    [CrossRef][PubMed]

13. Eisenberg E, Levanon EY (2013) Human housekeeping genes, revisited. Trends Genet 29:569–574
    [CrossRef][PubMed]

14. Dheda K, Huggett JF, Bustin SA et al (2004) Validation of housekeeping genes for normalizing RNA expression in real-time PCR. BioTechniques 37:112–119
    [PubMed]

15. Dieffenbach CW, Lowe TM, Dveksler GS (1993) General concepts for PCR primer design. PCR Methods Appl 3:S30–S37

[CrossRef][PubMed]

16. Bustin SA, Benes V, Garson JA et al (2009) The MIQE guidelines: minimum information for publication of quantitative real-time PCR experiments. Clin Chem 55:611–622
[CrossRef][PubMed]

17. Shen Z, Qu W, Wang W et al (2010) MPprimer: a program for reliable multiplex PCR primer design. BMC Bioinformatics 11:143
[CrossRef][PubMed][PubMedCentral]

18. Ernberg I, Falk K, Minarovits J et al (1989) The role of methylation in the phenotype-dependent modulation of Epstein-Barr nuclear antigen 2 and latent membrane protein genes in cells latently infected with Epstein-Barr virus. J Gen Virol 70:2989–3002
[CrossRef][PubMed]

19. Altiok E, Minarovits J, Hu LF et al (1992) Host-cell-phenotype-dependent control of the BCR2/BWR1 promoter complex regulates the expression of Epstein-Barr virus nuclear antigens 2-6. Proc Natl Acad Sci U S A 89:905–909
[CrossRef][PubMed][PubMedCentral]

20. Gregory CD, Rowe M, Rickinson AB (1990) Different Epstein-Barr virus-B cell interactions in phenotypically distinct clones of a Burkitt's lymphoma cell line. J Gen Virol 71:1481–1495
[CrossRef][PubMed]

21. Hatfull G, Bankier AT, Barrell BG et al (1988) Sequence analysis of Raji Epstein-Barr virus DNA. Virology 164:334–340
[CrossRef][PubMed]

22. Salamon D, Banati F, Koroknai A et al (2009) Binding of CCCTC-binding factor in vivo to the region located between Rep* and C-promoter of Epstein-Barr virus is unaffected by CpG methylation and does not correlate with Cp activity. J Gen Virol 90:1183–1189
[CrossRef][PubMed]

23. Bellan C, Lazzi S, Hummel M et al (2005) Immunoglobulin gene analysis reveals 2 distinct cells of origin for EBV-positive and EBV-negative Burkitt lymphomas. Blood 106:1031–1036
[CrossRef][PubMed]

24. Piccaluga PP, De Falco G, Kustagi M et al (2011) Gene expression analysis uncovers similarity and differences among Burkitt lymphoma subtypes. Blood 117:3596–3608
[CrossRef][PubMed]

25. Woisetschlaeger M, Strominger JL, Speck SH (1989) Mutually exclusive use of viral promoters in Epstein-Barr virus latently infected lymphocytes. Proc Natl Acad Sci U S A 86:6498–6502
[CrossRef][PubMed][PubMedCentral]

9. Analysis of Viral and Cellular MicroRNAs in EBV-Infected Cells

Rebecca L. Skalsky[1]✉

(1) Vaccine and Gene Therapy Institute, Oregon Health and Science University, 505 NW 185th Avenue, Beaverton, OR, USA

✉ **Rebecca L. Skalsky**
   Email: skalsky@ohsu.edu

Abstract
MicroRNAs are small, noncoding RNAs that posttranscriptionally regulate gene expression. The discovery of this relatively new mode of gene regulation as well as studies showing the prognostic value of viral and cellular miRNAs as biomarkers, such as in cancer progression, has stimulated the development of many methods to characterize miRNAs. EBV encodes 25 viral precursor microRNAs within its genome that are expressed during lytic and latent infection. In addition to viral miRNAs, EBV infection induces the expression of specific cellular oncogenic miRNAs, such as miR-155, miR-146a, miR-21, and others, that can contribute to the persistence of latently infected cells. This chapter describes several current techniques used to identify and detect the expression of viral and cellular miRNAs in EBV-infected cells.

Key words BHRF1 – BART – MicroRNA – RISC – RNA isolation – Deep sequencing – RIP-seq – Primer extension – Stem-loop qRT-PCR – Luciferase assay

1 Introduction

MicroRNAs (miRNAs) are important regulators of many, if not most, biological processes, including homeostasis, cell growth and differentiation, and responses to stimuli such as viral infection. These ~22 nt small, noncoding RNAs

posttranscriptionally regulate gene expression by guiding the RNA-induced silencing complex (RISC) to sequence-specific sites on target mRNAs, thereby repressing translation and/or inducing mRNA degradation. Virus infection can trigger dramatic changes in the host miRNA repertoire which consequently alters the host transcriptional and translational environment [1–7]. In B cells, for example, EBV induces high levels of oncogenic miR-155 which is required for the growth of these cells [1, 3, 8], while in EBV-positive epithelial cells, many tumor suppressor miRNAs are downregulated [4]. Notably, miRNA signatures have been linked to EBV status in B-cell lymphomas [6, 9, 10]. Given the many studies associating miRNA expression patterns with disease states [5–6, 9–12], miRNAs have significant value as biomarkers. Techniques such as miRNA profiling by deep sequencing and stem-loop qRT-PCR , described here, have been applied to a variety of cell types and tumors to investigate cellular and viral miRNAs during lytic and latent EBV infection.

Viral miRNAs were first identified in 2004 in EBV-infected cells [13]; initially, the expression of five EBV miRNAs (miR-BHRF1 -1,miR-BHRF1-2,miR-BHRF1-3, miR-BART1 , and miR-BART2) was demonstrated by cloning of small RNAs (18–24 nt) from EBV B95-8-infected BL41 cells and confirmed by Northern blot analysis. Over the last 10 years, additional EBV miRNAs have been identified by sequencing studies [15–17], and there is now evidence for >300 viral miRNAs expressed by herpesviruses and other DNA and RNA tumor virus families (reviewed in [5] and mirbase.org). At least 44 mature miRNAs arise from the 25 EBV precursor miRNAs (pre-miRNAs): three miRNAs flank the BHRF1 ORF encoding a viral Bcl2 homolog, and two large clusters of miRNAs arise from introns within the BART region (Fig. 1).
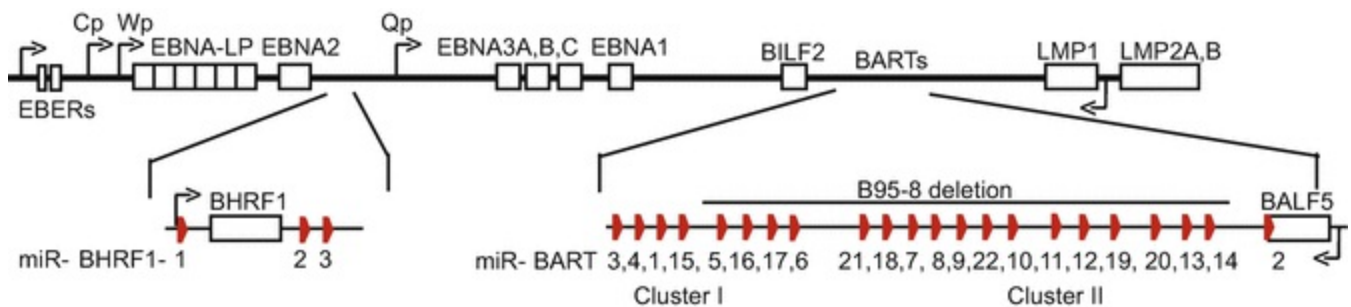
Fig. 1 Genomic locations of the EBV miRNA clusters

EBV miRNAs, like the majority of their cellular counterparts, are expressed from RNA polymerase II-driven long primary miRNA (pri-miRNA) transcripts which undergo multiple biogenesis steps in the nucleus and cytoplasm to generate a mature, RISC -associated miRNA [18]. Pri-miRNAs fold into long hairpins which are cleaved by nuclear Drosha into ~60 nt pre-miRNAs. Following nuclear export, the pre-miRNA is cleaved by cytoplasmic Dicer, and one strand of the ~22 nt miRNA duplex becomes associated with an Argonaute (Ago) protein and incorporated into RISC as the mature

miRNA [5, 18–20]. An understanding of these biogenesis steps has significantly aided in developing experimental strategies to identify and detect novel viral miRNA species [13–16], ectopically express miRNAs ([21–23] and described in [24]), and isolate miRNA-ribonucleoprotein (RNP) complexes to determine miRNA targets [21–23, 25–27]. High-throughput methods aimed at identifying miRNA targets in EBV-infected cells, such as PAR-CLIP [21–23, 27] and HITS-CLIP [26] (the PAR-CLIP protocol is described in detail elsewhere [28]), have benefited from this knowledge and led to the direct identification of hundreds of EBV miRNA targets related to cell survival, apoptosis , signaling, and immune evasion.

Broken into two major sections, this chapter describes current protocols (1) to identify and characterize miRNAs, including RISC -associated miRNAs, in EBV-infected cells using deep sequencing and bioinformatics tools and (2) to detect the expression of individual miRNAs using primer extension, stem-loop qRT-PCR, and luciferase assays.

2 Materials and Reagents

All reagents, tubes, pipette tips, and work areas should be RNase-free. Solutions should be prepared with ultrapure, nuclease-free water. Appropriate work practices and institutional disposal guidelines must be followed for working with phenol (TRIzol® Reagent), chloroform, and radioactivity.

2.1 RNA Isolation from EBV-Infected Cell Lines

1. TRIzol® Reagent (Life Technologies).

2. Chloroform.

3. Isopropanol (isopropyl alcohol).

4. Glycogen or GlycoBlue (optional).

5. 95 % ethanol (optional).

6. Nuclease-free water.

2.2 RISC Immunoprecipitation (RIP)

1. RIP lysis buffer: 50 mM HEPES, 150 mM KCl, 2 mM EDTA, 1 mM NaF, 0.5 % NP40, 0.5 mM DTT, and EDTA-free complete protease inhibitor cocktail tablets (Roche). For 50 mL of RIP lysis buffer, combine 2.5 mL 1 M HEPES, pH 7.5, 1.875 mL 4 M KCl, 0.2 mL 0.5 M EDTA, 50 μL 1 M NaF, 50 μL NP40 (or IGEPAL), 25 μL 1 M DTT, and 45.3 mL nuclease-free water. Dissolve protease inhibitor tablets according to manufacturer's instructions.

2. Citrate-phosphate buffer: To prepare 1 L, combine 4.7 g citrate phosphate and 9.32 g Na_2HPO_4. Bring volume up to 1 L with ultrapure water. The pH should be pH 5.0.

3. Dynabeads®, Protein G (Life Technologies) and magnetic bead separator (i.e., DynaMag).

4. Anti-Ago2 (clone 9E8.2, Millipore) or pan-Ago antibody (Abcam ab57113 recognizes Ago1, Ago2, and Ago3; Diagenode 2A8 recognizes all four human Ago proteins) [29]. Alternatively, a FLAG- tagged Ago2 can be introduced into cells, and RISC-miRNAs can be immunoprecipitated with monoclonal antibodies to FLAG (i.e., clone M2, Sigma) [21].

5. RNase inhibitor (i.e., RNaseOUT Recombinant Ribonuclease Inhibitor, Life Technologies).

6. NT2 buffer: 50 mM Tris-HCl, pH 7.4, 150 mM NaCl, 1 mM $MgCl_2$, and 0.05 % NP40. To prepare 50 mL of NT2 buffer, combine 2.5 mL 1 M Tris-HCl, pH 7.4, 7.5 mL 1 M NaCl, 50 μL 1 M $MgCl_2$, 25 μL NP40 (or IGEPAL), and 40 mL nuclease-free water.

7. Proteinase K, PCR grade.

2.3 Deep Sequencing of Small RNAs

1. Total or RIP RNA (up to 1 μg).

2. Illumina TruSeq small RNA kit (or kit compatible with the platform of choice).

3. Thermocycler and nuclease-free 0.2 μL tubes.

4. 10 % Tris/borate/EDTA (TBE) polyacrylamide gel, 1× TBE buffer, and electrophoresis apparatus.

5. 0.3 M NaCl, glycogen, and 100 % ice cold ethanol for precipitation.

2.4 Primer Extension

1. Total RNA (5–10 μg, in water).

2. Primer design: DNA oligonucleotides used for miRNA detection by primer extension should be ~14–17 nt in length and perfectly complementary to the 3′-end of the miRNA of interest to allow extension of 5–7 nt.

3. Size markers: DNA or RNA oligonucleotides of discrete sizes (i.e., 18 and 24 nt in length) can be radiolabeled for use as size markers. Alternatively, the Decade Marker System (Life Technologies) can be used. Label according to manufacturer's instructions.

4. [γ-^{32}P] ATP (3000 Ci/mmol, 10 mCi/mL).

5. MicroBioSpin6 columns (BioRad).

6. The following reagents are included within the Primer Extension System (Promega):

    T4 polynucleotide kinase (PNK) (NEB).

    T4 PNK 10× buffer.

    2× AMV primer extension buffer.

    40 mM sodium pyrophosphate.

    AMV reverse transcriptase (RT).

    Nuclease-free, ultrapure water.

    2× loading dye.

7. 15 % TBE-Urea polyacrylamide gel, 1× Tris/borate/EDTA (TBE) buffer, and electrophoresis apparatus.

2.5 Stem-Loop qRT-PCR

For detection of many EBV and human miRNAs, predesigned assays are commercially available. Commercial miRNA PCR arrays are also available for profiling large sets of known miRNAs. For custom assays, design the following:

1. miRNA-specific stem-loop RT primer, where *NNNNNN* is complementary to the miRNA 3′-end:
   5′-GTC GTA TCC AGT GCA GGG TCC GAG GTA TTC GCA CTG GAT ACG CA*N NNN NN*-3′.

2. miRNA-specific forward PCR primer, where *NNN NNN NNN NNN NNN N* is equivalent to the first 16 nt of the miRNA: 5′-GCG C*NN NNN NNN NNN NNN NN*-3′.

3. Reverse PCR primer: 5′-GTG CAG GGT CCG AGG T-3′.

4. miRNA-specific TaqMan® MGB-labeled probe, where *NNN NNN* is complementary to the 3′-end of the miRNA: 5′-TGG ATA CGA C*NN NNN N*-3′.

5. Reagents for the RT reaction (performed on a thermocycler): 5 µM annealed miRNA-specific stem-loop RT primer, 10 mM dNTPs, MultiScribe reverse transcriptase (Life Technologies), RNase inhibitor, RNA template (50 ng/µL) (*see* Subheading 3.1), nuclease-free water, and 10× RT buffer, 100 mM Tris-HCl, pH 8, 500 mM KCl, and 5.5 mM MgCl$_2$.

6. Reagents for the qPCR reactions (performed on a real-time PCR machine): 2× Universal PCR Master Mix (Life Technologies) or comparable, 50 µM forward and reverse PCR primers, 10 µM TaqMan® MGB probe, nuclease-free water, and 96-well optical plates suitable for real-time PCR.

2.6 Luciferase Indicator Assays

1. HEK293T cells, grown in Dulbecco's modified Eagle's medium supplemented with 10 % fetal bovine serum and antibiotics.

2. Dual-luciferase reporter vector such as psiCHECK-2 (Promega) with two perfectly complementary binding sites for a miRNA of interest cloned into the 3′-UTR of either renilla or firefly luciferase.

3. Source of viral or cellular miRNA with appropriate negative controls. This can be a miRNA expression vector such as pcDNA3 or lentiviral vector [21, 23, 24] containing ~200 nt of the primary miRNA cloned downstream of a promoter OR miRNA mimics (see [30] for custom design).

4. Transfection reagent such as Lipofectamine 2000 (Life Technologies) and Opti-MEM I reduced serum media.

5. Black-walled, clear-bottom 96-well tissue culture plates for transfections. Alternatively, transfections can be performed in 12-, 24-, or 48-well plates and lysates transferred to appropriate tubes/plates prior to addition of DLR substrate.

6. Dual-Luciferase Reporter (DLR) Assay System (Promega).

7. Luminometer capable of reading 96-well plates.

---

3 Methods

3.1 Identifying miRNAs in EBV-Infected Cells Using Small RNA Deep Sequencing

3.1.1 Isolating RNA from EBV-Infected Cells

1. Pellet suspension cells (~$1000 \times g$ for 5 min) and wash once with phosphate-buffered saline (PBS). For adherent cells, remove media and wash $1\times$ PBS. Add 1 mL TRIzol® per 1×10^7 cells and pipette up and down to lyse cells (*see* **Note 1**).

2. Perform phenol-chloroform extraction to isolate RNA from TRIzol®. Add 0.2 mL chloroform per 1 mL TRIzol. Vortex or invert to mix, and then centrifuge at >10,000

$\times$ g at 4 °C for 15 min to separate the aqueous (top) and organic (bottom) layers. Transfer aqueous layer to a new tube (if 1 mL TRIzol® was used, this volume should be about 0.5 mL). Optional: Perform additional chloroform extraction by adding one-volume chloroform to the aqueous layer, vortex or invert to mix, and centrifuge 10 min >10,000 $\times$ g to separate the layers. Transfer top layer to a new tube.

3. Precipitate RNA by adding 0.75 volumes of isopropanol to the aqueous layer, and incubate for >15 min at −80 °C or >30 min at −20 °C. For isolation of RNA from low cell numbers (<1 $\times$ 10^6), add 1 µL of glycogen during this step. Pellet RNAs at >15,000 $\times$ g at 4 °C for 30 min. Remove all liquid and allow RNA pellet to air-dry for 2–3 min. Resuspend RNA in 50 µL nuclease-free water. Optional: The RNA pellet can be washed one to two times with ice cold 95 % ethanol prior to resuspension in water (*see* **Note 2**).

3.1.2 Isolating RISC -Associated miRNAs by Ago Immunoprecipitation (RIP)

The majority of assays to investigate miRNA levels use total RNA or size-fractionated RNA as input. Recent studies have demonstrated that the level of a miRNA in total RNA fractions does not accurately predict its inhibitory potential; rather, the level of RISC association is a more accurate indicator for miRNA activity [29]. The RIP protocol below is modified from a protocol by Keene et al. [31] to isolate RISC-associated RNAs using antibodies against Ago2, a key RISC component. This RIP method, following by deep sequencing (RIP-seq), has been used recently to interrogate RISC-associated miRNAs in lymphoblastoid cell lines (LCLs) [22]:

1. Grow enough cells to obtain ~1 mL dry cell pellet (~50–100 $\times$ 10^6 cells or ~1–1.5 L of EBV B95-8 LCLs). Pellet cells by centrifugation at ~1000 $\times$ g for 5 min and wash two times with PBS (*see* **Note 3**). Resuspend pellet in three volumes of RIP lysis buffer and incubate on ice for 10 min. Clear lysate by centrifugation at >10,000 $\times$ g at 4 °C for 15 min. Transfer lysate to a new tube (*see* **Note 4**).

2. Prepare magnetic Dynabeads (protein G) by transferring 30 µL beads to 1.5 mL

tube and washing two times with 0.5 mL citrate-phosphate buffer. Resuspend beads in 60 µL of RIP lysis buffer and add 10 µL of anti-Ago2 antibody. Incubate on rotator for 45 min at room temperature.

3. Remove unbound antibody using the magnetic separator and wash beads one time with 1 mL of RIP lysis buffer. Resuspend beads in 60 µL RIP lysis buffer and add in full to cell lysate (*see* **Note 5**). Incubate at 4 °C on a rotator for 2–18 h.

4. Collect beads on ice using the magnetic separator and discard supernatant. Wash beads ten times in NT2 buffer (*see* **Note 6**).

5. Resuspend beads in 300 µL NT2 buffer (*see* **Note 7**). Add 10 µL RNase inhibitor and 30 µL (~25–30 µg) proteinase K to the bead mixture. Incubate at 55 °C for 30 min to release antibody/RISC-bound RNAs. Flick the tube every 5–10 min to mix.

6. Add 1 mL TRIzol$^®$ to the bead mixture to isolate RNAs. Proceed to the chloroform extraction and **steps 2** and **3** in Subheading 3.1.1 above. Addition of glycogen is necessary during RNA precipitation and recovery. Resuspend RNA pellet in 10 µL nuclease- free water (*see* **Note 8**).

3.1.3 Deep Sequencing of Small RNAs

Among the most commonly used platforms for high-throughput sequencing of RNAs are 454 (Roche), SOLiD (Life Technologies/Applied Biosystems), and Illumina. SOLiD and Illumina are preferred for small RNAs since both technologies yield millions of short reads. Two to five million reads generally provide enough complexity to have coverage of all miRNA isoforms in a given sample. Using the Illumina HiSeq2000 platform (50 cycle, single-end reads), we generally multiplex 10–12 samples in a sequencing lane. This yields about 300 million reads total, with at least 25 million high-quality reads per sample. Sequencing library preparation kits are commercially available for each platform. When comparing multiple biological samples, it is highly recommended to use the same sequencing platform.

We have previously used the Illumina TruSeq small RNA kit with either 0.5–1 µg total RNA (*see* Subheading 3.1.1) or 0.2–0.5 µg RIP RNA as input (*see* Subheading 3.1.2) [22, 29]. RNAs are sequentially ligated to Illumina adapter sequences. Following adapter ligation, RNAs are reverse transcribed using primers complementary to the 3′-adapter, and cDNAs are PCR amplified with bar-coded primers for multiplexing. Importantly, a pilot PCR should be performed for each library to ensure that amplification occurs within the linear range. The pilot PCR is necessary to maintain

library complexity and avoid over-amplifying highly expressed miRNAs. This can be set up using 15 % of the cDNA mixture and amplifying for 10, 12, 14, 16, and 18 cycles using the conditions outlined in the Illumina TruSeq manufacturer's protocol. cDNAs are gel purified using a 10 % TBE polyacrylamide gel run at 200 V in 1× TBE buffer. Following staining with ethidium bromide or SYBR Safe, excise the ~145 nt cDNA band, place the gel slice in a 1.5 mL tube with 0.5 mL 0.3 M NaCl, and passively elute on a rotator at 4 °C for 16 h. The eluted cDNA is precipitated by transferring the 0.5 mL supernatant to a clean tube and adding 1 μL glycogen and two volumes of 100 % ethanol. Incubate at 20 °C for 30 min and pellet by centrifugation at >10,000 × *g*.

3.1.4 Bioinformatics Analysis of Sequencing Reads

Sequences should be obtained in fastq format (*see* **Note 9**). A number of open source tools are available for filtering and aligning reads:

Preprocessing the reads:

For command-line users, the fast-x toolkit (http://hannonlab.cshl.edu/fastx_toolkit/) provides scripts to remove adapter sequences and filter out low-quality and short reads <15 nt. A web-based version, Galaxy (www.usegalaxy.org), is available for those requiring access to resources for computationally intensive analyses.

Aligning reads and determining miRNAs:

Strategy I: Using Bowtie [32] (or comparable alignment tool), align reads concurrently to the human (HG19) and appropriate EBV (i.e., AJ507799) genomes. For Bowtie or Bowtie2 alignments, we allow up to two mismatches and up to 25 unique locations for miR-seq and RIP -seq alignments (-v 2 -m 25). Genomic locations with reads falling into the best stratum (--best --strata) are kept for further analysis. To annotate miRNAs, compare read locations to the coordinates/sequences of the human and EBV miRNAs from the most current version of miRBase (www.mirbase.org).

Strategy II: Use Perl-based scripts from miRDeep2 [33] to align reads and quantify miRNA read counts. miRDeep2 has dependencies on Bowtie and also requires miRNA sequences from the most current version of miRBase .

Identifying differentially expressed (DE) miRNAs:

Once read counts per miRNA are obtained, we use the Bioconductor software package edgeR [34, 35] to normalize libraries and define DE miRNAs.

3.2 Detecting Individual miRNAs in EBV-Infected Cell Lines and Tissue Samples

3.2.1 Primer Extension

Primer extension analysis is an effective method to identify 5′-end variations in viral and cellular miRNAs [36, 37] and often has a better sensitivity than Northern blotting to detect miRNAs. Unlike Northern blotting which allows for detection of both the precursor and mature miRNA, only the mature miRNA isoforms can be detected by primer extension:

1. Label the probe. Set up the following reaction in a nuclease-free, sterile 1.5 mL tube: 2 μL (10 pmol) primer (5 μM stock), 1 μL 10x T4 PNK buffer, 5 μL nuclease-free water, 1 μL T4 PNK, and 1 μL [γ-32P] ATP (3000 Ci/mmol, 10 mCi/mL). Incubate at 37 °C for 10–30 min. To remove unincorporated radionucleotides, add 90 μL of nuclease-free water to the labeling reaction, and pipette the entire volume onto prepared MicroBioSpin column. Spin for 2 min at 800 × *g* and collect labeled probe into a new tube (*see* **Note 10**).

2. Perform primer extension (*see* **Note 11**). Set up the following reaction in a nuclease-free 1.5 mL tube: 5 μg total RNA (*see* **Note 12**), 1 μL labeled primer probe, 5 μL 2× AMV PE buffer, and nuclease-free water to 11 μL. Incubate at 95 °C for 2 min to denature RNA and then, anneal at 37 °C for 20 min.

3. At room temperature, set up the following: 11 μL annealed primer/RNA from **step 2**, 1.4 μL sodium pyrophosphate, 5 μL 2× AMV PE buffer, 1.6 μL nuclease-free water, and 1 μL AMV RT (should be added last). Pipette up and down to mix. Incubate for 5 min at room temperature, and then extend for 30 min at 42 °C. To terminate reaction, add 20 μL 2× formamide loading buffer and heat inactivate at 95 °C for 10 min.

4. Analyze primer extension products on a 15 % TBE urea gel (*see* **Note 13**). Prepare a vertical gel containing 15 % acrylamide (19:1 acrylamide-bis), 7 M urea, and 1× TBE buffer. Boil samples (including negative control reaction) and size markers briefly prior to loading. Run at 250 V in 1× TBE buffer until the bromophenol blue dye is within 1 cm of the bottom. Expose gel to X-ray film overnight at −80 °C or to a phosphorimaging screen.

3.2.2 Stem-Loop qRT-PCR

qRT-PCR-based assays are perhaps the most widely used method for detecting individual miRNAs due to their relative ease and little hands-on time. miRNA stem-

loop qRT-PCR relies on knowing the precise 3′-end of a miRNA. Several studies have profiled miRNAs in EBV-infected cells using deep sequencing [16, 17, 21–23, 26, 38]; thus, the 3′-ends of these miRNAs are generally known:

1. Set up the following for reverse transcription by preparing master mix for multiple samples: 0.2 μL dNTPs, 2 μL 10× RT buffer, 0.2 μL RNase inhibitor, 0.3 μL stem-loop RT primer (5 μM stock), 1 μL MultiScribe RT, 100 ng RNA, and nuclease-free water to 20 μL (*see* **Note 14**).

2. Incubate at 16 °C for 30 min to anneal RT primer and then at 42 °C for 30 min. Heat inactivate at 85 °C for 10 min.

3. Set up the following for TaqMan® qPCR (prepare master mixes for multiple samples): 10 μL 2× Universal PCR Master Mix, 0.3 μL each forward and reverse PCR primer (50 μM stock), 0.3 μL TaqMan® MGB probe (10 μM stock), and nuclease-free water to 18 μL. Pipette 18 μL of the PCR mix into each well of a 96-well qPCR plate. Add 2 μL cDNA (10 % of RT reaction from above) to each well. At minimum, technical duplicates should be set up for each experiment.

4. Perform qPCR using the following conditions: 40 cycles each consisting of (step 1) 2 min at 50 °C, (step 2) 10 min at 95 °C, and (step 3) 15 s at 95 °C and 1 min at 60 °C.

3.3 Detecting EBV miRNA Activity Using Luciferase Indicator Assays

Luciferase reporter assays are commonly used to measure miRNA activity following ectopic miRNA expression (i.e., for miRNA target validation, when a 3′-UTR of a gene of interest is cloned behind luciferase) or following disruption of miRNA function (i.e., to demonstrate inhibition in cells containing a sponge inhibitor, decoy, or locked nucleic acid inhibitor directed against a specific miRNA) [21–24, 30]. miRNA luciferase indicators are highly effective at demonstrating miRNA activity from miRNA expression plasmids (Fig. 2) as well as in infected cells [21, 23, 27]:
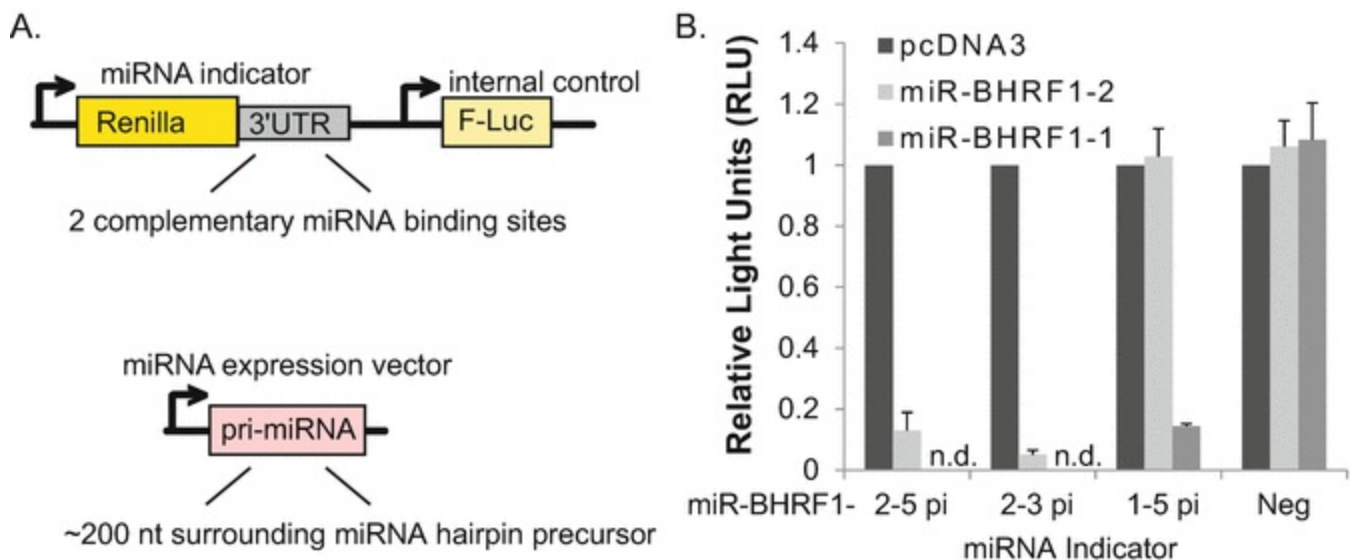
Fig. 2 (**a**) Example of luciferase reporter (miRNA indicator) and miRNA expression vector design. (**b**) EBV BHRF1 miRNAs inhibit luciferase expression from miRNA indicators. HEK293T cells, plated in 96-well black, clear-bottom plates, were co-transfected with 20 ng miRNA indicator and 250 ng miRNA expression vector using Lipofectamine 2000 according to manufacturer's protocol. 48 h post-transfection, cells were lysed in 1× passive lysis buffer and analyzed on a luminometer using the DLR (Dual-Luciferase Reporter) Assay System. Light values are relative to an internal control and normalized to empty vector (pcDNA3). A luciferase vector lacking miRNA-binding sites is used as a negative control (Neg). Shown is the average of two independent experiments performed in triplicate. n.d. = not determined for miR-BHRF1-1

1. Plate HEK293T cells (1×10^6 cells per plate) in 96-well black-well plates in complete media one day prior to transfection.

2. Per well, combine 20 ng luciferase indicator vector (i.e., psiCheck2 containing two tandem miRNA-binding sites within the luciferase 3′-UTR), 250 ng miRNA expression plasmid (or control) (*see* **Note 15**), Opti-MEM reduced serum media, and transfection reagent according to manufacturer's protocol, and add dropwise onto cells.

3. Incubate for 48–72 h to allow for miRNA expression. Lyse cells in 1× passive lysis buffer, and analyze luciferase activity using the DLR system and luminometer (*see* **Note 16**).

---

4 Notes

1. Lysate can be stored at −80 °C for several weeks or placed on ice prior to **step 2**.

2. The use of <95 % ethanol (i.e., 70 % ethanol) is not recommended for washing as this can partially elute small RNAs from the RNA pellet.

3. The pellet can be stored at −80 °C for several months. Avoid freeze-thaw cycles.

4. 25 μL of cleared lysate can be saved for Western blot (WB) analysis.

5. The slurry can be spiked with 1–2 μL RNase inhibitor to prevent RNA degradation.

6. Washing is critical to eliminate background. 25 μL of the supernatant following IP as well as portions of the wash steps can be saved for WB analysis.

7. 25 μL of resuspended beads can be saved and boiled in Laemmli buffer for WB analysis along with other saved samples (*see* **Notes 3** and **5**) to ensure adequate Ago2 IP.

8. Recovered RNA can be used directly for qRT-PCR analysis or to generate deep-sequencing libraries (RIP -seq). 0.5–2 μg of RNA is a common yield from ten million cells.

9. The Illumina platform provides reads in basespace format (fastq). For SOLiD users, reads are in colorspace format (csfasta) and require alternate workflows other than described here. Note that for either platform sequencing files are several gigabytes in size and require appropriate computational resources for storage and manipulation.

10. Purified probe for primer extension can be stored at −80 °C or used immediately. Measuring radionucleotide incorporation on a scintillation counter is recommended.

11. Master mixes for the primer mixture and extension mixture should be prepared when analyzing multiple RNA samples. Additionally, a negative control reaction should be prepared for each primer probe containing water in place of RNA template.

12. At least 5–10 μg of high-quality, total RNA is recommended for detection of most miRNAs. This amount can be increased to 15 μg for lowly expressed miRNAs.

13. Due to the small size of the primer extension product (~15 nt probe, ~22 nt product), a 15 % denaturing polyacrylamide gel is recommended. Wells of the gel should be rinsed with 1× TBE buffer to remove urea prior to loading samples.

14. Appropriate controls for assaying viral miRNAs include RNA from uninfected cells or from cells infected with a miRNA knockout virus (i.e., EBV BHRF1 miRNA mutant viruses [40, 21, 39]). Standard curves can be generated using RNA oligonucleotides that match the specific miRNA sequence. Separate RT reactions need to be set up for each standard curve dilution.

15. Suggested controls include additional miRNA expression plasmids that should not interact with the luciferase indicator vector as well as a control luciferase vector lacking miRNA-binding sites ("Neg" in Fig. 2). Technical replicates, i.e., triplicates, should be set up for each condition. psiCheck2 expresses both *Renilla* and firefly luciferase. If another type of luciferase vector is used, an internal control luciferase plasmid should be spiked into the transfections.

16. The level of luciferase indicator knockdown via a miRNA with perfect complementarity to the inserted binding sites should be in the range of >75–90 %. The 25–75 % inhibition is normally observed for luciferase 3′-UTR reporters with mismatches to the miRNA of interest, i.e., a 3′-UTR containing a miRNA seed match or an indicator with imperfect sites.

Acknowledgments

References

1. Cameron JE, Fewell C, Yin Q et al (2008) Epstein-Barr virus growth/latency III program alters cellular microRNA expression. Virology 382:257–266

[CrossRef][PubMed][PubMedCentral]

2. Cameron JE, Yin Q, Fewell C et al (2008) Epstein-Barr virus latent membrane protein 1 induces cellular MicroRNA miR-146a, a modulator of lymphocyte signaling pathways. J Virol 82:1946–1958
[CrossRef][PubMed]

3. Jiang J, Lee EJ, Schmittgen TD (2006) Increased expression of microRNA-155 in Epstein-Barr virus transformed lymphoblastoid cell lines. Genes Chromosomes Cancer 45:103–106
[CrossRef][PubMed]

4. Marquitz AR, Mathur A, Chugh PE et al (2014) Expression profile of microRNAs in Epstein-Barr virus-infected AGS gastric carcinoma cells. J Virol 88:1389–1393
[CrossRef][PubMed][PubMedCentral]

5. Skalsky RL, Cullen BR (2010) Viruses, microRNAs, and host interactions. Annu Rev Microbiol 64:123–141
[CrossRef][PubMed][PubMedCentral]

6. Forte E, Luftig MA (2011) The role of microRNAs in Epstein-Barr virus latency and lytic reactivation. Microbes Infect 13:1156–1167
[CrossRef][PubMed][PubMedCentral]

7. Mrazek J, Kreutmayer SB, Grasser FA et al (2007) Subtractive hybridization identifies novel differentially expressed ncRNA species in EBV-infected human B cells. Nucleic Acids Res 35:e73
[CrossRef][PubMed][PubMedCentral]

8. Linnstaedt SD, Gottwein E, Skalsky RL et al (2010) Virally induced cellular miR-155 plays a key role in B-cell immortalization by EBV. J Virol 84:11670–11678
[CrossRef][PubMed][PubMedCentral]

9. Navarro A, Gaya A, Martinez A et al (2008) MicroRNA expression profiling in classic Hodgkin lymphoma. Blood 111:2825–2832
[CrossRef][PubMed]

10. Leucci E, Onnis A, Cocco M et al (2010) B-cell differentiation in EBV-positive Burkitt lymphoma is impaired at posttranscriptional level by miRNA-altered expression. Int J Cancer 126:1316–1326
[PubMed]

11. Calin GA, Ferracin M, Cimmino A et al (2005) A MicroRNA signature associated with prognosis and progression in chronic lymphocytic leukemia. N Engl J Med 353:1793–1801
[CrossRef][PubMed]

12. Zhang G, Zong J, Lin S et al (2015) Circulating Epstein-Barr virus microRNAs miR-BART7 and miR-BART13 as biomarkers for nasopharyngeal carcinoma diagnosis and treatment. Int J Cancer 136:E301–E312
[CrossRef][PubMed]

13. Pfeffer S, Zavolan M, Grasser FA et al (2004) Identification of virus-encoded microRNAs. Science 304:734–736
[CrossRef][PubMed]

14. Grundhoff A, Sullivan CS, Ganem D (2006) A combined computational and microarray-based approach identifies novel microRNAs encoded by human gamma-herpesviruses. RNA 12:733–750
[CrossRef][PubMed][PubMedCentral]

15. Cai X, Schafer A, Lu S et al (2006) Epstein-Barr virus microRNAs are evolutionarily conserved and differentially expressed. PLoS Pathog 2:e23

[CrossRef][PubMed][PubMedCentral]

16. Chen SJ, Chen GH, Chen YH et al (2010) Characterization of Epstein-Barr virus miRNAome in nasopharyngeal carcinoma by deep sequencing. PLoS One 5:e12745
[CrossRef][PubMed][PubMedCentral]

17. Zhu JY, Pfuhl T, Motsch N et al (2009) Identification of novel Epstein-Barr virus microRNA genes from nasopharyngeal carcinomas. J Virol 83:3333–3341
[CrossRef][PubMed][PubMedCentral]

18. Bartel DP (2004) MicroRNAs: genomics, biogenesis, mechanism, and function. Cell 116:281–297
[CrossRef][PubMed]

19. Bartel DP (2009) MicroRNAs: target recognition and regulatory functions. Cell 136:215–233
[CrossRef][PubMed][PubMedCentral]

20. Ambros V (2004) The functions of animal microRNAs. Nature 431:350–355
[CrossRef][PubMed]

21. Skalsky RL, Corcoran DL, Gottwein E et al (2012) The viral and cellular microRNA targetome in lymphoblastoid cell lines. PLoS Pathog 8:e1002484
[CrossRef][PubMed][PubMedCentral]

22. Skalsky RL, Kang D, Linnstaedt SD et al (2014) Evolutionary conservation of primate lymphocryptovirus microRNA targets. J Virol 88:1617–1635
[CrossRef][PubMed][PubMedCentral]

23. Gottwein E, Corcoran DL, Mukherjee N et al (2011) Viral microRNA targetome of KSHV-infected primary effusion lymphoma cell lines. Cell Host Microbe 10:515–526
[CrossRef][PubMed][PubMedCentral]

24. Gottwein E, Cullen BR (2007) Protocols for expression and functional analysis of viral microRNAs. Methods Enzymol 427:229–243
[CrossRef][PubMed]

25. Dolken L, Malterer G, Erhard F et al (2010) Systematic analysis of viral and cellular microRNA targets in cells latently infected with human gamma-herpesviruses by RISC immunoprecipitation assay. Cell Host Microbe 7:324–334
[CrossRef][PubMed]

26. Riley KJ, Rabinowitz GS, Yario TA et al (2012) EBV and human microRNAs co-target oncogenic and apoptotic viral and human genes during latency. EMBO J 31:2207–2221
[CrossRef][PubMed][PubMedCentral]

27. Kang D, Skalsky RL, Cullen BR (2015) EBV BART MicroRNAs target multiple pro-apoptotic cellular genes to promote epithelial cell survival. PLoS Pathog 11:e1004979
[CrossRef][PubMed][PubMedCentral]

28. Hafner M, Landthaler M, Burger L, et al. (2010) PAR-CliP-a method to identify transcriptome-wide the binding sites of RNA binding proteins. *J Vis Exp* 41: pii: 2034

29. Flores O, Kennedy EM, Skalsky RL et al (2014) Differential RISC association of endogenous human microRNAs predicts their inhibitory potential. Nucleic Acids Res 42:4629–4639

[CrossRef][PubMed][PubMedCentral]

30. Hook LM, Landais I, Hancock MH et al (2014) Techniques for characterizing cytomegalovirus-encoded miRNAs. Methods Mol Biol 1119:239–265
[CrossRef][PubMed]

31. Keene JD, Komisarow JM, Friedersdorf MB (2006) RIP-Chip: the isolation and identification of mRNAs, microRNAs and protein components of ribonucleoprotein complexes from cell extracts. Nat Protoc 1:302–307
[CrossRef][PubMed]

32. Langmead B, Trapnell C, Pop M et al (2009) Ultrafast and memory-efficient alignment of short DNA sequences to the human genome. Genome Biol 10:R25
[CrossRef][PubMed][PubMedCentral]

33. Friedlander MR, Mackowiak SD, Li N et al (2012) miRDeep2 accurately identifies known and hundreds of novel microRNA genes in seven animal clades. Nucleic Acids Res 40:37–52
[CrossRef][PubMed]

34. Robinson MD, McCarthy DJ, Smyth GK (2010) edgeR: a Bioconductor package for differential expression analysis of digital gene expression data. Bioinformatics 26:139–140
[CrossRef][PubMed]

35. Anders S, McCarthy DJ, Chen Y et al (2013) Count-based differential expression analysis of RNA sequencing data using R and Bioconductor. Nat Protoc 8:1765–1786
[CrossRef][PubMed]

36. Manzano M, Forte E, Raja AN et al (2015) Divergent target recognition by coexpressed 5′-isomiRs of miR-142-3p and selective viral mimicry. RNA 21:1606–1620
[CrossRef][PubMed][PubMedCentral]

37. Manzano M, Shamulailatpam P, Raja AN et al (2013) Kaposi's sarcoma-associated herpesvirus encodes a mimic of cellular miR-23. J Virol 87:11821–11830
[CrossRef][PubMed][PubMedCentral]

38. Motsch N, Alles J, Imig J et al (2012) MicroRNA profiling of Epstein-Barr virus-associated NK/T-cell lymphomas by deep sequencing. PLoS One 7:e42193
[CrossRef][PubMed][PubMedCentral]

39. Feederle R, Haar J, Bernhardt K et al (2011) The members of an Epstein-Barr virus microRNA cluster cooperate to transform B lymphocytes. J Virol 85:9801–9810
[CrossRef][PubMed][PubMedCentral]

40. Feederle R, Linnstaedt SD, Bannert H et al (2011) A viral microRNA cluster strongly potentiates the transforming properties of a human herpesvirus. PLoS Pathog 7:e1001294
[CrossRef][PubMed][PubMedCentral]

10. Isolation and Characterization of Exosomes Released by EBV-Immortalized Cells

Gulfaraz Khan[1]✉ and Waqar Ahmed[1]

(1) Department of Microbiology and Immunology, College of Medicine and Health Sciences, United Arab Emirates University, Tawam Hospital Campus, 17666 Al Ain, United Arab Emirates

✉ **Gulfaraz Khan**
    Email: g_khan@uaeu.ac.ae

Abstract
Epstein-Barr virus is an oncogenic herpesvirus associated with several human malignancies. Although the details of the molecular steps involved in EBV-mediated cell transformation and immune evasion are not fully known, a number of viral products, including EBV latent proteins and non-protein coding RNAs have been shown to be involved, directly or indirectly in these processes. In recent years, a growing body of data indicates that some viruses are able to transport selected products to neighboring cells and induce biological changes by exploiting the exosome secretory pathway. Exosomes are nanovesicles secreted by virtually all cell types and present in most body fluids. Here, we describe the protocols used in our laboratory to isolate and characterize exosomes from EBV-infected, noninfected, and transfected cell lines.

Key words EBV – Exosomes – Differential ultracentrifugation – Electron microscopy – CD63 – Flotillin – RT-PCR – Western blotting

1 Introduction

Exosomes are nanosize membrane vesicles (50–150 nm in diameter) excreted by many different cells types, including B-cells, T-cells, dendritic cells, mast cells, epithelial

cells, and neurons [1, 2]. Exosomes are present in most body fluids, including blood, urine, saliva, and breast milk [3]. These nanovesicles are generated through inward budding of cytoplasmic endosomal-derived membranes of multi-vesicular bodies (MVBs) [4]. These MVBs can either be targeted for lysosomal degradation or transported to the plasma membrane and subsequently released as exosomes [4]. Morphologically, exosomes have been described as "cup or dish-like" structures after fixation, staining, and visualization by transmission electron microscopy . Whether these features are unique to exosomes or artifacts introduced by sample processing is unclear [5]. Initially, exosomes were thought to be artifacts or cell's waste products, but in recent years it has emerged that exosomes are in fact an important means of intercellular transport and communication [6, 7]. Exosomes have been shown to contain a number of membrane-associated proteins such as CD63 , endosome-associated proteins such as flotillin , heat shock proteins such as Hsp40 and endosomal sorting complex required for transport (ESCRT) such as Alix [5, 8]. Some of these proteins are believed to be involved in the transport of the exosomal cargo, which includes proteins, lipids, mRNAs, and microRNAs (miRNAs) [7, 8]. Moreover, a growing body of data indicates that some viruses can also hijack this physiological pathway for the excretion of their products [9]. What impact exosomes released from viral-infected cells have on recipient cells is poorly understood. Most likely, this will depend on the type of cell and exosomal cargo being excreted.

An important step in any study aimed at understanding exosomes and their biological role in the pathogenesis of viral infections is the isolation and characterization of exosomes. Because cells release many types of microvesicles [10], it is essential that exosomes are isolated and their identity confirmed before any down-stream investigations are performed [11]. In our laboratory we use differential ultracentrifugation to isolate exosomes from various cell lines, including EBV-infected, noninfected, and transfected cells. The identity of the isolated nanovesicles is checked by transmission electron microscopy and confirmed by western blotting for exosomal markers CD63 [12] and Flotillin [13]. In this chapter, the details of these protocols are described. In the next chapter (*Functional analysis of exosomes derived from EBV-infected cells*), we describe the methods we use for investigating the uptake and the physiological effect of EBV exosomes on recipient cells. Although our protocols are based on using EBV-infected cells, in principle the same protocols could be adopted for studying exosomes from other virus-infected cells.

2 Materials

2.1 Cell Culture and Exosome Isolation

1. CO_2 incubator set at 37 °C and 5 % CO_2.

2. Tissue culture media:

    (a) Media # 1: RPMI 1640 (without L-glutamine), supplemented with 2 mM L-glutamine, 10 % FBS, 10 µL/mL antibiotic antimycotic, 50 µg/mL gentamicin.

    (b) Media # 2: DMEM with L-glutamine, supplemented with 10 % FBS, 10 µL/mL antibiotic antimycotic, 50 µg/mL gentamicin.

3. Cells (*see* Table 1).

    Table 1 Type of cell lines used and their culture requirements

Name of cell line	Type of cell line	Culture requirements
B95.8	Marmoset B-cell (EBV+)	Media #1 (*see* Subheading 2.1)
EBV-LCL	Human EBV-immortalized B-cell (EBV+)	Media #1 (*see* Subheading 2.1)
Jurkat	Human T-cell (EBV-)	Media #1 (*see* Subheading 2.1)
Namalwa	Burkitt lymphoma-derived B-cell (EBV+)	Media #1 (*see* Subheading 2.1)
BL30	Burkitt lymphoma-derived B-cell (EBV-)	Media #1 with 1 mM sodium pyruvate, 10 mM α-TG and 20 µM BCA
BL30-B95.8	Burkitt lymphoma-derived B-cell (EBV+)	Media #1 with 1 mM sodium pyruvate,1 0 mM α-TG and 20 µM BCA
293 T	Human embryonic kidney epithelial cell (EBV-)	Media #2 (*see* Subheading 2.1)
293 T-Hebo	Human embryonic kidney epithelial cell (transfected with pHebo plasmid)	Media #2 with 150 µg/mL of hygromycin
293 T-ER1	Human embryonic kidney epithelial cell (transfected with EBER1- pHebo plasmid)	Media #2 with 150 µg/mL of hygromycin
293 T-ER2	Human embryonic kidney epithelial cell (transfected with EBER2-pHebo plasmid)	Media #2 with 150 µg/mL of hygromycin

4. Heat-inactivated fetal bovine serum (FBS).

5. Exosome depleted heat-inactivated fetal bovine serum (FBS) (*see* **Note 1**).

6. L-glutamine (200 mM).

7. Antibiotic antimycotic mix (10,000 U/mL penicillin, 12,500 µg/mL streptomycin, 25 µg/mL amphotericin B).

8. Gentamicin (50 mg/mL).

9. Sodium pyruvate (100 mM).

10. α-thioglycerol (α-TG) (50 mM), dissolved in PBS, filter-sterilized, aliquoted, and stored at −20 °C.

11. Bathocupronic disulfonic acid (BCA) (10 mM), dissolved in PBS, filter-sterilized, aliquoted, and stored at −20 °C.

12. Hygromycin (50 mg/mL).

13. Phosphate buffered saline (PBS), pH 7.4.

14. Trypsinization solution: 0.25 % Trypsin, 0.02 % EDTA in HBSS media.

15. 0.4 % Trypan blue.

16. Tissue culture flask T75.

17. Refrigerated ultracentrifuge.

18. 50 mL polypropylene falcon tubes.

19. Beckman polyallomer tubes or polycarbonate bottles, appropriate for the ultracentrifuge rotor.

2.2 Transmission Electron Microscopy

1. 2 % uranyl acetate.

2. 1× PBS.

3. Autoclaved water (ddH$_2$O).

4. 200 mesh formvar-carbon-coated copper grid.

5. Micropipette.

6. 5 mL syringes.

7. Philips CM10 transmission electron microscope (TEM) .

2.3 SDS-PAGE and Western Blot for Exosome Markers CD63 and Flotillin

1. Antibodies specific for exosome markers CD63 or flotillin. Suitable monoclonals for these markers are widely available. We have used clones MEM-259 for CD63 and EP446Y for flotillin.

2. Prestained molecular weight markers.

3. PVDF transfer membrane.

4. Tween 20.

5. PBST solution: In 1000 mL of PBS buffer add 1 mL of Tween 20.

6. 5 % blocking buffer: 2.5 g of fat free milk in 50 mL PBST.

7. RIPA buffer (*see* **Note 2**).

8. RLN buffer (*see* **Note 3**).

9. 6× loading buffer (*see* **Note 4**).

10. 10× SDS running buffer/electrophoresis buffer (*see* **Note 5**).

11. Transfer buffer (*see* **Note 6**)

12. 10 % SDS polyacrylamide gel (resolving gel) (*see* **Note 7**).

13. 4 % SDS polyacrylamide gel (stacking gel) (*see* **Note 8**).

14. ECL Plus kit.

15. Fluorescent imaging system (we use Typhoon).

2.4 RNA Isolation from Exosomes and RT-PCR for EBERs

1. TRIzol Reagent.

2. Exosomes.

3. Molecular biology grade chloroform, isopropanol, ethanol.

4. Refrigerated centrifuge.

5. Spectrophotometer, e.g., Nanodrop instrument.

6. Reverse transcription kit (Promega).

7. DNase 1.

8. Primers for EBER-1 and 2 (*see* Table 2).

Table 2 Sequence of EBER primers used for RT-PCR

Primer	Sequence (5' - 3')
EBER-1 forward primer	AGG ACC TAC GCT GCC C
EBER-1 reverse primer	AAA ACA TGC GGA CCA CCA GC
EBER-2 forward primer	AGG ACA GCC GTT GCC CTA GT
EBER-2 reverse primer	AAA AAT AGC GGA CAA GCC GAA T

9. PCR mastermix.

10. Taq polymerase.

11. PCR thermocycler.

3 Methods

3.1 Cell Culture and Exosome Isolation

1. Grow cells in the respective growth media (*see* Table 1) at 37 °C, 5 % CO_2 incubator. Change media two or three times a week by aspirating half of the old media and replacing it with an equal volume of fresh media to maintain the culture. Cells should be split as follows: 1:5 for B95.8, EBV-LCL, Namalwa and Jurkat; 1:3 for BL30 and BL30-B95.8; 1:10 for 293 T ; 1:5 for 293 T-Hebo, 293 T-ER1 and 293 T-ER2 (*see* **Note 9**).

2. For exosome isolation, 0.5×10^6 cells/mL should be grown in media containing exosome depleted FBS for 72 h.

3. Cell viability should be determined using trypan blue exclusion assay. Cell viability should be at least 95 % to continue to the next step (*see* **Note 10**).

4. Carefully remove the culture supernatant without disturbing the settled cells and centrifuge at 2000 × *g* for 20 min at 4 °C to remove cells and cellular debris (*see* **Note 11**).

5. Carefully remove the supernatant, leaving approximately 1–2 mL behind, and

transfer it to an ultracentrifuge tube and spin at 10,000 × g for 30 min at 4 °C. This will further remove the cellular debris.

6. Remove the supernatant and transfer it to a fresh ultracentrifuge tube and spin at 100,000 × g for 1 h at 4 °C.

7. Carefully remove the supernatant (leaving behind about 1 mL), and resuspend the exosome pellet in 1 mL of PBS. At this stage, exosome suspensions from all the tubes from the same cells can be pooled into a single ultracentrifuge tube.

8. Fill the tube with cold PBS and ultracentrifuge at 100,000 × g for 1 h at 4 °C.

9. Remove all the PBS as much as possible and resuspend the exosome pellet in 100 μL of PBS (if the total volume of the original culture supernatant was 80-100ml). Determine the total exosomal protein concentration using the Bradford Assay

10. Use immediately or store at −80 °C.

3.2 Transmission Electron Microscopy on Exosomes

1. Thaw the isolated exosomes and keep them on ice.

2. Add 10 μL of exosome suspension onto freshly glow discharged 200 mesh formvar-carbon-coated copper grid.

3. Let the grid absorb the suspension by incubating for 5 min at room temperature.

4. Wash the grids by adding a drop of ddH$_2$O using a syringe, let it stand for 1 min and absorb the drop using a filter paper.

5. Negatively stain the exosomes by adding a drop of 2 % uranyl acetate and incubate for 2 min at room temperature.

6. Absorb the extra uranyl acetate with filter paper.

7. Save the grid in a petri dish or use it immediately for examination under the electron microscope.

8. Under TEM, exosomes appear as membranous vesicles in the range of 50–150 nm with a "cup-shaped" morphology (Fig. 1a) [14].
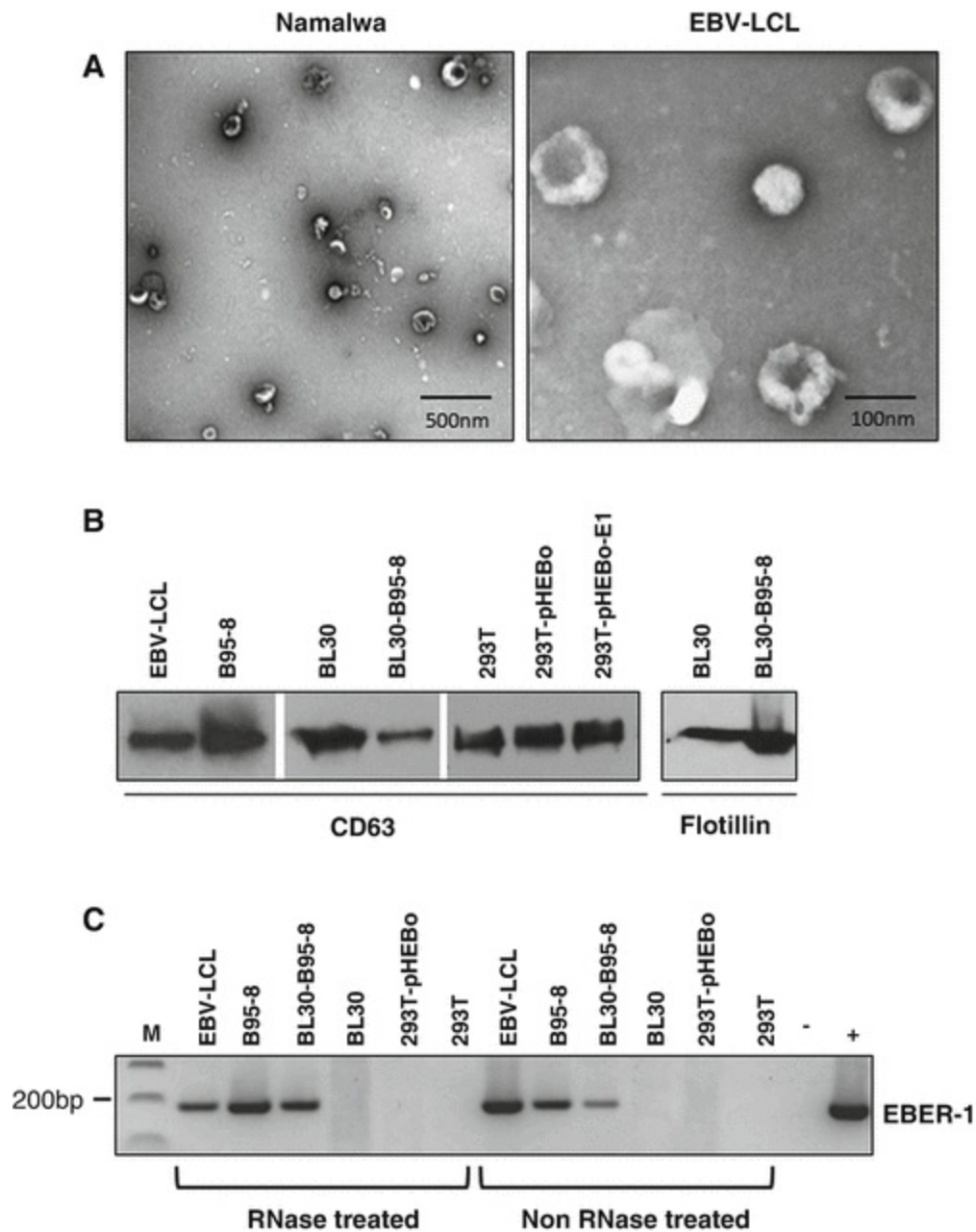
Fig. 1 Transmission electron microscopy of exosomes isolated by differential ultracentrifugation from two different EBV-positive cell lines. (**a**) Under TEM, exosomes appear as "cup-shaped" vesicles ranging from 50–150 nm. (**b**) The identity of isolated exosomes can be confirmed by Western blot for the exosomal markers, CD63 , and flotillin . (**c**) RT- PCR for EBER-1 showing presence of EBV RNA in exosomes. Pre-treatment of

exosomes with RNase prior to RNA extraction and RT-PCR, does not eliminate EBER amplification, indicating that EBERs are present within the exosomes and thus protected from RNase digestion (Figure adapted from ref. 14.)

3.3 SDS-PAGE and Western Blot for Exosomal Markers CD63 and Flotillin

1. For 100 μL of exosomes in PBS, add 40 μL of RLN buffer (*see* **Note 12**) and incubate the samples on ice for 10 min. Use 5 μL for the Bradford assay to determine exosomal protein concentration of each sample (*see* **Note 13**).

2. Depending on the exosomal protein volume, add 6 x loading dye (final dye concentration should be 1×).

3. Assemble the glass plates (1.5 mm) for western blotting (*see* **Note 14**).

4. Prepare the resolving gel (*see* **Note 7**).

5. Pour the gel solution between the glass plates with a pipette, leave about 1/4 of the space free for the stacking gel. Carefully cover the top of the resolving gel with isopropanol and wait until the resolving gel polymerizes (~30 min). A clear line will appear between the gel and the isopropanol when polymerization is complete.

6. Discard the isopropanol solution and wash gently with ddH$_2$O.

7. Prepare the stacking gel (*see* **Note 8**).

8. Pour the stacking gel on top of the resolving gel and insert the comb (*see* **Note 15**). Allow the gel to polymerize for at least 30 min.

9. Remove combs carefully and wash the wells twice with ddH$_2$O. Place the gel into the electrophoresis tank, fill the tank (bottom and top reservoirs) with fresh 1 x running buffer (*see* **Note 16**), making sure that the wells of the gel are covered with the buffer.

10. Load each sample (*see* **Note 17**) and prestained molecular weight markers.

11. Apply a current of 80 V for ~2 h.

12. Stop the electrophoresis, disassemble the gel apparatus, remove the gel carefully, and proceed with staining the gel or Western blot procedures.

13. Electrotransfer the SDS-PAGE resolved proteins from the gel to a PVDF membrane using wet/tank blotting system (*see* **Note 18**). Apply a current of 30 V for overnight at 4 °C.

14. Next day, incubate the PVDF membrane in 20 mL of blocking buffer (5 % nonfat milk in PBST) for 1 h at room temperature on a rocker with constant agitation.

15. Transfer the membrane to hybridization bags, add 5 mL of anti-CD63 and/or anti-flotillin monoclonal antibody diluted 1/500 and 1/1000 in 1 % milk PBST, respectively. Seal the bag and make sure there are no leaks.

16. Incubate for 1 h at room temperature on a rocker with constant agitation.

17. Remove the primary antibody and wash the PVDF membrane in PBST for 10 min (×3).

18. Repeat **steps 15**–**17** using HRP-labeled anti-mouse secondary antibody (diluted 1:20,000) for CD63 and HRP-labeled anti-rabbit secondary antibody (diluted 1:20,000) for flotillin.

19. Incubate the blot for 5 min in the appropriate HRP-substrate. We use fluoro-chemiluminescent detection reagents e.g., Pierce ECL Plus Substrate.

20. Visualize the blot using autoradiography or fluorescent image analyzer, e.g., Typhoon.

21. Bands at ~60 and ~48 kDa indicate the presence of CD63 and flotillin,

respectively. (Fig. 1b) (*see* **Note 19**) [14].

3.4 RNA Isolation from Exosomes and RT-PCR for EBERs

1. Add 500 µL of TRizol Reagent to 100 µL of isolated exosomes.

2. Add 100 µL of chloroform and shake the tubes vigorously for 15 s and then incubate the tubes at room temperature for 3 min.

3. Centrifuge at 12,000 × g at 4 °C for 15 min. Three layers will be visible after the centrifugation.

4. Transfer the aqueous phase to a new tube and add 500 µL of isopropanol to the aqueous phase and invert gently several times. Incubate at room temperature for 10 min.

5. Centrifuge at 12,000 × g at 4 °C for 10 min (*see* **Note 20**). A small white pellet will be visible at the bottom of the tube.

6. Discard the supernatant carefully and wash pellet by adding 1 mL of 75 % ethanol. Briefly vortex and then centrifuge at 7500 × g at 4 °C for 5 min.

7. Discard the ethanol and air dry the tubes for 15 min (*see* **Note 21**).

8. Resuspend the pellet in 20 µL of nuclease free water.

9. To eliminate any contaminating DNA, all RNA samples should be treated with DNase I. Appropriate PCR can be done to check for DNA contamination (*see* **Note 22**).

10. Reverse transcribe isolated RNA into cDNA using Reverse Transcription Kit (Promega), following the manufacturer's instructions.

11. Aliquot the cDNA and store at −80 °C until required.

12. Perform RT-PCR for EBERs using EBER1 and EBER2-specific primers (*see*

Table 2).

13. Set up each RT-PCR reaction as follows: 1 U of *Taq* polymerase, 0.5 mM dNTPs, 1× PCR reaction buffer, 2 mM MgCl$_2$ and 10 pmol of each primer and 1–2 μL of cDNA in 30 μL reactions.

14. Set the amplification conditions as follows: An initial 5 min denaturation step at 94 °C followed by 30 cycles of 94 °C for 1 min, 51 °C/46 °C (EBER-1/EBER-2 respectively) for 30 s and 72 °C for 60 s with a final elongation step at 72 °C for 7 min.

15. Separate the amplified products on a 2 % agarose gel stained with ethidium bromide. Bands at 166 bp and 172 bp indicate the presence of EBER-1 and EBER-2, respectively (Fig. 1c).

4 Notes

1. FBS is known to contain exosomes. To avoid contamination by these exosomes, cells should be grown in exosome depleted media. Exosome depleted FBS is commercially available, but it can also be prepared by centrifuging standard FBS at 100,000 × *g* at 4 °C for 6 h. This will pellet the exosomes, and supernatant can be carefully removed and stored at −20 °C until required.

2. RIPA buffer: 50 mM Tris, pH 7.4, 150 mM NaCl, 1 % Triton X-100, 1 % Sodium deoxycholate, 0.1 % SDS, made in ddH$_2$O and filter-sterilized. For 1 mL of RIPA buffer add 50 μL of β-Mercaptoethanol and 10 μL of 100 mM PMSF just before use.

3. RLN buffer: 50 mM Tris, pH 8.0, 140 mM NaCl, 1.5 mM MgCl$_2$, 0.5 % NP40, made in ddH$_2$O.

4. 6× loading buffer: 5.91 g of Trizma base, 6 g of SDS, 48 mL of glycerol, 9 mL of

β-merceptoethanol, 30 mg of bromophenol blue, volume made up to 100 mL in dH$_2$O.

5. 10× SDS running buffer: Dissolve 10 g SDS, 30.2 g Tris base and 144 g glycine in dH$_2$O and make up to 1000 mL.

6. 10× Transfer buffer (for 1500 mL): 45.4 g of Trizma base, 216 g of Glycine, 500 mL of dH$_2$O, mix and make up to 1500 mL with dH$_2$O. Make fresh 1× transfer buffer before using. 1× transfer buffer (for 1000 mL): 100 mL of 10× transfer buffer, 200 mL methanol, made up to 1000 mL with dH$_2$O.

7. Resolving gel: 8 mL of autoclaved dH$_2$O, 5 mL of 1.5 M Tris buffer, pH 8.8, 6.7 mL of 30 % acrylamide, 200 µL of 10 % SDS, 200 µL of 10 % APS, 20 µL of TEMED. This recipe is for casting two gels (7 mL for each gel). Add APS and TEMED at last to start the polymerization. For a native gel do not add 10 % SDS in the gel preparation.

8. Stacking gel: 6.1 mL of autoclaved dH$_2$O, 2.5 mL of 0.5 M Tris buffer, pH 6.8, 1.34 mL of 30 % acrylamide, 100 µL of 10 % SDS, 100 µL of 10 % APS, 20 µL of TEMED. Add APS and TEMED last to avoid polymerization.

9. For suspension cells (B95.8, EBV-LCL, Namalwa, Jurkat), aspirate the media without disturbing the cells settled at the bottom of the flask and add fresh media. For adherent cells (293 T, 293 T-Hebo, 293 T -ER1 and 293 T-ER2), aspirate the media, wash the cells with PBS and trypsinize for 1 min and neutralize by adding fresh media (double the volume of trypsin). 293 T cells are very sensitive and fragile. Care should be taken not to trypsinize them for longer time as this will harm the cells.

10. Cultures with cell viabilities of above 95 % should be used to avoid any cell debris contaminating the subsequent exosome fractions.

11. Pre-cool everything before use especially the centrifuge tubes as heating may affect exosomes preparation.

12. For nondenaturing SDS-PAGE, RLN buffer, but not RIPA buffer should be used. Protease inhibitor cocktail should be added to RLN and RIPA buffer to avoid protein degradation. For the Bradford assay, add the RLN buffer first and homogenize the exosomal proteins by pipetting and then use 5 µL of the exosome proteins for the assay. Add protease inhibitor cocktail after the Bradford assay, as this may affect the reading.

13. When performing western blot on exosomal extracts, it is important to load equal quantity of exosomes excreted from each cell type (e.g., infected and noninfected), if comparison is to be made. One method of estimating the amount of exosomes present in an isolate is by quantifying the total exosomal protein concentration. This can be done using the Bradford Assay.

14. Glass plates should be cleaned with ethanol before use.

15. It is important to use the comb of the same thickness as that of the glass slide. Using a comb of less thickness will result in the polymerization of the whole gel with no proper well formation. The maximum volume that can be loaded using a 1.5 mm comb is 45 µL per well.

16. Use the appropriate buffer depending on the type of gel. Running buffer and loading dye should be made without SDS for the native gel assay.

17. We usually load 25–35 µg of exosomal proteins per sample. For the denaturing gels, add 1× loading dye in the sample and heat at 100 °C in a water bath for 5 min before loading the samples on the gel. For native gels, add 1× loading dye in each sample and load directly onto the gel.

18. Pre-cool the 1× transfer buffer and add cold pack in the tank to keep the buffer cold throughout the transfer process.

19. The size of the bands will depend on the antibody clones used for the detection of CD63 and flotillin.

20. The RNA pellet is often not visible. Marking the outside of the ultracentrifuge tube prior to centrifugation can help in estimating the location of the pellet.

21. Air dry the tubes properly as droplets of ethanol can result in inhibition of downstream applications. You can leave the tubes for more than 15 min if the ethanol has not dried completely.

22. For RNA extracted from EBV exosomes, PCR for the EBV BamHI-W-fragment can be performed. Negative results indicate that there is no contaminating DNA present.

Acknowledgements

References

1. Kadiu I, Narayanasamy P, Dash PK, Zhang W, Gendelman HE (2012) Biochemical and biologic characterization of exosomes and microvesicles as facilitators of HIV-1 infection in macrophages. J Immunol 189:744–754
[CrossRef][PubMed][PubMedCentral]

2. Pant S, Hilton H, Burczynski ME (2012) The multifaceted exosome: biogenesis, role in normal and aberrant cellular function, and frontiers for pharmacological and biomarker opportunities. Biochem Pharmacol 83:1484–1494
[CrossRef][PubMed]

3. Inal JM, Kosgodage U, Azam S, Stratto ND, Antwi-Baffour S, Lange S (2013) Blood/plasma secretome and microvesicles. Biochim Biophys Acta 1834:2317–2325
[CrossRef][PubMed]

4. Colombo M, Raposo G, Théry C (2014) Biogenesis, secretion, and intercellular interactions of exosomes and other extracellular vesicles. Annu Rev Cell Dev Biol 30:255–289
[CrossRef][PubMed]

5. van der Pol E, Böing AN, Harrison P, Sturk A, Nieuwland R (2012) Classification, functions, and clinical relevance of extracellular vesicles. Pharmacol Rev 64:676–705
[CrossRef][PubMed]

6. Cocucci E, Racchetti G, Meldolesi J (2009) Shedding microvesicles: artefacts no more. Trends Cell Biol 19:43–51
[CrossRef][PubMed]

7. Villanueva MT (2014) Microenvironment: small containers, important cargo. Nat Rev Cancer 14:764
[CrossRef][PubMed]

8. Hurley JH, Odorizzi G (2012) Get on the exosome bus with ALIX. Nat Cell Biol 14:654–655
    [CrossRef][PubMed]

9. Meckes DG, Raab-Traub N (2011) Microvesicles and viral Infection. J Virol 85:12844–12854
    [CrossRef][PubMed][PubMedCentral]

10. Raposo G, Stoorvogel W (2013) Extracellular vesicles: exosomes, microvesicles, and friends. J Cell Biol 200:373–383
    [CrossRef][PubMed][PubMedCentral]

11. Witwer KW, Buzás EI, Bemis LT et al (2013) Standardization of sample collection, isolation and analysis methods in extracellular vesicle research. J Extracell Vesicles 2

12. Verweij FJ, van Eijndhoven MAJ, Hopmans ES et al (2011) LMP1 association with CD63 in endosomes and secretion via exosomes limits constitutive NF-kB activation. EMBO J 30:2115–2129
    [CrossRef][PubMed][PubMedCentral]

13. Okabayashi S, Kimura N (2010) LGI3 interacts with flotillin-1 to mediate APP trafficking and exosome formation. Neuroreport 21:606–610
    [CrossRef][PubMed]

14. Ahmed W, Philip PS, Tariq S, Khan G (2014) Epstein-Barr virus-encoded small RNAs (EBERs) are present in fractions related to exosomes released by EBV-transformed cells. PLoS One 9:e99163
    [CrossRef][PubMed][PubMedCentral]

11. Functional Analysis of Exosomes Derived from EBV-Infected Cells

Gulfaraz Khan[1]✉ and Pretty S. Philip[1]

(1) Department of Microbiology and Immunology, College of Medicine and Health Sciences, United Arab Emirates University, Tawam Hospital Campus, 17666 Al Ain, United Arab Emirates

✉ **Gulfaraz Khan**
   Email: g_khan@uaeu.ac.ae

Abstract
Exosomes are diverse bioactive extracellular nanovesicles excreted by different cell types. These tiny membrane-bound vesicles, once thought to be functionally insignificant, are now believed to be important vehicles for transport and intercellular communication. Exosomes have been shown to contain a broad range of molecules, from miRNAs to proteins to soluble factors. Moreover, an accumulating body of evidence indicates that some viruses can hijack the exosomal excretory pathway to influence the microenvironment surrounding the infected cells. In this chapter, we describe the protocols we use to examine the impact of exosomes isolated from EBV-infected cells on different cell types.

Key words EBV – Exosomes – Exosome uptake – Apoptosis – Caspase activation

1   Introduction

Epstein-Barr virus is a common herpesvirus infecting more than 90 % of individuals worldwide. Following primary infection, EBV establishes life-long persistence in resting memory B-lymphocytes, even in the face of a competent immune system. The virus has evolved multiple mechanisms by which it can evade the immune system and

persist in its host [1]. In recent years, studies have uncovered a potentially new strategy by which EBV could modulate the immune system for its survival, namely by hijacking the exosome excretory pathway. These nanovesicular bodies, initially considered to be garbage bags for abandoned membrane parcels and molecular fragments, are in fact important transport vehicles for a variety of molecules ranging from mRNA to miRNA, and from proteins to soluble factors [2]. Over 4500 proteins, 1600 mRNA, and 750 microRNAs (miRNAs) have been identified in exosomes derived from different cell types [3, 4]. Depending on their cargo, exosomes can induce various cellular changes in target cells, including antiviral activity and immune modulation [5, 6]. Several viruses, including EBV have also been shown to utilize the exosome pathway to excrete specific viral and cellular components. Moreover, the mechanism of exosome biogenesis has considerable overlap with the assembly and release of enveloped viruses such as EBV [7, 8]. Indeed, several studies now indicate that exosomes released from cells infected with some viruses, can induce local immune tolerance and contribute to virus-associated pathogenesis [9, 10]. For example, recently it was reported that exosomes isolated from nasopharyngeal carcinoma and from EBV-immortalized lymphoblastoid cell lines (LCLs) have anti-proliferative or apoptotic effects on recipient cells [11, 12]. In another study, it was shown that exosomes isolated from EBV LCLs contained Fas-ligand and MHC class II molecules and these exosomes could induce cell death of antigen specific T_H cells [13]. Taken together, there is now convincing evidence that EBV can manipulate its microenvironment by secreting exosomes loaded with bioactive cargo. However, the mechanisms involved in selecting the cargo to be packaged into EBV exosomes and the molecular details of the biological effects induced by these exosomes, remain to be elucidated. Here we describe the protocols we use in our laboratory for investigating proliferative/apoptotic effects of EBV exosomes released from various types of latently infected cells.

2 Materials

2.1 Fluorescent Labeling of EBV Exosomes

1. 50–100 μg of purified exosomes.

2. PKH 67 linker kit (Sigma) (*see* **Note 1**).

3. Beckman polyallomer tubes or polycarbonate bottles, appropriate for the ultracentrifuge rotor.

2.2 EBV Exosomes Uptake Assay

1. Coverslips to grow cells 22 × 22 mm.

2. 293 T cells, growing culture.

3. DMEM with 10 % FBS.

4. Trypsinization solution: 0.25 % trypsin, 0.02 % EDTA in HBSS media.

5. 70 % ethanol.

6. 6-well plates for tissue culture.

7. DAPI for nuclear staining.

2.3 Effect of EBV Exosomes on Recipient Cells

1. 293 T cells: Human embryonic kidney epithelial cell (EBV negative).

2. BL30 cells: Burkitt lymphoma derived B-cell (EBV negative).

3. CellTiter-Glo® Luminescent Cell Viability Assay (Promega).*

4. Caspase-Glo® 3/7 Assay (Promega).*

5. Caspase-Glo® 8 Assay (Promega).*

6. Caspase-Glo® 9 Assay (Promega).*

7. White 96 MicroWell Nunclon delta (flat bottom) microplates.

8. Exosome-depleted heat-inactivated FBS (*see* **Note 2**).

9. Tissue culture media:

   (a) For BL30 cells: RPMI 1640 (without L-glutamine), supplemented with 2 mM L-glutamine, 10 % FBS, 10 µL/mL antibiotic antimycotic, 50 µg/mL gentamicin.

   (b) For 293 T cells: DMEM with L-glutamine, supplemented with 10 % FBS, 10 µL/mL antibiotic antimycotic, 50 µg/mL gentamicin.

   *Prepare the reagent according to manufacturer's instructions.

3 Methods
3.1 Fluorescent Labeling of EBV Exosomes

1. Isolate EBV exosomes as described in the Chapter *Isolation and characterization of exosomes released by EBV-immortalized cells* and determine the total exosomal protein concentration using the Bradford Assay (*see* **Note 3**).

2. If using previously isolated exosomes stored at −80 °C, then thaw them on ice.

3. Dilute 100 µg of EBV exosomes in diluent C (1:1) provided with the labeling kit. This should be done inside the laminar flow hood (*see* **Note 4**).

4. Dilute PKH67 dye in diluent C (1:50) (*see* **Note 5**).

5. Add 20 µL of diluted PKH67 to the diluted exosomes from **step 3**. Mix by pipetting. For negative control, add 20 µL of diluted PKH67 to PBS (*see* **Note 6**).

6. Incubate at room temperature for 3 min in dark.

7. Add 0.1 % BSA or exosome-depleted FBS to terminate the reaction.

8. Centrifuge at 70,000 × *g* for 1 h at 4 °C in ultracentrifuge tubes.

9. Carefully remove the supernatant without disturbing the EBV exosome pellet.

10. Wash the pellet in PBS by centrifuging for 30 min at 70,000 × *g* at 4 °C.

11. Decant the buffer and resuspend the pellet in 100 µL PBS 1 µg/µL.

12. Use immediately or store at −80 °C.

3.2 EBV Exosomes Uptake Assay

1. Grow the recipient cells to be used for the EBV exosome uptake assay in their respective media. The protocol described here is for 293 T cells (*see* **Note 7**). For 293 T cells the passage number should not be more than 10.

2. Wash the 22 × 22 mm coverslips by dipping them in autoclaved ddH$_2$O several times (*see* **Note 8**). Then rinse them in 70 % ethanol (prepared in autoclaved water). Use petri dishes for these washing steps.

3. Keep the sterilized coverslips under UV for 30 min.

4. In the meantime, check the viability of 293 T cells using trypan blue exclusion assay (*see* **Note 9**). Cell viability should be at least 95 % to continue to the next step.

5. Place the sterile coverslips in 6 well tissue culture plates. Use a sterile forceps.

6. Plate 1 × 10^5 293 T cells in 150 µL of DMEM to the center of the sterile coverslip and incubate at 37 °C for 24 h in a 5 % CO$_2$ incubator (*see* **Note 10**).

7. Examine the cells under the microscope to confirm their presence and normal morphology (*see* **Note 11**).

8. Carefully wash the cells by aspirating the media and adding PBS drop by drop (*see* **Note 12**).

9. Dilute the labeled EBV exosomes in DMEM media containing exosome-depleted FBS (*see* **Note 2**) according to the experimental requirements. In our studies, we use 12.5 μg of labeled exosomes in 150 μL of media.

10. Add 150 μL (12.5 μg) of the labeled EBV exosomes to the 293 T cells on each coverslip and incubate for 24–30 h at 37 °C in a 5 % CO_2 incubator. Use PBS-PKH67 as a negative control for the exosome uptake assay.

11. Wash the recipient 293 T cells on the coverslip with PBS (×2) (*see* **Note 13**).

12. Fix with cold acetone for 30 min at 4 °C or 4 % paraformaldehyde for 30 min at room temperature.

13. Wash 3–4 times with PBS.

14. Counter stain the cells with DAPI (*see* **Note 14**). Add 100 μL of 5 μg/mL of DAPI to the cells on the coverslip and incubate for 5 min in dark.

15. Wash with PBS (×5).

16. Mount the cells using fluorescence mounting medium (*see* **Note 15**).

17. Examine under fluorescent microscope (Fig. 1).
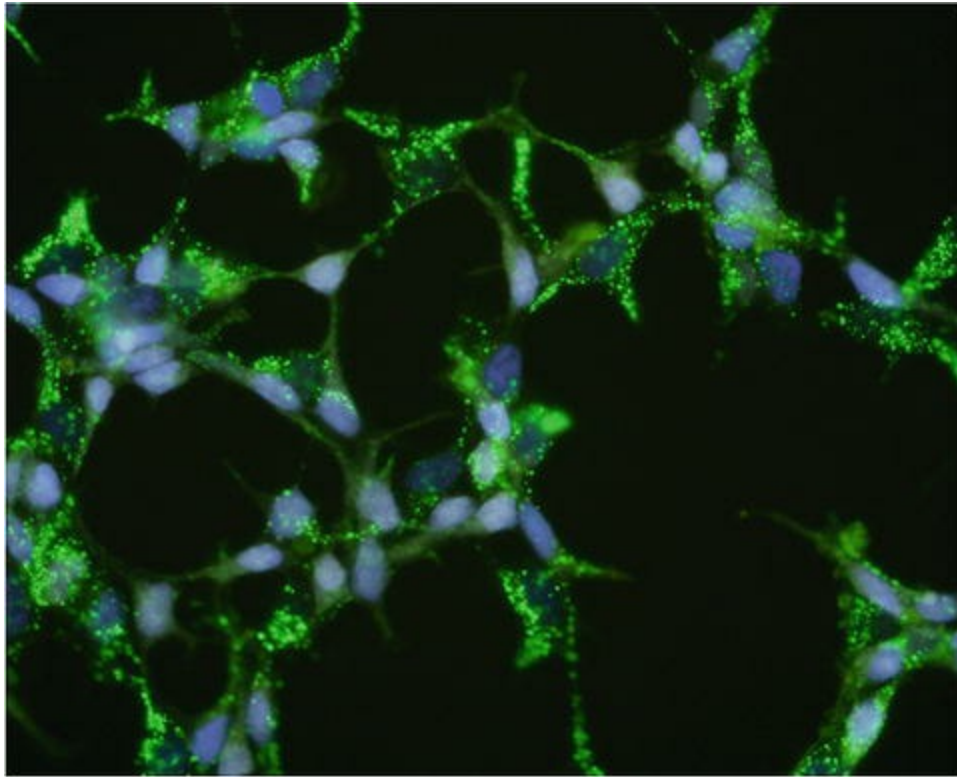
Fig. 1 Strong punctate fluorescent green signals are clearly evident in the cytoplasm of 293 T cells exposed to PKH67 labeled EBV exosomes from EBV-LCL. DAP1 (blue) was used as a nuclear counter stain. (Original magnification 40×)

3.3 Effect of EBV Exosomes on Recipient Cells

Exosomes are nanovesicles which are released from all cell types under normal and pathological conditions. It is now well accepted that these membrane-bound vesicles can be taken up by neighboring cells and induce physiological changes in the recipient cells [6]. The effect will depend on the type of cargo present in the exosomes and the type of cells receiving these exosomes. The following protocol can be used to examine the effect of exosomes on cell proliferation, apoptosis , and caspase activation . This protocol takes 3–4 days to complete, depending on the cell type being used (adherent or suspension cultures) and the length of exposure to exosomes. The protocol described here is for 293 T cells (adherent cells) and BL30 cells (suspension cells).

1. Grow the recipient cells to be tested (293 T and/or BL30) in their respective growth media (*see* **Note 16**).

2. Determine the cell viability of 293 T and BL30 cells using trypan blue exclusion assay. Since 293 T cells are adherent cells, they require gentle trypsinization to

remove them from the culture flask (*see* **Note 9**).

3. For 293 T, plate 2500 cells/100 µL/well in white 96 microwell plate (in duplicates or triplicates) and incubate them overnight to allow them to "settle" before exposing them to EBV exosomes. BL30 cells can be exposed to EBV exosomes without the need to "settle."

4. Next day, remove the media from 293 T cells and add 100 µL of exosome-depleted media (*see* **Note 2**). For BL30, plate 5000 cells/100 µL/well in exosome-depleted media.

5. Add the appropriate amount of exosomes depending on the experiment. We regularly used 12.5 µg of exosomes for the apoptosis assay (*see* **Note 3**). For negative controls, PBS is added instead of exosomes (*see* **Note 17**).

6. Incubate the cells at 37 °C in 5 % CO_2 for 48 h (*see* **Note 18**).

7. To check cell proliferation/cell viability, commercially available kits can be used. We use CellTiter-Glo® Luminescent Cell Viability Assay (Promega) (*see* **Note 19**). Thaw the reagents from the kit at room temperature.

8. To determine cell viability, add 100 µL of the cell viability reagent (CellTiter-Glo® Reagent) and incubate for 10 min on a rocking platform in dark (*see* **Note 20**).

9. Read the plates in the plate reader or the luminometer (*see* **Note 21**) (e.g., Perkin Elmer, 2030 multi-label reader, Victor Tm X3) with the luminescence settings.

10. For determining caspase activity, after incubation with exosomes (**step 6**), add 100 µL of the Caspase-Glo® Reagent from the appropriate kit (*see* **Note 22**).

11. Incubate the plate for 3 h on the rocker in dark and read the plate in the plate reader or the luminometer.

12. The mean readings of the replicates should be analyzed relative to the mean readings of the negative controls (without exposure to exosomes). Data can be represented in the form of a bar chart.

---

4 Notes

1. PKH67 has a long aliphatic tail, resulting in more stable labeling and less cell-to-cell transfer. It is estimated to have an in vivo half-life of 10–12 days.

2. FBS is known to contain exosomes. Thus, only exosome-depleted serum should be used. Exosome-depleted FBS is commercially available, but it can also be prepared in the lab by centrifuging standard FBS at 100,000 × *g* for 6 h at 4 °C (see the chapter *Isolation and characterization of exosomes released by EBV-immortalized cells*).

3. The quantity of exosomes isolated from culture supernatants will vary depending on the cell type and the isolation procedure. Moreover, the concentration will vary from batch to batch and this can have a significant impact on downstream functional assays. One way to standardize this is to measure the total exosomal protein concentration using the Bradford Assay.

4. Since the labeled exosomes are going to be used for tissue culture purpose, it is recommended to maintain the sterility by performing the procedures inside a laminar flow safety cabinet.

5. PKH67 staining and the subsequent steps should be done in the dark.

6. Including a negative control, i.e., equivalent volume of PBS instead of exosomes, is important as it can help to differentiate between any nonspecific background staining and genuine signals.

7. 293 T cells are cultured in DMEM with L-glutamine, supplemented with 10 % FBS, 10 μL/mL antibiotic antimycotic, 50 μg/mL gentamicin.

8. Use sterile petri dishes inside the hood.

9. 293 T cells are adherent cells and require gentle trypsinization for 1 min followed by neutralization using fresh DMEM media (double the volume of trypsinization solution). 293 T cells are very sensitive and fragile. Care should be taken not to trypsinize them for longer time as this will damage the cells.

10. Make sure to add the cells at the center of the coverslips and do not tilt once they are added.

11. Do this with as little movement as possible to avoid disturbing the cells. If a digital camera is used, then an image of the cells can be taken for future reference.

12. Tilt the plate slightly and aspirate the media from the coverslips using a p200 pipette. While washing, ensure not to disturb the 293 T cells in the center. Also make sure the cells look healthy and at least 80–90 % have normal morphology.

13. PKH67 is a membrane dye, and it will label all membranes. Hence, failure in washing it away, will results in significant background signal.

14. DAPI stock solution is 5 mg/mL in ddH2O. DAPI readily dissolves in water, but does not dissolve directly in PBS, even with heat and sonication. For long-term storage, the solution can be aliquoted and stored at -20 °C. Working solution is diluted 1:1000 in PBS, giving a final DAPI concentration of 5 μg/mL.

15. The fluorescence is stable for 2 days at 4 °C. Wrap the slides in aluminum foil and keep them refrigerated.

16. BL30 cells are cultured in RPMI 1640 (without L-glutamine), supplemented with 2 mM L-glutamine, 10 % FBS, 10 μL/mL antimycotic, 50 μg/mL gentamicin, 1 mM sodium pyruvate, 10 mM α-thioglycerol and 20 μM bathocupronic disulfonic acid. For 293 T cells, *see* **Note 7** above.

17. Including negative controls, i.e., cells not exposed to exosomes is essential. In our exosome isolation protocol (see previous chapter), we resuspend our final exosome pellets in PBS, hence we use PBS for a negative control. The volume of PBS used for negative controls should be equivalent to the volumes of exosome used.

18. Recipient cells can be exposed to EBV exosomes for shorter or longer time, but in our hands, we have found that 48 h exposure is most optimal for measuring maximum apoptotic effects of exosomes.

19. The CellTiter-Glo® Luminescent Cell Viability Assay measures the viability of cells in culture based on quantitation of the ATP present, an indicator of metabolically active cells. It is a very simple assay involving the addition of a single reagent (CellTiter-Glo® Reagent) directly to cells.

20. It is important to do the experiment in the dark. Exposure to light can affect the luminescence and can give incorrect readings.

21. Although we take our readings soon after the end of the 10 min incubation period, the luminescent signal is fairly stable for several hours and a slight delay in taking the readings will not affect the results.

22. Promega Caspase-Glo Assays are available for measuring the activity of several different caspases, e.g., 3/7, 8, and 9. Although we describe the assay using 100 µL of Caspase-Glo® Reagent to 100 µL of sample, this can be adapted to smaller volumes (e.g., 50 µL), provided the 1:1 ratio of Caspase-Glo® Reagent to sample volume is maintained.

Acknowledgements

References

1. Ressing ME, van Gent M, Gram AM, Hooykaas MJG, Piersma SJ, Wiertz EJHJ (2015) Immune evasion by Epstein-Barr virus. Curr Top Microbiol Immunol 391:355–381
[PubMed]

2. Villanueva MT (2014) Microenvironment: small containers, important cargo. Nat Rev Cancer 14:764
[CrossRef][PubMed]

3. Valadi H, Ekström K, Bossios A, Sjöstrand M, Lee JJ, Lötvall JO (2007) Exosome-mediated transfer of mRNAs and microRNAs is a novel mechanism of genetic exchange between cells. Nat Cell Biol 9:654–659
[CrossRef][PubMed]

4. Zhao L, Liu W, Xiao J, Cao B (2015) The role of exosomes and "exosomal shuttle microRNA" in tumorigenesis and drug resistance. Cancer Lett 356:339–346
[CrossRef][PubMed]

5. van der Pol E, Böing AN, Harrison P, Sturk A, Nieuwland R (2012) Classification, functions, and clinical relevance of extracellular vesicles. Pharmacol Rev 64:676–705
[CrossRef][PubMed]

6. Li J, Liu K, Liu Y et al (2013) Exosomes mediate the cell-to-cell transmission of IFN-α-induced antiviral activity. Nat Immunol 14:793–803
[CrossRef][PubMed]

7. Mori Y, Koike M, Moriishi E et al (2008) Human herpesvirus-6 induces MVB formation, and virus egress occurs by an exosomal release pathway. Traffic 9:1728–1742
[CrossRef][PubMed][PubMedCentral]

8. Jolly C, Sattentau QJ (2007) Human immunodeficiency virus type 1 assembly, budding, and cell-cell spread in T cells take place in tetraspanin-enriched plasma membrane domains. J Virol 81:7873–7884
[CrossRef][PubMed][PubMedCentral]

9. Izquierdo-Useros N, Naranjo-Gomez M, Erkizia I et al (2010) HIV and mature dendritic cells: trojan exosomes riding the trojan horse? PLoS Pathog 6:e1000740
[CrossRef][PubMed][PubMedCentral]

10. Benito-Martin A, Di Giannatale A, Ceder S, Peinado H (2015) The new deal: a potential role for secreted vesicles in innate immunity and tumor progression. Front Immunol 6:66
[CrossRef][PubMed][PubMedCentral]

11. Keryer-Bibens C, Pioche-Durieu C, Villemant C et al (2006) Exosomes released by EBV-infected nasopharyngeal carcinoma cells convey the viral Latent Membrane Protein 1 and the immunomodulatory protein galectin 9. BMC Cancer 6:283
[CrossRef][PubMed][PubMedCentral]

12. Mrizak D, Martin N, Barjon C et al (2015) Effect of nasopharyngeal carcinoma-derived exosomes on human regulatory T cells. J Natl Cancer Inst 107:363–376
[CrossRef][PubMed]

13. Klinker MW, Lizzio V, Reed TJ, Fox DA, Lundy SK (2014) Human B cell-derived lymphoblastoid cell lines constitutively produce Fas ligand and secrete MHCII + FasL+ killer exosomes. Front Immunol 5:1–10
[CrossRef]

12. Terminal Repeat Analysis of EBV Genomes

Ferenc Bánáti[1] ✉, Anita Koroknai[2] and Kálmán Szenthe[1]

(1) RT-Europe Nonprofit Research Ltd., Vár 2, Szigetköz building, H-9200 Mosonmagyaróvár, Hungary
(2) Department of Retroviruses, National Center for Epidemiology, Microbiological Research Group, Albert Florian Str. 2-6, H-1097 Budapest, Hungary

✉ **Ferenc Bánáti**
   Email: fbanati@yahoo.co.uk

Abstract
Epstein-Barr virus (EBV) was the first human virus associated directly with human malignancies. During EBV infection of various host cells the double-stranded linear EBV DNA carried by the virions undergoes circularization. Since there are variable numbers of terminal repetitions (TRs) at the ends of the linear EBV genome, the resulting circular episomes enclose a variable number of TRs. Thus, in cells carrying viral episomes, the sizes of the terminal restriction enzyme fragments of EBV is affected by the number of TRs (Raab-Traub and Flynn Cell 47:883-889, 1986). Southern blot analysis revealed that in monoclonal proliferations, arising from a single cell, there was only a single band representing the joined EBV termini, whereas multiple terminal restriction enzyme fragments that differ in size were characteristic for oligoclonal or polyclonal proliferations. Using suitable probes, one can distinguish the episomal form from the linear EBV genomes that are formed during lytic EBV replication or during integration into the host genome. TR analysis is a useful tool for the determination of EBV clonality in different clinical samples and in cell lines carrying EBV genomes. A single terminal restriction enzyme fragment may indicate EBV infection at an early phase of clonal cell proliferation, whereas polyclonal EBV genomes may derive from multiple infections of proliferating cells.

1 Introduction

TR analysis, i.e., the study of EBV clonality in EBV-associated neoplasms may reveal the order of distinct pathogenic events such as viral infection and cell proliferation. In case of benign or malignant cell proliferations, a monoclonal EBV genome may indicate a causative relationship between viral infection and tumorigenesis. In contrast, polyclonal EBV genomes may indicate that the infection occurred after the massive cell division suggesting that the tumor initiation anticipated EBV infection.

The unique features of productive, lytic EBV replication and the circularization of the viral genome in newly infected cells permits the analysis of EBV clonality by the molecular biological analysis of the length of the terminal restriction enzyme fragment that carries variable numbers of direct tandem terminal repeats (TRs) [1–3] (also *see* Fig. 1). This approach is based on conventional genomic DNA digestion using restriction endonucleases followed by the determination of the size of the DNA fragment that harbors the terminal repeat, using agarose gel-based separation and Southern blotting [4]. Most studies applied radioactively labeled hybridization probes. Here we describe a non-isotopic method for TR analysis.
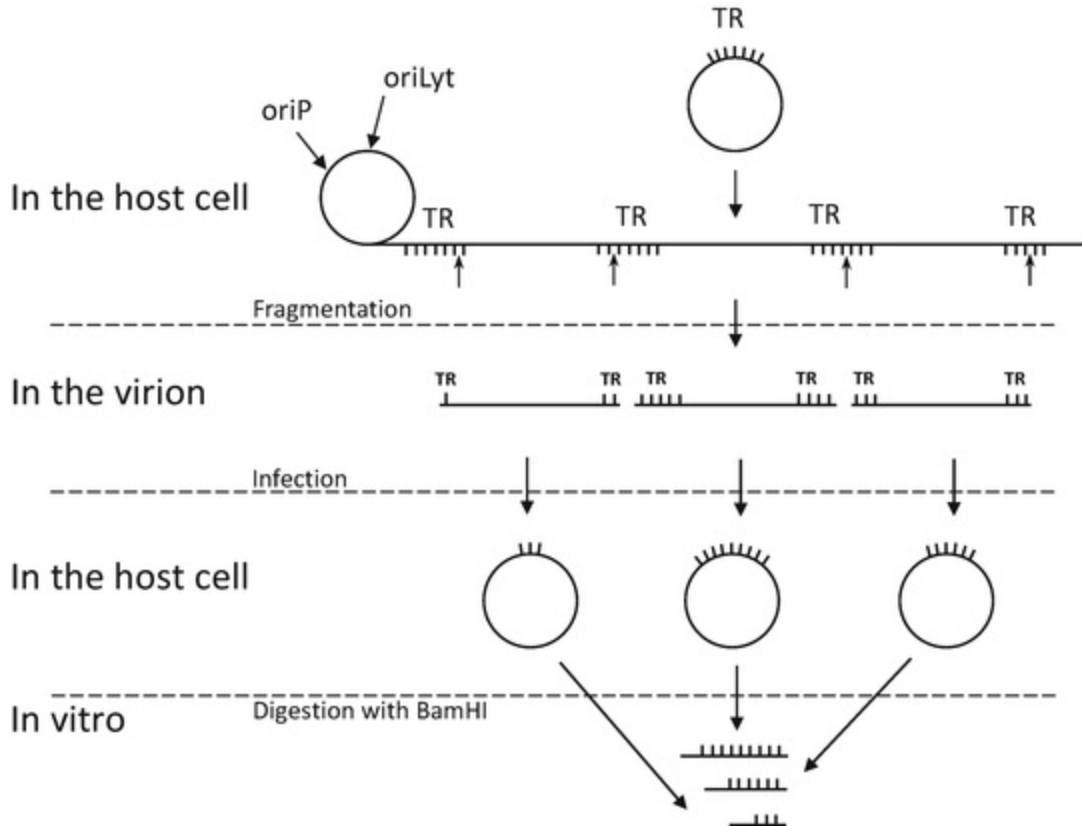
Fig. 1 EBV life cycle and TR fragment length analysis. Within the host cell during lytic replication EBV forms a

concatemeric repeat of its genome. Before encapsidating into the virion the concatemers are fragmented between two terminal repeat (TR) units according to an unclarified mechanism resulting in different numbers of TR units at both ends. After virions having different TR sizes, due to a variable number of repeating units, infect cells, the clonality can be determined by methods like terminal repeat analysis, "measuring" the length of the complete terminal repeat region

The length of a single TR of the EBV genome is 538 bp. This fragment contains all the sequences required for the cleavage of the concatemers generated during lytic replication and encapsidation of the linear double-stranded genomes during the build-up of the virions. Accordingly, it was demonstrated that a TR-negative mutant-EBV produced predominantly empty virions, without DNA, in spite of the fact that rare infectious viruses carrying TR-negative EBV genomes were also observed. These data suggested that virion formation and egress may occur even in the absence of viral DNA packaging [5]. The number of TRs generated during concatemeric amplification and—accordingly—the length of the terminal restriction enzyme fragment representing the joint EBV termini in the circular episomes formed in newly infected cells is highly variable. The exact mechanism behind this phenomenon is not clearly understood, although an enzymatic and an immunoglobulin gene rearrangement-like scheme have already been suggested [2, 6]. The length of the detected terminal restriction enzyme fragment is proportional to the number of TRs enclosed into the episome. Besides, viral integration can also be detected using terminal repeat analysis [7, 8].

Viral episomes carried by EBV positive cell lines cultivated in vitro and EBV positive tumors growing in vivo can be characterized by the number of their TRs and the sizes of their terminal restriction fragments. The TR repeat number (the length of the terminal fragment) inversely correlated with LMP2A mRNA amount and directly with cell doubling time, pointing at a selection mechanism favoring a shorter TR region containing less repeats with higher LMP2A expression and LMP2A -driven carcinogenesis. Usually 4–20 repeat units can be observed [3].

The clinical importance of the clonality of EBV carrying cell populations is evidenced in a series of key publications [9–19]. These studies are fundamental in the determination of how the proliferations emerge and develop from a single host cell or due to multiple, independent events involving EBV infection.

2 Materials
2.1 Digestion and Purification of Genomic DNA

1. 200U *Bam*HI restriction endonuclease per sample (100,000 U/mL) (*see* **Note 1**).

2. Appropriate 10× restriction digest buffer.

3. 10 µg sample DNA.

4. DNA isolation kit or solutions.

2.2 Labeling of DNA Probe for the Detection of EBV Terminal Repeat

1. PCR enzyme or Klenow fragment.

2. DIG DNA Labeling Mix (1 mM dATP, 1 mM dCTP, 1 mM dGTP, 0.65 mM dTTP, 0.35 mM DIG-dUTP) (*see* **Note 2**).

3. Template/sample DNA.

4.
Primers:	Forward primer:	GTATGCCTGCCTGTAATTGTTG
	Reverse primer:	ACGAAAGCCAGTAGCAGCAG

   10 µM each. These primers amplify the region between nts 68-723 of the EBV genome (GenBank NC_007605.1).

5. Agarose, molecular biology grade, for gel electrophoresis.

6. 10× TBE buffer: 89 mM Tris-borate, 2 mM EDTA, pH 8.3.

7. DNA molecular weight marker for PCR products.

8. DNA gel stain, e.g., ethidium bromide or equivalent.

9. PCR product purification kit.

2.3 Southern Blot

1. Agarose for molecular biology, for gel electrophoresis.

2. 10× TBE buffer: 89 mM Tris-borate, 2 mM EDTA, pH 8.3).

3. DNA Molecular Weight Marker III, DIG-labeled: The mixture contains 13 fragments with the following base pair lengths: 125, 564, 831, 947, 1,375, 1,584, 1,904, 2,027, 3,530, 4,268, 4,973, 5,148, and 21,226 bp.

4. DNA gel stain, e.g., ethidium bromide or equivalent.

5. Hybond N membrane or equivalent (*see* **Note 3**).

6. Whatman paper.

7. Depurination solution: HCl, 250 mM.

8. Denaturation solution: 1.5 M NaCl, 0.5 M NaOH.

9. Neutralization solution: 1.5 M NaCl, 0.5 M Tris–HCl, pH 7.5.

10. Transfer buffer, 20× SSPE: 3 M NaCl, 0.2 M NaH_2PO_4, 20 mM EDTA, pH 7.4 (*see* **Note 4**).

11. Pre-hybridization solution: 50 % deionized formamide, 5× SSC (20× SSC: 3 M NaCl, 0.3 M Na-citrate, pH 7.0), 0.1 % N-lauroylsarcosine, 0.02 % SDS, 2 % Skim Milk Powder.

12. Hybridization solution: Pre-hybridization solution + labeled probe, 100 ng.

13. Low stringency buffer: 2× SSC, 0.1 % SDS.

14. High stringency buffer: 0.1 × SSC, 0.1 % SDS.

15. Maleate buffer: 150 mM NaCl, 100 mM maleate, pH 7.5.

16. Blocking reagent for nucleic acid hybridization and detection, Roche.

17. 10 µL Anti-Digoxigenin-AP, Fab fragments, per 100 cm^2 membrane, Roche.

18. Washing buffer: Maleate Buffer, 0.3 % Tween-20.

19. Detection buffer: 0.1 M NaCl, 0.1 M Tris–HC l pH 9.5.

20. X-ray film, developer and fixer solution.

3 Methods

3.1 Digestion and Purification of Genomic DNA

Digest 10 µg sample DNA with *Bam*HI restriction enzyme as follows:

1. Mix together 33 µL dH$_2$O, 5 µL 10× restriction digest buffer, 2 µL *Bam*HI restriction endonuclease (100,000 U/mL) and 10 µL sample DNA (1 µg/µL).

2. Incubate at 37 °C for at least 1 h.

Isolate digested DNA with classical or silica-based methods and elute DNA in small volume (<20 µL) of TE buffer: 1 mM EDTA, 10 mM Tris, pH 8.0.

*Bam*HI cuts EBV genomic DNA more than 40 times. The fragment that contains the terminal repeats is cut at positions 166,156/166,160 and 3955/3959 resulting in a 9693 bp product (EBV reference genome GenBank NC_007605.1). Within this reference DNA sequence four terminal repeat units can be observed.

3.2 Labeling of the Probe for EBV TR Detection

Mix together the following components: 5 µL DIG DNA Labeling, 1 µL of each oligo (10 µM each); 5 µL 10× PCR reaction buffer without MgCl$_2$; 5 µL MgCl$_2$ (25 mM); 2.5U polymerase and 1 µL genomic DNA of the cell line of interest in 50 µL total volume.

The PCR conditions are summarized in Table 1.

Table 1 Thermal profile of amplification-based probe labeling of an EBV sequence

Process	Temperature (°C)	Time (min)	Cycles
Denaturation and Enzyme activation	95	3.5	1×

Denaturation	95	0.5	40×
Annealing	60	0.5	
Elongation	72	1	
Final extension	72	3	1×
Cooling	4	Infinite	1×

The effectiveness of labeling is to be determined using agarose gel electrophoresis with 1 % agarose gel and 1× TBE or equivalent. The incorporated digoxigenin results in a size shift, thus unlabeled product has to be included in the run to see the efficiency of the labeling reaction. A typical photo showing the size difference between labeled and unlabeled products is shown in Fig. **2** .
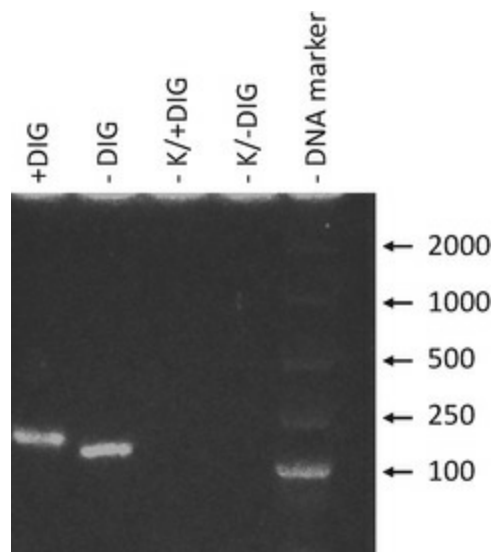
Fig. 2 A representative result of PCR-based DIG-labeling. +DIG: PCR mix contained Digoxigenin-conjugated dUTP, −DIG: PCR mix without Digoxigenin-conjugated dUTP, −K/+DIG and − DIG are the negative controls of + DIG and − DIG samples. DNA marker band sizes from above are as follows: 2000, 1000, 500, 250, 100 bps. A shift in product size due to digoxigenin incorporation can be observed upon successfull labeling

In the case of the above-mentioned EBV probe the size is expected to be 656 bp. After successful labeling the product has to be purified with a PCR clean-up kit or similar procedures.

3.3 Southern Blot

1. Run the prepared genomic DNA (see Subheading 3.1) and the Dig-labeled DNA marker side-by-side in a 0.8 % agarose gel using 1× TBE for 15 min at 50 V (2.5 V/cm) and 135 min at 100 V (5 V/cm).

2. Submerge agarose in depurination solution for 10 min and shake gently.

3. Soak gel in denaturation solution twice for 20 min to denature separated dsDNA to single stranded.

4. Wash gel two times for 20 min in neutralization solution with gentle shaking.

5. Change buffer to 20× SSPE and let the gel soak for 10 min to get it ready for DNA transfer.

6. For capillary transfer assembly, *see* Fig. **3** .
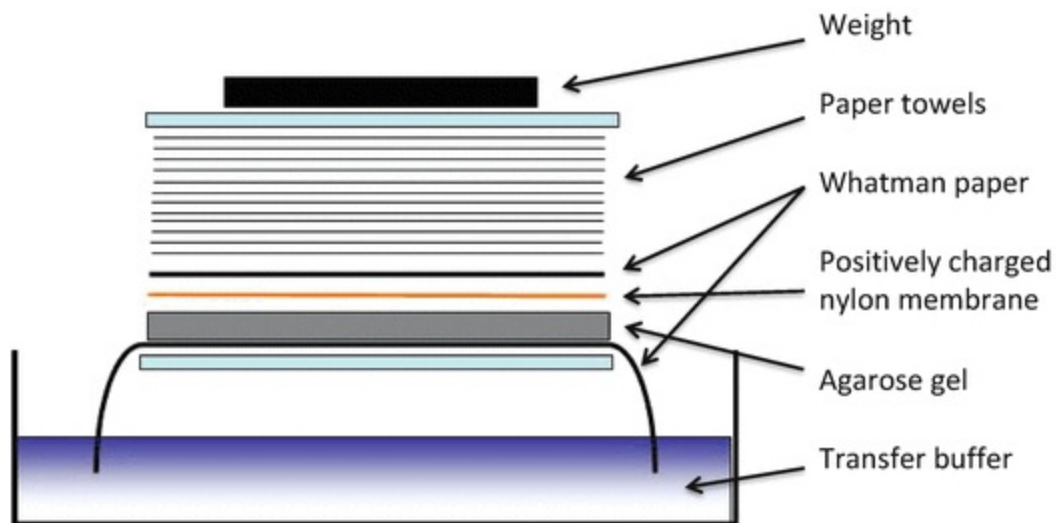
Fig. 3 Capillary transfer of DNA, Southern blot assembly. Whatman paper is soaked and submerged into the transfer buffer. On the top of the paper the agarose is placed just below the nylon membrane. To apply capillary effect, a Whatman paper and a pile of paper towels is gently pressed on the top with the help of a glass plate and some weight

7. After overnight blotting the membrane-DNA binding is stabilized with 4 min UV light exposure (*see* **Notes 4** and **5**).

8. Thereafter, the membrane is pre-hybridized in 10 mL Standard buffer at 42 °C.

9. Discard buffer and add 5 mL Standard buffer supplemented with denatured (95 °C,

3 min) DIG-labeled probe and incubate at 42 °C overnight.

10. Wash membrane in low stringency buffer 2× for 15 min at room temperature (RT) with continuous shaking.

11. Wash membrane in high stringency buffer 2× for 15 min at 65 °C with continuous shaking.

12. Incubate membrane in maleate buffer with 1 % blocking reagent (Roche) for 1 h.

13. Soak membrane for 30 min in 50 mL 1 % blocking reagent (same as before) supplemented with anti-digoxigenin-AP in 1:5000 dilution (10 μL) (*see* **Note 6**).

14. Antibody surplus is discarded with washing the blot in washing buffer for 15 min, 2× at RT.

15. Put membrane into detection buffer for 5 min.

16. Cover the surface of the membrane with a 1000 μL (in the case of 100 cm^2 membrane) 1:200 diluted CDP-Star (the substrate of alkaline phosphatase conjugated to Anti-DIG antibody) in detection buffer for 5 min (*see* **Note 6**).

17. Detect signal using X-ray film or equivalent method or instrument.

A typical result is shown in Fig. **4** . The lengths of specific products presented in the figure are between ca 10 and 25 Kbp with obvious differences among cell lines. In all EBV-carrying cell lines only one band could be visualized except the B95-8 cell line with spontaneous lytic activation.
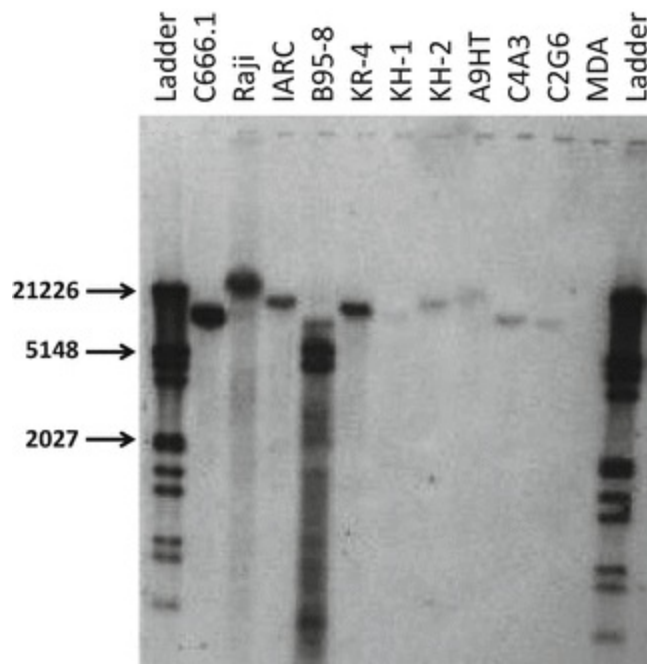
Fig. 4 Southern blot result of a terminal repeat analysis experiment. Cell lines used in the presented experiment are as follows: EBV carrying cell lines: C666.1 , C2G6, C4A3—epithelial cell lines; Raji —endemic Burkitt's lymphoma; IARC, KR-4-Lymphoblastoid cell lines immortalized by in vitro EBV infection; B95-8 marmoset cell line; KH-1, KH-2, A9HT hybrid cell lines; EBV negative control cell line: MDA—breast carcinoma cell line

4 Notes

1. Depending on the aim of the study different restriction endonucleases can be used.

2. There are many ways of DNA fragment labeling, e.g., one can supplement a PCR mix with digoxigenin-dUTP or with labeled oligos before the PCR reaction, or different end-labeling approaches can also be used, like ligation.

3. Instead of nylon membranes, nitrocellulose is also suitable, although DNA has to be stabilized with baking. Nylon membranes bind DNA much stronger and can be cross-linked covalently with UV light. Nitrocellulose is more fragile and cannot be reprobed as many times as nylon. Nitrocellulose is not suitable for smaller DNA fragments below 500 bps, but usually gives less background.

4. Transfer of DNA may be performed with applying vacuum or positive pressure instead of simple capillary effect.

5. Duration of the capillary transfer depends on the size of the DNA fragment of

interest. When using a depuration step resulting in broken DNA of about 1-2 Kbp, shorter time might suffice for >90 % transfer efficiency, but it has to be empirically determined.

6. Other enzyme-substrate systems for visualization are available besides alkaline phosphatase/CDP-star (e.g., HRPO or NBT/BCIP), and as a consequence the developing method is highly dependent on the infrastructure of the laboratory.

References

1. Raab-Traub N, Flynn K (1986) The structure of the termini of the Epstein-Barr virus as a marker of clonal cellular proliferation. Cell 47(6):883–889
   [CrossRef][PubMed]

2. Zimmermann J, Hammerschmidt W (1995) Structure and role of the terminal repeats of Epstein-Barr virus in processing and packaging of virion DNA. J Virol 69(5):3147–3155
   [PubMed][PubMedCentral]

3. Moody CA, Scott RS, Su T, Sixbey JW (2003) Length of Epstein-Barr virus termini as a determinant of epithelial cell clonal emergence. J Virol 77(15):8555–8561
   [CrossRef][PubMed][PubMedCentral]

4. Southern EM (1975) Detection of specific sequences among DNA fragments separated by gel electrophoresis. J Mol Biol 98(3):503–517
   [CrossRef][PubMed]

5. Feederle R, Shannon-Lowe C, Baldwin G, Delecluse HJ (2005) Defective infectious particles and rare packaged genomes produced by cells carrying terminal-repeat-negative Epstein-Barr virus. J Virol 79(12):7641–7647. doi:10.1128/JVI.79.12.7641-7647.2005
   [CrossRef][PubMed][PubMedCentral]

6. Chiu SH, Wu MC, Wu CC, Chen YC, Lin SF, Hsu JT et al (2014) Epstein-Barr virus BALF3 has nuclease activity and mediates mature virion production during the lytic cycle. J Virol 88(9):4962–4975. doi:10.1128/JVI.00063-14
   [CrossRef][PubMed][PubMedCentral]

7. Gulley ML, Raphael M, Lutz CT, Ross DW, Raab-Traub N (1992) Epstein-Barr virus integration in human lymphomas and lymphoid cell lines. Cancer 70(1):185–191
   [CrossRef][PubMed]

8. Fan H, Gulley ML (2001) Molecular methods for detecting Epstein-Barr virus (part ii): structural analysis of Epstein-Barr virus DNA as a marker of clonality. Methods Mol Med 49:313–319. doi:10.1385/1-59259-081-0:313
   [PubMed]

9. Lewin N, Minarovits J, Weber G, Ehlin-Henriksson B, Wen T, Mellstedt H et al (1991) Clonality and methylation status of the Epstein-Barr virus (EBV) genomes in in vivo-infected EBV-carrying chronic lymphocytic leukemia

(CLL) cell lines. Int J Cancer 48(1):62–66
[CrossRef][PubMed]

10. Gulley ML, Eagan PA, Quintanilla-Martinez L, Picado AL, Smir BN, Childs C et al (1994) Epstein-Barr virus DNA is abundant and monoclonal in the Reed-Sternberg cells of Hodgkin's disease: association with mixed cellularity subtype and Hispanic American ethnicity. Blood 83(6):1595–1602
[PubMed]

11. Gulley ML, Pulitzer DR, Eagan PA, Schneider BG (1996) Epstein-Barr virus infection is an early event in gastric carcinogenesis and is independent of bcl-2 expression and p53 accumulation. Hum Pathol 27(1):20–27
[CrossRef][PubMed]

12. van de Rijn M, Cleary ML, Variakojis D, Warnke RA, Chang PP, Kamel OW (1996) Epstein-Barr virus clonality in lymphomas occurring in patients with rheumatoid arthritis. Arthritis Rheum 39(4):638–642
[CrossRef][PubMed]

13. Lin CT, Chen W, Hsu MM, Dee AN. Clonal versus polyclonal Epstein-Barr virus infection in nasopharyngeal carcinoma cell lines. Laboratory investigation; a journal of technical methods and pathology. 1997;76(6):793-8.

14. Ryan JL, Kaufmann WK, Raabtraub N, Oglesbee SE, Carey LA, Gulley ML (2006) Clonal evolution of lymphoblastoid cell lines. Lab Invest 86(11):1193–200. doi:10.1038/labinvest.3700472
[CrossRef][PubMed]

15. Arai A, Yamaguchi T, Komatsu H, Imadome K, Kurata M, Nagata K et al (2014) Infectious mononucleosis accompanied by clonal proliferation of EBV-infected cells and infection of CD8-positive cells. Int J Hematol 99(5):671–675. doi:10.1007/s12185-014-1548-4
[CrossRef][PubMed]

16. Brown NA, Liu CR, Wang YF, Garcia CR (1988) B-cell lymphoproliferation and lymphomagenesis are associated with clonotypic intracellular terminal regions of the Epstein-Barr virus. J Virol 62(3):962–969
[PubMed][PubMedCentral]

17. Raab-Traub N, Rajadurai P, Flynn K, Lanier AP (1991) Epstein-Barr virus infection in carcinoma of the salivary gland. J Virol 65(12):7032–7036
[PubMed][PubMedCentral]

18. Pathmanathan R, Prasad U, Chandrika G, Sadler R, Flynn K, Raab-Traub N (1995) Undifferentiated, nonkeratinizing, and squamous cell carcinoma of the nasopharynx. Variants of Epstein-Barr virus-infected neoplasia. Am J Pathol 146(6):1355–1367
[PubMed][PubMedCentral]

19. Pathmanathan R, Prasad U, Sadler R, Flynn K, Raab-Traub N (1995) Clonal proliferations of cells infected with Epstein-Barr virus in preinvasive lesions related to nasopharyngeal carcinoma. N Engl J Med 333(11):693–698. doi:10.1056/NEJM199509143331103
[CrossRef][PubMed]

13. Characterization of EBV Promoters and Coding Regions by Sequencing PCR-Amplified DNA Fragments

Kalman Szenthe[1]✉ and Ferenc Bánáti[1]✉

(1) RT-Europe Nonprofit Research Ltd., Vár 2, Szigetköz Building, Mosonmagyaróvár, 9200, Hungary

✉ **Ferenc Bánáti**
   Email: fbanati@yahoo.co.uk

Abstract
DNA sequencing approaches originally developed in two directions, the chemical degradation method and the chain-termination method. The latter one became more widespread and a huge amount of sequencing data including whole genome sequences accumulated, based on the use of capillary sequencer systems and the application of a modified chain-termination method which proved to be relatively easy, fast, and reliable. In addition, relatively long, up to 1000 bp sequences could be obtained with a single read with high per-base accuracy. Although the recent appearance of next-generation DNA sequencing (NGS) technologies enabled high-throughput and low cost analysis of DNA, the modified chain-terminating methods are often applied in research until now. In the following, we shall present the application of capillary sequencing for the sequence characterization of viral genomes in case of partial and whole genome sequencing, and demonstrate it on the BARF1 promoter of Epstein Barr virus (EBV).

Key words Capillary sequencing – Whole genome sequencing – EBV

1 Introduction

1.1 Sequencing in General

Molecular biological methods relying on DNA or RNA sequences are widespread in basic research. The very same methods (e.g., polymerase chain reaction, DNA/RNA micro array, Southern/Northern blot, molecular cloning, RFLP and certain kind of sequencing) are frequently used in diagnostics or in the development of diagnostic methods as well. In 1953, Watson and Crick defined the structure of DNA; thenceforth, a series of methods have been invented to determine primary DNA sequences including whole-genome sequences of organisms, and DNA sequence data were utilized in diverse areas of research and diagnostics. In 1977 two groups established two different sequencing approaches: Sanger and colleagues established the dideoxy chain-terminating method [1], and Maxam and Gilbert established the chemical degradation method [2]. The first one formed the basis of more recent sequencing methods (e.g., capillary sequencing and certain kind of next-generation sequencing (NGS) approaches), while the second one formed the basis for special methods, e.g., the dimethyl sulfate (DMS) in vivo footprinting [3–6] assay.

While the original Sanger method was based on ^{32}P radioactive isotope labeling and detection, the newer methods used the same approach, but replaced the hazardous radioactive label: instead of isotope labeling, fluorescein dye-labeled dideoxy nucleotides or—in certain cases—fluorescein dye-labeled universal sequencing primers (e.g., Pharmacia Biotech (Amersham Biosciences) ALF express Genetic analyzer; [7]) were introduced. The disadvantage of the original method and the method using fluorescein-dye is that, due to a single dye (or radioactivity) four different reactions had to be prepared for the four dideoxy nucleotides, and the products had to be run in four separate wells on a slab gel electrophoresis system. To reduce the laboratory work and hands-on time, a new labeling method was developed with four different dyes linked to the different dideoxy nucleotides (ddATP, ddCTP, ddGTP, ddTTP) [8] and later [9] a single capillary (10- to 100-μm internal diameter size) filled with matrix replacing the slab gel system. The matrix could be produced from linear polyacrylamide (LPA), polyethylene oxide (PEO), hydroxyethylcellulose (HEC), polydimethylacrylamide (PDMA), polyvinylpyrrolidone (PVP), polyethylene glycol with a fluorocarbon tail, or polyacryloylaminopropanol, a copolymer of acrylamide or allylglucopyranose [10]. Mathies and colleagues published a protocol using two fluorescent dyes [9], but currently capillary sequencing mostly uses a four-colored approach. The LPA matrix provided the best resolution and a fair read-length (ca 500-1000 bp) [11]. The capillary approach facilitated the development of parallel DNA sequencing runs of multiple samples using a 96-well plate or systems using multiple 96-well plates in parallel.

Currently, despite the spread of next-generation sequencing (NGS) approaches, DNA sequencing based on capillary electrophoresis is still a common method for the

sequencing of PCR-amplified DNA fragments. It is worth to be mentioned that the high throughput NGS approaches can also be applied to this purpose, but these platforms are profitable only at high sample numbers.

The exact steps of the capillary sequencing protocols are platform specific. A typical sequencing process is presented in Fig. 1. In the following, we shall describe an optional way using the MegaBace 1000 Sequencing System (Amersham Biosciences, GE Healthcare Life Sciences).
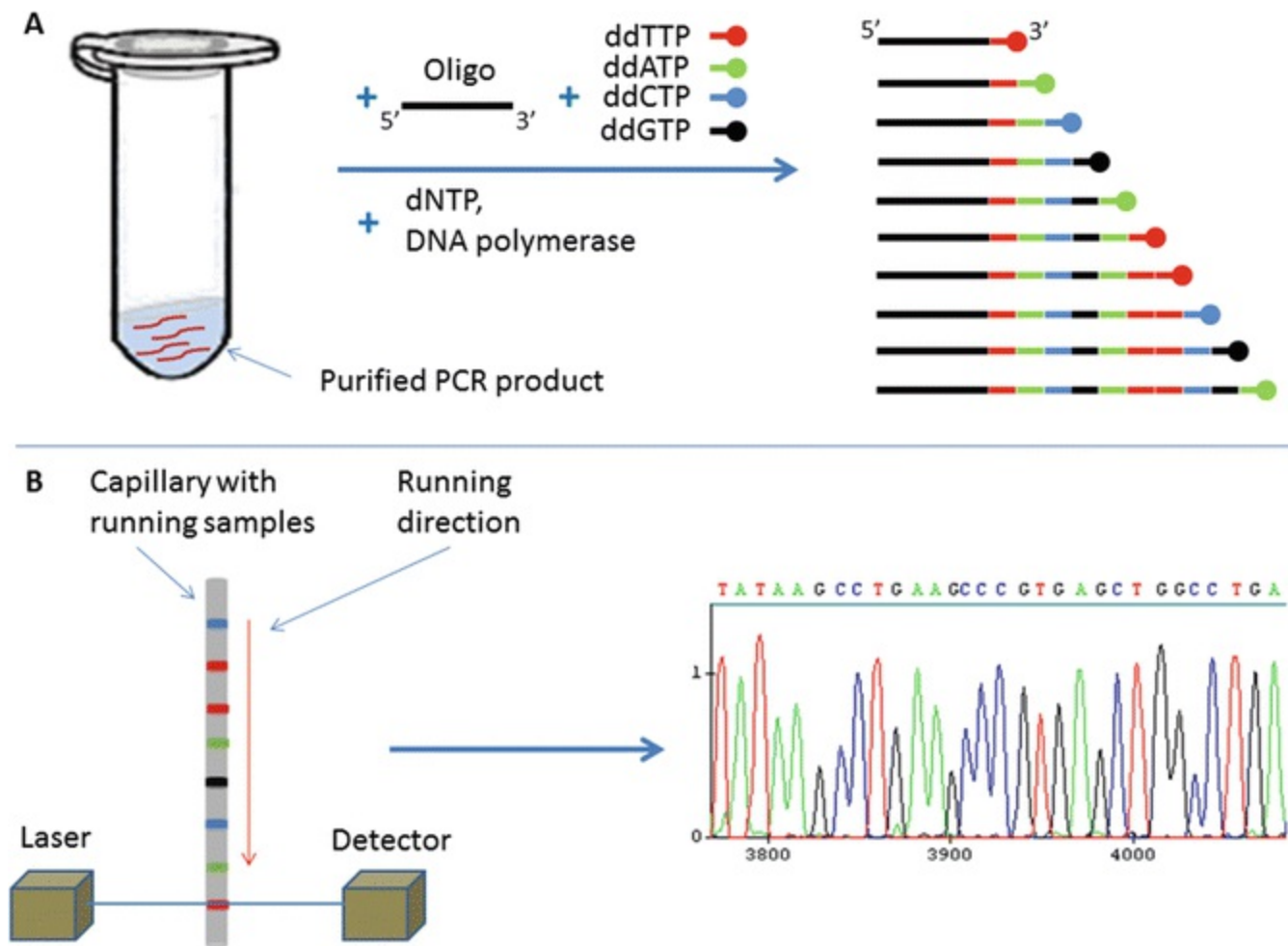
Fig. 1 Sequencing process. (**a**) The sequencing reaction contains an oligonucleotide primer, template DNA, e.g., purified PCR product, ddNTPs, each labeled with a different fluorochrome, dNTPs, DNA polymerase, and an appropriate buffer. (**b**) After purification, the products of the sequencing reaction are separated by length using capillary electrophoresis filled with LPA matrix. The shorter products run faster. The laser induces the specific fluorochrome attached to the ddNTP which terminated the chain elongation in the sequencing reaction. The detector detects the fluorochrome-specific, emitted light. Based on fluorescence detection, the software discriminates the distinct ddNTPs and thus establishes the DNA sequence of initial template for the PCR product

1.2 Capillary Sequencing Using the EBV Model System

In the following, we shall present the application of sequencing (principally the capillary sequencing) for the sequence characterization of viral genomes, as

demonstrated on EBV (Epstein Barr virus) genomes.

The first whole genome sequence for Epstein Barr virus was established through a shotgun sequencing approach by Baer and colleagues, using B95-8 (GenBank accession number V01555), a virus produced by an EBV-carrying marmoset B-lymphoblastoid cell line [12]. Earlier some partial B95-8 sequence results were published by Cheung et al. [13] and Dambaugh et al. [14]. The B95-8 cell line is frequently used, because it continuously produces the virus, due to the activation of the lytic cycle in a subpopulation of the cells. Other groups detected a few deletions in other cell lines, e.g., Daudi, P3HR-1 [15] and Raji [16]. Later, a "wild type" EBV reference sequence (EBVwt) was created, based on the B95-8 sequence, by decreasing the number of IR1 internal repeat units and inserting a Raji-derived viral sequence to restore the B95-8 deletion [17]. The "wild type" EBV sequence (EBVwt, AJ507799) is available at http://www.ncbi.nlm.nih.gov/nuccore/AJ507799.

In addition to the earlier results of "classical" sequencing methods, currently there are several new details coming from NGS experiments. Lin and colleagues sequenced the EBV strains from the Mutu I and Akata cell lines after IgM and IgG lytic cycle activation, respectively [18]. Another group sequenced the EBV strain carried by the nasopharyngeal carcinoma cell line C666.1 using an NGS system and corrected, verified, and extended the results with capillary sequencing [19]. Recently, Palser and colleagues also used NGS to determine 71 novel EBV genome sequences from different clinical sample types and locations collected worldwide [20].

In addition to whole genome sequencing, the capillary sequencing method is also useful for partial genome (usually PCR-amplicon) sequencing. Partial genome sequencing is generally useful for targeted preparatory work which precedes the analysis of DNA methylation experiments, i.e., the sequencing of bisulfite -treated DNA. In this case, it is necessary to establish the actual primary DNA sequence under examination, before further oligonucleotide design is performed (for more detail please see Chap. 15).

Subsequently, we shall present an example of partial genome sequencing using the capillary sequencer, for the EBV gene encoding the BARF 1 transcript.

The Epstein-Barr virus (EBV) *Bam*HI-A rightward frame 1 (BARF1) gene can be regarded as a viral oncogene in epithelial cells, and it has immune-modulating functions [21]. The BARF1 gene is encoded in the *Bam*HI A fragment of the EBV genome. Its protein product has autocrine and paracrine effects and may play an important role in the development of certain EBV-associated malignancies. It is classified as an early gene of the lytic cycle of EBV, nonetheless it is also expressed in latently infected epithelial cells such as nasopharyngeal carcinoma (NPC) cells, EBV-associated gastric cancer (GC) cells and EBV positive epithelial and lymphoid cell lines as well as in certain EBV-associated lymphomas [22, 23]. In latently EBV-infected cell lines lytic genes other than BARF1 are not expressed. Due to its high expression level during viral

latency in epithelial cells, the classification of BARF1 as lytic cycle gene has become questionable [22].

2 Materials

2.1 Cell Lines

Cells were cultured in RPMI 1640 medium containing 10 % FCS (Fetal Calf Serum), 2 mM glutamine, 50 U/mL streptomycin at 5 % CO_2 content and 37 °C. Cell lines and their main characteristics are shown in Table 1.

Table 1 Cell lines and their main characteristics

Cell line	Cell type or stage of B cell maturation	EBV	Reference
CBM1-Ral-STO	Lymphoblastoid	+	[24]
KR-4			[25]
Rael	Endemi c, EBV-positive BL;	+	[24]
Mut u-BL-I-cl-216	late germinal center B cell		[26]
Mutu-BL-III-cl-99			[26]
Raji			[27]
MDA-MB-231	Breast carcinoma cell line	−	[28]
C4A3		+	[29]
C2G6		+	[29]
C666.1	Nasopharyngeal carcinoma cell line	+	[30]

2.2 Isolation of DNA

1. 1× PBS (Phosphate buffered saline): 137 mM NaCl, 2.7 mM KCl, 10 mM Na_2HPO_4, 2 mM KH_2PO_4, adjust pH to 7.4 with HCl.

2. TE buffer: 10 mM Tris–HCl, pH 8.0, 1 mM EDTA.

3. Extraction buffer: 10 mM Tris–HCl, pH 8.0, 0.1 M EDTA, pH 8.0, 20 μg/mL RNase A, 0.5 % SDS.

4. Proteinase K.

5. Phenol, saturated with 0.5 M Tris–HCl, pH 8.

6. Chloroform.

7. Ammonium acetate.

2.3 PCR

1. FastStart™ Taq DNA Polymerase: Roche.

2. Oligonucleotide sets used:

   BARF1fw: 5′-cac gta gat gtc cct gtg ata gg-3′

   BARF1rev: 5′-gtc cag cta cct cat gtt cag g-3′

   BARF3fw: 5′-cgt agt ggt cgt tgt aca ctg c-3′

   BARF3rev: 5′-caa ggt gaa ata ggc aag tgc-3′

   BARF5fw: 5′-ctt tac tca tca cgc aac acc-3′

   BARF5rev: 5′-cag ctg acc tca atc tct gg-3′.

2.4 PCR Purification

1. GeneJET PCR Purification Kit, Thermo Scientific.

2.5 Sequencing Reaction

1. DYEnamic™ ET dye terminator, Amersham Biosciences, GE Healthcare Life Sciences.

2.6 Purification of the Sequencing Reaction Products

1. Illustra AutoSeq G-50 columns: GE Healthcare Life Sciences.

2. Absolute ethanol.

3. Ammonium acetate: 7.5 M, included in DYEnamic™ ET dye terminator kit.

4. GenElute™-LPA: Sigma-Aldrich.

5. loading solution: 70 % formamide, 1 mM EDTA, included in DYEnamic™ ET dye terminator kit.

---

3 Methods

3.1 Isolation of DNA

For DNA isolation nowadays there are numerous options. Silica-based genomic DNA isolation kits (e.g., GeneJET Genomic DNA Purification Kit, Thermo Scientific) could be fast and profitable solutions. These kits have detailed manuals, so in the following we shall describe a classical option using basic laboratory chemicals.

1. Centrifuge cell suspension (ca. 5×10^7 cells) for $1500 \times g$ at 4 °C for 10 min.

2. Wash the cell pellet in $1\times$ PBS twice (between the washing steps centrifuge the samples with $1500 \times g$ at 4 °C for 10 min).

3. Resuspend the pellet in 1 mL TE buffer.

4. Add 10 mL of Extraction buffer to the 1 mL of cell suspension and incubate at 37 °C for 1 h.

5. Add 100 µg/mL (final concentration) Proteinase K and incubate at 50 °C for 3 h.

6. Cool to room temperature (RT) and add an equal volume of saturated (0.5 M Tris–HCl, pH 8) phenol.

7. Stir at RT for 10 min and centrifuge at $5000\times g$ for 15 min.

8. Pipette the upper aqueous phase into a new tube and repeat the phenolic purification twice.

9. Add equal volume of chloroform to the upper aqueous phase, stir, centrifuge, and remove aqueous phase.

10. Add 0.2 volume of 10 M ammonium acetate and 2 volumes of absolute ethanol to the aqueous phase, mix gently, and centrifuge at 12,000× *g* 10 min at 4 °C.

11. Wash pellet twice with 70 % ethanol and then dry the pellet at RT (between the washing steps centrifuge the samples at 12,000× *g* at RT for 5 min).

12. Dissolve the pelleted DNA in sterile TE buffer. Analyze the solution using a spectrophotometer at 260 and 280 nm. The final concentration should be about 1 μg/μL DNA.

3.2 PCR Reaction

The specific PCR reaction process depends on the system used (PCR kit, primers, and PCR instrument). In general, a PCR reaction contains DNA polymerase, reaction buffer, dNTPs, $MgCl_2$, specific oligos, and template DNA. In the following, we suggest an optional approach, using the FastStart™ Taq DNA Polymerase, according to the manufacturer's instructions.

1. Thermal profile: 95 °C for 3 min once, then 95 °C for 40 s, 65 °C for 40 s and 72 °C for 1 min alternating for 45 cycles, and finally an elongation step at 72 °C for 8 min.

2. To verify the quality and quantity of PCR product it is recommended to use agarose gel electrophoresis.

3. The product of the PCR reaction must be purified from the oligos and other reaction components prior to the sequencing reaction using a purification kit, e.g., Thermo Scientific, GeneJET PCR Purification Kit.

3.3 Sequencing Reaction

The actual sequencing reaction process depends on the system used. Subsequently, we shall describe an optional way using the MegaBace 1000 Sequencing System (Amersham Biosciences, GE Healthcare Life Sciences) (*see* **Note 1**).

1. Add 1.5 µL dH$_2$O, 0.5 µL oligo (10 µM) and 8 µL DYEnamic™ ET dye terminator (Amersham Biosciences, GE Healthcare Life Sciences) premix (final volume: 20 µL) per 10 µL of sample into a PCR tube. The premix contains dNTPs, ddNTPs with fluorochromes, DNA polymerase (sequenase), and reaction buffer. In this specific kit, the dNTP contains dITP instead of dGTP.

2. Thermal profile: 95 °C for 20 s once, then 95 °C for 20 s, 58 °C for 15 s and 60 °C for 1 min, alternating for 30 cycles.

3.4 Purification of the Sequencing Reaction Product

There are several options for the purification of the sequencing reaction product, among which only two, a fast gel filtration-based solution (illustra AutoSeq G-50 columns; GE Healthcare Life Sciences) and a simple ethanol precipitation are mentioned here. Because the illustra AutoSeq G-50 kit has a detailed manual supplied by the producer, subsequently we shall describe only the second option using basic laboratory chemicals. This inexpensive approach results in long read-lengths and good sequencing results.

1. Add 55 µL absolute ethanol and 2.5 µL ammonium acetate (7.5 M, included in the DYEnamic™ ET dye terminator kit), 2 µL 0.25 mg/mL GenElute™-LPA (Sigma-Aldrich).

2. Incubate the samples on −20 °C for 15 min and then centrifuge them at 14,000× *g* at 4 °C for 20 min.

3. Discard the supernatant from the pellet, and wash it with 70 % ethanol once. After the washing step centrifuge the samples at 12,000× *g* at RT for 5 min).

4. Dry the pellet, but do not overdry (!), and dissolve it in 15 µL loading solution (70 % formamide, 1 mM EDTA, included in the DYEnamic™ ET dye terminator kit). The samples in loading solution can be stored for a few months.

3.5 Sequencing Run

We used the MegaBACE 1000 platform to analyze the purified fragments. This instrument applies LPA matrix (*see* **Note 2**) loaded into the 96 or 2 × 96 well PCR

plates, and the submerging capillaries enable the separation of fragments between 600 and 1000 bases depending on the secondary structures and other physicochemical characteristics. The detection is performed with a four color detector and thus using four different dyes. The resulting electropherogram can be opened with the appropriate Amersham software (MegaBACE™ Sequence Analyzer) and can be exported for further processing. Quantitative analysis may be performed, while paying attention to the fact that the different dyes yield fluorescence with different intensities and that the raw data can not be accessed on this platform.

The protocol regarding the adjustment of the electrophoresis, detection, and data management parameters is beyond the scope of this chapter, because these parameters depend largely on the specific sequencing machine used. Some empirical hints to accomplish the sequencing runs are given in Subheading 4 (*see* **Notes 3 – 6**).

3.6 Results of BARF1 Sequencing

Our sequencing of the BARF1 promoter of several virus strains revealed eleven new polymorphisms, among them ten substitutions and one deletion, *see* Table 2. In case of other virus-infected cell lines there was no change compared to the NCBI Reference Sequence: AJ507799.

Table 2 Results of BARF1 sequencing

Position in the reference sequence (AJ507799)	Polymorphisms
164109	C2G6 cell line: cytosine to thymine transversion
164147	Rael cell line: cytosine to thymine transversion
164148	CBM1 cell line: guanine deletion, Rael cell line: guanine to adenine transversion
164154	Mutu I and Mutu III cell lines: guanine to thymine transversion
164724	C666.1 cell line: cytosine to thymine transversion
164938	Rael and CBM1 cell lines: guanine to thymine transversion
165087	C666.1 cell line: thymine to cytosine transversion
165131	Mutu I and Mutu I II cell lines: thymine-cytosine transversion
165219	Mutu III cell line: guanine to adenine transversion
165486	Mutu III cell line: cyto sine to thymine transversion

A typical electropherogram is presented in Fig. 2 showing an example of the BARF1 promoter sequence from the C666.1 cell line, prepared using the MegaBace sequence Analyzer software.

Fig. 2 Electropherogram of BARF1 sequence of the EBV genome from the C666.1 nasopharyngeal carcinoma cell line

4 Notes

1. We prepared sequencing reactions with all oligos used in the PCR amplifications. In many cases, bidirectional sequencing with the lower and the upper oligos is a better approach than unidirectional sequencing, because of the more reliable results of overlapping sequences and because it enables the user to sequence larger PCR products in this way. In many cases the PCR amplification oligos are usable for sequencing reactions, but sometimes, due to unwanted secondary structures of oligos, it is necessary to design oligos specially for the sequencing reaction or to reoptimize the amplification oligos.

2. The MegaBace 1000 sequencing system uses LPA matrix (MegaBACE Long Read Matrix), which enables read lengths around 600–800 bases per sample.

3. The capillary should occasionally be washed with warm distillated water, but never warmer than 50 °C, because the high temperature can harm the capillary.

4. The results of sequencing runs are highly dependent on the quality and quantity of the PCR product and the sequencing reaction. In certain cases, the dilution of the

purified sequencing product enhances sequencing quality and as a consequence, has a positive impact on the electropherogram.

5. For further useful details please check the following webpage : https://www.gelifesciences.com/gehcls_images/GELS/Related%20Content/Files/1314729545976/litdocMega_manual_complete_20110830212541.pdf.

6. We used the MegaBACE™ Sequence Analyzer software, but other, freely available software can be also used.

References

1. Sanger F, Nicklen S, Coulson AR (1977) DNA sequencing with chain-terminating inhibitors. Proc Natl Acad Sci U S A 74:5463–5467
   [CrossRef][PubMed][PubMedCentral]

2. Maxam AM, Gilbert W (1977) A new method for sequencing DNA. Proc Natl Acad Sci U S A 74:560–564
   [CrossRef][PubMed][PubMedCentral]

3. Mueller PR, Wold B (1989) In vivo footprinting of a muscle specific enhancer by ligation mediated PCR. Science 246:780–786
   [CrossRef][PubMed]

4. Garrity PA, Wold BJ (1992) Effects of different DNA polymerases in ligation-mediated PCR: Enhanced genomic sequencing and in vivo footprinting. Proc Natl Acad Sci U S A 89:1021–1025
   [CrossRef][PubMed][PubMedCentral]

5. Niller HH, Glaser G, Knüchel R et al (1995) Nucleoprotein complexes and DNA 5′-ends at oriP of Epstein-Barr virus. J Biol Chem 270:12864–12868

6. Szenthe K, Koroknai A, Banati F et al (2013) The 5′ regulatory sequences of active miR-146a promoters are hypomethylated and associated with euchromatic histone modification marks in B lymphoid cells. Biochem Biophys Res Commun 433:489–495
   [CrossRef][PubMed]

7. Szenthe K, Koroknai A, Banati F et al (2013) The role of DNA hypomethylation, histone acetylation and in vivo protein-DNA binding in Epstein-Barr virus-induced CD23 upregulation. Biochem Biophys Res Commun 435:8–15
   [CrossRef][PubMed]

8. Prober JM, Trainor GL, Dam RJ et al (1987) A system for rapid DNA sequencing with fluorescent chain-terminating dideoxynucleotides. Science 238:336–341
   [CrossRef][PubMed]

9. Huang XC, Quesada MA, Mathies RA (1992) DNA sequencing using capillary array electrophoresis. Anal Chem 64:2149–2154
   [CrossRef][PubMed]

10. Dolnik V (1999) DNA sequencing by capillary electrophoresis (review). J Biochem Biophys Methods 41:103–119
[CrossRef][PubMed]

11. Ausubel FM, Albright LM, Ju J (1999) DNA sequencing. Curr Protoc Mol Biol 7:1–7.0.15

12. Baer R, Bankier AT, Biggin MD et al (1984) DNA sequence and expression of the B95-8 Epstein-Barr virus genome. Nature 310:207–211
[CrossRef][PubMed]

13. Cheung A, Kieff E (1982) Long internal direct repeat in Epstein-Barr virus DNA. J Virol 44:286–294
[PubMed][PubMedCentral]

14. Dambaugh TR, Kieff E (1982) Identification and nucleotide sequences of two similar tandem direct repeats in Epstein-Barr virus DNA. J Virol 44:823–833
[PubMed][PubMedCentral]

15. Jones MD, Foster L, Sheedy T et al (1984) The EB virus genome in Daudi Burkitt's lymphoma cells has a deletion similar to that observed in a non-transforming strain (P3HR-1) of the virus. EMBO J 3:813–821
[PubMed][PubMedCentral]

16. Hatfull G, Bankier AT, Barrell BG et al (1988) Sequence analysis of Raji Epstein-Barr virus DNA. Virology 164:334–340
[CrossRef][PubMed]

17. de Jesus O, Smith PR, Spender LC et al (2003) Updated Epstein-Barr virus (EBV) DNA sequence and analysis of a promoter for the BART (CST, BARF0) RNAs of EBV. J Gen Virol 84:1443–1450
[CrossRef][PubMed]

18. Lin Z, Wang X, Strong MJ et al (2013) Whole-genome sequencing of the Akata and Mutu Epstein-Barr virus strains. J Virol 87:1172–1182
[CrossRef][PubMed][PubMedCentral]

19. Tso KK, Yip KY, Mak CK et al (2013) Complete genomic sequence of Epstein-Barr virus in nasopharyngeal carcinoma cell line C666-1. Infect Agent Cancer 8:29
[CrossRef][PubMed][PubMedCentral]

20. Palser AL, Grayson NE, White RE et al (2015) Genome diversity of Epstein-Barr virus from multiple tumor types and normal infection. J Virol 89:5222–5237
[CrossRef][PubMed][PubMedCentral]

21. Hoebe EK, Wille C, Hopmans ES et al (2012) Epstein-Barr virus transcription activator R upregulates BARF1 expression by direct binding to its promoter, independent of methylation. J Virol 86:11322–11332
[CrossRef][PubMed][PubMedCentral]

22. Fiorini S, Ooka T (2008) Secretion of Epstein-Barr Virus-encoded BARF1 oncoprotein from latently infected B cells. Virol J 5:70
[CrossRef][PubMed][PubMedCentral]

23. Hoebe EK, Le Large TY, Greijer AE et al (2013) BamHI-A rightward frame 1, an Epstein-Barr virus-encoded oncogene and immune modulator. Rev Med Virol 23:367–383
[CrossRef][PubMed][PubMedCentral]

24. Ernberg I, Falk K, Minarovits J et al (1989) The role of methylation in the phenotype dependent modulation of

Epstein–Barr nuclear antigen 2 and latent membrane protein genes in cells latently infected with Epstein–Barr virus. J Gen Virol 70:2989–3002
[CrossRef][PubMed]

25. Altiok E, Minarovits J, Hu LF et al (1992) Host-cell-phenotype-dependent control of the BCR2/BWR1 promoter complex regulates the expression of Epstein-Barr virus nuclear antigens 2-6. Proc Natl Acad Sci U S A 89:905–909
[CrossRef][PubMed][PubMedCentral]

26. Gregory CD, Rowe M, Rickinson AB (1990) Different Epstein–Barr virus–B cell interactions in phenotypically distinct clones of a Burkitt's lymphoma cell line. J Gen Virol 71:1481–1495
[CrossRef][PubMed]

27. Epstein MA, Achong BG, Barr YM et al (1966) Morphological and virological investigations on cultured Burkitt tumor lymphoblasts (strain Raji). J Natl Cancer Inst 37:547–559
[PubMed]

28. Cailleau R, Young R, Olive M et al (1974) Breast tumor cell lines from pleural effusions. J Natl Cancer Inst 53:661–674
[PubMed]

29. Wakisaka N, Kondo S, Yoshizaki T et al (2004) Epstein-Barr virus latent membrane protein 1 induces synthesis of hypoxia-inducible factor 1 alpha. Mol Cell Biol 24:5223–5234
[CrossRef][PubMed][PubMedCentral]

30. Cheung ST, Huang DP, Hui AB et al (1999) Nasopharyngeal carcinoma cell line (C666-1) consistently harboring Epstein-Barr virus. Int J Cancer 83:121–126
[CrossRef][PubMed]

14. The Use of Chromatin Precipitation Coupled to DNA Sequencing (ChIP-Seq) for the Analysis of Zta Binding to the Human and EBV Genome

Anja Godfrey[1], Sharada Ramasubramanyan[2] and
Alison J. Sinclair[1] ✉

(1) School of Life Sciences, University of Sussex, JMS Bldg 3C19, Brighton, BN1
     9QG, UK
(2) V ClinBio Labs Pvt Ltd., Central Research Facility, Sri Ramachandra University,
     Porur, Chennai, 600 016, India

✉ **Alison J. Sinclair**
   Email: A.J.Sinclair@sussex.ac.uk

Abstract
Determining which components of the transcription machinery associate with the viral
and cellular genome, and how this changes at specific stages of the viral life cycle is
paramount to understanding how the distinct transcriptional programs associated with
primary infection, latency, and disease are established and how they are reprogrammed
during initiation and execution of the viral lytic replication cycle. Chromatin
precipitations linked to next generation DNA sequencing (ChIP-Seq) allow for the
interactions of proteins with DNA to be mapped across both viral and cellular genomes.
This can be applied to viral and cellular transcription factors, coactivators and
corepressors, modified histones, and modulators of chromatin.

Key words Chromatin – Immunoprecipitation – DNA – ChIP – DNA sequencing –
Transcription factor

1 Introduction

Every cell in an organism has an identical genome, which contains all of the information required for the lifetime of that organism, but many genes are required only in specialized cells or in response to particular conditions. Highly controlled mechanisms that regulate the expression of such genes are paramount to the specialization of cells, thus allowing for the complexity and survival of the organism. This is achieved through a myriad of controls that ensure that an environment that is either favorable or unfavorable to transcriptional activation exists surrounding the transcriptional start site of each gene [1].

The Epstein Barr virus (EBV) has highly controlled and distinct programs of gene expression . The EBV genome consists of ~170 kb of double strand DNA. Following infection of cells the genome is transported to the nucleus, where it becomes associated with histon es and so resembles cellular DNA. During viral latency one of the four distinct patterns of viral gene expression is established (termed latency 0 to latency III) [2]. These have relevance for viral persistence a nd for virus-associated disease. Cells exhibiting these latency patterns can be activated to initiate the viral lytic replicatio n cycle, during which most viral genes are expressed. In addition, an important but currently less well-defined pattern of gene expression occurs immediately following infection of B-cells, and during some diseases, which is termed pre-latency or abortive lytic replication.

The relevant proteins include histones, specific posttranslational modifications of histones, transcription factors, coactivators and corepressors, and proteins that enable and change chromatin architecture. Several EBV genes encode transcription factors that either interact directly (e.g., Zta (Zebra) and Rta), or indirectly (e.g., EBNA1 , -2, - 3 and -LP) with DNA [2].

ChIP-Seq has been valuable in determining information about the binding sites of individual EBV transcription factors with the human, and in some cases viral, genomes [3–9]. In addition, the Encyclopedia of DNA elements (ENCODE) project [10] includes an EBV-infected cell displaying latency III pattern of gene expression , and the wealth of data available from ENCODE has been mapped to the EBV genome. This generated an atlas of interactions in Latency III [11].

The ChIP-Seq technique takes a genome-wide approach to determine the interactions of proteins with DNA. This involves the use of cross-linkers to "fix" adjacent protein-protein and protein-DNA interactions within live cells, followed by isolation of a specific protein, together with any other proteins, and DNA that protein is associated with. The precipitated DNA and a sample of the starting DNA are then isolated, the cross-links are reversed and samples are prepared for sequencing. The libraries are then subject to next generation sequencing . The resulting DNA sequencing reads are mapped to genome sequences. For virus-infected cells, this can be undertaken

for both the viral genome and the host cell genome from the same sequence library as shown for the viral transcription factor Zta [9, 12].

2 Materials

2.1 Chromatin Preparation and Precipitation

1. Formaldehyde: 37 % (v/v).

2. Glycine: 1 M.

3. PBS: 137 mM NaCl, 2.7 mM KCl, 10 mM Na_2HPO_4, 1.8 mM KH_2PO_4.

4. Cell Lysis Buffer: 85 mM KCl, 0.5 % (v/v) NP-40, and 5 mM PIPES pH 8.0.

5. SDS lysis buffer: 1 % (w/v) SDS, 10 mM EDTA, 50 mM Tris pH 8.0.

6. IP Dilution Buffer: 0.01 % (w/v) SDS, 1.1 % (v/v) Triton X-100, 1.2 mM EDTA, 16.7 mM Tris pH 8.0, 167 mM NaCl.

7. Low salt wash buffer: 0.1 % (w/v) SDS, 1 % (v/v) Triton X-100, 2 mM EDTA, 20 mM Tris pH 8.0, 150 mM NaCl.

8. High salt wash buffer: 0.1 % (w/v) SDS, 1 % (v/v) Triton X-100, 2 mM EDTA, 20 mM Tris pH 8.0, 500 mM NaCl.

9. LiCl wash buffer: 250 mM LiCl, 1 % (v/v) NP-40, 1 % (w/v) Na-deoxycholate, 1 mM EDTA, 10 mM Tris pH 8.0.

10. Elution buffer: 10 mM Tris–HCl, 1 mM EDTA, 1 % (w/v) SDS.

11. Protein A sepharose beads.

12. Protein G sepharose beads.

13. Blocking buffer: PBS, 0.5 % (w/v) BSA (fraction V), passed through a 0.2 μm filter).

14. RNase A: 20 mg/mL.

15. Proteinase K (20 mg/mL).

2.2 ChIP Library Preparation

1. Library preparation kits: NEB Next ChIP-Seq Library Prep Reagent Set for Illumina, NEBNext Multiplex Oligos for Illumina (Index Primers Set 1).

2. Deoxynucleotide (dNTP) solution mix: Kit component, 10 mM dATP, 10 mM dGTP, 10 mM dCTP, 10 mM dTTP, supplied in Milli-Q water (Millipore Corporation) as a sodium salt at pH 7.5.

3. Phosphorylation reaction buffer (10×): Kit component, 500 mM Tris–HCl, 100 mM MgCl2, 100 mM DTT, 10 mM ATP, pH 7.5 at 25 °C.

4. Enzymes: Kit components, T4 DNA Polymerase, DNA polymerase I: Large (Klenow) fragment, T4 Polynucleotide Kinase, Klenow Fragment (3′→5′exo–), quick T4 DNA ligase, USER enzyme.

5. NEBuffer 2 for Klenow fragment (3′ → 5′exo–): Kit component, 50 mM NaCl, 10 mM Tris–HCl, 10 mM $MgCl_2$, 1 mM DTT, pH 7.9 at 25 °C.

6. Deoxyadenosine 5′- Triphosphate (dATP): Kit component, 1 mM, supplied in Milli-Q water as a sodium salt at pH 7.5.

7. Quick ligation reaction buffer (2×): Kit component, 132 mM Tris–HCl, 20 mM $MgCl_2$, 2 mM dithiothreitol, 2 mM ATP, 15 % (v/v) Polyethylene glycol (PEG 6000), pH 7.6 at 25 °C.

8. NEBNext Adaptor: Kit component, 15 μM, 5′-/5Phos/GAT CGG AAG AGC ACA CGT CTG AAC TCC AGT C/ideoxyU/A CAC TCT TTC CCT ACA CGA CGC

TCT TCC GAT C*T-3′, where the * indicates a phosphorothioate bond.

9. High-Fidelity 2× PCR Master Mix: Sample kit component.

10. Universal PCR primer: Kit component, 25 µM (*see* **Note 1**), 5′-AAT GAT ACG GCG ACC ACC GAG ATC TAC ACT CTT TCC CTA CAC GAC GCT CTT CCG ATC*T-3′, where the * indicates a phosphorothioate bond.

11. NEBNext Multiplex Oligos for Illumina: Kit component, e.g., Index 1: 5′-CAA GCA GAA GAC GGC ATA CGA GAT CGT GAT GTG ACT GGA GTT CAG ACG TGT GCT CTT CCG ATC-s-T-3′, where -s- indicates a phosphorothioate bond (*see* **Note 2**).

12. Qiagen MinElute PCR Purification and Gel Extraction Kits.

13. PB buffer: Kit component, high concentration of guanidine hydrochloride and isopropanol.

14. MinElute Columns: Kit component.

15. QIAquick spin columns: Kit component.

16. 2 mL collection tubes: Kit component.

17. PE buffer: Kit component.

18. EB buffer: Kit component, 10 mM Tris-Cl, pH 8.5.

19. QG buffer: Kit component.

20. Thermal cycler.

21. Agarose.

22. TAE buffer (1×): 4.84 g Tris base, 1.14 mL acetic acid, pH 8.0. Make up to 1 L

with sterile water.

23. Loading buffer: 50 mM Tris, pH 8.0, 40 mM EDTA, 40 % w/v sucrose.

24. 100 bp DNA ladder (New England Bio Labs Quick-Load 100 bp DNA Ladder).

25. 1 kb DNA ladder (Bioline HyperLadder).

26. Electrophoresis equipment (Bio-Rad Mini-Sub Cell GT System #170-4467 and power source).

27. Dark Reader Transilluminator (Clare Chemical Research).

28. Disposable scalpels.

29. 96–100 % (v/v) ethanol.

30. Isopropanol.

31. Microcentrifuge.

32. Agilent 2100 Bioanalyzer.

33. Agilent High Sensitivity DNA Kit.

34. High Sensitivity DNA Chip: Kit component.

35. Electrode Cleaner: Kit component.

36. Syringe: Kit component.

37. Spin Filters: Kit component.

38. High Sensitivity DNA Ladder: Kit component , 13 DNA fragments from 50 to 7000 bp.

39. High Sensitivity DNA Markers: Kit component, lower marker at 35 bp, upper marker at 10,380 bp.

40. High Sensitivity DNA Dye Concentrate: Kit component.

41. High Sensitivity DNA Gel Matrix: Kit component.

42. IKA MS3 vortex mixer with chip adaptor (Agilent).

43. Electrode cleaner (Agilent).

3 Methods

3.1 Chromatin Preparation and Precipitation

1. Centrifuge 1×10^8 cells at $1710 \times g$ for 5 min, resuspend in 5 mL of cell culture medium to 2×10^7/mL.

2. Add formaldehyde to cell culture medium to a final concentration of 1 % and incubate for 15 min at 20 °C while rocking.

3. Add 625 μL of 1 M glycine, to a final concentration of 0.125 M.

4. Centrifuge cells at $1710 \times g$ for 5 min resuspend in 5 mL of PBS.

5. Centrifuge cells at $1710 \times g$ for 5 min resuspend cells in 3 mL of Cell Lysis Buffer.

6. Incubate on ice for 10 min.

7. Centrifuge at $1710 \times g$ 5 min, and discard supernatant (*see* **Note 3**).

8. Resuspend nuclei in 2 mL SDS lysis buffer.

9. Sonicate nuclear lysate on ice (e.g., using a Branson Model 250 Microtip sonicator) 10×10 s pulses, in a volume of 100 μL with a 21 % output, vortexing the sample after every minute (*see* **Note 4**).

10. Snap freeze and store nuclear chromatin extracts at −80 °C.

11. Mix 1 mL of Protein-A Sepharose beads with 1 mL of Protein-G Sepharose beads (*see* **Note 5**) and 10 mL of IP Dilution Buffer (*see* **Note 6**).

12. Centrifuge beads at $1710 \times g$ for 5 min, and discard supernatant.

13. Add 10 mL of IP Dilution Buffer, centrifug e beads at $1710 \times g$ for 5 min and discard supernatant.

14. Resuspend beads in 5 mL of blocking buffer and incubate at 4 °C while rotating for 30 min.

15. Centrifuge beads at $1710 \times g$ for 5 min and discard supernatant.

16. Resuspend beads in 2 mL of IP dilution buffer.

17. Defrost 2 mL of chromatin and transfer it to a 50 mL falcon tube.

18. Add 18 mL IP dilution buffer.

19. Remove 400 μL and freeze. Label as "input chromatin."

20. Add 1 mL of the blocked protein A-G beads to the remaining 19.4 mL and incubate for 30 min at 4 °C.

21. Centrifuge beads at $1710 \times g$ for 5 min and transfer supernatant into a new 50 mL tube.

22. Add 40 μg of antibody and incubate for 1 h on a rotator.

23. Add 1 mL of blocked protein A-G beads and rotate tubes overnight.

24. Centrifuge beads at $1710 \times g$ for 5 min and add 20 mL low salt wash buffer. Incubate for 10 min on a rotator.

25. Centrifuge beads at $1710 \times g$ for 5 min and add 20 mL high salt wash buffer. Incubate for 10 min on a rotator.

26. Centrifuge beads at $1710 \times g$ for 5 min and add 20 mL LiCl wash buffer. Incubate for 10 min on a rotator.

27. Centrifuge beads at $1710 \times g$ for 5 min and add 20 mL TE buffer. Incubate for 10 min on a rotator.

28. Centrifuge beads at $1710 \times g$ for 5 min and discard supernatant.

29. Add 3 mL of TE/1 % (v/v) SDS at room temperature and incubate the solution at 65 °C for 20 min.

30. Centrifuge beads at $1710 \times g$ for 5 min. Transfer the supernatant to a new tube.

31. Defrost the "input chromatin" control and add 3 mL of TE/1 % (w/v) SDS at room temperature.

32. Incubate the input chromatin and the precipitated chromatin at 65 °C overnight to reverse the cross-links.

33. Add 60 μL of RNAse A and 3 mL of TE to each and incubate at 37 °C for 2 h (*see* **Note 7**).

34. Add 60 μL of proteinase K to each tube and incubate at 55 °C for 2 h (*see* **Note 7**).

35. Purify DNA using the Qiagen MinElute PCR purification kit (*see* **Note 11**). Add ethanol (96–100 %) to buffer PE before use. All centrifugation steps are carried out in a microcentrifuge set to $11,710 \times g$ at room temperature (*see* **Note 12**).

36. Add 15 mL PB buffer to the samples and mix.

37. Place the MinElute column in a provided 2 mL collection tube.

38. Apply 700 µL of the samples to the column and centrifuge for 1 min.

39. Discard the flow-through and place the MinElute column back into the same tube.

40. Repeat **steps 38** and **39** until all of the sample has been centrifuged.

41. Add 750 µL PE buffer to the column, let it stand for 3 min, and centrifuge for 1 min.

42. Discard the flow-through and place the column back into the same tube. Centrifuge the column for an additional minute.

43. Place the MinElute column into a sterile 1.5 mL microcentrifuge tube.

44. Add 42 µL EB buffer to the center of the membrane, let the column stand for 1 min, then centrifuge for 1 min.

45. Add the eluate back to the center of the column, let it stand for 1 min, then centrifuge for 1 min.

3.2 ChIP Library Preparation

1. The NEBNext ChIP-Seq Library Prep Reagent Set is used in combination with the NEBNext Multiplex Oligos for Illumina (Index Primers Set 1), the MinElute PCR purification kit (Qiagen), and the Gel Extraction kit (Qiagen) to prepare the input and ChIP libraries.

2. To end-repair the ChIP and input DNA, measure the concentration of your ChIP

and input samples (*see* **Note 8**).

3. Suspend 10 ng (*see* **Note 9**) of ChIP or input DNA in sterile water to a final volume of 40 µL.

4. Dilute DNA polymerase I, Large (Klenow) Fragment by mixing 1 µL of enzyme with 4 µL of sterile water.

5. Mix the following components in a sterile microcentrifuge tube:

    (a) 20 µL of Phosphorylation Reaction Buffer (10×).

    (b) 4 µL of T4 DNA Polymerase.

    (c) 4 µL of T4 polynucleotide kinase.

    (d) 8 µL of dNTP mix.

    (e) 4 µL of diluted DNA Polymerase I, Klenow Fragment.

6. Add 10 µL of this mix to each sample of the 40 µL ChIP and input DNA.

7. Incubate in a thermal cycler at 20 °C for 30 min (*see* **Note 10**).

8. Purify DNA using the Qiagen MinElute PCR purification kit (*see* **Note 11**). Add ethanol (96–100 % (v/v)) to buffer PE before use. All centrifugation steps are carried out in a microcentrifuge set to $11,710 \times g$ at room temperature (*see* **Note 12**).

9. Add 250 µL PB buffer to the samples and mix.

10. Place the MinElute column in a provided 2 mL collection tube.

11. Apply all traces of the samples to the column and centrifuge for 1 min.

12. Discard the flow-through and place the MinElute column back into the same tube.

13. Add 750 µL PE buffer to the column, stand for 3 min, and centrifuge for 1 min.

14. Discard the flow-through and place the column back into the same tube. Centrifuge the column for an additional minute.

15. Place the MinElute column into a sterile 1.5 mL microcentrifuge tube.

16. Add 35 µL EB buffer to the center of the membrane, let the column stand for 1 min, then centrifuge for 1 min.

17. Add the eluate back to the center of the column, let it stand for 1 min, then centrifuge for 1 min.

18. For dA-tailing of end-repaired DNA, mix the following components in a sterile microcentrifuge tube:

    (a) 20 µL NEBuffer 2 (10×).

    (b) 40 µL Deoxyadenosine 5′-Triphosphate.

    (c) 4 µL Klenow Fragment (3′→5′ exo–).

19. Add 16 µL of this mix to the 34 µL of DNA sample (*see* **Note 13**).

20. Incubate in a thermal cycler for 30 min at 37 °C.

21. Repeat **steps 8–17**, but using 11 µL EB buffer.

22. For the adaptor ligation, dilute the NEBNext Adaptor for Illumina (15 µM) 10-fold in sterile water to a final concentration of 1.5 µM.

23. Mix the following components in a sterile microcentrifuge tube:

    (a) 60 µL of Quick Ligation Reaction Buffer (2×).

    (b) 4 µL of Diluted NEBNext Adaptor (1.5 µM).

    (c) 16 µL of Quick T4 ligase.

24. Add 20 µL of this mix to the 10 µL end-repaired, dA-tailed DNA.

25. Incubate the reaction in a thermal cycler for 15 min at 20 °C (*see* **Note 10**).

26. Add 3 µL USER enzyme, mix by pipetting up and down, and incubate at 37 °C for 15 min.

27. Repeat **steps 8–17**, but using 150 µL PB and 24 µL EB buffer.

28. To PCR enrich the adaptor ligated DNA, mix the following components in a sterile microcentrifuge tube:

    (a) 23 µL adaptor ligated DNA.

    (b) 25 µL NEBNext High-Fidelity 2× PCR Master Mix.

    (c) 1 µL universal PCR primer (25 µM).

    (d) 1 µL Index Primer (one of 12 per sample, e.g., Input: Index 4, ChIP1: Index 6, ChIP2: Index 12).

29. PCR cycling conditions (Table 1):

Table 1 PCR cycling conditions

Cycle step	Temperature (°C)	Time (s)	Cycles
Initial denaturation	98	30	1
Denaturation	98	10	15
Annealing	65	30	
Extension	72	30	
Final extension	4	hold	1

30. Repeat **steps 8–17**, but using 16 µL EB buffer.

31. To size select the library, prepare the required number of 2 % (w/v) agarose gels with 1× TAE buffer (*see* **Note 14**).

32. Add 6 µL loading buffer to the samples and to 15 µL of the 100 bp DNA ladder.

33. Use 1× TAE buffer as running buffer. Load the sample and marker ladders onto the gel(s), leaving at least one space between ladder and samples (*see* **Note 15**).

34. Run the gel at 120 V until the marker dye has reached the bottom of the gel (approximately 60 min).

35. Weigh out three sterile microcentrifuge tubes and label them with their weight.

36. View the gels on the Dark Reader Transilluminator (*see* **Note 16**).

37. Excise the 175–225 bp region of the gel with a clean, disposable scalpel (*see* **Note 17**). Minimize the size of the gel slice by removing excess agarose. Place the selected gel slice into a labeled microcentrifuge tube.

38. Use the Qiagen gel extraction kit to purify the DNA from the agarose slice. All centrifugation steps are carried out in a microcentrifuge set to $11{,}710 \times g$ at room temperature (*see* **Note 12**).

39. Weigh the tubes containing the gel slice and calculate the weight of the agarose.

40. Add three volumes of QG buffer to one volume of gel (i.e., add 300 μL of QG to 100 mg of gel). For gel slices over 400 mg, use more than one tube.

41. Incubate on bench (*see* **Note 18**) for at least 10 min until the gel slice has completely dissolved. Vortex the tube every 2 min during the incubation time.

42. Heat EB buffer to 50 °C.

43. Add one gel volume of isopropanol to the sample (i.e., if the gel slice weight 100 mg, add 100 μL) and mix (*see* **Note 19**).

44. Place the QIAquick spin column in a provided 2 mL collection tube.

45. Apply the sample to the column and centrifuge for 1 min. The maximum volume of the column is 750 μL. For higher sample volumes, load the spin column again after centrifugation.

46. Discard flow-through and place the column back into the same collection tube.

47. Add 500 μL QG buffer to the column and centrifuge for 1 min.

48. Discard flow-through.

49. Add 750 μL of PE buffer to the column and let it stand for 3 min, then centrifuge for 1 min.

50. Discard flow-through a nd centrifuge the column for an additional minute.

51. Place the column into a sterile 1.5 mL microcentrifuge tube.

52. Add 55 μL of EB buffer directly to the center of the column membrane and let the column stand for 1 min, then centrifuge for 1 min.

53. Repeat **steps 8–17**, but using 14 μL EB buffer.

54. Use 1 μL of the purified library sample for quality control on a Bioanalyzer (*see* **Note 20**) using the Agilent High Sensitivity DNA Kit:

55. Let the High Sensitivity DNA dye concentrate and High Sensitivity DNA gel matrix equilibrate to room temperature (*see* **Note 21**).

56. Vortex the vial with High Sensitivity DNA dye concentrate for 10 s and spin down. Making sure that the DMSO is completely thawed.

57. Pipette 15 μL of the dye concentrate into a High Sensitivity DNA gel matrix vial (*see* **Note 22**).

58. Return the dye concentrate to 4 °C to store, protecting it from light.

59. Cap the tube, vortex for 10 s. Make sure that the gel and dye are mixed properly.

60. Transfer the gel—dye mix to the top receptacle of the spin filter.

61. Spin for 10 min at 2400 × g at room temperature in a microcentrifuge.

62. Discard the filter and label the tube (*see* **Note 23**).

63. Ensure that the base plate of the chip priming station is in position C and that the adjustable clip is set to the lowest position.

64. Place a new High Sensitivity DNA chip onto the chip priming station.

65. Placing the pipette tip at the center of the well, pipette 9 μL of the gel—dye mix (which is at room temperature) to the bottom of the well located in the right (fourth) column and third row.

66. Set a timer to 1 min and make sure that the plunger is positioned at 1 mL. Then close the chip priming station.

67. Press the syringe plunger down until it is held by the clip, then start the timer.

68. Release the plunger after exactly 1 min.

69. Make sure that the plunger moves back at least to the 0.3 mL mark.

70. Wait 5 s before slowly pulling back the plunger to the 1 mL position.

71. Open the chip priming station and pipette 9 μL of the gel—dye mix into the three empty wells of the right (fourth) column.

72. Return the gel—dye mix to 4 °C to store, protecting it from light.

73. Pipette 5 μL of the High Sensitivity DNA marker into each of the empty wells (first three columns) (*see* **Note 24**).

74. Pipette 1 μL of the High Sensitivity DNA ladder into the well marked with the ladder symbol (third column, fourth row).

75. Pipette 1 μL of sample (*see* **Note 25**) or 1 μL of marker (for otherwise empty wells) into each well of the first three columns, except the well with the ladder symbol.

76. Carefully place the chip horizontally into the vortex adapter and vortex for 1 min at 2400 rpm.

77. Place the chip carefully into the receptacle of the Bioanalyzer, making sure that the run is started within 5 min.

78. Carefully close the lid (*see* **Note 26**) and start the chip run. Use the dsDNA assay and fill in the sample name table.

79. After the run is finished dispose of the chip.

80. Slowly fill one of the wells of the electrode cleaner (*see* **Note 27**) with 350 µL sterile water.

81. Place the electrode cleaner in the Bioanalyzer, then close the lid and leave it for about 10 s.

82. Remove the electrode cleaner and wait another 10 s to allow the water on the electrodes to evaporate.

83. For a good quality sample, the electropherogram should show no peak in the 100 bp region, with a high peak around 200 bp (*see* Fig. 1). If there is a peak in the adaptor region (as indicated by the blue box), the sample is contaminated and sequencing may not yield successful results.
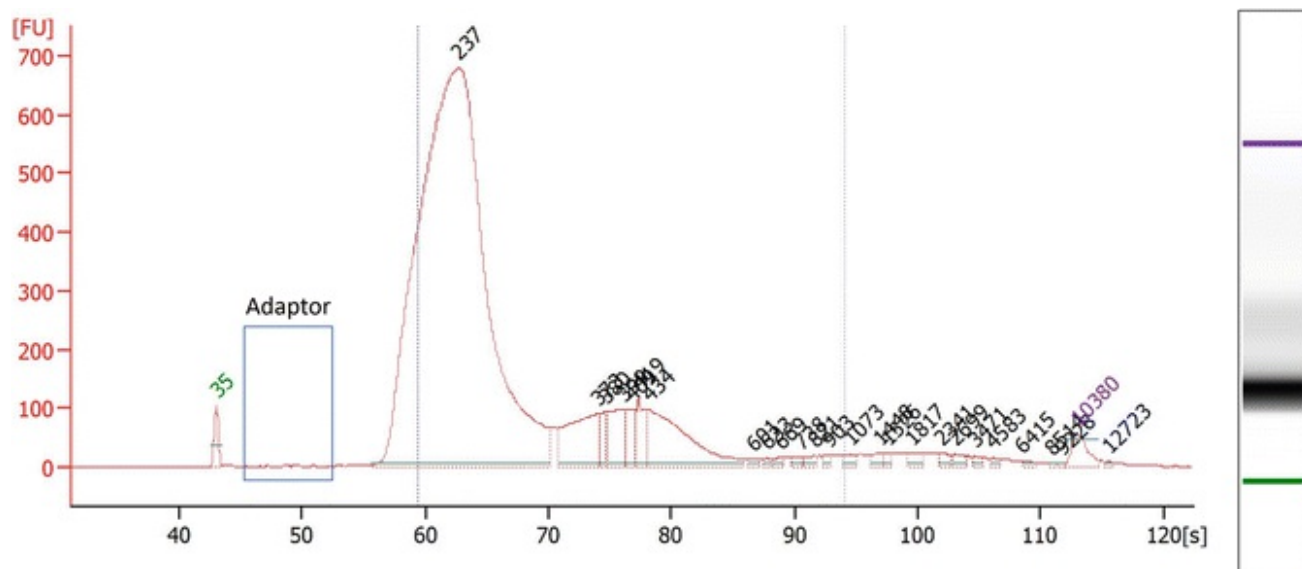
Fig. 1 Bioanalyzer Electropherogram showing fluorecense units [FU] on the *y*-axis and seconds [s] on the *x*-axis, with numbers above peaks indicating the fragment size in base pairs (bp). A single high peak around 200 bp and no peak in the 100 bp Adapotor region has been detected

4 Notes

1. Concentrations of universal PCR Primer and the Index Primers contained in the NEB kit have changed from 25 to 10 µM. Refer to the most recent protocol for use.

2. 12 Index Primers are included in the NEBNext Multiplex Oligos for Illumina (Index Primers Set 1) kit for producing barcoded libraries. Refer to the manual for sequence information. If fewer than 2 indexes per lane are used, NEB recommends the combination of the following indexes for best demultiplexing results:

   (a) Pool of 2 samples: Index 6 and 12.

   (b) Pool of 3 samples: Index 4, 6, and 12.

   (c) Pool of 6 samples: Index 2, 4, 5, 6, 7, and 12.

3. After the addition of cell lysis buffer all steps are undertaken at 4 °C unless specified.

4. Sonication is critical. The ideal fragment size for ChIP sequencing is 200 bp. Appropriate conditions will vary with each sonicator and can be checked by undertaking a time course of sonication, incubating at 65 °C overnight to reverse the cross-links. This is followed by purifying the DNA and analyzing size distribution on an agarose gel. Figure 2 shows the results of two different sonication protocols. The gel on the left shows a sub-ideal chromatin sonication for ChIP-Seq purposes. The gel on the right, using the second chromatin sonication protocol, shows a good fragmentation around 200 bp.
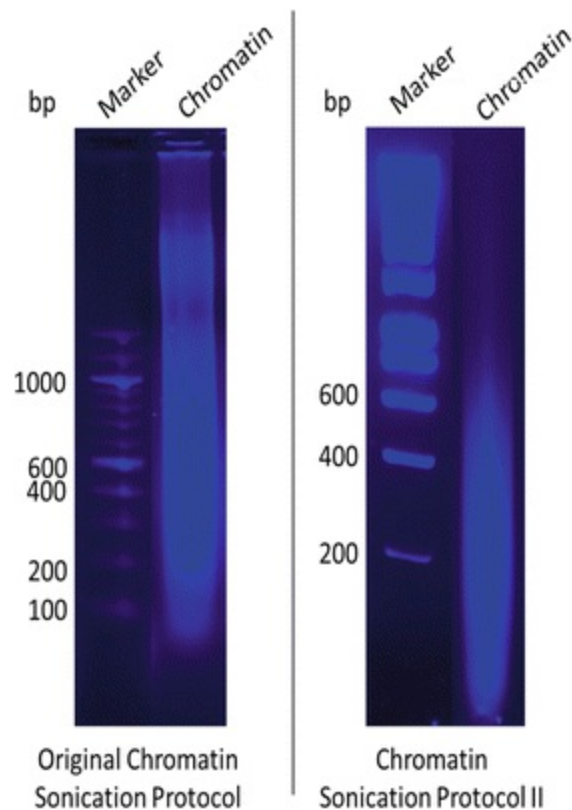
Fig. 2 Agarose gel showing the size, in base pairs (bp), of sonicated chromatin fragments, using two different chromatin sonication protocols (*left* and *right*)

5. Protein A and Protein G sepharose beads should be stored at 4 °C in 70 % (v/v) ethanol, then washed with IP dilution buffer prior to use.

6. Add protease inhibitor cocktail (Sigma) and 1 mM PMSF to all buffers just before use.

7. Proteinase K and RNAase can be stored as aliquots at −20 °C.

8. We found that the Qubit Fluorometer worked well for this step. The concentration of our ChIP samples was too low to be measured accurately using a NanoDrop Spectrophotometer.

9. The kit calls for 10 ng of DNA, but we have previously used 18 ng to ensure maximum library concentration. In our experience, this did not seem to impair the quality of the final library.

10. Our laboratory tends to be around 20 °C. We incubate this reaction on the bench rather than in a thermal block cycler and still get good results.

11. If using the Qiagen kit, it is important for the efficiency of this purification process that centrifugation steps are actually carried out at room temperature.
    Alternatively, it is possible to clean up the sample using AMPure XP Beads (Beckman Coulter, Inc.).

12. Qiagen suggests that buffer QG from the GelExtraction kit may be used to remove salt and proteins from samples. Do not use buffer QG outside of the gel extraction during the library preparation.

13. The sample was eluted in 35 µL, but a small amount will remain in the column; hence, the DNA is already in the correct 34 µL volume required for the following step.

14. Make sure that the comb creating the sample wells in the agarose gel is precisely straight to ensure that the sample and markers run exactly vertically on the gel. If the samples and markers run at an angle, it is more difficult to be sure of the exact size to select on the gel, which can lead to adaptor contamination.

15. It is important to select the correct sample size, we suggest running each sample with two markers on each side, as shown in the scheme below.

Marker 1	Marker 2	Sample	Marker 1	Marker 2

16. The Dark Reader Transilluminator allows the visualization of the DNA on the gel for excision of the desired size while avoiding UV exposure that may be harmful to the DNA sample.

17. Make sure not to cut out any of the light adaptor band (below 150 bp). It is advisable to take a photograph of the gel before and after the excision.

18. Do not heat the samples to 55 °C as stated in the GelExtraction kit protocol.

19. Do not centrifuge the sample at this point.

20. If you are unable to perform quality control of your sample using a bioanalyzer, your sequencing facility may be able to perform this step for you. In this case, we recommend performing a qPCR analysis of a target that is known/thought to be enriched before sending your samples off.

21. Make sure to protect the DNA dye concentrate from light.

22. Use the indicated volumes. Different volumes at the same ratio can produce inaccurate results.

23. Shield the gel—dye mix from light and store at 4 °C. It is sufficient for five chips. Use within 6 weeks of preparation.

24. Even if you have less than 11 samples, do not leave any wells empty; otherwise, the chip will not run properly.

25. Samples should be dissolved in 10 mM Tris and 1 mM EDTA for optimal results. However, we have achieved good results with our samples in EB buffer.

26. Never use force to close the lid or drop the lid onto the chip. This may damage the electrodes or cause liquid spills leading to bad results.

27. A more thorough c lean may be required when switching between different types

of assay.

Acknowledgment

References

1. Kimura H (2013) Histone modifications for human epigenome analysis. J Hum Genet 58:439–445
[CrossRef][PubMed]

2. Longnecker R, Kieff E, Cohen JI (2013) In: Knipe D, Howley P (eds.), Fields Virology, 6th edn. Lippincott Williams & Wilkins (Philadelphia, Pennsylvania, United States)

3. Bergbauer M, Kalla M, Schmeinck A, Gobel C, Rothbauer U, Eck S, Benet-Pages A, Strom TM, Hammerschmidt W (2010) CpG-methylation regulates a class of Epstein-Barr virus promoters. PLoS Pathog 6:e1001114
[CrossRef][PubMed][PubMedCentral]

4. Holdorf MM, Cooper SB, Yamamoto KR, Miranda JL (2011) Occupancy of chromatin organizers in the Epstein-Barr virus genome. Virology 415:1–5
[CrossRef][PubMed]

5. Ramasubramanyan S, Osborn K, Flower K, Sinclair AJ (2012) Dynamic chromatin environment of key lytic cycle regulatory regions of the Epstein-Barr virus genome. J Virol 86:1809–1819
[CrossRef][PubMed][PubMedCentral]

6. Woellmer A, Arteaga-Salas JM, Hammerschmidt W (2012) BZLF1 governs CpG-methylated chromatin of Epstein-Barr Virus reversing epigenetic repression. PLoS Pathog 8:e1002902
[CrossRef][PubMed][PubMedCentral]

7. Jiang S, Willox B, Zhou H, Holthaus AM, Wang A, Shi TT, Maruo S, Kharchenko PV, Johannsen EC, Kieff E et al (2014) Epstein-Barr virus nuclear antigen 3C binds to BATF/IRF4 or SPI1/IRF4 composite sites and recruits Sin3A to repress CDKN2A. Proc Natl Acad Sci U S A 111:421–426
[CrossRef][PubMed]

8. McClellan MJ, Wood CD, Ojeniyi O, Cooper TJ, Kanhere A, Arvey A, Webb HM, Palermo RD, Harth-Hertle ML, Kempkes B et al (2013) Modulation of enhancer looping and differential gene targeting by Epstein-Barr virus transcription factors directs cellular reprogramming. PLoS Pathog 9:e1003636
[CrossRef][PubMed][PubMedCentral]

9. Ramasubramanyan S, Osborn K, Al-Mohammad R, Naranjo Perez-Fernandez IB, Zuo J, Balan N, Godfrey A, Patel H, Peters G, Rowe M et al (2015) Epstein-Barr virus transcription factor Zta acts through distal regulatory elements to directly control cellular gene expression. Nucleic Acids Res 43:3563–3577
[CrossRef][PubMed][PubMedCentral]

10. Kellis M, Wold B, Snyder MP, Bernstein BE, Kundaje A, Marinov GK, Ward LD, Birney E, Crawford GE, Dekker J et al (2014) Defining functional DNA elements in the human genome. Proc Natl Acad Sci U S A 111:6131–6138
[CrossRef][PubMed][PubMedCentral]

11. Arvey A, Tempera I, Tsai K, Chen HS, Tikhmyanova N, Klichinsky M, Leslie C, Lieberman PM (2012) An atlas of the Epstein-Barr virus transcriptome and epigenome reveals host-virus regulatory interactions. Cell Host Microbe 12:233–245
[CrossRef][PubMed][PubMedCentral]

12. Ramasubramanyan S, Kanhere A, Osborn K, Flower K, Jenner RG, Sinclair AJ (2012) Genome-wide analyses of Zta binding to the Epstein-Barr virus genome reveals interactions in both early and late lytic cycles and an epigenetic switch leading to an altered binding profile. J Virol 86:12494–12502
[CrossRef][PubMed][PubMedCentral]

15. Analysis of Viral Epigenotypes Using Bisulfite Sequencing: A Detailed Protocol for the Crucial Bisulfite Modification and PCR Amplification Steps

Daniel Salamon[1]✉

(1) Department of Microbiology, Tumor and Cell Biology, Karolinska Institutet, Nobels väg 16, SE-171 77 Stockholm, Sweden

✉ **Daniel Salamon**
   Email: Daniel.salamon@ki.se

Abstract
Characterization of viral DNA methylation patterns is essential to understand its function in viral pathogenesis. Bisulfite modification, followed by polymerase chain reaction (PCR) and sequencing is the most effective method for the high resolution methylation mapping of viral genomes. Since the bisulfite modification and PCR steps are the most critical ones, an optimized protocol for these two steps is presented, with special attention to potential pitfalls.

Key words Virus – DNA methylation – Bisulfite modification – Polymerase chain reaction – Primer design – Sequencing

1 Introduction

DNA methylation plays an important role in the control of the latent and/or lytic state of several viruses [1–3]. High resolution methylation mapping of episomal and/or integrated viral genomes is essential to understand the function of DNA methylation in these viruses [4]. Current high resolution methylation mapping techniques are based on

sodium bisulfite modification of purified DNA. During this reaction unmethylated cytosines convert to uracils and are therefore amplified as thymines, while methylated cytosines remain unconverted and amplified as cytosines in the subsequent amplification steps [5, 6]. Although the sequence of bisulfite modified DNA can be analyzed with several different techniques, sequencing is the most effective method to measure DNA methylation levels at one nucleotide resolution. Sequencing can be either region-specific or genome-wide. Since the length of most viral genomes is relatively small compared to the human genome, their DNA methylation patterns are analyzed particularly by region-specific sequencing. This type of sequencing starts with the PCR amplification of the bisulfite modified region of interest, followed by sequencing the PCR product directly [7–12] or after cloning [5, 6]. Direct sequencing allows fast, semi-quantitative measurement of the average methylation level at each cytosine, but provides no information about methylation pattern heterogeneity (for a representative result *see* Fig. 1). Furthermore, accurate quantification of DNA methylation level from the raw direct sequencing data is often difficult, although correction algorithm retrieving imbalanced and overscaled signals is available [11]. The advantage of indirect sequencing is that it determines cytosine methylation pattern for each individual amplicon. On the other hand, cloning biases may affect the result [16], and the need for sequencing a high number of clones for statistical accuracy makes this method expensive, labor-intensive and time-consuming. While the selection of the appropriate region-specific sequencing technique greatly depends on the available laboratory resources, the bisulfite modification and PCR steps can easily be accomplished in any laboratory. Hence, and because the bisulfite modification and PCR steps are the most critical ones, this chapter covers only these two parts of the whole method.
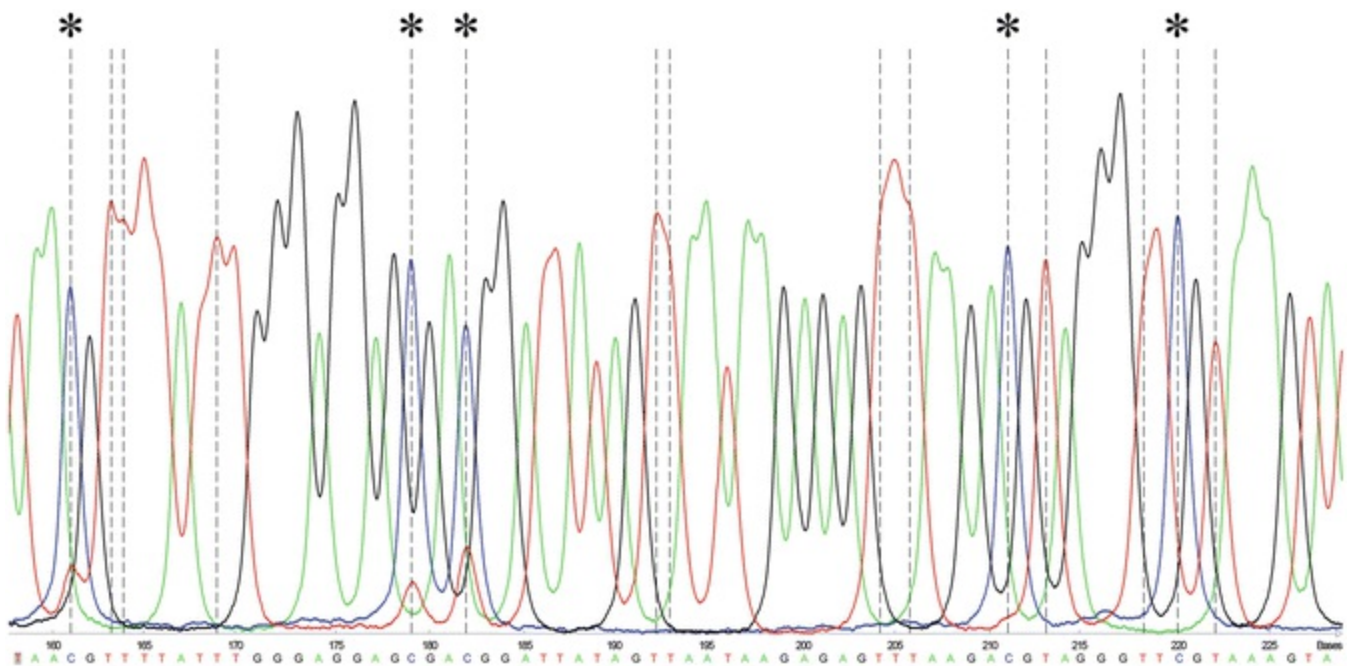
Fig. 1 Raw direct sequencing data of the C-promoter (Cp) of Epstein-Barr virus (EBV), obtained from bisulfite modified C2G6 DNA. DNA purified from the C2G6 cell line [13] was bisulfite modified and amplified in a nested PCR with primers specific for the Cp of EBV [14]. One of the nested primers was biotin labeled, while the other carried 15 bases of the M13 universal primer sequence at its 5′ end. The second PCR product was purified with streptavidin-coated magnetic beads, and the biotin-labeled strand was sequenced with the fluorescein-labeled M13 universal primer as described by Myöhänen et al. [7]. The reaction product was separated on an acrylamide gel using an automated DNA sequencer. The Cp region is shown between nucleotides 11,041 and 11,111 (according to the prototype B95-8 sequence [15]). *Vertical dashed lines* indicate positions of cytosines in the unmodified DNA sequence. *Stars above the lines* indicate positions of cytosines within cytosine–guanine dinucleotides (CpG)

2   Materials

Freshly prepare all solutions using DNase/RNase-free distilled water. Unless otherwise specified, prepare and store all reagents at room temperature. Do not vortex the solutions unless indicated otherwise. Use filter tips. Strictly follow waste disposal regulations when disposing of waste materials.

1.   Purified genomic or viral DNA dissolved in water (*see* **Note 1**).

2.   3 and 5 M sodium hydroxide solutions: Add 12 or 20 g of sodium hydroxide pellets to 80 mL of water, while stirring with a magnetic stirring bar (*see* **Note 2**). After the pellets have completely dissolved, make up to a final volume of 100 mL with water. Sterilization is not required.

3.   10 mM hydroquinone solution (*see* **Note 3**): Dissolve 55 mg hydroquinone without vigorous shaking in 45 mL water. Make up to a final volume of 50 mL with water and sterilize by filtration.

4.   3.6 M sodium bisulfite solution, pH 5.0 (*see* **Note 3**): Dissolve 2.256 g of sodium bisulfite (e.g., Sigma-Aldrich) without vigorous shaking in 4.5 mL water. Adjust the pH to 5.0 with the addition of 370 μL freshly prepared 5 M sodium hydroxide. Make up to a final volume of 5 mL with water and sterilize by filtration.

5.   Mineral oil, molecular biology grade.

6.   One of the appropriate GeneClean Kits (e.g., MP Biomedicals).

7.   10 M ammonium acetate solution: Dissolve 385.4 g molecular biology grade

ammonium acetate in 400 mL of water. Make up to a final volume of 500 mL with water and sterilize by filtration.

8. 20 mg/mL glycogen, molecular biology grade.

9. FastStart High Fidelity PCR System, dNTPack (e.g., Roche) (*see* **Note 4**).

10. Oligonucleotide primers (*see* **Note 5**).

---

3 Methods

Perform all procedures at room temperature unless otherwise specified. Do not vortex the samples unless indicated (bisulfite modified DNA is highly fragile). Use filter tips.

3.1 Bisulfite Modification of Purified Genomic DNA

1. Adjust the volume of the DNA solution (containing 50 ng–5 µg DNA) to 40 µL with DNase/RNase-free distilled water. Add 4.4 µL freshly prepared 3 M sodium hydroxide, vortex gently, spin down and incubate at 37 °C for 15 min.

2. Add 24.4 µL 10 mM hydroquinone solution and mix by pipetting. Add 424 µL 3.6 M sodium bisulfite solution, mix by pipetting and dispense five 98 µL aliquots into 0.5 mL PCR tubes. Overlay the aliquots with 100 µL of mineral oil and incubate in a thermocycler (*see* **Note 6**) at 95 °C for 1 min, followed by five cycles of 95 °C for 3 min, 57 °C for 57 min (*see* **Note 7**).

3. Recover the bisulfite treated DNA solution from under the mineral oil layer (*see* **Note 8**), and purify the DNA using one of the GeneClean Kits or another system appropriate for the purification of single-stranded DNA, according to the manufacturer's instructions. Elute or resuspend the purified DNA in 100 µL DNase/RNase-free distilled water in a 1.5 mL Eppendorf tube.

4. Add 11 µL freshly prepared 3 M sodium hydroxide, mix by pipetting and incubate at 37 °C for 15 min.

5. Add 0.5 µL 20 mg/mL glycogen (*see* **Note 9**), 47 µL 10 M ammonium acetate and

500 µL 100 % ethanol, mix by pipetting and incubate overnight at −20 °C.

6. Centrifuge at maximum speed in a microfuge for 20 min at 4 °C . Carefully decant the supernatant. Add 800 µL 70 % ethanol. Spin at maximum speed in a microfuge for 5 min at 4 °C. Carefully decant the supernatant. Air-dry for a few minutes and then dissolve the pellet in an appropriate volume of DNase/RNase-free distilled water.

7. Quantify modified DNA by spectrophotometric measurement or any other more specific method (*see* **Note 10**). Store the bisulfite modified DNA at −20 °C (*see* **Note 11**).

3.2 PCR Amplification of Bisulfite Modified Genomic DNA

1. Amplify the bisulfite modified DNA with the FastStart High Fidelity PCR System, dNTPack, according to the manufacturer's instructions, with minor modifications. The 50 µL PCR contains 5 µL FastStart High Fidelity Reaction Buffer (10× conc. with 18 mM $MgCl_2$ (*see* **Note 12**)), 1 µL PCR Grade Nucleotide Mix (to obtain a 200 µM final concentration of each dNTP), 0.6 µM final concentration of each primer, 5–250 ng bisulfite modified DNA, 0.5 µL (5 U/µL) FastStart High Fidelity Enzyme Blend, and DNase/RNase-free distilled water up to 50 µL.

2. Incubate the reaction in a thermocycler at 95 °C for 2 min, followed by 35 cycles of 95 °C for 30 s, 50–72 °C (*see* **Notes 12** and **13**) for 30 s, 72 °C for 0.5 - 3 min (*see* **Note 14**) and then 72 °C for 7 min. For products larger than 3 kb incubate the reaction in a thermocycler at 94 °C for 2 min, followed by ten cycles of 94 °C for 30 s, 50–68 °C (*see* **Notes 12** and **13**) for 30 s, 68 °C for 3–5 min (*see* **Note 14**), followed by 30 cycles of 94 °C for 30 s, 50–68 °C (*see* **Notes 12** and **13**) for 30 s, 68 °C for 3–5 min (*see* **Note 13**) with an extra 20 s of 68 °C after each successive cycle, and then 68 °C for 7 min.

3. If further amplification is necessary, dilute the first PCR product 100× with DNase/RNase-free distilled water and use 1 µL in a nested PCR with similar conditions, but containing 0.2 µM final concentration of each nested primer.

4. Visualize an aliquot of the PCR product on a 1–2 % agarose gel.

4 Notes

1. Any methods and kits can be used to isolate genomic or viral DNA, which provides pure, protein free DNA [16]. Fragment size reduction of high-molecular-weight DNA is unnecessary. Control reactions with fully methylated and unmethylated DNA (commercially available; for a detailed list see Hernandez et al. [17]) are also recommended to run in parallel with experimental samples to monitor the efficiency of conversion.

2. Preparation of concentrated sodium hydroxide solution is accompanied by an exothermic reaction. To avoid breakage, the glass beaker can be placed in a container of ice. Avoid skin contact.

3. Hydroquinone and sodium bisulfite are toxic chemicals. Avoid skin contact and inhalation. Weigh in a safety cabinet. Hydroquinone and sodium bisulfite solutions are light sensitive, and therefore should be protected from light.

4. Most commercially available Taq polymerases sufficiently amplify bisulfite modified DNA. However, high cycle number PCR amplification with Taq polymerase may lead to the accumulation of sequence errors, resulting in the appearance of false negative and/or false positive cytosine methylation [16]. This bias is especially important, if the PCR products are cloned before sequencing. Therefore, a higher fidelity polymerase, which tolerates uracil in the DNA template is recommended to use for high cycle number PCR amplification of bisulfite modified DNA.

5. Primers should be designed under the assumption that all cytosines (C) outside of CpGs convert to uracil during bisulfite modification. Since the two DNA strands are no longer complementary after bisulfite modification, separate primer pairs must be designed for each. Modified DNA essentially contains only three bases, increasing the probability of nonspecific primer annealing. Therefore, optimal primer sequences are usually longer (~24–30 base pairs) than in conventional PCR. The primer binding site should not contain cytosines of CpGs, to ensure equal amplification of both unmethylated and methylated templates. If a primer must reside on a cytosines(s) of a CpG(s) degenerate bases(s) must be used at that(those) positions(s): Y (cytosine or thymine) instead of cytosine in the forward primer, while R (adenine or guanine) instead of guanine must be used in the

reverse primer. On the other hand, the presence of non-CpG cytosines in the primer binding site is favorable, as it may avoid the amplification of insufficiently converted DNA. Since bisulfite modified DNA is usually highly fragmented, the optimal length of the PCR product is less than 500 bp. Several free online tools are also available to support the design of primers specific for bisulfite modified DNA [17]. Take into account the potential sequence differences between viral strains. If necessary, determine the sequence of the analyzed region in the particular viral strain before designing primers. For primers less than 35 bases in length desalting is a sufficient method of purification. For longer primers additional purification is recommended.

6. The bisulfite conversion reaction is light sensitive and must take place in the dark (use a thermocycler with a non-transparent lid).

7. Alternatively, when the starting DNA amount is below 200 ng, the aliquots can be incubated in a thermocycler at 98 °C for 8 min, followed by 55 °C for 60 min. This protocol may increase DNA yield, without significantly decreasing conversion efficiency.

8. Although minimal residual oil may not affect the purification process, the oil layer can easily be removed after snap freezing the aliquots and pipetting off the unfrozen oil.

9. Addition of glycogen as a carrier may not be needed, if the starting DNA amount is more than 1 µg. Other carriers like linear acrylamide, tRNA, or salmon sperm DNA are also suitable.

10. Choose a quantification method which is capable to measure single stranded DNA. Use settings for single-stranded DNA during spectrophotometric measurement.

11. Under these conditions the modified DNA is stable for at least 6 months.

12. Optimal adjustment of $MgCl_2$ concentrations and annealing temperatures may prevent false priming and the potential bias in the amplification efficiency of differentially methylated alleles [16, 18, 19].

13. Depending on the melting temperatures of the primers.

14. Depending on the length of the product to be amplified (~1 min/kb).

Acknowledgment

References

1. Ay E, Banati F, Mezei M et al (2013) Epigenetics of HIV infection: promising research areas and implications for therapy. AIDS Rev 15:181–188
   [PubMed]

2. Chen HS, Lu F, Lieberman PM (2013) Epigenetic regulation of EBV and KSHV latency. Curr Opin Virol 3:251–259
   [CrossRef][PubMed][PubMedCentral]

3. Johannsen E, Lambert PF (2013) Epigenetics of human papillomaviruses. Virology 445:205–212
   [CrossRef][PubMed]

4. Fernandez AF, Rosales C, Lopez-Nieva P et al (2009) The dynamic DNA methylomes of double-stranded DNA viruses associated with human cancer. Genome Res 19:438–451
   [CrossRef][PubMed][PubMedCentral]

5. Frommer M, McDonald LE, Millar DS et al (1992) A genomic sequencing protocol that yields a positive display of 5-methylcytosine residues in individual DNA strands. Proc Natl Acad Sci U S A 89:1827–1831
   [CrossRef][PubMed][PubMedCentral]

6. Clark SJ, Harrison J, Paul CL et al (1994) High sensitivity mapping of methylated cytosines. Nucleic Acids Res 22:2990–2997
   [CrossRef][PubMed][PubMedCentral]

7. Myöhänen S, Wahlfors J, Jänne J (1994) Automated fluorescent genomic sequencing as applied to the methylation analysis of the human ornithine decarboxylase gene. DNA Seq 5:1–8
   [CrossRef][PubMed]

8. Paul CL, Clark SJ (1996) Cytosine methylation: quantitation by automated genomic sequencing and GENESCAN analysis. Biotechniques 21:126–133
   [PubMed]

9.

Colella S, Shen L, Baggerly KA et al (2003) Sensitive and quantitative universal Pyrosequencing^{TM} methylation analysis of CpG sites. Biotechniques 35:146–150
[PubMed]

10. Tost J, Dunker J, Gut IG (2003) Analysis and quantification of multiple methylation variable positions in CpG islands by Pyrosequencing. Biotechniques 35:152–156
[PubMed]

11. Lewin J, Schmitt AO, Adorjan P et al (2004) Quantitative DNA methylation analysis based on four-dye trace data from direct sequencing of PCR amplificates. Bioinformatics 20:3005–3012
[CrossRef][PubMed]

12. Han W, Cauchi S, Herman JG et al (2006) DNA methylation mapping by tag-modified bisulfite genomic sequencing. Anal Biochem 355:50–61
[CrossRef][PubMed]

13. Arbach H, Viglasky V, Lefeu F et al (2006) Epstein-Barr virus (EBV) genome and expression in breast cancer tissue: effect of EBV infection of breast cancer cells on resistance to paclitaxel (Taxol). J Virol 80:845–853
[CrossRef][PubMed][PubMedCentral]

14. Salamon D, Takacs M, Ujvari D et al (2001) Protein-DNA binding and CpG methylation at nucleotide resolution of latency-associated promoters Qp, Cp, and LMP1p of Epstein-Barr virus. J Virol 75:2584–2596
[CrossRef][PubMed][PubMedCentral]

15. Baer R, Bankier AT, Biggin MD et al (1984) DNA sequence and expression of the B95-8 Epstein-Barr virus genome. Nature 310:207–211
[CrossRef][PubMed]

16. Warnecke PM, Stirzaker C, Song J et al (2002) Identification and resolution of artifacts in bisulfite sequencing. Methods 27:101–107
[CrossRef][PubMed]

17. Hernández HG, Tse MY, Pang SC et al (2013) Optimizing methodologies for PCR-based DNA methylation analysis. Biotechniques 55:181–197
[CrossRef][PubMed]

18. Warnecke PM, Stirzaker C, Melki JR et al (1997) Detection and measurement of PCR bias in quantitative methylation analysis of bisulphite-treated DNA. Nucleic Acids Res 25:4422–4426
[CrossRef][PubMed][PubMedCentral]

19. Shen L, Guo Y, Chen X et al (2007) Optimizing annealing temperature overcomes bias in bisulfite PCR methylation analysis. Biotechniques 42:48–58
[CrossRef][PubMed]

16. Analysis of Viral Epigenotypes Using Chromatin Immunoprecipitation

Ferenc Bánáti[1]✉ and Kálmán Szenthe[1]

(1) RT-Europe Nonprofit Research Ltd., Vár 2, Dunacsunyi ut, Szigetköz building, Mosonmagyaróvár, H-9200, Hungary

✉ **Ferenc Bánáti**
Email: fbanati@yahoo.co.uk

Abstract
Chromatin Immunoprecipitation (ChIP) is a method used to detect DNA-protein interactions in vivo. ChIP has been widely applied to assess the abundance of various epigenetic regulators, including modified histones, in various regions of cellular and viral chromatin. During the procedure, DNA binding proteins are covalently cross-linked to DNA, and the isolated chromatin is broken into pieces of 300–500 bps in length on average. Thereafter, using specific antibody directed against the protein of interest the covalently cross-linked DNA is pulled down together with Protein A or G carrying beads that bind the Fc fragment of the antibody. After the reversal of crosslinks and DNA isolation, one may analyze the precipitated DNA fragments by quantitative and qualitative methods to assess the relative abundance of the examined protein in a region or within the genome studied in vivo. In addition to the analysis of transcription factor binding, ChIP has proved to be a reliable method to map histone modifications across cellular and viral epigenomes.

Key words Protein-DNA interaction – In vivo – Chromatin – Epigenetics

1 Introduction
The field of epigenetics originated from developmental biology and embryogenesis as

the term "epigenetics" was coined by Conrad H. Waddington in 1942 who described the epigenetic landscape mechanism in cell fate determination in the late 1950s (reviewed in [1–3]). Originally, epigenetics stood for "The science concerned with the causal analysis of development." In those days the mechanisms behind phenotypic differences notwithstanding identical genomes was beyond the scope of knowledge, and only in 1975 was it proposed that 5-methyl cytosine may play a role in influencing gene activity [4, 5]. The importance of nucleosomal chromatin arrangement and chromatin remodeling complexes was discovered and extensively studied from the late 1980s [6]. Many different histone modifications were implicated and demonstrated to play a role in genetic regulations alone or in combinations [7]. As the time went on, the term epigenetics gained another meaning, such as the study of changes in gene function that are mitotically and/or meiotically heritable and that do not entail a change in DNA sequence [8].

1.1 Epigenotypes

The main role of epigenetic regulations is to assure and coordinate the expression of genetic information at the right time and in the right place and amount via the modulation of the chromatin structure and the binding of different transcription factors. These mechanisms manifest at the gene expression level and influence all the important biological processes within a cell. Epigenetic dysregulation can be involved however, in tumorigenic processes [9–11]. The main epigenetic mechanisms in mammals affecting gene regulation are DNA methylation and hydroxymethylation at CpG palindrome dinucleotides, modification of histon e side chains with acetyl, methyl, phosphoryl, ubiquitin, sumoyl groups [12] and the binding of Polycomb/Trithorax protein complexes. Generally, cytosine methylation of regulatory sequences flanking RNA polymerase II-transcribed promoters results in the inhibition of gene expression [11]. The effect of histone modifications on gene activity is very complex and depends on other modifications; some possess inhibiting, others have activating properties [7]. These modifications are associated with lysine and arginine side chains. Polycomb and Trithorax group proteins with blocking and upregulating activity also modify histone tails and form stable complexes with the DNA [13–15].

In addition to host cell genomes, complex viral genomes are also regulated via epigenetic mechanisms. The relevance of epigenetic gene regulation in latent herpesvirus infections was documented and reviewed by several research groups [16–18]. Latency, an important property of all three herpesvirus subfamilies (α, β, γ), enables the long-term maintenance of viral genomes within the host cell's nucleus without lytic replication . In case of several herpesviruses, distinct patterns of gene expression can be observed in the latent phase of infection. In latent EBV infection only a small proportion of the approximately 70 viral genes is expressed. Depending on C

and Q promoter usage directing the transcription of Epstein-Barr virus Nuclear Antigens (EBNAs) and in combination with the expression of Latent Membrane proteins (LMPs), numerous latency gene expression patterns were observed, classified as EBV latency types. Because these latency types are associated with discrete epigenetic marks, the epigenotypes of EBV were directly linked to the viral latency types [19].

Due to the developments in ChIP-coupled methods, the examination of activating and inhibitory histone modifications and the exploration of modified cytosines can be efficiently performed within viral genomic regions or even within complete viral genomes choosing the appropriate ChIP-based protocol (see more details about ChIP methods below).

In this chapter, we focus on the use of ChIP for the characterization of epigenetic marks, especially histone modifications of latent EBV episomes. For the analysis of the other major epigenetic mark , CpG methylation, *see* chapter 15 by Salamon, D.

1.2 Chromatin Immunoprecipitation

The history of Chromatin Immunoprecipitation began ca 30 years ago, when Lis and coworkers (1984) examined in vivo protein-DNA interactions in bacteria and *Drosophila melanogaste r* [20, 21]. The methodology was developed further by Solomon et al. (1988) applying formaldehyde instead of UV crosslinking [22]. In these early times the detection of the isolated DNA was based on nucleic acid hybridization. The method was not as widely used as nowadays until the early 2000s when quantitative real-time PCR (qPCR) was added in practice as a subsequent quantification method after DNA isolation [23]. When omitting cross linking agents, native chromatin can also be sheared using micrococcal nucleases. This ChIP approach is also called native or N-ChIP permitting mainly the examination of nucleosomal arrangement and to a lesser extent transcription factor occupancy. N-ChIP has several advantages and disadvantages compared to X-ChIP (cross-linking ChIP) based on treatment with crosslinking agents. For more details *see* refs. 24, 25. The schematic view of X-ChIP is presented in Fig. 1.
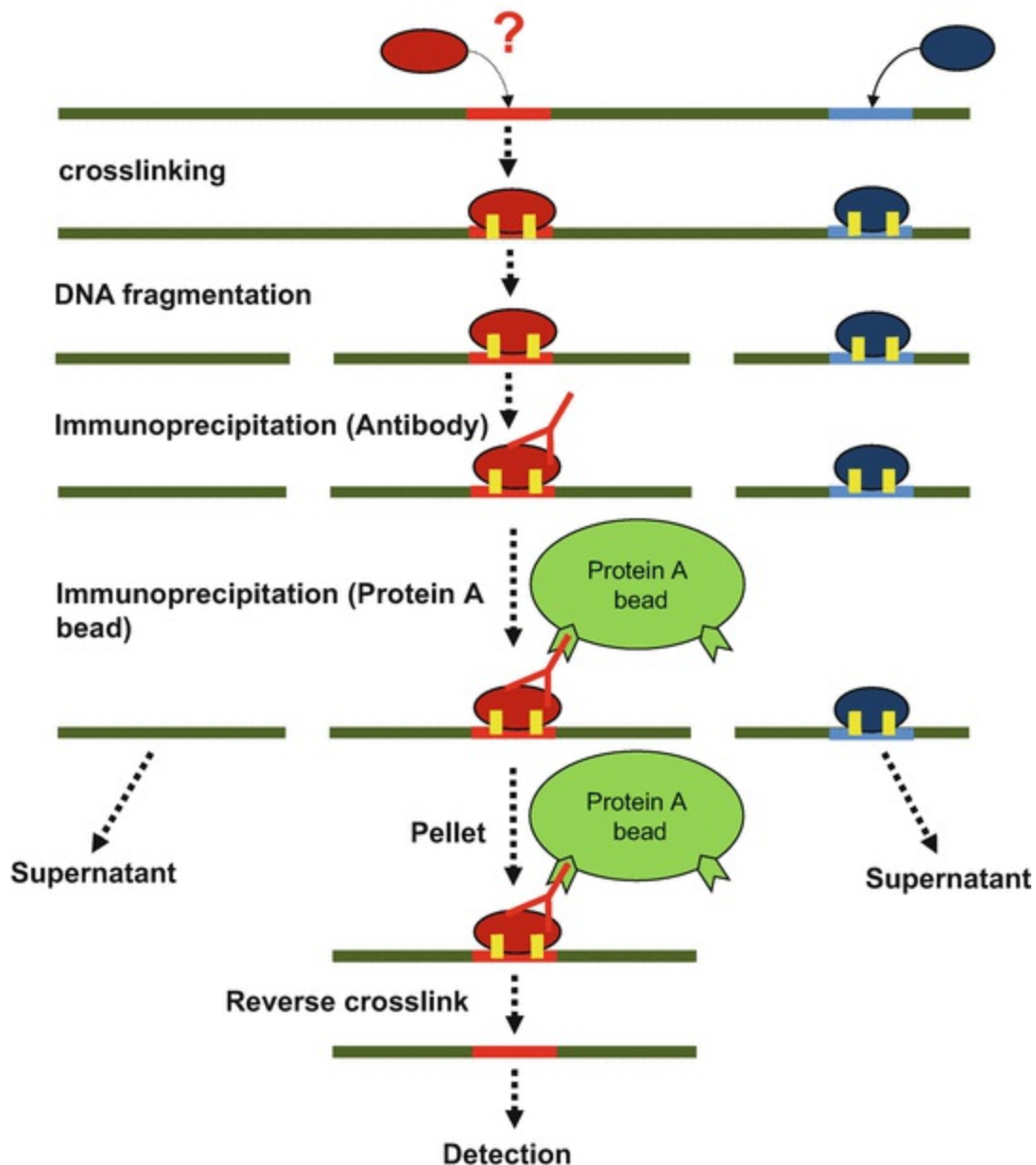
Fig. 1 Schematic overview of ChIP method. DNA and DNA-binding proteins are covalently crosslinked followed by chromatin shearing. Chromatin fragments are immunoprecipitated using bead-coupled specific antibodies against proteins of interest. The purified DNA, following the reversal of crosslinking, is analyzed by the method of choice.

As for the last steps of the workflow more and more sophisticated high-throughput methods have been developed, and not only the capacity and speed of ChIP improved, but the field of its applicability became much wider, too. Besides detection methods, sophisticated improvements enable users to examine not only cultured cells, but even tissue samples as a starting material. The improvements in the ChIP protocol resulted in differently named methods like Carrier ChIP (CChIP), Quick and quantitative ChIP (Q2ChIP), Fast ChIP (qChIP), MicroChIP (μChIP), or Matrix ChIP. Some aspects and main advantages are summarized in Table 1.

Table 1 List of differen t ChIP applications and their main characteristics

Designation	Abbreviation	Summary	Reference
Carrier ChIP	CChIP	ChIP is carried out of ca 100 cells mixed with carrier Drosophila cells to reduce loss of target chromatin	[31]
Quick and quantitative ChIP	Q^2ChIP	Starting with 10^6 cells in crosslinking and sonication. The immunoprecipitation is done with a 100-cell aliquote using fast protocol and quantitative real-time PCR detection	[32]
Fast ChIP	qChIP	The binding of antibody to target is facilitated with ultrasonic bath, the DNA isolation is Chelex-100-based. In 5 h 24 PCR-ready ChIP DNA can be produced	[33]
MicroChIP	µChIP	A 1-day protocol with small cell number (100–1000) or tiny tissue biopsies	[34, 35]
Matrix ChIP		Potentially automatable 96-well plate-based assay with simplified process	[36]
Pathology tissue-ChIP	PAT-ChIP	Developed protocol enables user to start with laser microdissected FFPE tissue sample	[37]
ChIP-nexus		ChIP coupled with exonuclease to gain nucleotide-level resolution	[38]
Ultra-low-input ChIP-seq	ULI-ChIP-seq	A combination of ChIP and NGS sequencing with 1000 cells as starting material using and micrococcal digestion (NChIP)	[39]

1.3 ChIP-Coupled Detection Methods

As mentioned above, with the continuous development of DNA analysis chemistry and instruments, the quantitative and qualitative assessment of immunoprecipitated DNA can be performed in many ways including classical and high-throughput methods as well. Below is an incomplete list and summary of the most dominant approaches used in this field.

1.3.1 ChIP, Classical

Real-time PCR is an appropriate method for quantitative analysis of DNA present in samples and as such, for defining the abundance of DNA fragments co-immunoprecipitated with proteins of interest in chromatin immunoprecipitation experiments. Although, in several cases probe-based detection is preferred, in general dye-based qPCR (SYBR Green, Eva Green etc.) provide us satisfying and reliable result. Intercalating dye converts excess energy of laser exposure into rotation energy in solution; thus it does not emit, until rotation is arrested due to binding to double-stranded DNA. The excess, emitted energy can be detected at 530 nm. The amount of the bound dye and thus the intensity of the detectable signal are proportional to the amount and length of the double-stranded DNA. Determination of the fluorescent signal intensity takes place at the end of the elongation step of each cycle. By checking the melting temperature of the qPCR products, the reaction specificity can be verified with continuous signal detection during heating from 55 °C to 95 °C.

1.3.2 ChIP-Seq

High-throughput techniques such as New Generation Sequencing (NGS) may also be coupled to ChIP. This approach allows the user to investigate all or most chromatin regions that are bound to a specific transcription factor or any other protein of interest. Besides, NGS within some limits may supply users with trustable, quantitative and comparable information (*see* **Note 1**).

1.3.3 ChIP-Chip, ChIP-on-Chip

Another high-throughput solution for the detection of fished DNA sequences is using some sort of microarray-based technique. As many different platforms with a wide range of data-points are available, one can choose the optimal solution depending on expected results, sample type, and other aspects. The limit of these chip slides is that one can detect only regions that are represented on the chip as a probe [26].

1.3.4 ChIP Associated Mass Spectrometry

In addition to the above-mentioned high-throughput methods, mass spectrometry has been developing in technology and capacity as well and was linked to ChIP. Isolated chromatin, using antibodies against histone -modifications or chromatin-associated proteins, can be analyzed further for co-immunoprecipitated proteins with mass spectrometry analysis and protein identification (ChroP, Chromatin Proteomics or ChIP-MS and m-ChIP) [27, 28].

With this armada of subsequent methods linked directly to chromatin immunoprecipitation and numerous available antibodies directed not only against proteins but also at methylated or hydroxymethylated cytosines or at methylated-cytosine-binding proteins (Me-DIP: methylated DNA immunoprecipitation; hMe-DIP: hydroxymethylated DNA immunoprecipitation; MeCP2 ChIP) and at different amino acid side-chain modifications, nearby transcription factor and cofactor binding, all epigenetic mechanisms can be quantitatively and qualitatively examined within entire viral and host genomes.

The list of methods presented above is by far not complete, and as methodologies are developing and coming up, the list is continuously broadening. For example, there are efforts to combine and correlate ChIP-seq data with mass spectrometry results, too.

The method presented below is based on the classical X-ChIP workflow described by Farnham et al. (2002), with some adaptations [8, 23, 29]. The presented results are unpublished data of Banati et al. on the EBER region of Epstein-Barr virus. This method applies "home-made" buffers with the entire protocol free of kits, except for the detection method, real-time PCR in this case (*see* **Note 2**).

2 Materials

2.1 Chromatin Preparation

1. 37 % Formaldehyde.

2. 2.5 M Glycine.

3. PBS: 137 mM NaCl, 2.7 mM KCl, 10 mM N a_2HPO_4, 1.8 mM KH_2PO_4, pH 7.4.

4. Cell lysis buffer: 5 mM Pipes, pH 8.0, 85 mM KCl, 0.5 % NP40 + freshly added protease inhibitor.

5. Nuclei lysis buffer: 50 mM Tris–HCl, pH 8.1, 10 mM EDTA, 1 % SDS + freshly added protease inhibitor.

2.2 Evaluation of Chromatin Shearing, Reverse Crosslinking, DNA Isolation

1. Proteinase K, 20 mg/mL.

2. RNase I, 10 mg/mL.

3. 5 M NaCl.

4. Column-based DNA extraction kit.

5. TE buffer: 10 mM Tris–HCl, pH 8.0, 0.1 mM EDTA.

6. 10 % SDS.

2.3 Immunoprecipitation

1. IP Dilution Buffer: 0.01 % SDS, 1.1 % Triton X-100, 1.2 mM EDTA, 16.7 mM Tris–HCl, pH 8.0, 167 mM NaCl.

2. Sonicated salmon sperm DNA, 10 µg/µL.

3. tRNS, 11 mg/mL.

4. 50 % Protein A bead (*see* **Note 3**).

5. LiCl detergent wash buffer: 10 mM Tris–HCl, pH 8.1, 1 mM EDTA, 250 mM LiCl, 1 % IGEPAL-CA630, 1 % deoxycholate.

6. Low salt buffer: 0.1 % SDS, 1 % Triton X-100, 2 mM EDTA, 20 mM Tris–HCl, pH 8.0, 150 mM NaCl.

7. High salt buffer: 0.1 % SDS, 1 % Triton X-100, 2 mM EDTA, 20 mM Tris–HCl, pH 8.0, 500 mM NaCl.

8. Elution buffer: 1 % SDS, 0.1 M $NaHCO_3$.

2.4 Activation of Protein A Bead

1. Protein A bead, agarose or sepharose coupled (*see* **Note 3**).

2. Lysis buffer: 1 % SDS, 10 mM EDTA, 50 mM Tris–HCl, pH 8.0 + freshly added protease inhibitor.

3. Dilution buffer: 1 % Triton X-100, 150 m M NaCl, 2 mM EDTA, 20 mM Tris–HCl, pH 8.0 + freshly added protease inhibitor.

4. BSA, 10 µg/µL.

5. Sonicated salmon sperm DNA, 10 µg/µL, (*see* **Note 4**).

2.5 Detection, Quantification of ChIP-ed DNA

1. Real-time PCR kit.

2. Positive control, DNA.

3. Negative control, TE buffer if DNA is eluted in TE.

4. PCR grade water.

3 Method
3.1 Chromatin Preparation

1. Take ca 4×10^7 cells in 44 mL media.

2. Add 1.22 mL 37 % formaldehyde (1 % final concentration) and incubate with gentle agitation for 10 min at RT.

3. Add 2.38 mL 2.5 M glycine (0.125 M final concentration) and incubate with gentle agitation for 5 min at RT.

4. Centrifuge tube at $1100 \times g$ for 5 min at 4 °C.

5. Wash cell pellet twice in 5 mL PBS.

6. Discard all the supernatant carefully.

7. Resuspend pellet in 1 mL cell lysis buffer and incubate on ice for 5 min.

8. Centrifuge sample at $1500 \times g$ for 5 min at 4 °C (nuclei will settle down).

9. Repeat **steps 6–8**.

10. Discard all the supernatant carefully.

11. Resuspend pellet in 2 mL nuclei lysis buffer and incubate on ice for 5 min.

12. Use own protocol to sonicate sample. This step is highly dependent on the instrument and/or method used, and accordingly we do not go into details (*see* **Note 5**).

13. Centrifuge sample on 4 °C for 5 min at $15,000 \times g$.

3.2 Evaluation of Chromatin Shearing, Reverse Crosslinking, DNA Isolation

1. Take 100 µL supernatant, add 6 µL 5 M NaCl and 2 µL RNase I, and incubate at 65 °C overnight (at least 2 h).

2. Add 4 µL Proteinase K and incubate at 50 °C for 1 h.

3. Purify DNA with classical Phenol-Chloroform-Isoamyl alcohol protocol (*see* **Note 6**).

4. Separate extracted DNA in 1 % conventional TBE or TAE agarose gel. Sheared chromatin size should be around 300–500 bases.

3.3 Immunoprecipitation

1. To 90 µL lysate add 810 µL IP dilution buffer, 18 µL sonicated salmon sperm DNA, 16 µL tRNA and 36 µL activated (!!!) Protein A bead.

2. Rotate sample for 30 min at RT.

3. Centrifuge sample at $1500 \times g$ for 3 min RT.

4. Divide supernatant into 2 tubes (ca 2×450 µL).

5. Add 2 µg antibody specific to the protein of interest to tube 1 (Ab + sample).

6. Add 2 µg nonimmunized rabbit IgG to tube 2 (Ab- samples).

7. Vortex samples and incubate at 4 °C overnight (ON) with gentle agitation (rotation).

8. Add 30 µL 50 % protein A bead, rotate at RT for 30 min.

9. Centrifuge at $1500 \times g$, 1 min. Save Ab- sample supernatant as total input chromatin (TIC) until the **step 15**. Discard Ab + supernatant.

10. Wash bead 1× in 1 mL Low salt buffer (cf. 1500 g, 1 min).

11. Wash bead 1× in 1 mL High salt buffer (cf. 1500 g, 1 min).

12. Wash bead 2× in 1 mL LiCl Wash buffer (cf. 1500 g, 1 min).

13. Wash bead 2× in 1 mL TE buffer (cf. 1500 g, 1 min).

14. Resuspend bead in 100 µL TE.

15. Add 1 µL RNase I and incubate at 65 °C ON. TIC sample can be processed in parallel. With TIC samples follow protocol from **step 20**.

16. Add 2 µL 10 % SDS, 5 µL Proteinase K and incubate at 50 °C for 1 h.

17. Centrifuge with 1500 × g, 2 min.

18. Isolate DNA from the supernatant using a silica column-based method.

19. Elute DNA in 50 µL TE.

20. Add 4.5 µL RNase I to TIC samples and incubate at 65 °C ON.

21. Add 9 µL 10 % SDS, 22.5 µL Proteinase K and incubate at 50 °C for 1 h.

22. Centrifuge with 1500 × g, 2 min.

23. Isolate DNA from the supernatant using a silica column-based method (PCR purification kit).

24. Elute DNA in 50 µL TE.

3.4 Bead Activation (*see* **Note** 7)

1. Add 600 µL TE to 0.15 g Protein A agarose bead and incubate for 1.5 h at RT.

2. Add 600 µL TE and wash the bead four times (centrifugation with 2000 × g for 5 min between washing steps).

3. After discarding supernatant add 600 µL TE resulting ca 1.2 mL 50 % bead (*see* **Note 8**).

4. Add 50 µL Sonicated Salmon Sperm DNA (ca 400 µg/mL final conc.) to 50 % bead.

5. Add 125 µL BSA (ca 90 µg/mL final conc.).

6. Store activated bead at 4 °C until use.

3.5 Detection, Quantification of ChIP-ed DNA

Here an example is shown; the actual parameters will vary, of course, depending on the actual experiment to be performed.

In this ChIP study, we used antibodies directed to modified histones to characterize the epigenetic marks in a region of the EBV genome. Quantitation of antibody-precipitated DNA sequences of different Epstein-Barr virus carrying cell lines permitted assessing the abundance of the activating histone modifications Acetylated Histone 3 (AcH3), Acetylated Histone 4 (AcH4), and dimethylated Lysine 4 of Histone 3 (H3K4me2) in the regulatory and coding sequences of EBER 1 and 2 genes. The primers used to detect EBER sequences are listed in Table 2.

Table 2 Primers used to detect EBER sequences in ChIP experiment

EBER region	Name of the primer (position in sequence)[a]	Sequence of primers 5′- 3′
EBER- CTCF	EBER-CTCF up (6136–6156)	tca cag cta aat gcc cac cag
	EBER-CTCF low (6339–6319)	ctc aga aaa cac gcc atc cac
EBER1	EBER1 up (6656–6676)	cta ggg agg aga cgt gtg tgg
	EBER1 low (6777–6757)	gct ggt act tga ccg agg acg
EBER2	EBER2 up (6988–7004)	cac cgc caa cgc tca gtg
	EBER2 low (7111–7091)	cga ata ccc ttc tcc cag agg

[a] according to the NC_007605 NCBI reference genome

qPCR reaction was done in 20 µL containing 10 µL 2× SensiFAST SYBR No-Rox Kit, 1 µL each of two primers (5 µM, each), 7 µL dH$_2$O and 1 µL template DNA. Amplification was performed as follows in Table 3.

Table 3 Thermal program of the qPCR used for the amplification of EBER sequences

Denaturation, enzyme activation	95 °C 2 min	1×
Denaturation	95 °C 10 s	40×
Annealing and elongation	60 °C 30 s [a]	
Tm calling	60–95 °C, 0,3 °C/s ramping	1×

[a] Fluorescence was measured at the end of this step

The concentration of the samples was determined with the help of a plotted standard curve obtained from a 10× dilution series of the most concentrated total input chromatin DNA.

A typical result is demonstrated in Fig. 2.
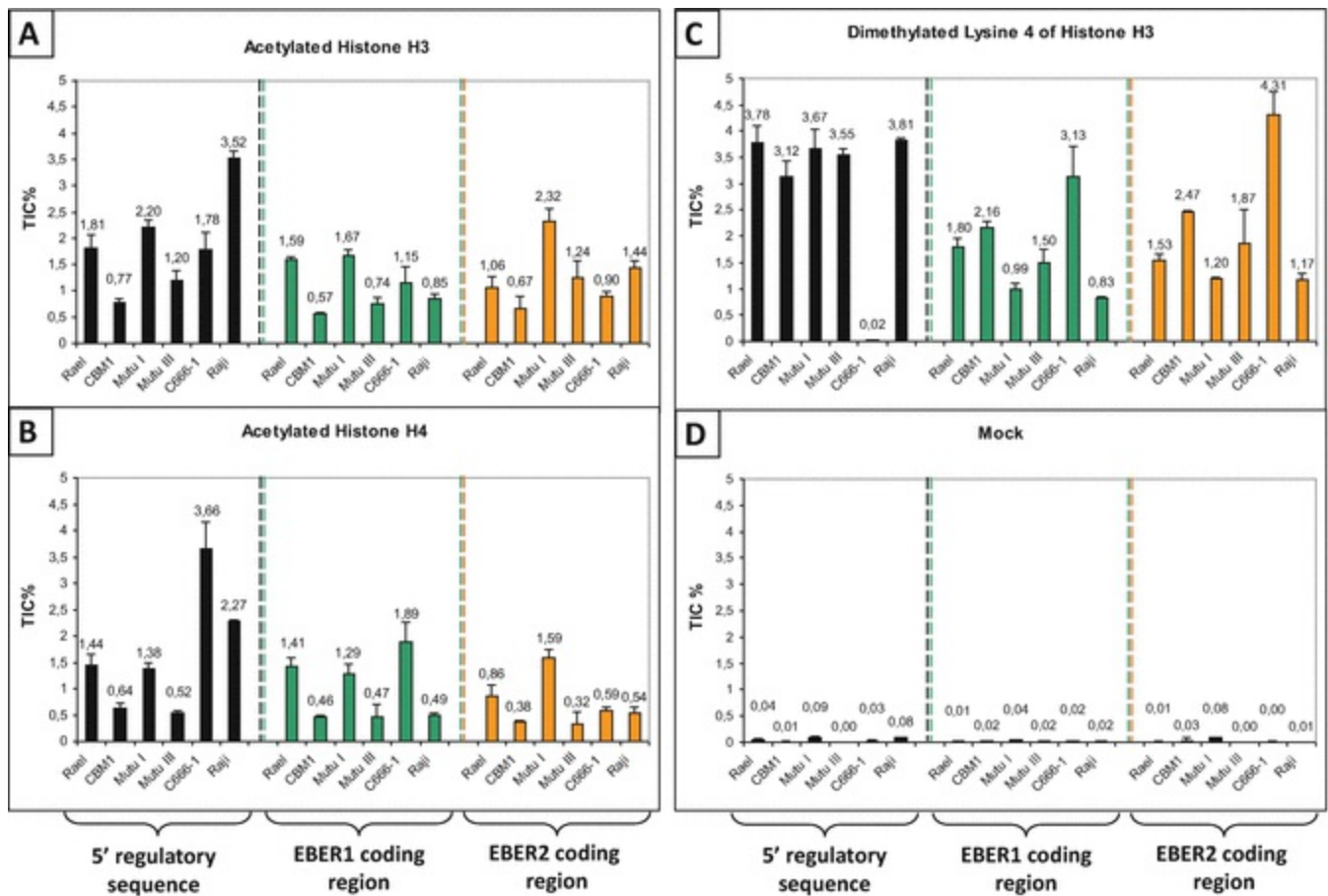
Fig. 2 ChIP results of EBE R region using modified histone specific and nonspecific antibodies. The abundance of different histone modifications is expressed as the percentage of the total input chromatin. Panel A: Acetylated Histone H3, panel B: Acetylated Histone H4. Panel C: dimethylated lysine 4 of Histone H3, panel D: Mock-precipitated samples. On the left side, the amount of modifications in the 5′ regulatory sequence (*black columns*), in the middle the EBER 1 coding sequence (*green columns*), on the *right* the EBER 2 coding sequence (*orange columns*) is shown in the examined cell lines

All of the examined histone modifications were found to be present in great amounts within the entire EBER locus in all of the investigated cell lines. There were minor differences between the individual cell lines in all cases. The Rael and Mutu I Burkitt's lymphoma cells carrying latency type I EBV genomes were more enriched in AcH3 throughout the EBER locus, compared to the CBM1 and Mutu III, latency type III cells that carry the same EBV strains with their latency I counterparts. The same tendency was observed in case of acetylated H4. The abundance of these histone modifications was variable in the C666-1 nasopharyngeal carcinoma cell line and the Raji Burkitt's lymphoma cell line. The H3K4me2 modification was approximately equally abundant in the 5′ promoter sequence of the lymphoid cell lines, but the C666-1 nasopharyngeal carcinoma cells lacked this modification in that region. In the coding sequences, the latency type I cell lines (Rael, Mutu I) had lower amounts of the H3K4me2 modification compared to their latency type III counterparts (CBM1, Mutu III, respectively). The C666-1 cells showed the highest amount, and the Raji cells showed the smallest amount of this modification in the EBER coding sequences.

4 Notes

1. For high-throughput ChIP experiments, the data handling might be extremely exhausting. To ease this problem, a Web-based analysis tool was created called MEME-ChIP [30].

2. The entire ChIP protocol can be performed within hours using commercial ChIP kits.

3. Magnetic or any other kind of beads might be suitable; however, the exact experimental conditions have to be individually adjusted.

4. Other DNA protecting agents can also be used.

5. To shear chromatin one can use ultrasound , physical braking (syringe, nitrogen), or specific nucleases (restriction endonucleases, micrococcal DNase, or limited DNase I treatment). In each case, the exact experimental conditions have to be adjusted experimentally.

6. Instead of classical methods column-based DNA purification kit or PCR clean-up kit can be used.

7. In case of ready to use beads and several all-inclusive ChIP kits there is no need for an extra bead activation step.

8. The exact amount of TE buffer needed has to be estimated based on the remaining bead volume to obtain 50 % bead solution.

References

1. Waddington CH (1942) Canalization of development and the inheritance of acquired characters. Nature 150(3811):563–565
[CrossRef]

2. Waddington CH (1957) The strategy of the genes; a discussion of some aspects of theoretical biology. Allen & Unwin, London

3. Waddington CH (2012) The epigenotype. 1942. Int J Epidemiol 41(1):10–13. doi:10.1093/ije/dyr184
[CrossRef][PubMed]

4. Holliday R, Pugh JE (1975) DNA modification mechanisms and gene activity during development. Science 187(4173):226–232
[CrossRef][PubMed]

5. Riggs AD (1975) X inactivation, differentiation, and DNA methylation. Cytogenet Cell Genet 14(1):9–25
[CrossRef][PubMed]

6. Han M, Grunstein M (1988) Nucleosome loss activates yeast downstream promoters in vivo. Cell 55(6):1137–1145
[CrossRef][PubMed]

7. Jenuwein T, Allis CD (2001) Translating the histone code. Science 293(5532):1074–1080. doi:10.1126/science.1063127
[CrossRef][PubMed]

8. Dupont C, Armant DR, Brenner CA (2009) Epigenetics: definition, mechanisms and clinical perspective. Semin Reprod Med 27(5):351–357. doi:10.1055/s-0029-1237423
[CrossRef][PubMed][PubMedCentral]

9. Laird PW, Jaenisch R (1996) The role of DNA methylation in cancer genetic and epigenetics. Annu Rev Genet 30:441–464. doi:10.1146/annurev.genet.30.1.441
[CrossRef][PubMed]

10. Pfeifer GP, Tang M, Denissenko MF (2000) Mutation hotspots and DNA methylation. Curr Top Microbiol Immunol 249:1–19
[PubMed]

11. Robertson KD, Jones PA (2000) DNA methylation: past, present and future directions. Carcinogenesis 21(3):461–467
[CrossRef][PubMed]

12. Strahl BD, Allis CD (2000) The language of covalent histone modifications. Nature 403(6765):41–45. doi:10.1038/47412
[CrossRef][PubMed]

13. Guitton AE, Berger F (2005) Control of reproduction by Polycomb Group complexes in animals and plants. Int J Dev Biol 49(5–6):707–716. doi:10.1387/ijdb.051990ag
[CrossRef][PubMed]

14. Schuettengruber B, Chourrout D, Vervoort M, Leblanc B, Cavalli G (2007) Genome regulation by polycomb and trithorax proteins. Cell 128(4):735–745. doi:10.1016/j.cell.2007.02.009
[CrossRef][PubMed]

15. Niller HH, Tarnai Z, Decsi G, Zsedenyi A, Banati F, Minarovits J (2014) Role of epigenetics in EBV regulation and pathogenesis. Future Microbiol 9(6):747–756. doi:10.2217/fmb.14.41
[CrossRef][PubMed]

16. Ernberg I, Falk K, Minarovits J, Busson P, Tursz T, Masucci MG, Klein G (1989) The role of methylation in the phenotype-dependent modulation of Epstein-Barr nuclear antigen 2 and latent membrane protein genes in cells latently infected with Epstein-Barr virus. J Gen Virol 70(Pt 11):2989–3002
[CrossRef][PubMed]

17. Day L, Chau CM, Nebozhyn M, Rennekamp AJ, Showe M, Lieberman PM (2007) Chromatin profiling of Epstein-Barr virus latency control region. J Virol 81(12):6389–6401. doi:10.1128/JVI.02172-06
[CrossRef][PubMed][PubMedCentral]

18. Takacs M, Banati F, Koroknai A, Segesdi J, Salamon D, Wolf H, Niller HH, Minarovits J (2010) Epigenetic regulation of latent Epstein-Barr virus promoters. Biochim Biophys Acta 1799(3–4):228–235
[CrossRef][PubMed]

19. Minarovits J (2006) Epigenotypes of latent herpesvirus genomes. Curr Top Microbiol Immunol 310:61–80
[PubMed]

20. Gilmour DS, Lis JT (1984) Detecting protein-DNA interactions in vivo: distribution of RNA polymerase on specific bacterial genes. Proc Natl Acad Sci U S A 81(14):4275–4279
[CrossRef][PubMed][PubMedCentral]

21. Gilmour DS, Lis JT (1985) In vivo interactions of RNA polymerase II with genes of Drosophila melanogaster. Mol Cell Biol 5(8):2009–2018
[CrossRef][PubMed][PubMedCentral]

22. Solomon MJ, Larsen PL, Varshavsky A (1988) Mapping protein-DNA interactions in vivo with formaldehyde: evidence that histone H4 is retained on a highly transcribed gene. Cell 53(6):937–947
[CrossRef][PubMed]

23. Weinmann AS, Farnham PJ (2002) Identification of unknown target genes of human transcription factors using chromatin immunoprecipitation. Methods 26(1):37–47. doi:10.1016/S1046-2023(02)00006-3
[CrossRef][PubMed]

24. Turner B (2001) ChIP with native chromatin: advantages and problems relative to methods using cross-linked

material. In: Mapping protein/DNA interactions by cross-linking. Institut national de la santé et de la recherche médicale, Paris

25. O'Neill LP, Turner BM (2003) Immunoprecipitation of native chromatin: NChIP. Methods 31(1):76–82
[CrossRef][PubMed]

26. Buck MJ, Lieb JD (2004) ChIP-chip: considerations for the design, analysis, and application of genome-wide chromatin immunoprecipitation experiments. Genomics 83(3):349–360
[CrossRef][PubMed]

27. Lambert JP, Mitchell L, Rudner A, Baetz K, Figeys D (2009) A novel proteomics approach for the discovery of chromatin-associated protein networks. Mol Cell Proteomics 8(4):870–882. doi:10.1074/mcp.M800447-MCP200
[CrossRef][PubMed][PubMedCentral]

28. Soldi M, Bonaldi T (2014) The ChroP approach combines ChIP and mass spectrometry to dissect locus-specific proteomic landscapes of chromatin. J Vis Exp (86). doi:10.3791/51220

29. Bakos A, Banati F, Koroknai A, Takacs M, Salamon D, Minarovits-Kormuta S, Schwarzmann F, Wolf H, Niller HH, Minarovits J (2007) High-resolution analysis of CpG methylation and in vivo protein-DNA interactions at the alternative Epstein-Barr virus latency promoters Qp and Cp in the nasopharyngeal carcinoma cell line C666-1. Virus Genes 35(2):195–202. doi:10.1007/s11262-007-0095-y
[CrossRef][PubMed]

30. Ma W, Noble WS, Bailey TL (2014) Motif-based analysis of large nucleotide data sets using MEME-ChIP. Nat Protoc 9(6):1428–1450. doi:10.1038/nprot.2014.083
[CrossRef][PubMed][PubMedCentral]

31. O'Neill LP, VerMilyea MD, Turner BM (2006) Epigenetic characterization of the early embryo with a chromatin immunoprecipitation protocol applicable to small cell populations. Nat Genet 38(7):835–841. doi:10.1038/ng1820
[CrossRef][PubMed]

32. Dahl JA, Collas P (2007) A quick and quantitative chromatin immunoprecipitation assay for small cell samples. Front Biosci 12:4925–4931
[CrossRef][PubMed]

33. Nelson J, Denisenko O, Bomsztyk K (2009) The fast chromatin immunoprecipitation method. Methods Mol Biol 567:45–57. doi:10.1007/978-1-60327-414-2_3
[CrossRef][PubMed]

34. Dahl JA, Collas P (2008) A rapid micro chromatin immunoprecipitation assay (microChIP). Nat Protoc 3(6):1032–1045. doi:10.1038/nprot.2008.68
[CrossRef][PubMed]

35. Dahl JA, Klungland A (2015) Micro chromatin immunoprecipitation (muChIP) from early mammalian embryos. Methods Mol Biol 1222:227–245. doi:10.1007/978-1-4939-1594-1_17
[CrossRef][PubMed]

36. Flanagin S, Nelson JD, Castner DG, Denisenko O, Bomsztyk K (2008) Microplate-based chromatin immunoprecipitation method, matrix ChIP: a platform to study signaling of complex genomic events. Nucleic Acids Res 36(3):e17. doi:10.1093/nar/gkn001
[CrossRef][PubMed][PubMedCentral]

37. Amatori S, Ballarini M, Faversani A, Belloni E, Fusar F, Bosari S, Pelicci PG, Minucci S, Fanelli M (2014) PAT-

ChIP coupled with laser microdissection allows the study of chromatin in selected cell populations from paraffin-embedded patient samples. Epigenetics Chromatin 7:18. doi:10.1186/1756-8935-7-18 [CrossRef][PubMed][PubMedCentral]

38. He Q, Johnston J, Zeitlinger J (2015) ChIP-nexus enables improved detection of in vivo transcription factor binding footprints. Nat Biotechnol 33(4):395–401. doi:10.1038/nbt.3121 [CrossRef][PubMed][PubMedCentral]

39. Brind'Amour J, Liu S, Hudson M, Chen C, Karimi MM, Lorincz MC (2015) An ultra-low-input native ChIP-seq protocol for genome-wide profiling of rare cell populations. Nat Commun 6:6033. doi:10.1038/ncomms7033 [CrossRef][PubMed]

17. Mice with Reconstituted Human Immune System Components as a Tool to Study Immune Cell Interactions in EBV Infection

Frank Heuts[1] and Noemi Nagy[2] ✉

(1)   Institute of Immunity and Transplantation, University College London Medical School, London, UK

(2)   Department of Microbiology, Tumor and Cell Biology, Karolinska Institutet, Nobels väg 16, Stockholm, SE-171 77, Sweden

✉ **Noemi Nagy**
    Email: noemi.nagy@ki.se

Abstract
Recent developments in mouse models that harbor part of a human immune system have proved extremely valuable to study the in vivo immune response to human specific pathogens such as Epstein-Barr virus. Over the last decades, advances in immunodeficient mouse strains that can be used as recipients for human immune cells have greatly enhanced the use of these models. Here, we describe the generation of mice with reconstituted human immune system (HIS mice) using immunocompromised mice transplanted with human $CD34^+$ hematopoietic stem cells. We will also describe how such mice, in which human immune cells are generated de novo, can be used to study EBV infection.

Key words $CD34^+$ – Humanized mice – Epstein-Barr virus – Latency

1   Introduction

Studies of human specific pathogens such as Epstein-Barr virus (EBV) have been

hampered by the lack of suitable small animal models for in vivo studies. Immunocompromised mice engrafted with human hematopoietic cells have proved to be extremely valuable in this respect; however, these models were limiting in that they were relying on the transfer of peripheral blood mononuclear cells (PBMCs) , and no immune cells developed de novo in these animals. Recent advances in immunodeficient mouse strains have allowed for the development of improved animal models. After transplantation with human CD34$^+$ hematopoietic stem cells, such mice develop human immune cells, notably T and B cells, allowing for infection with human tropic viruses such as EBV and the subsequent immune response [1, 2]. Here, we describe how to generate mice with human immune system components (HIS mice) by transplantation of human hematopoietic stem cells into newborn immunodeficient mice, and how such mice can be used successfully to study EBV infection in vivo through manipulation of cell populations in vivo and subsequent ex vivo experiments.

2 Materials

2.1 Generation of HIS Mice

1. Newborn NOD/Lt-*scid IL2rγ* ^{null} (NSG) mice (*see* **Note 1**).

2. Irradiation source (*see* **Note 2**).

3. 100 mm^2 petri dish.

4. CD34$^+$ human hematopoietic stem cells (*see* **Note 3**) purified using the human CD34 $^+$ isolation kit (e.g., Miltenyi Biotec or equivalent products from other vendors).

5. Sterile phosphate buffer saline (PBS).

6. Eppendorf tubes.

7. 25 μL Hamilton syringe (Model 702 RN SYR (25 μL with replaceable needle) with 30 gauge, Small Hub RN NDL, 1 in., point style 4 (Sharp 10–12° beveled needle)).

8. Eppendorf tubes containing anticoagulant, for example 2 mM EDTA in PBS.

2.2 EBV Infection and Immune System Manipulation In Vivo

1. Antibodies for depletion (*see* **Note 4**).

2. Sterile PBS.

3. 27 gauge needles.

4. 1 mL syringes.

5. EBV stock of known titer.

6. Weighing scales.

2.3 Processing of Organs

1. Sterile PBS.

2. 70 µm cell strainers.

3. 22.1 cm^2 petri dishes.

4. 2 mL syringes.

5. Ammonium chloride lysing solution: 8 .25 g NH_4Cl, 1 g $KHCO_3$ and 200 µL 0.5 M EDTA dissolved in 1 L ddH$_2$O and pH adjusted to 7.2.

6. Complete RPMI medium: RPMI with 10 % fetal calf serum (FCS), 100 U/mL penicillin, 100 µg/mL streptomycin.

2.4 Flow Cytometric Analysis of Tissues and Cell Cultures

1. FACS buffer: 2 % fetal bovine serum in PBS.

2. Fluorescent conjugated antibodies (*see* **Note 5**).

3. Fc blocking reagent.

4. BD FACS lysing solution.

5. Flow cytometer.

6. Flow cytometry analysis software.

2.5 Real-Time RT-PCR

1. Total RNA isolation kit, for example Quick-RNA Miniprep (Zymo Research) or kits from other suppliers can be used (*see* **Note 6**).

2. cDNA synthesis kit, for example SuperScript VILO (Invitrogen) or from other suppliers.

3. SYBR Green-based real-time RT-PCR kit, for example LightCycler FastStart DNA Master SYBR Green I kit (Roche) or similar.

4. Primers (*see* **Note 7**).

5. Ultrapure DNase/RNase-free distilled water.

6. Nuclease free, aerosol-resistant pipette tips (with filter).

7. Nuclease free Eppendorf tubes (1.5 mL).

2.6 In Vitro Measurement of Splenocyte Proliferation

1. Complete RPMI medium: RPMI with 10 % fetal calf serum (FCS), 100 U/mL penicillin, 100 µg/mL streptomycin.

2. Stock solution of 1 mg/mL Cyclosporin A.

3. 96 well plate (flat bottom).

4. Methyl-^{3}H-Thymidine.

5. Glass fiber filters (e.g., from Perkin Elmer).

6. Cell harvester for a 96-well plate.

7. Scintillation liquid (e.g., Betaplate scint from Perkin Elmer).

8. β-counter.

3 Methods
3.1 Generation of HIS Mice

1. All work on NSG mice should be performed in a sterile environment to prevent possible infections.

2. Set up NSG breeder pairs and monitor for newborns.

3. Transfer newborn recipients 24–48 h after birth into a sterile 100 mm^2 Petri dish containing some bedding of the breeding cage.

4. Irradiate recipient newborn mice with 1 Gray.

5. Prepare CD34$^+$ cells for transplantation to concentration of 4×10^6/mL in PBS in an Eppendorf vial (*see* **Notes 8** and **9**).

6. Preload the Hamilton syringe with 25 μL CD34$^+$ cell suspension.

7. Inject 1×10^5 CD34$^+$ progenitor cells intrahepatically 4 h after irradiation. In order to prevent the cell suspension from leaking out of the liver and abdomen the injection should be performed as in Fig. 1. Gently scruff the mouse between thumb and index finger and puncture the skin in the neck, avoiding the carotic nerve. Move the needle over the rib cage, through the diaphragm into the liver until the needle enters one of the lobes. Gently inject the cell suspension. If cells are injected correctly the lobe will turn pale and swell up slightly.

Fig. 1 For injection of human CD34$^+$ cells, newborn mice should be held between thumb and index finger. 25 μL of cell suspension needs to be injected into one lobe of the liver as shown

8. After injection carefully retract the needle and return the newborn to the cage with the mother.

9. Wean the transplanted mice at 3 weeks of age.

10. Allow reconstitution to take place until the mice are 8–12 weeks old (*see* **Note 10**).

11. Collect a 50 μL blood sample in a tube containing anticoagulant and analyze for engraftment of human hematopoietic cells by flow cytometry (Subheading 3.4.1).

12. Use mice with sufficient engraftment levels for EBV infection (*see* **Note 11**).

3.2 EBV Infection of Humanized Mice

1. Prior to and during infection with EBV, selected human immune cells can be depleted through intraperitoneal injection of antibodies targeting these populations (*see* **Note 4**).

2. Prepare EBV by diluting in PBS so that 100 μL of suspension contains the desired viral titer for infection.

3. Inject mice intraperitoneally with 100 μL of virus suspension.

4. Monitor health by checking weight, behavior, and appearance three times weekly and if applicable treat with depleting antibody.

5. Sacrifice mice at the desired time point and harvest tissues of interest for analysis (*see* **Note 12**).

3.3 Processing of Organs

1. Create single cell suspensions of lymph nodes and spleen by straining through a 70 μm cell strainer into a 22.1 cm^2 petri dish containing 1 mL PBS using the plunger of a 2 mL syringe.

2. Collect single cell suspension and transfer into 15 mL polypropylene tube.

3. Wash in 10 mL PBS and centrifuge cells at 400 × *g* for 10 min at 4 °C.

4. Aspirate supernatant.

5. Resuspend splenic cells in 2 mL ammonium chloride lysing solution to lyse red blood cells. Leave for 10 min at room temperature. This step is not required for lymph node cell suspensions. For preparation of lymph nodes continue at **step 7** in this protocol.

6. Stop lysis by adding 10 mL of PBS and centrifuge cells at $400 \times g$ for 10 min at 4 °C.

7. Resuspend pelleted cells in 1 or 3 mL of complete RPMI for lymph node or spleen cell suspensions respectively.

8. Count cell number in a haemocytometer and proceed with ex vivo analysis.

3.4 Flow Cytometry

3.4.1 Flow Cytometric Analysis of Blood Samples

1. Transfer 80 µL of anticoagulated blood into a 6 mL polystyrene FACS tube.

2. Add 20 µL of antibody mastermix containing antihuman CD45, CD3, and CD19 antibodies (*see* **Note 5**) and Fc blocking reagent in FACS buffer.

3. Incubate for 10 min at 4 °C.

4. Wash once in 1 mL FACS buffer and centrifuge cells at $400 \times g$ for 5 min at 4 °C.

5. Aspirate supernatant.

6. Resuspend pellet in 1.5 mL BD FACS lysing solution and incubate for 12 min at room temperature.

7. Add 3 mL FACS buffer to every sample and centrifuge cells at $400 \times g$ for 5 min at 4 °C.

8. Resuspend cell pellet in 250 μL of FACS buffer and acquire samples on a flow cytometer.

9. Analyze B and T cell populations within the human CD45 positive cell population using flow cytometry analysis software such as FlowJo.

3.4.2 Flow Cytometry of Tissue Samples and Cultured Cells

1. Prepare 100 μL antibody mixture for labeling the cells per sample by mixing the required antibodies at the right concentration (*see* **Note 5**) and the Fc blocking reagent in FACS buffer.

2. Transfer 1×10^6 cells to be analyzed into a 6 mL polystyrene FACS tube.

3. Wash once in 1 mL FACS buffer and centrifuge cells at $400 \times g$ for 5 min at 4 °C.

4. Aspirate supernatant.

5. Resuspend cell pellet in 100 μL of the prepared antibody mixture and incubate the samples for 10 min at 4 °C protected from light.

6. Wash once in 1 mL FACS buffer and centrifuge cells at $400 \times g$ for 5 min at 4 °C.

7. Resuspend cell pellet in 250 μL of FACS buffer and acquire samples on a flow cytometer.

8. Analyze B and T cell populations within the human CD45 positive cell population using flow cytometry analysis software such as FlowJo.

3.5 Latency Type Determination/EBV Gene Expression by

Real-Time RT-PCR of Splenic Cells

In vivo generation of the various latency types can be ascertained by determining the presence and relative abundance of the different EBV transcripts initiated from the latency type specific promoters. C (Cp) and W (Wp) promoters identify latency III cells, while Qp is characteristic of latency I and latency IIa cells [3]. Other EBV encoded genes, e.g., EBNA2 , LMP1, EBER1/2, can be determined as well.

1. Pellet 1–3 × 10^6 cells from the suspension prepared from the spleen or other organs as described at Subheading 3.3 in a nuclease free Eppendorf tube (1.5 mL). Discard completely the supernatant (medium) with an aerosol-resistant tip. Proceed directly to total RNA purification or quick freeze the pellet at −80 °C where it can be kept until a later time point when RNA is purified.

2. Purify total RNA according to the manufacturer's protocol (*see* **Note 13**) and measure RNA concentration with your method of choice, for example by Nanodrop. High quality RNA should have an *A260/A280* ratio >1.8, and *A260/A230* ratio >1.8.

3. Perform cDNA synthesis according to the manufacturer's instructions. If SuperScript VILO kit is used, the amount of input total RNA can be anywhere between 100 ng and 2.5 μg in a 20 μL reaction, where the maximum volume of RNA can be 14 μL. cDNA can be stored at −20 °C.

4. To perform the real-time RT-PCR reaction, dilute cDNA in ultrapure DNase/RNase-free distilled water to achieve the concentration equivalent of starting with 100 ng of RNA. For example if 1.5 μg total RNA was used in the cDNA synthesis reaction, then a 15 times dilution should be performed (*see* **Note 14**). Two microliters of this diluted cDNA will be used in a 20 μL real-time PCR reaction.

    The PCR mix for one reaction contains 10.8 μL H_2O; 3.2 μL 25 mM $MgCl_2$; 1 μL of 5 μM forward and reverse primers each (giving a total final concentration of 0.5 μM), 2 μL of the 10× concentrated LightCycler FastStart reaction mix SYBR Green I with the admixed LightCycler FastStart enzyme and 2 μL of the diluted template (cDNA).

5. Run the PCR reaction: initially denature the mix at 95 °C for 10 min and then run 40 cycles of 95 °C for 8 s, 60 °C for 5 s, 72 °C for 8 s.

6. Calculate the relative level of each transcript by using the standard curve method (*see* **Note** 15). For normalization use the relative values of the simultaneously measured EF1α transcripts, used as housekeeping gene (*see* **Note** 16). EBV genes are only expressed in human B cells; thus, the relative expression values have to be related to the number of B cells present in the cell suspension used as starting material. For this, the results of the FACS analysis described in Subheading 3.4.2 are used. If the percentage of B cells in the human lymphocyte gate is "N" for a given spleen, then the relative EBV gene expression in B cells in that spleen = relative expression obtained in the PCR reaction/N × 100.

3.6 Proliferative Capacity of EBV-Infected B Cells from Spleen or Lymph Nodes and Effect of T Cells

Cell-mediated immunity against EBV that has been generated in vivo can be monitored in vitro as the capacity of T lymphocytes to inhibit virus induced proliferation of B cells. EBV specific T cells that are present would inhibit the in vitro growth of transformed B cells. This test is a modified version of the classical, so called outgrowth inhibition (regression) test [4]. Unlike in the standard outgrowth inhibition assay, in this present version, we do not "super-infect" in vitro the lymphocyte population derived from the infected mice's spleen. In this way, the test also gives information about the proliferative capacity of the in vivo infected B cells, thus indirectly about their latency types. Cells with latency I or IIa lack EBNA2 expression; thus they do not have inherent proliferative capacity in vitro. Therefore, proliferating B cell cultures would be detected after 4 weeks if the B cells present in the spleen express latency III program and the number of EBV specific T cells is too low to inhibit them. In order to measure only the proliferative capacity of the B cells, in half of the cultures we inhibit T cell function with Cyclosporin A .

1. Seed the cells in doubling dilutions from 2×10^5 to 0.12×10^5/well (five different concentrations). Set up at least ten replicates for each dilution. For this purpose, resuspend 5×10^6 cells from the single cell suspension prepared from the spleen (described at Subheading 3.3.) in 2.5 mL complete RPMI medium. This will give a concentration of 2×10^6 cells/mL.

2. Distribute 100 µL of complete medium into rows 2–5 of a 96-well plate with flat bottom (leave the first row empty).

3. Distribute 200 µL cell suspension into the first row (which does not contain medium) of the plate.

4. Starting from this row, prepare the serial doubling dilutions by transferring 100 µL of cell suspension into the next row, admix with the medium already present there, and transfer 100 µL into the next row. Repeat this until the last row, from where after the mixing step 100 µL cell suspension is discarded. This will provide you with 0.12×10^5 cells/well in the last row.

5. Add 100 µL complete medium to half of the wells of each cell concentration (total of 200 µL/well).

6. To the other half of the wells, add 100 µL complete medium that contains 1 µg/mL Cyclosporin A (CsA). Thus, the final concentration will be 0.5 µg/mL CsA and this will inhibit the T cell functions. To prepare the 1 µg/mL Cs A, add 3.5 µL from the stock solution (1 mg/mL) to 3.5 mL medium.

7. Feed the cells weekly by replacing 100 µL culture medium with 100 µL fresh complete RPMI medium. For the CsA containing cultures replace the old medium with 100 µL medium that contains 0.5 µg/mL CsA.

8. After 4 weeks, evaluate the growth of transformed B cells by visual examination, by recording the presence of cell clumps. At this time point, only transformed B cells are present in the cultures, T cells do not survive.

9. To obtain a more objective evaluation of the B cell growth, after the visual examination of the cultures, use ^{3}H-Thymidine incorporation to measure cell proliferation (*see* **Note 17**). For this, add 1 µCi ^{3}H-Tymidine to each well. Incubate for 16 h, during which proliferating cells will incorporate the labeled nucleotide into newly synthesized DNA.

10. Harvest the cells from the plate on a glass fiber filter, using a cell harvester.

Air dry the filter and seal it in a plastic bag. Add 4 mL scintillation fluid to the filter and measure radioactivity in a β-counter. Counts per minute (cpm) values are proportional with the number of proliferating cells present in each well.

Cultures grown in medium with CsA (no T cells were active) that incorporate ^{3}H-Thymidine, correspond to wells where B cells expressing latency III were present.

The lower the cell number/well that still gives positive result, the higher the frequency of these B cells was in the spleen at the time of sacrifice. Comparing cpm values of cultures with the same starting cell number, grown with or without CsA, gives information about the presence of EBV specific T cells. They were present, if cpm is lower in cultures with functioning T cells (no CsA) than in the absence of T cells (CsA added).

---

4 Notes

1. While various immunodeficient mouse strains can be used for engraftment with human CD34$^+$ cells, NOD/Lt-*scid* IL2Rγ^{null} (NSG) mice have been shown superior over other strains. It should also be noted that there are no reports in which immunodeficient strains on the C57BL/6J background have been successfully engrafted with human CD34$^+$ cells [5].

2. A ^{137}Cs source is used in this protocol, but other radiation sources can be used. We recommend however performing a titration to establish the right dosage if another source is used.

3. Human CD34$^+$ cells are commonly isolated from fetal liver, cord blood, or G-CSF mobilized PBMCs . Cord blood is a readily accessible source for most researchers and stem cells obtained from this source have been shown to give good engraftment results. Notably, larger numbers of CD34$^+$ cells can be obtained from fetal liver, and in addition to this, fewer stem cells are required to obtain satisfying levels of chimerism in the mice [6]. However, access to fetal liver is more restricted than cord blood. Engraftment of CD34$^+$ cells isolated from G-CSF mobilized blood is less efficient compared to CB and HFL derived cells [6]. Additionally, getting access to this source of CD34$^+$ cells is limited due to ethical constraints.

4. We and others have successfully depleted human CD4 or CD8 T cells by injecting humanized mice intraperitoneally with 100 μg OKT-4 or 50 μg OKT-8 in 100 μL PBS for 3 consecutive days every 2 weeks [2, 7]. Antibody treatment needs to be started 3 days prior to EBV inoculation to ascertain that the targeted cell subset has been depleted before exposure to EBV. Antibodies targeting other subsets of

cells can be used provided that a dose and treatment regimen is established.

5. The choice of antibodies for flow cytometric analysis depends on the question being asked; however, antibodies against human CD45 (clone 5B1), CD3 (clone UCHT1), and CD19 (clone HIB19) should be included in any panel used. The correct concentrations to be used for all antibodies should be established on human peripheral blood mononuclear cells.

6. If EBERs and/or miRNAs are going to be detected by PCR, make sure you use an RNA purification kit and protocol that allows recovery of RNAs smaller than 200 nt as well.

7. The following primer pairs were designed for the different EBV genes to be used in the capillar y LightCycler (Roche) instrument, but are expected to perform well in other, for example the Applied Bioscience instruments. The working solution of different primers is 5 µM. The primers are based on the B95-8 sequence; thus, their suitability for other EBV strains has to be tested.

Primer pair	Sequence
Cp	5′-GAT CAG ATG GCA TAG AGA CAA GGA C-3′
	5′-AGG CTG TTT CTT CAG TCG GTT TAG-3′
Wp [8]	5′-CGC CAG GAG TCC ACA CAA AT-3′
	5′-GAG GGG ACC CTC TGG CC-3′
Qp	5′-GAT AGC GTG CGC TAC CGG AT-3′
	5′-TGC AGA ATC AGC TCT CCC AAA C-3′
Fp	5′-TGC GAA AAC GAA AGT GCT TGA-3′
	5′-TGC AGA ATC AGC TCT CCC AAA C-3′
EBER1	5′-TGC TAG GGA GGA GAC GTG TGT-3′
	5′-GAA GAC GGC AGA AAG CAG AGT-3′
EBER2	5′-GCC CTA GTG GTT TCG GAC ACA-3′
	5′-GGA CAA GCC GAA TAC CCT TCT-3′
LMP1	5′-GCA GGA GGG TGA TCA TCA GT-3′
	5′-GTC CTC TAT TCC TTT GCT CTC ATG-3′
EBNA2	5′-GGA CAC AAG AGC CAT CAC CT-3′
	5′-CAA AGC ATT CGC ATA GCA GA-3′
EF1α	5′-CTG AAC CAT CCA GGC CAA AT-3′
	5′-GCC GTG TGG CAA TCC AAT-3′

The EF1α primer pair for the housekeeping gene is human specific; thus, the results will not be influenced by the contaminating mouse cells present in the starting material (cell suspension).

8. If a fresh source of CD34$^+$ cells is available on the day of transplantation, freshly isolated cells can be used. Alternatively, isolated CD34$^+$ cells can be frozen in 10 % dimethyl sulfoxide in fetal calf serum using a controlled rate freezer and thawed on the day of transplantation. Thawed cells should be enumerated prior to injection and resuspended in PBS at the correct concentration.

9. 1×10^5 CD34$^+$ cells are sufficient to achieve 50 % chimerism in recipient mice [2]. If more donor cells are available a larger number of cells can be injected to improve reconstitution [6].

10. T cell reconstitution is complete 12 weeks after reconstitution. Blood samples analyzed at earlier time points may display a large variability in frequencies of T cells.

11. What is considered a sufficient level of engraftment will depend on the experimental setup. The investigators should establish experimentally which level of engraftment is sufficient to answer their question.

12. EBV-infected HIS mice can develop tumors, predominantly in the spleen although we have occasionally observed tumors in other anatomical locations such as liver and thymus.

13. DNase treatment must be performed during RNA purification, since EBERs do not contain intronic sequences, and our primer set for the housekeeping gene of choice (EF1α) does not span over intronic sequences either.

14. Dilution is important because higher concentrations of cDNA will affect the signal baseline in SYBR Green reactions.

15. Include in all PCR runs a standard sample of cDNA prepared from an established LCL (for Cp and other transcrip ts specific for latency III) and a cDNA from a typical type I cell line (for example: Rael) for Q promoter activity. In this way,

results of test samples run in different occasions can be compared/related to each other.

16. Actin and GAPDH are often used as reference (housekeeping) genes for relative quantification of gene expression . However, we found that expression of these genes was very different in samples derived from infe cted compared to noninfected mice. This was most likely a consequence of the presence of high numbers of activated and proliferating T and B cells in the infected mice. After testing a number of other genes suggested in the literature [9], we selected EF1α as a housekeeping gene, since it was expressed at much more stable levels in this system.

17. Instead of ^{3}H-Tymidine incorporation, MTT [3-(4,5-Dimethylthiazol-2-yl)-2,5-diphenyltetrazoliumbromid] or other methods can be used to evaluate the quality of the cultures (living cell number) in a more objective way than just visual examination.

References

1. Traggiai E, Chicha L, Mazzucchelli L et al (2004) Development of a human adaptive immune system in cord blood cell-transplanted mice. Science 3(04):104–107
[CrossRef]

2. Heuts F, Rottenberg ME, Salamon D et al (2014) T cells modulate Epstein-Barr virus latency phenotypes during infection of humanized mice. J Virol 88:3235–3245
[CrossRef][PubMed][PubMedCentral]

3. Rickinson AB, Kieff E (2001) Epstein–Barr virus. In: Knipe DM, Howley PM (eds) Fields virology, vol 2, 4th edn. Lippincott Williams and Wilkins, Philadelphia, pp 2575–2628

4. Moss DJ, Rickinson AB, Pope JH (1978) Long-term T-cell-mediated immunity to Epstein-Barr virus in man. I Complete regression of virus-induced transformation in culture of seropositive donor leukocytes. Int J Cancer 22:662–668
[CrossRef][PubMed]

5. Ono A, Hattori S, Kariya R, Iwanaga S (2011) Comparative study of human hematopoietic cell engraftment into BALB/c and C57BL/6 strain of rag-2/jak3 double-deficient mice. BioMed Research 2011:539748. doi:10.1155/2011/539748

6. Lepus CM, Gibson TF, Gerber SA et al (2009) Comparison of human fetal liver, umbilical cord blood, and adult blood hematopoietic stem cell engraftment in NOD-scid/gammac−/−, Balb/c-Rag1−/−gammac−/−, and C.B-17-scid/bg immunodeficient mice. Hum Immunol 70:790–802
[CrossRef][PubMed][PubMedCentral]

7. Strowig T, Chicha L, Mazzucchelli L et al (2009) Priming of protective T cell responses against virus-induced tumors in mice with human immune system components. J Exp Med 206:1423–1434
[CrossRef][PubMed][PubMedCentral]

8. Bell AI, Groves K, Kelly GL et al (2006) Analysis of Epstein-Barr virus latent gene expression in endemic Burkitt's lymphoma and nasopharyngeal carcinoma tumour cells by using quantitative real-time PCR assays. J Gen Virol 87:2885–2890
[CrossRef][PubMed]

9. Hamalainen HK, Tubman JC, Vikman S et al (2001) Identification and validation of endogenous reference genes for expression profiling of T helper cell differentiation by quantitative real-time RT-PCR. Anal Biochem 299:63–70
[CrossRef][PubMed]

18. Generation and Analysis of Humanized Mouse Model of EBV Infection

Ken-Ichi Imadome[1] and Shigeyoshi Fujiwara[2, 3] ✉

(1) Division of Advanced Medicine for Virus Infections, National Research Institute for Child Health and Development, 2-10-1 Okura, Setagaya-ku, Tokyo 157-8535, Japan

(2) Department of Allergy and Clinical Immunology, National Research Institute for Child Health and Development, 2-10-1 Okura, Setagaya-ku, Tokyo 157-8535, Japan

(3) Division of Hematology and Rheumatology, Department of Medicine, Nihon University School of Medicine, 30-1 Oyaguchikamimachi, Itabashi-ku, Tokyo 173-8610, Japan

✉ **Shigeyoshi Fujiwara**
   Email: fujiwara-s@ncchd.go.jp

Abstract
The recent development of severely immunodeficient mouse strains enabled the production of new-generation humanized mice, in which major components of the human immune system are reconstituted. These new-generation humanized mice can be infected with human pathogenic viruses that do not infect regular mice and target cells of the hematoimmune system. Here we describe the method for preparing humanized mice, infecting them with EBV, and for their virological and immunological analyses. The results obtained from our own mouse models are briefly described.

Key words Epstein-Barr virus – Humanized mouse – Lymphoproliferative disease – Rheumatoid arthritis – Latent infection – Immune response – T cell – ELISPOT assay – MHC class I tetramer

1 Introduction

Humans are the only natural host of EBV infection and very few mammal species, including the cotton-top tamarin, can be infected with the virus experimentally. Although cotton-top tamarins have been used as an in vivo model of EBV-induced lymphomagenesis, they are an endangered species now and cannot be used in experiments anymore. Small animal models, particularly useful in the evaluation of novel drugs and therapies, have not been available for EBV. The development of C.B-17 *scid* mice in 1980s enabled the generation of *scid*-hu PBL mice that were generated by intraperitoneal injection of human peripheral blood mononuclear cells (PBMCs) in C.B-17 *scid* mice. Injection of PBMCs isolated from EBV-seropositive donors induced the development of EBV-positive B-cell lymphoma in *scid*-hu PBL mice, whereas those from seronegative donors did not [1]. *Scid*-hu PBL mice were thus utilized as a small animal model of EBV-induced B-cell oncogenesis. However, this early version of humanized mouse was actually a xenotransplantation model and was not suitable for direct analysis of in vivo events induced by EBV infection, including immune responses.

The development of severely immunodeficient mouse strains, such as NOD/Shi-*scid* *Il2rg* ^null^ (NOG) [2], BALB/c *Rag2* $^{-/-}$ *Il2rg* $^{-/-}$ (BRG) [3], and NOD/LtSz-*scid Il2rg* $^{-/-}$ (NSG) [4], enabled reconstitution of functional human immune system components in mice by transplanting them with human hematopoietic stem cells (HSCs) [5]. Mice thus prepared are often called new-generation humanized mice and are a powerful tool to study the development and function of the human immune system. In addition, these new-generation humanized mice have been used to reproduce key features of viral infections that target cells of the human hematoimmune system [6]. In vivo infection models for viruses including Epstein-Barr virus (EBV), human immunodeficiency virus type 1 (HIV-1), Dengue virus, and Kaposi's sarcoma-associated herpesvirus (KSHV) have been prepared using new-generation humanized mice [6]. Pathogenesis of these viruses and novel experimental therapeutics for them have been studied in these mice [6]. We have used NOG mice to prepare a humanized mouse model of EBV infection and reproduced key features of human EBV infection, including B-cell lymphoproliferative disease (LPD), erosive arthritis resembling rheumatoid arthritis, cell-mediated and humoral immune responses specific to the virus, and asymptomatic persistent infection similar to EBV latency in humans [7–10].

In this chapter, we describe our protocol for the preparation of new-generation humanized mice, inoculation of EBV to the mice, and virological and immunological characterization of infected mice. Although the entire process of preparing and analyzing these models consists of numerous individual steps requiring various virological and immunological techniques, we describe here only techniques essential

for studies with humanized mice. Standard techniques in EBV virology and immunology should be found elsewhere in this book.

2 Generation of Humanized Mice

2.1 Materials

2.1.1 Immunodeficient Mouse Strains

NOD/Shi-*scid Il2rg* ^{null} (NOG) [2], BALB/c *Rag2* $^{-/-}$ *Il2rg* $^{-/-}$ (BRG) [3], and NOD/LtSz-*scid Il2rg* $^{-/-}$ (NSG) [4] are representative immunodeficient mouse strains used most often for preparation of new-generation humanized mice. NOG and BRG mice are available from Taconic Biosciences Inc. (Hudson, NY), whereas NSG mice can be purchased from the Jackson Laboratory (Bar Harbor, ME). A specific pathogen free (SPF) facility, such as a vinyl isolator, a biobubble, or a barrier room, is required for maintaining these severely immunodeficient mice. The authors' group uses the bioBUBBLE (Kurea, Japan) and the IVC system (TECNIPPLAST, Japan). Immunodeficient mice need to be fed with sterilized water and food. Sterile disposable instruments or those sterilized by autoclaving should be used in all experiments with immunodeficient mice. Sterile caps, masks, gowns, and gloves should be worn always when handling these mice. Regular monitoring for microbiological agents should be carried out at least once a month. The immunodeficient mouse strains named above are considered living modified organisms (LMOs), and experiments with them should be carried out in compliance with laws and guidelines concerned.

2.1.2 Cord Blood

Cord blood is the recommended source of HSCs. Bone marrow-derived stem cells can be also used, but the speed and efficiency of reconstitution are less favorable than cord blood-derived ones (Imadome K, unpublished results). In addition, it is difficult to obtain bone marrow samples from healthy persons due to ethical considerations. The majority of adults are considered EBV carriers and bone marrow is likely to contain EBV-infected cells, unless they are shown to be seronegative. The author's group has been using cord blood supplied by a cord blood bank. A fraction of cord blood samples deposited to cord blood banks do not clear the criteria for transplantation to patients and are available for experiments, if informed consent is obtained. Frozen samples of cord blood are available from public resources such as the RIKEN Biobank (Tsukuba, Japan) and commercially (e.g., Lonza, Basel, Switzerland), although the efficiency of humanization with these materials is not comparable to fresh cord blood and varies from lot to lot. Experiments using cord blood should follow the Helsinki declaration and the protocol for them should be approved by an internal review board (IRB).

2.1.3 Commercially Available Kits for Isolation of HSCs

We use the CD34 MicroBead kit (Miltenyi Biotec, Bergisch Gladbach, Germany) and the protocol for isolating HSCs shown below is mostly based on the instruction supplied in the kit.

2.1.4 Antibodies for Characterization of Reconstituted Human Immune System Components

We use the following antibodies: FITC-anti-CD10, PE-anti-IgD, ECD-anti-CD45, PC5-anti-CD20, PC7-anti-CD19, FITC-anti-HLA-DR, PE-anti-CD8, ECD-anti-CD45, PC5-anti-CD3, PC7-anti-CD4, PE-anti-CD3, PC5-anti-CD56, and PC7- anti-CD16. All antibodies are available from BD Biosciences (Franklin Lakes, NJ, USA), except for FITC-anti-HLA-DR that can be purchased from Beckman-Coulter (Brea, CA, USA).

2.2 Methods

2.2.1 Isolation of CD34$^+$ Hematopoietic Stem Cells from Cord Blood (See *Note* 1)

Isolation of Mononuclear Cells

1. Transfer cord blood from a cord blood bag with a pipet into a 50 mL sterile tube containing 5 mL of phosphate-buffered saline (PBS) supplemented with 200 U/mL heparin and store at 4 °C prior to use (*see* **Note** 2).

2. Dilute the cord blood sample 1:1 with RPMI-1640 medium and put it slowly on a cushion of lymphocyte separation media (Promo Cell, Heidelberg, Germany).

3. Centrifuge at 400 × *g* for 30 min at room temperature (RT).

4. Collect the mononuclear cell band with a glass pipet and dilute 1:1 with RPMI-1640 medium and transfer to a sterile 15 mL tube.

5. Centrifuge the cell suspension at 400 × *g* for 10 min at RT and discard the supernatant fluid.

6. Resuspend the cell pellet with 10 mL of RPMI-1640 medium.

7. Determine cell number and viability.

8. Centrifuge cell suspension at $400 \times g$ for 10 min and aspirate supernatant completely.

*Isolation of CD34+ Cells by Magnetic Labeling (See **Note 3**)*

1. Resuspend cell pellet in 300 µL of RPMI-1640 medium (*see* **Notes 4** and **5**).

2. Add 100 µL of FcR Blocking Reagent (supplied by the kit).

3. Add 100 µL of CD34 MicroBeads (supplied by the kit).

4. Mix well and keep at 2–8 °C for 30 min (*see* **Note 6**).

5. Wash cells by adding 5–10 mL of RPMI-1640 medium, centrifuge at $400 \times g$ for 10 min, and aspirate supernatant completely.

6. Resuspend cells in 500 µL of RPMI-1640 medium.

7. Place an appropriate MACS column (supplied by the kit) in the magnetic field of a suitable MACS Separator (supplied by the kit) (*see* **Note 7**).

8. Rinse the column with the appropriate amount of RPMI-1640 medium: 500 µL for MS and 3 mL for LS.

9. Apply the cell suspension to the column. The flow-through contains unlabeled cells.

10. Wash the column three times with the appropriate amount of RPMI-1640 medium: MS, 3×500 µL; LS, 3×3 mL.

11. Remove the column from the separator and place it on a collection tube.

12. Pipet the appropriate amount (1 mL for MS and 5 mL for LS) of RPMI-1640

medium onto the column and let labeled cells drop down (*see* **Note 8**).

2.2.2 *Transplantation of HSCs to Immunodeficient Mice (See Note 9)*

1. Resuspend CD34+ stem cells isolated as described above in PBS at $1–10 \times 10^4$ cells/300 µL and inject the total volume slowly (taking 5–10 s) via the tail vein (*see* **Note 10**).

2.2.3 2.2.3 *Monitoring of Reconstitution of Human Immune System Components in Mice*

1. Take 100 µL of blood from the tail vein (*see* **Note 11**) and transfer to a 12 × 75 mm test tube containing an appropriate amount (*see* **Note 12**) of antibody and mix well.

2. Keep the tube shielded from light at RT (20–25 °C) for 15–30 min.

3. Add 500 µL of OptiLyse C (Beckman Coulter) and stir well.

4. Keep the tube shielded from light at RT (20–25 °C) for 10 min.

5. Add 500 µL of PBS and stir well.

6. Keep the tube shielded from light at RT (20–25 °C) for 10 min.

7. Add 2 mL of PBS and stir well.

8. Centrifuge the tube at $400 \times g$ for 5 min and remove the supernatant.

9. Resuspend the cells in 500 µL of PBS containing 2 % BSA and keep the sample shielded from light at 2–8 °C until measurement by a flow cytometer .

3 Inoculation of EBV to Humanized Mice

3.1 Material

3.1.1 EBV

EBV can be prepared from the culture supernatants of several virus-producer cell lines, such as Akata and B95-8 . Akata is a human cell line that was derived from a Japanese patient with Burkitt lymphoma and produces a type-1 strain EBV. B95- 8 is a B-cell line of the cotton-top tamarin origin transformed by a type-1 EBV strain isolated from a patient with infectious mononucleosis .

3.2 Methods

3.2.1 Preparation of an Akata EBV Inoculate

1. Resuspend Akata cells at 5×10^6 cells/mL in fresh culture medium containing a final concentration of 0.5 % (vol/vol) polyclonal rabbit anti-human IgG (Dako, Denmark).

2. Incubate the cells at 37 °C in 5 % CO_2 atmosphere for 6 h.

3. Wash the cells once with fresh culture medium, resuspend them at 1×10^6 cells/mL in fresh culture medium, and transfer them to a culture flask of an appropriate size.

4. Culture the cells at 37 °C in 5 % CO_2 atmosphere for 42 h.

5. Collect supernatant by centrifugation at $400 \times g$ for 5 min at 4 °C.

6. Filter the supernatant through a 0.45 μm sterile filter membrane.

7. The supernatant fluid is kept at −80 °C until use (*see* **Note 13**).

3.2.2 Preparation of a B95-8 EBV Inoculate

1. Propagate B95-8 cells in 40 mL of culture medium using a T-75 flask.

2. Change the half of the medium every 4–5 days until full confluency is gained.

3. Remove cells from the flask with a cell scraper, resuspend them in 100 mL fresh culture medium, and transfer them to a T-150 flask.

4. Incubate for 7 days at 37 °C in 5 % CO_2 atmosphere.

5. Centrifuge the cells at 400 × g for 5 min at 4 °C.

6. Collect the supernatant and filter it through a filter membrane 0.45 μm.

7. The supernatant fluid is kept at −80 °C until use (*see* **Note** **13**).

3.2.3 Intravenous or Intraperitoneal Injection

Following transplantation of HSC s to NOG mice, B cells are reconstituted 2–3 months post-transplantation, whereas T cells develop significantly later, 5–6 months post-transplantation (Fig. 1). Therefore, efficient T-cell responses are induced when mice are infected 5–6 months following transplantation; more aggressive EBV-induced lymphoproliferation results when mice are infected at earlier time points [8].
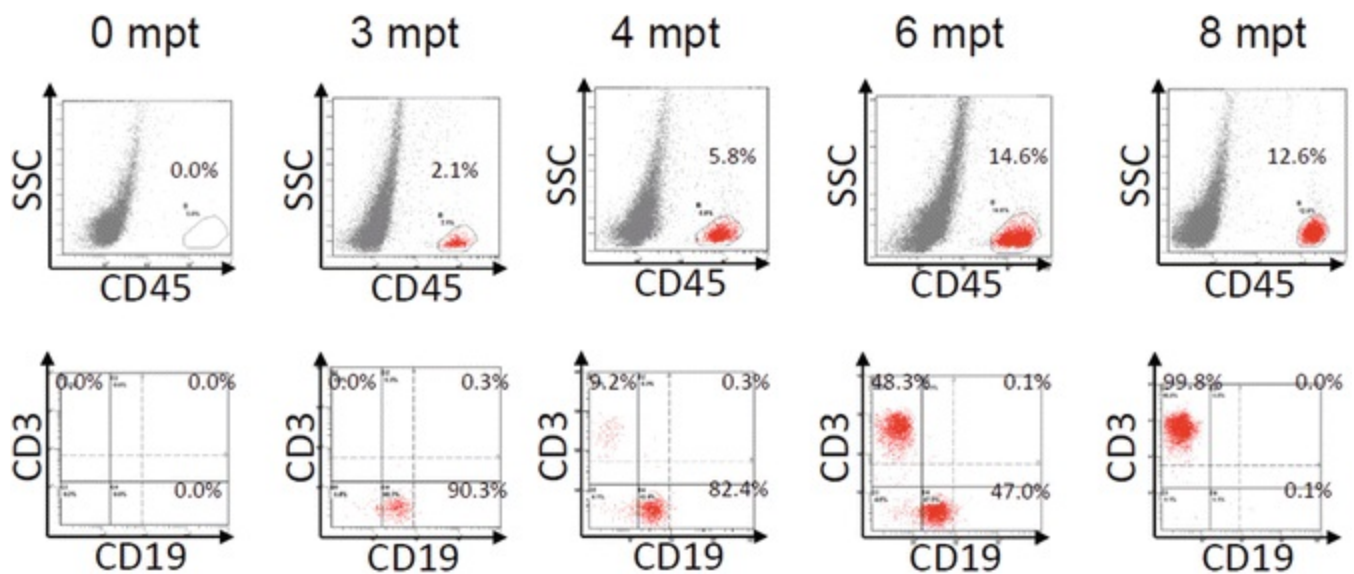
Fig. 1 Differentiation of human lymphocytes in a NOG mouse transplanted with human HSCs. Percentage of cells positively stained with human-specific antibodies to CD45, CD3, and CD19 were determined at 0, 3, 4, 6, and 8 months post-transplantation (mpt). B cells differentiated first around three mpt, whereas T cells appeared first four mpt and reached the peak level at six mpt

Inject EBV inoculate (100 μL containing an appropriate titer) intravenously through the tail vein with a 29 Gauge (0.33 × 13 mm) needle. The same amount of virus can be injected intraperitoneally (*see* **Note 14**).

---

4 Analyses of EBV-Infected Mice

4.1 Monitoring EBV DNA Load (*See* **Note 15**)

4.1.1 Materials

1. DNA isolation kit (e.g., QIAamp DNA Mini Kit from QIAGEN, Venlo, Netherlands).

2. Primers and a probe for real-time PCR derived from the EBV-encoded BALF5 open reading frame: upstream primer, 5′-CGG AAG CCC TCT GGA CTT C-3′; downstream primer, 5′-CCC TGT TTA TCC GAT GGA ATG-3′; fluorogenic probe, 5′-TGT ACA CGC ACG AGA AAT GCG CC-3′.

3. Reagents kit for real-time PCR (e.g., AmpliTaq Gold DNA Polymerase with Gold Buffer & $MgCl_2$ from Applied Biosystems, Waltham, MA, USA).

4.1.2 Methods

1. Take 100 μL of blood from the tail vein.

2. Purify DNA following the instruction provided in the kit and determine DNA concentration.

3. Perform standard real-time PCR as described elsewhere [11].

4.2 Characterization of Peripheral Blood Lymphocyte Phenotypes

Following infection with EBV, a drastic increase in the number of peripheral blood CD8+ T cells is recognized. These CD8+ T cells have an activated phenotype with the expression of HLA-DR. Some mice show a slight increase in the number of peripheral blood NK cells. These changes in the number and phenotype of lymphocytes, examined

by flow cytometry as described in Subheading 2.2.3, can be used as a marker for successful infection.

4.3 ELISPOT Assay to Count EBV-Specific T-Cells

4.3.1 Materials

1. A CD8+ T-cell isolation kit (e.g., Anti-Human CD8 Particles from BD Biosciences).

2. An ELISPOT assay kit (e.g., IMMUNOCYTO IFN-γ ELISPOT Kit provided by MBL, Nagoya, Japan).

3. 96-well microplates for ELISPOT assay (such as Millipore MAHA S45 10 and MAIP S45 10).

4. Lymphoblastoid cell lines transformed by EBV that are used as a stimulator of IFN-γ production or as a mock stimulator (*see* **Note 16**).

5. Sensitization buffer: 20 mM HEPES, pH 7.4, 150 mM NaCl, 0.5 mM $CaCl_2$.

6. Wash buffer: 0.05 % Tween 20 in the sensitization buffer.

4.3.2 Methods

Isolation of CD8+ T Cells

1. Sacrifice mice with Somnopentyl and collect total blood by cardiac puncture.

2. Isolate mononuclear cells as described in Subheading 2.2.1.

3. Count cells, wash them with an excess volume of 1× BD IMag buffer (supplied by the kit), and carefully aspirate all the supernatant.

4. Vortex the BD IMag Anti-Human CD8 Magnetic Particles-DM (supplied by the kit) thoroughly, and add 50 μL of particles for every 10^7 total cells.

5. Mix thoroughly by gentle pipetting and incubate at RT for 30 min.

6. Bring the volume up to $1–8 \times 10^7$ cells/mL with $1\times$ BD IMag buffer (supplied by the kit), and immediately place the tube on the BD IMagnet (supplied by the kit). I ncubate for 8–10 min.

7. With the tube on the BD IMagnet, carefully aspirate off the supernatant. This supernatant contains the negative fraction.

8. Remove the tube from the BD IMagnet, and add 1 mL of $1\times$ BD IMag buffer to the same volume as in the **step 6**. Gently resuspend cells by pipetting, and return the tube to the BD IMagnet for another 2–4 min.

9. With the tube on the BD IMagnet, carefully aspirate off the supernatant and discard.

10. Repeat **steps 8** and **9**.

11. After the final wash step, resuspend the positive fraction in culture medium.

Preparation of Microplates

1. Add 100 µL of 70 % ethanol to a polyvinylidene difluoride (PVDF) plate (such as Millipore MAIP S45 10) and keep at RT for 10 min (*see* **Note 17**).

2. Remove 70 % ethanol and add 100 µL of sensitization buffer.

3. Aspirate the buffer and add 100 µL of appropriately diluted antibody to each well.

4. Seal the plate and incubate at 4 °C overnight.

5. Aspirate the antibody solution.

6. Wash the plate with 200 µL/well of sensitization buffer and aspirate. Repeat this

step 5 times.

7. Block the plate by adding 200 μL of culture medium to each well and incubate at RT for 30 min.

ELISPOT Analysis

1. Mix CD8+ T cells with autologous LCL in fresh culture medium containing 50 U/mL human IL-2 so that the cell density for the former will be $2.5–10 \times 10^4$ cells/well and that for the latter $1–10 \times 10^2$ cells/well. Dispense 200 μL of this cell suspension to each well of the microplate (*see* **Note 18**).

2. Incubate for 17 h in 5 % CO_2 incubator at 37 °C.

3. Aspirate supernatant of each well carefully and add 200 μL of wash buffer to each well.

4. Aspirate supernatant of each well carefully.

5. Repeat **step 3–4** to wash each well four times.

6. Add 100 μL of diluted Biotinylated anti-human IFN-γ monoclonal antibody (supplied by the kit) to each well.

7. Overlay the plate with a plate seal and incubate the plate for 2 h at RT.

8. Wash each well, according to **step 3–5**.

9. Add 100 μL of diluted streptavidin-conjugated alkaline phosphatase (supplied by the kit) to each well.

10. Overlay the plate with a plate seal and incubate the plate for 1 h at RT.

11. Wash each well, according to **step 3–5**.

12. Add 1000 µL of diluted BCIP/NBT chromogen Substrate (supplied by the kit) to each well.

13. Overlay the plate with a plate seal and incubate the plate for 10–20 min at RT in the dark. This incubation should continue until the red-purple spots on the plate become visible.

14. Stop color development by adding 200 µL of deionized water to each well.

15. Aspirate water.

16. Repeat **step 14–15** to wash each well nine times.

17. Leave the plate to dry completely.

18. Count spots with a stereomicroscope or an automated ELISPOT reader.

4.4 Quantitation of EBV-Specific T Cells with MHC Class I Tetramers (*See* **Notes 19** and **20**)

4.4.1 Materials

1. Human MHC class I tetramers presenting EBV-derived peptides
   PE-labeled HLA-A*0201, 0301, 1101, 2402 and HLA-B*1501, 0801, 3501 tetramers presenting epitopes derived from five immunodominant EBV proteins, LMP2 , BRLF1, BMLF1, EBNA3A , and EBNA3B are available from Medical and Biological Laboratories (MBL), Nagoya, Japan. The following protocol is based on the instruction provided in the kit (T-Select HLA class I human Tetramer-PE, MBL).

4.4.2 Methods

1. Prepare PBMC as described above and resuspend them at 4×10^6 cells/mL in PBS.

2. Add 40 µL human FcR blocking reagent (provided in the kit) to 50 µL (2×10^5

cells) of the PBMC suspension and incubate for 5 min at RT.

3. Add 10 μL of the tetramer solution (provided in the kit).

4. Incubate for 20 min at RT or for 30 min at 4 °C.

5. Add 20 μL of anti-CD8 antibody (*see* **Note 21**) and incubate for 30 min at 4 °C.

6. Add an appropriate amount of PBS containing 2 % FCS and centrifuge the tube at 400 × *g* for 5 min.

7. Aspirate or decant the supernatant carefully.

8. Resuspend the pellet in 500 μL of PBS containing 0.5 % Paraformaldehyde.

9. Store prepared samples at 4 °C protected from light for a minimum of 1 h (maximum 24 h) prior to analysis by flow cytometry.

---

5 Notes

1. During this procedure, cells should be kept cold and precooled solutions should be used to suspend them. This will prevent capping of antibodies on the cell surface and nonspecific cell labeling.

2. Cord blood should be used on the day of collection. This will help isolating HSCs of better quality.

3. The volumes for buffers and solutions given below are for up to 10^8 total cells. When working with fewer than 10^8 cells, use the same volumes as indicated. When working with higher cell numbers, scale up all reagent volumes and total volumes accordingly (e.g., for 2×10^8 total cells, use twice the volume of all indicated reagent volumes and total volumes).

4. For optimal isolation of HSCs it is important to obtain a single cell suspension

before magnetic labeling. Pass cells through 30 μm nylon mesh (for example, cell strainer provided by BD Biosciences) to remove cell clumps which may clog the column.

5. We use RPMI-1640 medium in place of the buffer (PBS, pH 7.2 containing 0.5 % BSA and 2 mM EDTA) suggested by the kit and obtain good results.

6. The recommended incubation temperature is 2–8 °C. Higher temperatures or longer incubation times may lead to nonspecific cell labeling. Incubation on ice may require increased incubation time.

7. An appropriate MACS Column and MACS Separator should be chosen according to the number of total cells and the number of CD34$^+$ cells; the criteria for this choice are given in the instruction provided by the manufacturer.

8. When the number of labeled cells is expected to be low, we spin the column at $400 \times g$ for 10 min.

9. Female mice at the age of 6–8 weeks are injected intravenously with 1–10×10^4 stem cells. There are several options for the method of transplanting HSCs. Mice can be irradiated (~300 cGy) before transplantation, although this may shorten the lifespan of mice [12]. Newborn mice can be also transplanted with HSCs; intrahepatic injection or injection via the facial vein is usually used [13].

10. A mouse fixation adjuster (Sanpratec Japan) can be used to retain mice.

11. Blood should be taken from mice at 8, 12, 16, 20, 24 weeks after transplantation of HSCs.

12. The amount of antibody to give optimal staining varies and should be determined on an empirical basis.

13. The 50 % transforming dose (TD$_{50}$) of individual virus preparations can be measured as described elsewhere [7].

14. We have used both intravenous and intraperitoneal routes for EBV inoculation. By comparison, intravenous injection gave more consistent results. We have also tried oral administration of EBV, without success.

15. EBV DNA starts to be detected in the peripheral blood of humanized NOG mice usually 3–4 weeks after inoculation and therefore measurement of EBV DNA load should be started before this time point.

16. A stimulator LCL needs to be established from the same cord blood sample as used for humanization of the particular mouse, or from B cells isolated from the mouse. This warrants that an LCL obtained is autologous to T cells isolated from the EBV-infected mouse. An allogenic LCL with mismatched MHC can be used as a mock stimulator.

17. Microplates with two kinds of membrane, mixed cellulose and PVDF, are available for ELISPOT assay; we usually have better results with PVDF membrane.

18. Each mouse has a different number of EBV-specific cells among total CD8+ T cells. Therefore, the number of CD8+ T cells and LCL cells per well, as well as the ratio of the two cell populations, should be varied to find an optimal condition for counting spots.

19. In primary EBV infection of humans, massive expansion of CD8+ T cells is evident. The majority of these CD8+ cells is specific to EBV and plays important roles in the immune control of primary infection. An approximate number of EBV-specific CD8+ T cells can be quantitated with human MHC c lass I tetramers. Reactivity with these tetramers is considered as a direct evidence for T-cell responses restricted by human MHC in humanized mice.

20. In the positive selection of T-cell progenitors in the thymus, those cells expressing TCR molecules reacting with the MHC molecule (plus a self-derived peptide) on thymic epithelial cells with low affinity will survive. Because the thymic epithelial cells of regular new-generation humanized mice are of the murine origin, T cell education in the thymus does not occur optimally, and the functions of human T cells in these mice are impaired. The NS G-HLA-A2.1 mouse strain (available from Jackson Laboratory) expresses the human HLA-A2.1 molecule

from a transgene, and therefore excellent T-cell responses to EBV are achieved when humanized with HSCs carrying this particular MHC allele [14].

21. We use the clone T8 provided by Becton Dickinson and have not obtained good results with other antibodies to CD8.

---

6 Brief Description of the Results with Our Humanized Model Mice

Most humanized NOG mice infected with EBV of $>10^3$ TD$_{50}$ developed a lymphoproliferative disease that is similar to typical cases of human EBV-associated lymphoproliferative disease with respect to histology (typically diffuse large B-cell lymphoma), marker expression (activated B-cell phenotype), and EBV gene expression (latency III) (Fig. 2) [7]. Mice infected with EBV of $<10^1$ TD$_{50}$ developed asymptomatic persistent infection that may be similar to EBV latency in humans. EBV-infected humanized NOG mice mounted efficient virus-specific T-cell responses that are restricted by human MHC class I, and depletion of either CD3- or CD8-positive cells by the administration of anti CD3 or anti-CD8 antibody, respectively, reduced the lifespan of infected mice significantly [7, 8]. In contrast, humoral immune responses were much less efficient, and only a minor fraction (3/30) of infected mice produced IgM antibodies to the viral capsid antigen component p18 ^{BFRF3} [7]. No IgG antibody directed to EBV proteins was detected. Basically similar results have been obtained from the humanized mouse model of EBV infection using different immunodeficient mouse strains as well as different procedures of reconstitution of human immune system components [15, 16]. Recently, characterization of EBV mutants in humanized mice has revealed novel functions of EBV genes that could not have been elucidated in in vitro studies with cultured cells [reviewed in 9]. Humanized mice prepared by transplanting human fetal liver and thymus tissues as well as autologous HSCs isolated from human liver are called BLT mice and mount better T-cell immune responses as compared with regular new-generation humanized mice [16].
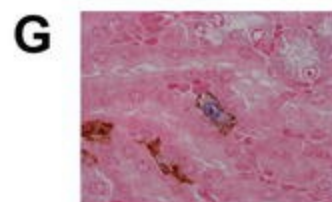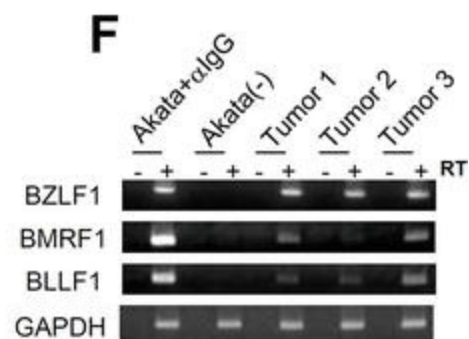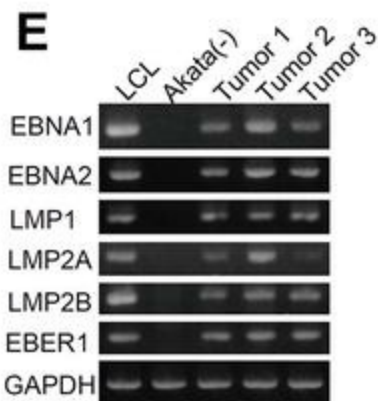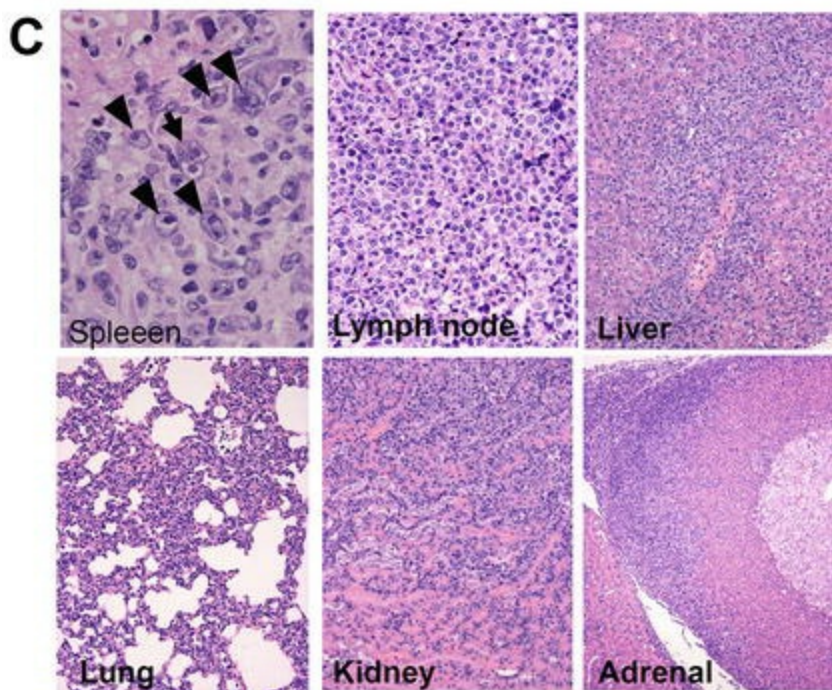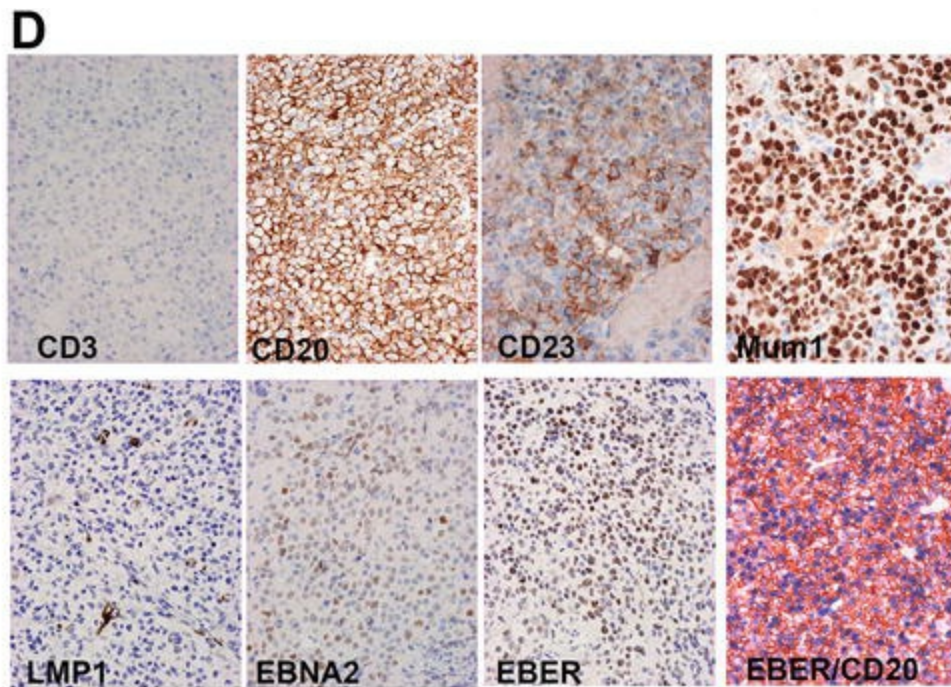
Fig. 2 EBV-induced lymphoproliferative disease in humanized NOG mice. (**a**) Photograph of a mouse showing tumors in the cervical area. (**b**) Photographs of spleens, liver, lymph node, and kidney from EBV-infected mice. The *upper-left panel* shows the spleen from an uninfected mouse. (**c**) Photomicrographs of HE-stained tissues. An *arrow* indicates a Reed-Sternberg-like cell and *arrowheads* indicate Hodgkin-like cells. (**d**) Immunohistochemical staining of lymphocyte surface markers (CD3, CD20, CD23, and Mum1) and EBV-encoded proteins (LMP 1 and EBNA2), as well as in situ hybridization for EBER in a lymph node of an infected mouse. The *bottom-right panel* represents double staining for EBER and CD20. (**e, f**) RT-PCR analysis of latent-cycle (**e**) and lytic-cycle (**f**) EBV gene expression in tumors from infected mice. Spleen tumors from three different mice were examined for the expression o f EBV genes indicated. RNA samples from an LCL (**e**) and anti-IgG-treated Akata cells (**f**) were used as positive controls, and those of EBV-negative Akata cells (**e, f**) were used as a negative control. Analysis was done with (+) or without (−) reverse transcriptase (RT) in **f**. (**g**) Double staining of EBER and CD20 in the spleen of a humanized NOG mouse inoculated with low-dose EBV. EBER is stained navy in the nucleus and CD20 is stained brown in the membrane. Reproduced with permission from J Infect Dis 198:673–682, 2008

Although B cells and epithelial cells are the major targets of EBV infection, the virus infects T or NK cells occasionally and induces their monoclonal or oligoclonal proliferation in a group of rare diseases termed EBV-associated T/NK-cell LPDs. Since we did not find any signs of EBV infection in T or NK cells in EBV-infected humanized mice described above, we transplanted PBMCs isolated from patients with EBV-associated T/NK-cell LPDs and succeeded in reproducing cardinal features of these diseases [17].

References

1. Mosier DE, Gulizia RJ, Baird SM, Wilson DB (1988) Transfer of a functional human immune system to mice with severe combined immunodeficiency. Nature 335:256–259
[CrossRef][PubMed]

2. Ito M, Hiramatsu H, Kobayashi K, Suzue K, Kawahata M, Hioki K et al (2002) NOD/SCID/gamma(c)(null) mouse: an excellent recipient mouse model for engraftment of human cells. Blood 100:3175–3182
[CrossRef][PubMed]

3. Traggiai E, Chicha L, Mazzucchelli L, Bronz L, Piffaretti JC, Lanzavecchia A et al (2004) Development of a human adaptive immune system in cord blood cell-transplanted mice. Science 304:104–107
[CrossRef][PubMed]

4. Ishikawa F, Yasukawa M, Lyons B, Yoshida S, Miyamoto T, Yoshimoto G et al (2005) Development of functional human blood and immune systems in NOD/SCID/IL2 receptor {gamma} chain(null) mice. Blood 106:1565–1573
[CrossRef][PubMed][PubMedCentral]

5. Shultz LD, Brehm MA, Garcia-Martinez JV, Greiner DL (2012) Humanized mice for immune system investigation: progress, promise and challenges. Nat Rev Immunol 12:786–798
[CrossRef][PubMed][PubMedCentral]

6. Akkina R (2013) New generation humanized mice for virus research: comparative aspects and future prospects. Virology 435:14–28
[CrossRef][PubMed][PubMedCentral]

7. Yajima M, Imadome K, Nakagawa A, Watanabe S, Terashima K, Nakamura H et al (2008) A new humanized mouse model of Epstein-Barr virus infection that reproduces persistent infection, lymphoproliferative disorder, and cell-mediated and humoral immune responses. J Infect Dis 198:673–682
[CrossRef][PubMed]

8. Yajima M, Imadome K, Nakagawa A, Watanabe S, Terashima K, Nakamura H et al (2009) T cell-mediated control of Epstein-Barr virus infection in humanized mice. J Infect Dis 200:1611–1615
[CrossRef][PubMed]

9. Fujiwara S, Imadome K, Takei M (2015) Modeling EBV infection and pathogenesis in new-generation humanized mice. Exp Mol Med 47:e135
[CrossRef][PubMed][PubMedCentral]

10. Kuwana Y, Takei M, Yajima M, Imadome K, Inomata H, Shiozaki M et al (2011) Epstein-Barr virus induces erosive arthritis in humanized mice. PLoS One 6:e26630
[CrossRef][PubMed][PubMedCentral]

11. Kimura H, Morita M, Yabuta Y, Kuzushima K, Kato K, Kojima S et al (1999) Quantitative analysis of Epstein-Barr virus load by using a real-time PCR assay. J Clin Microbiol 37:132–136
[PubMed][PubMedCentral]

12. Watanabe S, Ohta S, Yajima M, Terashima K, Ito M, Mugishima H et al (2007) Humanized NOD/SCID/IL2Rgamma(null) mice transplanted with hematopoietic stem cells under nonmyeloablative conditions show prolonged life spans and allow detailed analysis of human immunodeficiency virus type 1 pathogenesis. J Virol 81:13259–13264
[CrossRef][PubMed][PubMedCentral]

13. Sato K, Misawa N, Nie C, Satou Y, Iwakiri D, Matsuoka M et al (2011) A novel animal model of Epstein-Barr virus-associated hemophagocytic lymphohistiocytosis in humanized mice. Blood 117:5663–5673
[CrossRef][PubMed]

14. Shultz LD, Saito Y, Najima Y, Tanaka S, Ochi T, Tomizawa M et al (2010) Generation of functional human T-cell subsets with HLA-restricted immune responses in HLA class I expressing NOD/SCID/IL2r gamma(null) humanized mice. Proc Natl Acad Sci U S A 107:13022–13027
[CrossRef][PubMed][PubMedCentral]

15. Strowig T, Gurer C, Ploss A, Liu YF, Arrey F, Sashihara J et al (2009) Priming of protective T cell responses against virus-induced tumors in mice with human immune system components. J Exp Med 206:1423–1434
[CrossRef][PubMed][PubMedCentral]

16. Melkus MW, Estes JD, Padgett-Thomas A, Gatlin J, Denton PW, Othieno FA et al (2006) Humanized mice mount specific adaptive and innate immune responses to EBV and TSST-1. Nat Med 12:1316–1322
[CrossRef][PubMed]

17. Imadome K, Yajima M, Arai A, Nakazawa A, Kawano F, Ichikawa S et al (2011) Novel mouse xenograft models reveal a critical role of CD4+ T cells in the proliferation of EBV-infected T and NK cells. PLoS Pathog 7:e1002326
[CrossRef][PubMed][PubMedCentral]

19. EBV-Directed T Cell Therapeutics for EBV-Associated Lymphomas

Lauren P. McLaughlin[1, 2] ✉, Stephen Gottschalk[3],
Cliona M. Rooney[4] and Catherine M. Bollard[2, 5]

(1) Department of Hematology/Oncology, Children's National Medical Center, 111 Michigan Ave., Washington, DC, 20010, USA
(2) The George Washington University, Washington, DC, USA
(3) Texas Children's Cancer Center, Texas Children's Hospital, Baylor College of Medicine, Houston, TX, USA
(4) Center for Cell and Gene Therapy, Texas Children's Hospital, Houston Methodist Hospital,, Baylor College of Medicine, Houston, TX, USA
(5) Center for Cancer and Immunology Research, Children's National Medical Center, Washington, DC, USA

✉ **Lauren P. McLaughlin**
   Email: lmclaugh@childrensnational.org

Abstract
Epstein Barr virus (EBV) is a human gamma herpes virus that establishes latency in B cells after primary infection. EBV generally only causes a mild, self-limiting viral illness but is also associated with several malignancies including posttransplantation lymphoproliferative disorder in the immunosuppressed host as well as Hodgkin and non-Hodgkin lymphoma in the immune competent host. The expression of EBV antigens by lymphoma has important applications as targets for adoptive T cell therapy. However, as many lymphomas only express subdominant EBV antigens that are less immunogenic, novel strategies are needed to manufacture EBV-specific T cell products specific for Latent Membrane Protein 1 (LMP1) and LMP2, which are expressed in lymphomas with type II and III latency. While several techniques for manufacturing EBV-CTLs are described in the literature, this chapter focuses on one method for

generating Good Manufacturing Practice (GMP)-compliant EBV-specific T cell products that are enriched with LMP1 and LMP2.

Key words Epstein Barr virus – Lymphoma – Adoptive T cell therapy – Good manufacturing practice

1 Introduction

1.1 Overview

Epstein Barr virus (EBV) is a gamma herpes virus that infects 90 % of the population. EBV establishes life-long latency in memory B cells and oral epithelial cells. In the immune competent host, circulating EBV-specific cytotoxic T lymphocytes (CTLs) maintain EBV-infected B cells at a level of less than 1 % of the B-cell pool. However, in the immunosuppressed host, uncontrolled proliferation of EBV-infected B cells contributes to lymphoproliferative disorders such as posttransplantation lymphoproliferative disorder (PTLD) after solid organ transplantation (SOT) or hematopoietic stem cell transplantation (HSCT). Moreover, a significant proportion of Hodgkin lymphomas (HL) and non-Hodgkin lymphomas (NHL) express EBV antigens even in the immune competent host. The expression of EBV antigens by lymphomas has significant implications for adoptive T cell therapy.

1.2 EBV-Encoded Proteins as Target Antigens for Immunotherapy

EBV latency varies in the number and type of EBV proteins expressed by B cells, and EBV-associated malignancies can be categorized by their EBV latency pattern (*see* Table 1). Type III latency malignancies such as PTLD express a full complement of EBV antigens, which makes these tumors highly immunogenic and thus prime candidates for adoptiv e T cell therapy with EBV-CTLs. However, PTLD only occurs in immune compromised hosts. In the immune competent host, approximately 40 % of HL and a significant proportion of NHL (20 % of diffuse large B-cell lymphomas and >90 % natural killer/T-cell NHL nasal type) are associated with type II EBV latency. Type II latency tumors only express the subdominant antigens LMP1, LMP2, EBV nuclear antigen 1 (EBNA1), and BARF1 [1–3]. LMP1 and LMP2 are expressed by Reed-Sternberg c ells in HL and by NHL tumor cells, and LMP-specific CTLs are present in most donors at a low frequency that can be activated and expanded in vitro [4]. Thus, LMP1 and LMP2 are suitable targets for type II and III latency lymphomas. Nasopharyngeal carcinomas (NPC) are also frequently EBV-associated with a type II latency pattern, and EBV-CTLs have been used to treat metastatic or locally recurrent

NPC but with less success than in EBV-associated lymphomas [5]. In type I latency such as seen in Burkitt's Lymphoma (BL), only EBNA1 and BARF1 are expressed, which are weakly immunogenic. While EBNA1 is expressed in most EBV infected cells, an internal glycine-alanine repeat prevents effective presentation to class I CD8+ T cells, making EBNA1 an unsuitable target for adoptive T cell therapy [6].

Table 1 Pattern of EBV latent gene expression

	Type I	Type II	Type III
EBV antigen expression	BARFO EBNA1	LMP1, LMP2 +/-BARFO EBNA1	LMP1, LMP2 BARFO EBNA1 EBNA2 EBNA3a,b,c LP
Associated malignancy	Burkitt's lyphoma	Hodgkin lymphoma DLBCL , NK/T cell lymphoma , NPC	PTLD

1.3 Clinical Applications of Adoptive T Cell Therapy for EBV-Associated Lymphomas

Adoptive T cell therapy has been used for over two decades to treat EBV-associated PTLD [7]. While using unselected donor lymphocyte infusions (DLIs) from EBV seropositive donors to restore EBV-specific immunity has yielded response rates of ~70 % [8–10], this approach carries the significant risk of severe graft-versus-host-disease (GVHD). Thus, investigators sought novel ways to restore EBV immunity while minimizing GVHD risk by manufacturing EBV-specific T cell products for infusions. One early method of manufacturing EBV-specific T cell products was developed to use EBV-transformed B-lymphoblastoid cells lines (LCLs) as antigen presenting cells (APCs) [11]. In a cohort of 101 patients who received EBV-specific CTLs post-HSCT as prophylaxis for EBV-associated PTLD, no patients developed disease compared to a 11.5 % incidence in the historical controls. Moreover, 11 out of 13 patients who had developed PTLD attained a durable CR after receiving donor-derived EBV-specific T-cells [12]. In a study of 49 patients with PTLD, Doubrovina et al. from Memorial Sloan Kettering Cancer Center demonstrated that DLI from EBV-seropositive donors ($n = 30$) and donor derived EBV-specific T cells ($n = 19$) had similar efficacies in vivo since approximately 70 % of patients in both groups attained complete or partial responses. However, the EBV-T-cell cohort had no cases of GVHD compared to a 17 % incidence in the patients who received DLI [10]. An alternative strategy to treat PTLD which is

generally an aggressive and rapidly progressing disease, the use of "off the shelf" third-party EBV-CTL products are being developed to avoid the time delays inherent when generating donor-specific products. Using this approach, a group from the United Kingdom reported an overall response rate of 52 % (17 of 33 patients) at 6 months using third-party EBV-CTLs in patients with PTLD after SOT ($n = 31$) or HSCT ($n = 2$) who had previously failed conventional therapy [13].

Given the significant successes using EBV-CTLs for the treatment and prevention of PTLD, this therapeutic also been used to treat refractory/relapsed EBV-positive HL and NHL. Circulating T cells specific for type II latency antigens are relatively uncommon in patients with type II latency lymphomas, and the immunosuppressive tumor microenvironment is thought to render these T cells anergic [14, 15]. Despite these limitations, autologous EBV-CTLs have been successfully expanded from patients with EBV+ Hodgkin lymphoma, but expansion is less robust when compared to healthy donors [16]. To enrich T cells specific for the EBV type II latency antigens present on EBV+ lymphomas that develop in immune competent hosts, the Baylor College of Medicine group developed a method of transducing dendritic cells and EBV-transformed B–lymphoblastoid cell lines (LCLs) with an adenoviral vector (Ad5f35) expressing LMP1 and/or LMP2 [17, 18]. Using this approach, in 50 patients with refractory/relapsed EBV-associated HL or NHL, 28 out of 29 patients who received LMP-specific T cells prophylactically after autologous SCT or chemotherapy remained in remission with an 82 % EFS at 2 years, and 13 of 21 patients with relapsed disease had a partial ($n = 2$) or complete ($n = 11$) tumor response [19, 20].

While patients with HL/NHL typically have good outcomes, the prognosis for patients with relapsed or refractory disease is often very poor. Moreover, there are significant short- and long-term effects associated with the standard therapies that include chemotherapy, radiation therapy, and possibly HSC T. Additionally, PTLD can be a very aggressive disease, and while PTLD often responds favorably to reduction in immunosuppression , this is often not feasible in SOT patients who require lifelong immunosuppression. Thus, EBV-CTLs offer a novel therapeutic for many patients who have previously failed therapy. Not only do EBV-CTLs help restore EBV-specific cellular immunity and have direct tumor killing, but there is also evidence that they recruit endogenous T cells specific for nonviral tumor antigens through epitope spreading [20].

Importantly, EBV-CTLs have proven to be not only efficacious but also safe since EBV-directed T cells (both autologous and donor-derived) have been well tolerated in vivo with minimal infusion related toxicities [20, 21]. Further, in the allogeneic donor-specific setting, despite a theoretical risk of GVHD , the adoptive transfer of allogeneic donor-derived virus-specific CTLs in 153 recipients resulted in no de novo cases of acute GVHD after infusion despite 73 instances of HLA mismatch [22]. Similarly, no cases of GVHD occurred in 33 patients who received third-party EBV-CTLs despite a

low degree of HLA matching ranging from 2/6 to 5/6 antigen match [13]. Thus, adoptive T cell therapy with EBV-specific T cells is a very promising therapy for patients with refractory/relapsed EBV-associated lymphomas that primarily have been used in the post-HSCT setting but have potential to be used as either a bridge to HSCT or adjuvant upfront therapy to decrease the short- and long-term side effects associated with conventional therapy.

2 Materials and Equipment

1. RPMI 1640 (Invitrogen).

2. Advanced RPMI 1640 (Invitrogen).

3. X-vivo 15 (Lonza).

4. Click's Medium (Irvine Scientific).

5. Heat-inactivated Fetal Calf Serum (Hyclone 1640).

6. Human AB serum (Gemini).

7. CTL medium: 45 % Advanced RPMI 1640, 45 % Click's Medium, 10 % Fetal Calf Serum, 2 mM L-Glutamine.

8. Complete medium: 90 % RPMI 1640, 10 % Fetal Calf Serum, 2 mM L-Glutamine.

9. Dulbecco's PBS (1×) (Invitrogen).

10. L-Glutamine, 200 mM (Invitrogen).

11. Acyclovir (Hospital pharmacy).

12. Cyclosporine A (Sandoz).

13. EBV-containing viral supernatant (CAGT, cell line B95.8).

14. Ad5f35ΔLMP1 -I-LMP2 (CAGT Vector Production Facility).

15. Ficoll (Lymphoprep, Cosmo Bio USA, Carlsbad, CA).

16. Interleukin-15 (CellGenix).

17. Interleukin-2 (hospital pharmacy).

18. 15 and 50 mL centrifuge tubes (Falcon).

19. 24-well and 96-well tissue culture plates (Falcon).

20. T-25 cm^2 vented flask (Falcon).

21. Serological pipets (Falcon).

22. Pipette tips (VWR).

23. Biosafety Cabinet.

24. Centrifuge, calibrated.

25. Microscope.

26. Irradiator.

27. Humidified incubator with atmosphere of 5 % CO_2 in air.

28. Hemacytometer.

29. Water bath.

30. Pipetman.

31. Pipet Aid.

---

3 Methods

Several groups have developed methods for activating and expanding T-cells specific for EBV antigens for clinical use. Moreover, EBV-CTLs can be generated from autologous or allogeneic sources (either HSCT donor or third-party). LCLs are generally used as antigen presenting cells for the expansion of EBV-specific T cells since they not only express type III latency antigens but also are excellent APCs as they express both HLA class I and II and several costimulatory ligands [23]. Dendritic cells or activated monocytes can also be used as APCs. However, monocytes cannot be used for the generation of autologous EBV-CTLs as they are not effective enough APCs to reactivate LMP-specific T cells from patients with lymphoma where such T cells are likely very low in frequency and anergic [24]. The Baylor College of Medicine group have developed a more rapid generation of EBV-CTLs that express LMP1, LMP2, and EBNA1 that uses an antigen-presenting complex (KATpx) consisting of activated autologous T cells pulsed with EBV peptides with a costimulatory HLA-negative K562 cell line [25]. This method is currently being tested in a Phase I clinical trial (NCT01555892). However, this chapter outlines the process of manufacturing an EBV/LMP-CTL product that has already been comprehensively evaluated in phase I studies ultimately for third-party use as an off the shelf therapeutic [19, 20, 24, 26, 27].

3.1 Blood Procurement and Preparation of Mononuclear Cells

1. Peripheral blood (up to 120 mL total in two aliquots of 60 mL) is collected from the allogeneic donor (*see* **Note 1**).

2. Dilute heparinized peripheral blood in an equal volume of PBS or RPMI 1640 at ambient temperature.

3. In a 50 mL centrifuge tube, carefully overlay approximately 10 mL of Lymphoprep with approximately 20 mL of diluted blood.

4. Centrifuge at 400 × *g* for 40 min.

5. Harvest PBMC interface into an equal volume of PBS or RPMI 1640.

6. Centrifuge at 450 × *g* for 10 min. Aspirate supernatant.

7. Resuspend in 40 mL PBS and count. Centrifuge at 400 × *g* for 5 min. Aspirate supernatant. PBMCs can now be frozen for later use or used to generate APCs and CTLs.

3.2 Generation of EBV-Transformed B Lymphoblastoid Cells Lines (EBV-LCL)

EBV-LCLs are used for the second and subsequent stimulations but require 4–6 weeks to generate depending on the donor. PBMCs are infected with a clinical grade, laboratory strain of EBV (B95-8) [28, 29] to manufacture EBV-LCL. EBV-LCLs are transduced with the Ad5f35-LMP1-I-2 vector [18], which enables EBV-LCL to overexpress LMP1 and LMP2 antigens to the T cells.

3.2.1 Generation of LCLs

1. Centrifuge 5–10 × 10^6 PBMC for 5 min at 400 × *g*. Remove supernatant.

2. Add 200 μL of concentrated B95.8 virus-supernatant to pelleted PBMCs and resuspend.

3. Add 1.8 mL of complete culture media containing cyclosporine (1 μg/mL).

4. Place 200 μL of cell mixture in each of five wells of a 96-well flat-bottomed plate. Place in incubator. Place 100 μL of cell mixture into another 10 wells and add 100 μL of CS A-containing medium to those 10 wells. Final volume per well is 200 μL.

5. Feed weekly by removing 100 μL and replacing with 100 μL fresh media. When cells are confluent and the media has changed color, the cells should be split from one well to two wells.

6. After 1–3 weeks, combine three wells into one well of a 24-well plate. Continue with weekly feeds (*see* **Note 2**).

7. Once cells are proliferating, remove cells from 24-well plate and place in a T-25 cm^2 vented flask with 5 mL complete medium plus 100 μM acyclovir.

8. Feed cells twice a week adding 100 μM acyclovir each time. LCLs should be cultured to the appropriate cell number needed for CTL stimulation and maintained in culture as stimulator cells for CTL (*see* **Note 3**).

3.2.2 *Adenovirus Transduction of LCL*

1. Aliquot up to 1×10^7 LCL per 15 mL centrifuge tube. Centrifuge at $400 \times g$ for 5 min to pellet cells. Aspirate supernatant.

2. Transfer adenovirus vector into the cells and pipette to mix (*see* **Note 4**).

3. Incubate at 37 °C for 90 min. Then resuspend cells in complete culture medium to a concentration of 5×10^6 cells per mL (*see* **Note 5**).

4. Add 2 mL of cell suspension to each well of a 24-well plate.

5. Incubate 1–2 days in 37 °C incubator.

6. LCL can now be used as stimulators or frozen for future use.

3.3 Initiation of EBV/LMP-Specific CTLs Using Adenovirus Vector-Transduced Adherent PBMC s

Day 0: Monocyte activation by adherence to plastic

1. Resuspend PBMC at 1×10^6 cells per mL in serum-free X-Vivo15.

2. Aliquot 2 mL cell suspension per well of a 24-well plate. Incubate overnight at 37 °C.

Day 1: Addition of adenovirus vector

3. Harvest nonadherent and adherent PBMCs. Use either a cell scraper or transfer pipette to dislodge adhered monocytes and combine with nonadherent cells.

4. Count and aliquot into centrifuge tubes at up to 1×10^7 cells per tube. Centrifuge for 5 min at $400 \times g$ and aspirate supernatant.

5. Add Adenovirus vector to pellet. Incubate for 120 min at 37 °C.

6. Wash cells four times.

7. Resuspend cells at 1×10^6 cells/mL in CTL medium. Add 10 ng/mL IL-15 for a final concentration of 5 ng/mL.

8. Aliquot 2 mL per well of a 24-well plate. Culture at 37 °C for 7 days.

Day 6–8: Media change

9. Remove 1 mL of medium per well and replace with 1 mL of fresh CTL medium.

*Days 9–12: Second stimulation of EBV-specific CTL (see **Note 6**)*

10. Harvest responder cells from 24-well plates. Centrifuge at $400 \times g$ for 5 min. Resuspend cells at 1×10^6 cells per mL in CTL medium.

11. Count and determine viability (*see* **Note 7**).

12. Aliquot 1 mL cells per well of a 24-well plate.

13. Irradiate LMP1/2- transduced LCL at 50 Gy, wash four times, and count.

14. Resuspend LCL at 2.5×10^5 cells per mL and aliquot 1 mL per well of responder T cells so that the ratio of CTL:LCL is 4:1. Culture in 37 °C (*see* **Note 8**).

15. 3–4 days after second stimulation, perform media change with IL-2. Prepare CTL media with 100–200 units/mL IL-2 (final concentration of 50–100 unit/mL). Remove 1 mL medium per well and replace with 1 mL fresh medium with IL-2 (*see* **Note 9**).

16. Culture for 3–4 days.

Days 16+: Third or subsequent stimulations

17. Harvest CTLs. Count and determine viability.

18. Resuspend CTLs at 1×10^6 cells per mL. Add 100–200 units/mL of IL-2 (final concentration of 50–100 units/mL). Aliquot 1 mL cells per well in a 24-well plate.

19. Irradiate LMP1/2 transduced LCL at 50 Gy, wash four times, and count.

20. Resuspend LCL at 2.5×10^5 cells per mL and aliquot 1 mL per well of responder T cells. Culture in 37 °C.

21. 3–4 days after stimulation, perform media change with IL-2. Prepare CTL media with 100–200 units/mL IL-2 (final concentration of 50–100 unit/mL). Remove 1 mL medium per well and replace with 1 mL fresh medium with IL-2 (*see* **Note 10**).

22. Culture for 3–4 days (*see* **Note 11**).

4 Notes

1. Blood should be kept at room temperature until it is processed, which should ideally be done within 24 h of blood procurement to ensure the highest yield of

PBMCs .

2. LCL will be ready to be transferred from 96-well plate to 24-well plate when they are confluent and in clumps. Feed harvested wells with medium as they often grow back. Additionally, for very fast growing cultures, nine wells of 96-well plate may be transferred directly into a T-25 cm^2 vented flask.

3. After LCL have been in T-25 cm^2 vented flasks for approximately 2 weeks, we recommend freezing three vials with at least 5×10^6 LCLs per vial for backup or future use. This procedure should produce a minimum of 2×10^7 LCL from 5 mL of peripheral blood.

4. For Ad5f35ΔLMP1-I- LMP2 transduction, the multiplicity of infection (MOI) is established for every new lot of vector. For example, if the MOI is 500 viral particles (v.p.) per cell in 500 μL and the adenovirus vector is 10^{12} v.p. per mL, add 5 μL adenovirus vector (diluted 1:10) per 1×10^6 cells.

5. Remember to keep cap of centrifuge tube loosened to allow for CO_2 exchange.

6. Second and subsequent CTL stimulations can also be performed in a G-Rex flask of the appropriate volume at a 5:1 ratio of CTL:LCL. We recommend 1–5 mL of CTLs at 1×10^6 cells per mL be used for a G-Rex10 or 10–20 mL of CTLs for a G-Rex100.

7. If viability is less than 60 %, centrifuge over Lymphoprep gradients to remove dead cells. Harvest interface, centrifuge, and resuspend in CTL medium. Count cells and wash one more time. Then resuspend cells at 1×10^6 cells per mL CTL medium and proceed with second stimulation. This can be done at each subsequent stimulation.

8. Culture 2 mL of irradiated LCL alone in one well as a control for irradiation.

9. The addition of IL-15 at the time of CTL initiation has been shown to increase the likelihood of expanding LMP1/2- specific CTLs independent of HLA type. IL-2 should not be used until the feed step during the second stimulation as it may

contribute to the expansion of non-antigen-specific T cells or even T regulatory cells [24].

10. If wells are confluent, cells can be split 1:1 into new wells and refed with fresh medium.

11. CTL can be cryopreserved for infusion from day 7 onward, but immunological analysis should not be done until at least Day 10 because of high background cytokine release.

Acknowledgments

References

1. Kuppers R, Engert A, Hansmann ML (2012) Hodgkin lymphoma. J Clin Invest 122:3439–3447
[CrossRef][PubMed][PubMedCentral]

2. Grogg KL, Miller RF, Dogan A (2007) HIV infection and lymphoma. J Clin Pathol 60:1365–1372
[CrossRef][PubMed][PubMedCentral]

3. Fox CP, Haigh TA, Taylor GS et al (2010) A novel latent membrane 2 transcript expressed in Epstein-Barr virus-positive NK- and T-cell lymphoproliferative disease encodes a target for cellular immunotherapy. Blood 116:3695–3704
[CrossRef][PubMed][PubMedCentral]

4. Sing AP, Ambinder RF, Hong DJ et al (1997) Isolation of Epstein-Barr Virus (EBV)-Specific cytotoxic T Lymphocytes that lyse reed-sternberg cells: implications for immune-medicated therapy of EBV hodgkin's disease. Blood 89:1978–1986
[PubMed]

5. Chia WK, Teo M, Wang WW et al (2014) Adoptive T-cell transfer and chemotherapy in the first-line treatment of metastatic and/or locally recurrent nasopharyngeal carcinoma. Mol Ther 22(1):132–139
[CrossRef][PubMed]

6. Levitskaya J, Coram M, Levitsky V et al (1995) Inhibition of antigen processing by the internal repeat region of the Epstein-Barr virus nuclear antigen-1. Nature 375(6533):685–688
[CrossRef][PubMed]

7. Rooney CM, Smith CA, Ng C et al (1995) Use of gene-modified virus-specific T lymphocytes to control Epstein-Barr virus-related lymphoproliferation. Lancet 345:9–13
[CrossRef][PubMed]

8. Papadopoulos EB, Ladanyi M, Emanuel D et al (1994) Infusions of donor leukocytes to treat Epstein-Barr virus-associated lymphoproliferative disorders after allogeneic bone marrow transplantation. N Engl J Med 330:1185–1191
[CrossRef][PubMed]

9. O'Reilly RJ, Lacerda JF, Lucas KG et al (1996) Adoptive cell therapy with donor lymphocytes for EBV-associated lymphomas developing after allogeneic marrow transplants. In: DeVita VT, Hellman S, Rosenberg SA (eds) Important advances in oncology 1996. Lippincott-Raven, Philadelphia, pp 149–166

10. Doubrovina E, Oflaz-Sozmen B, Prockop SE et al (2012) Adoptive immunotherapy with unselected or EBV-specific T cells for biopsy-proven EBV$^+$ lymphomas after allogeneic hematopoietic cell transplantation. Blood 119(11):2644–2656
[CrossRef][PubMed][PubMedCentral]

11. Heslop HE, Ng CYC, Li C et al (1996) Long-term restoration of immunity against Epstein-Barr virus infection by adoptive transfer of gene-modified virus-specific T lymphocytes. Nat Med 2:551–555
[CrossRef][PubMed]

12. Heslop HE, Slobod KS, Pule MA et al (2010) Long-term outcome of EBV-specific T-cell infusions to prevent or treat EBV-related lymphoproliferative disease in transplant recipients. Blood 115(5):925–935
[CrossRef][PubMed][PubMedCentral]

13. Haque T, Wilkie GM, Jones MM et al (2007) Allogeneic cytotoxic T-cell therapy for EBV-positive posttransplantation lymphoproliferative disease: results of a phase 2 multicenter clinical trial. Blood 110(4):1123–1131
[CrossRef][PubMed]

14. Young LS, Rickinson AB (2004) Epstein-Barr virus: 40 years on. Nat Rev Cancer 4(10):757–768
[CrossRef][PubMed]

15. Tierney J, Steven N, Young LS et al (1994) Epstein-Barr virus latency in blood mononuclear cells: analysis of viral gene transcription during primary infection and in the carrier state. J Virol 68(11):7374–7385
[PubMed][PubMedCentral]

16. Roskrow MA, Suzuki N, Gan Y-J et al (1998) EBV-specific cytotoxic T lymphocytes for the treatment of patients with EBV positive relapsed Hodgkin's disease. Blood 91:2925–2934
[PubMed]

17. Bollard CM, Straathof KC, Huls MH et al (2004) The generation and characterization of LMP2-specific CTLs for use as adoptive transfer from patients with relapsed EBV-positive Hodgkin disease. J Immunother 27(4):317–327
[CrossRef][PubMed]

18. Chia WK, Wang WW, Teo M et al (2012) A phase II study evaluating the safety and efficacy of an adenovirus DLMP1-LMP2 transduced dendritic cell vaccine in patients with advanced metastatic nasopharyngeal carcinoma.

Ann Oncol 23(4):997–1005
[CrossRef][PubMed]

19. Bollard CM, Gottschalk S, Leen AM et al (2007) Complete responses of relapsed lymphoma following genetic modification of tumor-antigen presenting cells and T-lymphocyte transfer. Blood 110(8):2838–2845
[CrossRef][PubMed][PubMedCentral]

20. Bollard CM, Gottschalk S, Torrano V et al (2014) Sustained complete responses in patients with lymphoma receiving autologous cytotoxic T lymphocytes targeting Epstein-Barr virus latent membrane proteins. J Clin Oncol 32(8):798–808
[CrossRef][PubMed]

21. Cruz CR, Hanley PJ, Liu H et al (2010) Adverse events following infusion of T cells for adoptive immunotherapy: a 10 year experience. Cytotherapy 12(6):743–749
[CrossRef][PubMed][PubMedCentral]

22. Bollard CM, Rooney CM, Heslop HE (2012) T-cell therapy in the treatment of post-transplant lymphoproliferative disease. Nat Rev Clin Oncol 9(9):510–519
[CrossRef][PubMed][PubMedCentral]

23. Hislop AD, Taylor GS, Sauce D et al (2007) Cellular responses to viral infection in humans: lessons from Epstein-Barr virus. Annu Rev Immunol 25:587–617
[CrossRef][PubMed]

24. Bollard CM, Gottschalk S, Huls MH et al (2011) Manufacture of GMP-grade cytotoxic T lymphocytes specific for LMP1 and LMP2 for patients with EBV-associated lymphoma. Cytotherapy 13(5):518–522
[CrossRef][PubMed][PubMedCentral]

25. Ngo MC, Ando J, Leen AM et al (2014) Complementation of antigen presenting cells to generate T lymphocytes with broad target specificity. J Immunother 37(4):193–203
[CrossRef][PubMed][PubMedCentral]

26. Perna SK, Gottschalk S, Torrano V et al (2015) Administration of LMP-specific cytotoxic T-lymphocytes to patients with relapsed EBV-positive lymphoma post allogeneic stem cell transplant. BBMT 21(2):S148

27. Miller R, Perna SJ, Gottschalk S et al (2015) Administration of LMP-specific cytotoxic T-lymphocytes to patients with relapsed EBV-positive lymphoma post allogeneic stem cell transplant. Cytotherapy 17(6):S18
[CrossRef]

28. Miller G, Lipman M (1973) Release of infectious Epstein-Barr virus by transformed marmoset leukocytes. Proc Natl Acad Sci U S A 70:190–194
[CrossRef][PubMed][PubMedCentral]

29. Smith CA, Ng CYC, Heslop HE et al (1995) Production of genetically modified EBV-specific cytotoxic T cells for adoptive transfer to patients at high risk of EBV-associated lymphoproliferative disease. J Hematother 4:73–79
[CrossRef][PubMed]

Index

A
Apoptosis

B
B cells
   B cell receptor (BCR)
   germinal center (GC)
   memory2
   naïve4
Bioinformatics, Computation
   Bowtie
   EBSeq1
   EdgeR1
   Fast-x toolkit1
   Galaxy1
   Integrative Genomics Viewer (IGV)
   miRbase1
   miRDeep1
   RSEM1
   STAR aligner1
Burkitt Lymphoma
   endemic (eBL)
   sporadic (sBL)

C
Cell culture
   B cell lines
      Akata5
      B95-8
      BL30
      Daudi1
      lymphoblastoid cell line (LCL)
      Mutu1
      Raji1

U

W